

**Design of Chiral  $\pi$ -Cu(II) Catalysts for  
the Enantioselective  $\alpha$ -Halogenation Reaction**

**Kazuki NISHIMURA**

Graduate School of Engineering, Nagoya University

Nagoya, 2022



## Contents

<b>Chapter 1</b>	Introduction and General Summary.....	1
<b>Chapter 2</b>	Enantio- and Site-selective $\alpha$ -Fluorination of <i>N</i> -Acyl-3,5-dimethylpyrazoles Catalyzed by Chiral $\pi$ -Cu(II) Complexes.....	24
<b>Chapter 3</b>	Thorpe–Ingold Effect and a High-Performance Chiral $\pi$ -Cu(II) Catalyst.....	218
<b>Chapter 4</b>	A $\pi$ -Cu(II)– $\pi$ Complex as an Extremely Active Catalyst for Enantioselective $\alpha$ -Halogenation of <i>N</i> -Acyl-3,5-dimethylpyrazoles.....	236
<b>Research Achievement</b> .....		279
<b>Acknowledgements</b> .....		283



# **Chapter 1**

## **Introduction and General Summary**

## 1-1. Introduction

The electrophilic  $\alpha$ -halogenation reaction of carbonyl compounds is one of the most important organic reactions. Halogen-containing products are not only useful synthetic intermediates but also pharmaceutically active drugs. The C–H bond is generally quite strong, and therefore unreactive (e.g.  $pK_a$  of  $\text{CH}_4 = \sim 56^1$ ). In the case of the  $\alpha$ -C–H bond, the anionic charge is delocalized over the oxygen. Thus, the  $pK_a$  values of  $\alpha$ -C–H bonds are relatively low compared to those of non-functionalized C–H bonds (Fig. 1).  $\alpha$ -Halogenation proceeds *via* the formation of enolate species from the deprotonation of carbonyl compounds, followed by nucleophilic attack of electrophilic halogenation reagents (Scheme 1). Over the past 100 years, the most commonly used halogenating reagents for this reaction have been the diatomic halides ( $\text{X}_2$ ), which are highly reactive for asymmetric catalysis and in some cases are nonselective. Over the past few decades, significant progress has been made in the development of catalytic, asymmetric halogenation reactions, largely due to the intense development of mild  $\text{X}^+$  source reagents.<sup>6,7</sup>

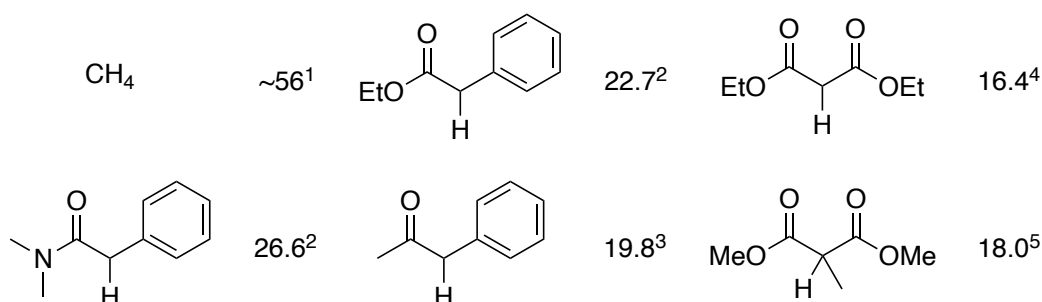
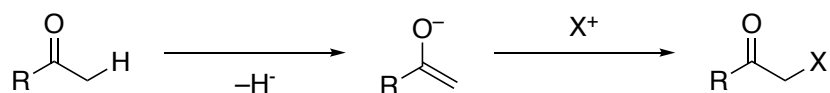


**Figure 1.**  $pK_a$  values of various carbonyl compounds in DMSO.

### **Scheme 1.** Electrophilic $\alpha$ -Halogenation of Carbonyl Compounds

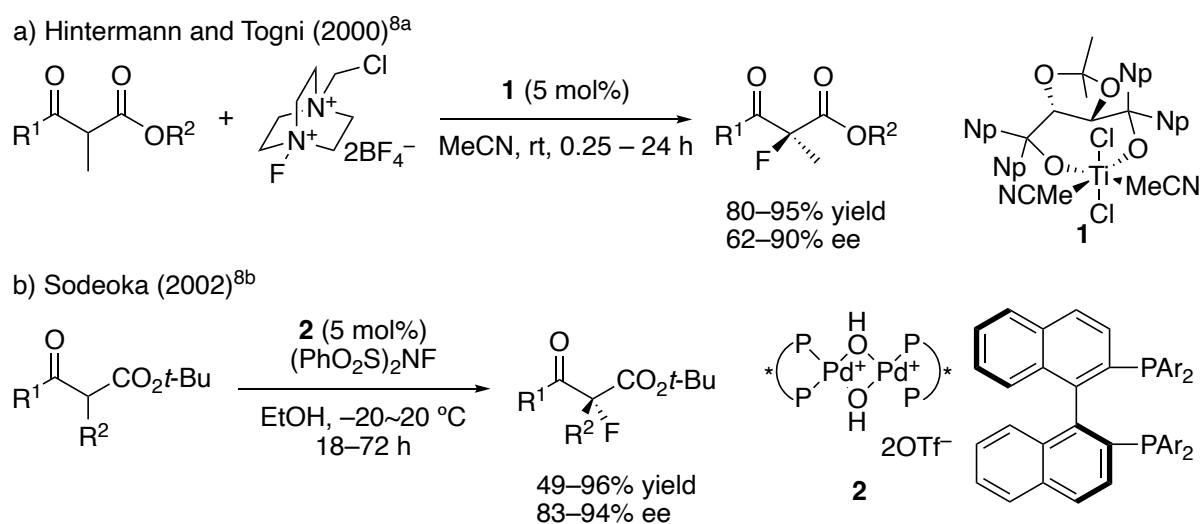


In particular, the strategy for catalytic enantioselective  $\alpha$ -halogenation can fall into one of several classes: (1) a chiral Lewis acid or Brønsted acid catalyst is used to activate a carbonyl moiety; (2) a chiral amine catalyst is used to generate an enamine derived from the reaction of a ketone or aldehyde; (3) a chiral phase-transfer catalyst is used to associate with enolate oxygen; and (4) a chiral

nucleophilic catalyst is used to generate a chiral ketene intermediate.

Hintermann and Togni developed the first enantioselective fluorination of  $\alpha$ -branched  $\beta$ -keto esters catalyzed by a chiral titanium complex (Scheme 2a).<sup>8a</sup> In 2002, Sodeoka's group reported elegant work using Lewis acidic palladium catalyst **2** (Scheme 2b).<sup>8b</sup> As shown in Figure 1,  $pK_a$  values of  $\beta$ -keto esters are quite low among carbonyl compounds. Thus, many researchers have established sophisticated systems for the catalytic asymmetric halogenation of  $\beta$ -keto esters by various Lewis acid catalysts<sup>8</sup>, phase-transfer catalysts<sup>9</sup>, and organocatalysts.<sup>10</sup>

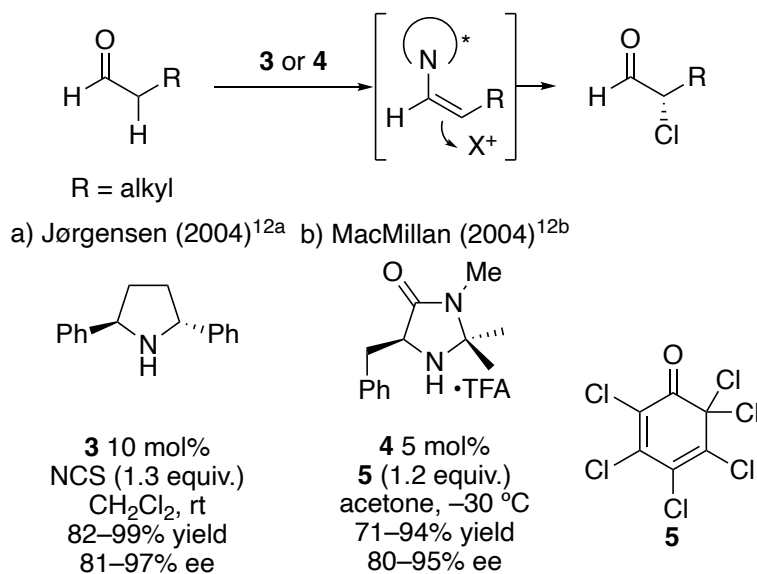
**Scheme 2.** Enantioselective  $\alpha$ -Halogenation of  $\beta$ -Keto Esters



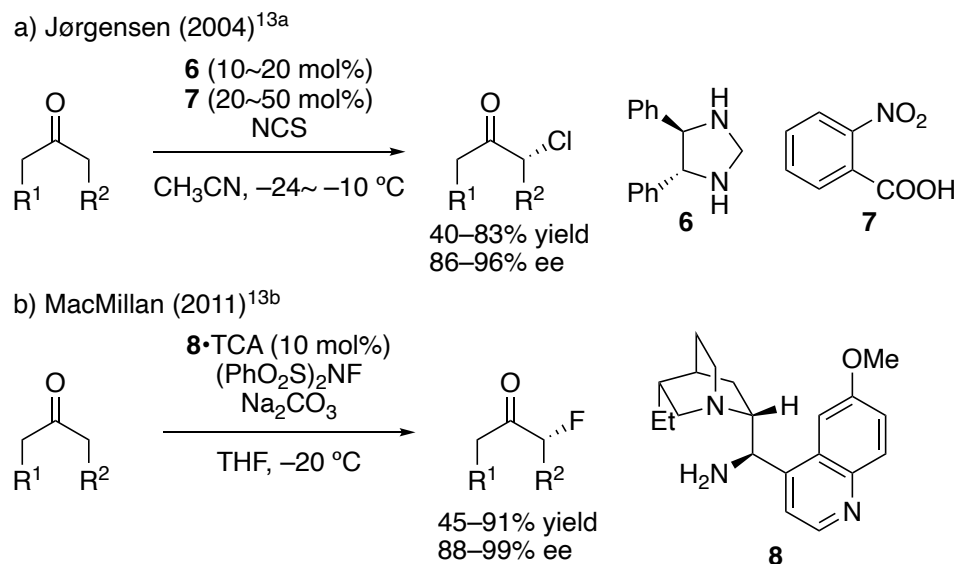
Another important protocol for the enantioselective  $\alpha$ -halogenation reaction employs enamine catalysis. Either primary or secondary amines react with aldehydes and ketones in the presence of an acid catalyst to generate highly nucleophilic enamines. *L*-Proline, the most famous chiral enamine catalyst has been used for decades in a variety of asymmetric reactions.<sup>11</sup> In 2004, the first organocatalytic asymmetric  $\alpha$ -chlorination of aldehydes was independently developed by MacMillan<sup>12a</sup> and Jørgensen<sup>12b</sup> (Schemes 3a and 3b). By taking advantage of enamine catalysts, many researchers have designed various types of basic catalysts<sup>12</sup> including *N*-heterocyclic carbene catalysts<sup>12c</sup> and primary amine catalysts<sup>12d</sup>. Jørgensen accomplished the first catalytic enantioselective  $\alpha$ -chlorination of ketones by using less sterically demanding catalyst **6** to promote

the formation of enamine.<sup>13a</sup> MacMillan's group also accomplished the first highly enantioselective  $\alpha$ -fluorination of ketones catalyzed by Cinchona-based alkaloid primary amine catalyst **8**.<sup>13b</sup>

**Scheme 3.** Enantioselective  $\alpha$ -Halogenation of Aldehydes



**Scheme 4.** Enantioselective  $\alpha$ -Halogenation of Ketones

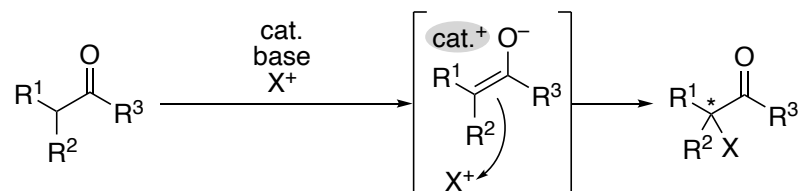


In 2002, Kim's group reported the first example of the use of a chiral quaternary ammonium phase-transfer catalyst for the enantioselective fluorination of  $\beta$ -keto esters.<sup>9a</sup> Generally, an inorganic base is involved and the generated anionic enolate species is associated with a positively charged chiral ammonium cation and provides significant facial discrimination (Scheme 5). Other



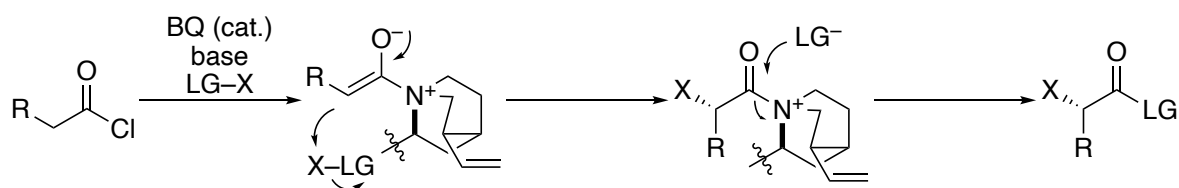
groups have demonstrated the use of phase-transfer catalysts to control enantioselectivity.<sup>9</sup>

**Scheme 5.** Phase-Transfer Catalysis for Enantioselective  $\alpha$ -Halogenation



Although several impressive examples of catalytic enantioselective  $\alpha$ -halogenation have been established with  $\beta$ -keto esters, aldehydes, and ketones, direct and enantioselective  $\alpha$ -halogenation of carboxylic acid derivatives has not been explored until now, mainly because of the higher  $pK_a$  values of  $\alpha$ -C–H bonds of simple esters and amides (Fig. 1). To address these problems, carboxylic acid derivatives have been designed to efficiently increase the acidity of an  $\alpha$ -proton. One of the pioneering works was the combination of acid chloride and a chiral nucleophilic catalyst in the presence of a base and *in situ*-generated ketene enolates. Enantioselective  $\alpha$ -halogenation then occurred with an electrophilic halogenating reagent (LG–X, LG = Leaving Group) and the reactive intermediate reacted with LG<sup>–</sup> (Scheme 5).<sup>14</sup>

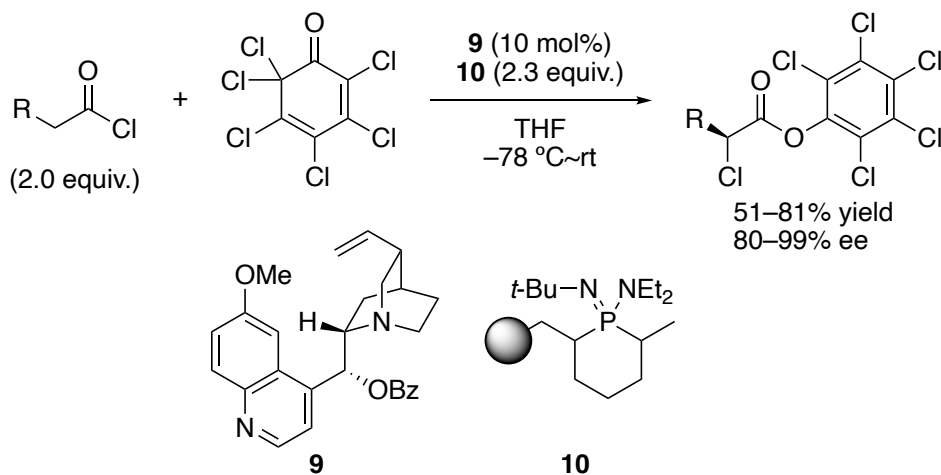
**Scheme 5.** Chiral Nucleophilic Catalyst for Enantioselective  $\alpha$ -Halogenation



In 2001, Lectka's group explored a significant breakthrough in asymmetric chlorination using simple acid halides catalyzed by cinchona alkaloid derivative **9** and a polymer-supported triaminophosphoamide imide (BEMP) **10** (Scheme 6).<sup>14a</sup> The resulting  $\alpha$ -chloroesters could be further functionalized with various nucleophiles. In 2004, they developed enantioselective  $\alpha$ -bromination using the same strategy.<sup>14b</sup> To the best of our knowledge, this is still the only example

of the catalytic enantioselective  $\alpha$ -bromination of carboxylic acid derivatives. Despite this excellent work, the yields tend to be low due to the instability of acid chloride and the formation of a nonhalogenated side product. Moreover, only a few successful examples have been reported using more stable carboxylic acid derivatives.

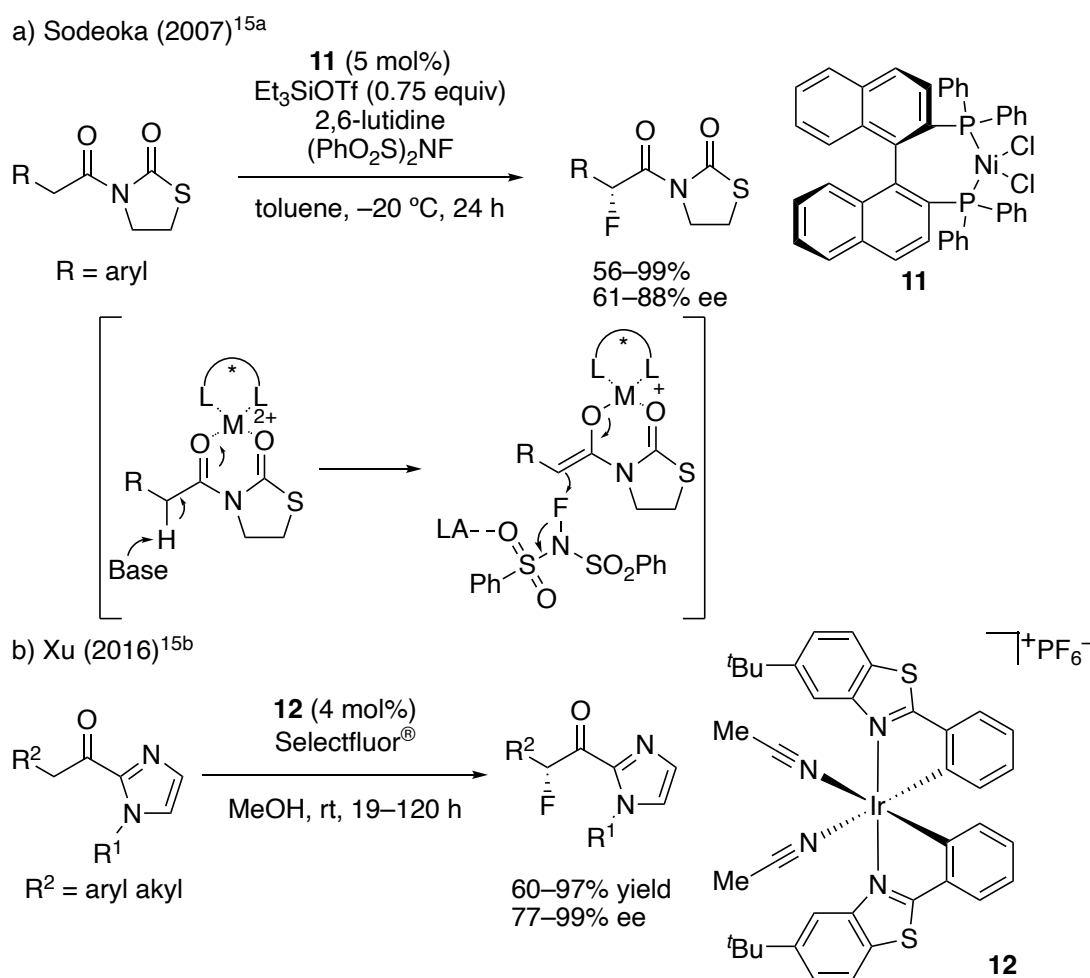
**Scheme 6.** Chiral Nucleophilic Catalyst for Enantioselective  $\alpha$ -Halogenation



In 2007, Sodeoka's group first disclosed the direct enantioselective  $\alpha$ -fluorination of carboxylic acid derivatives by using a catalytic amount of  $\text{NiCl}_2/\text{BINAP}$ , triethylsilyl triflate, and 2,6-lutidine (Scheme 7a).<sup>15a</sup> Up until then, only a few synthetically useful diastereoselective fluorination reactions of ester derivatives were reported.<sup>16</sup> No catalytic system had been reported, presumably due to the difficulty in the *in situ* generation of enol species under catalytic conditions. The use of an auxiliary to activate the carbonyl group and to decrease the  $\pi$ -donation of the amide might be effective for increasing the acidity of an  $\alpha$ -C–H proton. Another important point of using an auxiliary is that the carbonyl group is expected to react *via* a bidentate metal enolate. They later extended this system to chlorination with triflyl chloride.<sup>15b</sup> However, the substrate scope was limited to aromatic substituted groups at the  $\alpha$ -position because of their  $pK_a$  values. In 2016, Xue's group developed iridium-catalyzed enantioselective fluorination using another type of activated pseudoamide, acyl imidazoles (Scheme 7b). Importantly, aliphatic groups at the  $\alpha$ -position also worked. These  $pK_a$  values are higher than those of aromatic groups, which means that these

compounds are more challenging substrate candidates. Although the substrate scope has been broadened to include aliphatic acyl derivatives, the reaction is very slow (reaction time: 1~5 days), and the removability of the imidazole moiety without racemization has not been confirmed. Given these limitations, there has been a need for the development of a more efficient and practical asymmetric catalytic system. Very recently, Megger's group demonstrated enantioselective fluorination and chlorination using a chiral-at-rhodium catalyst.<sup>15d</sup> However, they could not obtain the desired products with an aliphatic side chain. Furthermore, the use of highly reactive and corrosive triflyl chloride is needed in the presence of a stoichiometric amount of base for an efficient reaction.

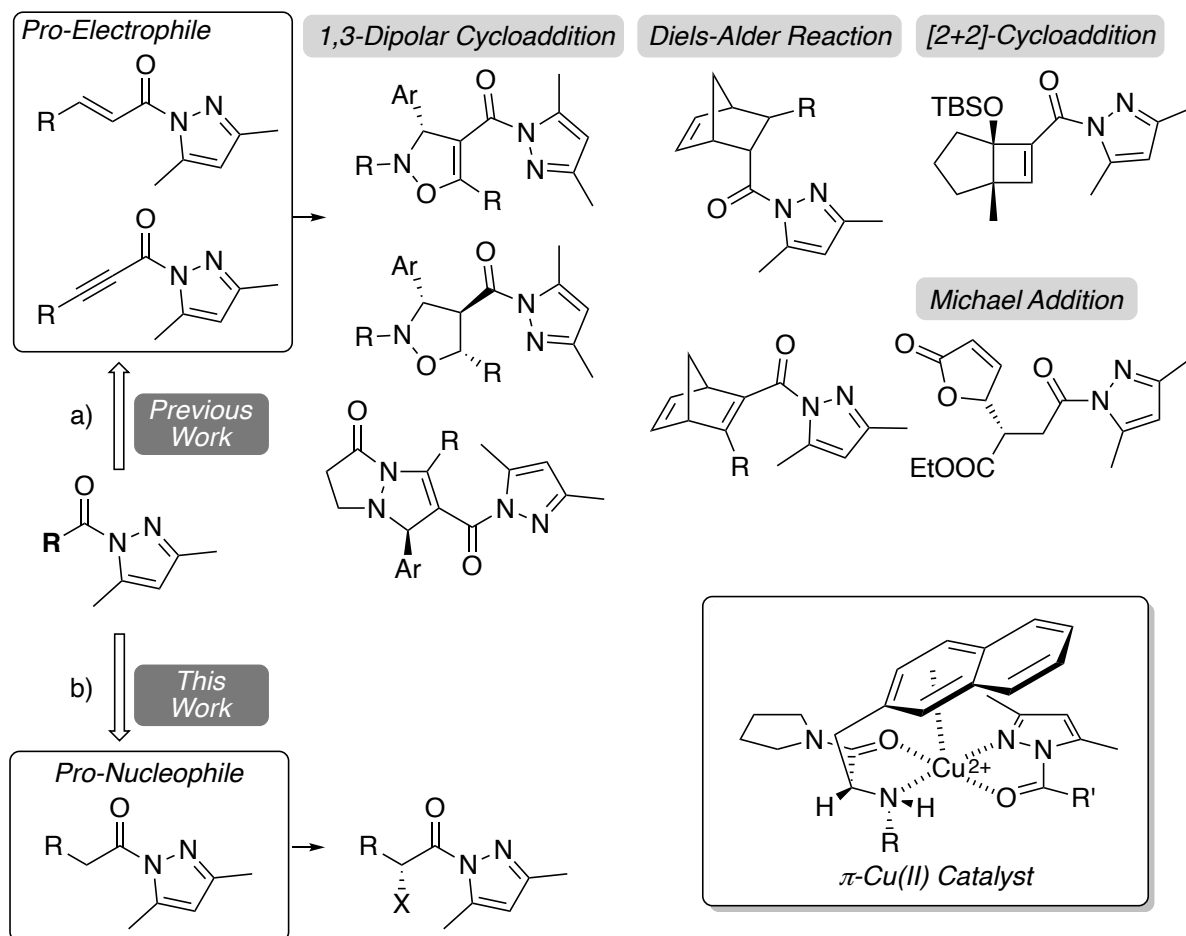
**Scheme 7.** Asymmetric  $\alpha$ -Fluorination of Carboxylic Acid Derivatives



## 1-2. Strategies for Novel Catalyst Design

Since 2006, Ishihara's group has developed  $\pi$ -Cu(II) complex-catalyzed enantioselective nucleophilic addition reactions and cycloaddition reactions to  $\alpha,\beta$ -unsaturated *N*-acylpyrazoles and propioloylpyrazoles, which are appropriate as electrophiles due to the electron-deficiency of the pyrazole moiety and because the pyrazole moiety might effectively coordinate to an appropriate Lewis acid in a bidentate manner (Scheme 8a).<sup>17</sup> In addition, several groups have reported that *N*-acylpyrazoles are useful amides as pronucleophiles for the same reason.<sup>18</sup>  $\pi$ -Cu(II) complexes are important because (1) they enable the inexpensive and simple design of a chiral ligand that is derived from commercially available 3-(2-naphthyl)-*L*-alanine; (2) an asymmetric environment is effectively created through  $\pi$ -Cu(II) interaction between the naphthalene ring of the ligand and Cu(II); and (3) most importantly, the design of intramolecular  $\pi$ -Cu(II) interaction in the complex releases the counterions and/or prevents the solvent from decreasing the Lewis acidity of Cu(II). Therefore, this thesis focuses on the use of highly active  $\pi$ -Cu(II) complexes in enantioselective  $\alpha$ -halogenation reactions, with the expectation of a broader substrate scope and a more efficient catalytic system (Scheme 8b) (Chapters 2 and 4). During the course of this research, we found a more suitable ligand to induce higher enantioselectivity. Thus, the investigation of the generality of the catalyst is described (Chapter 3).

### Scheme 8. $\pi$ -Cu(II) Complexes for Enantioselective Reactions



### 1-3. Enantio- and Site-selective $\alpha$ -Fluorination of *N*-Acyl-3,5-dimethylpyrazoles Catalyzed by Chiral $\pi$ -Cu(II) Complexes

Some large natural organohalides are fluorinated compounds.<sup>19</sup> Most terrestrial fluorine atoms are bound in an insoluble form, hindering uptake by bio-organisms. Until 1957, no fluorine-containing drug had been developed. One of the earliest synthetic fluorinated drugs was the antineoplastic agent 5-fluorouracil.<sup>20</sup> Since then, over 150 drugs have come to the market and now account for ~20% of all pharmaceuticals,<sup>21</sup> with even higher numbers for agrochemicals (up to 30%).<sup>21c</sup> Top-selling fluorinated pharmaceuticals include the antidepressant fluoxetine (Prozac),<sup>22a</sup> the cholesterol-lowering drug atorvastatin (Lipitor),<sup>22b</sup> and the antibacterial ciprofloxacin (Ciprobay)<sup>22c</sup> (Fig. 2).

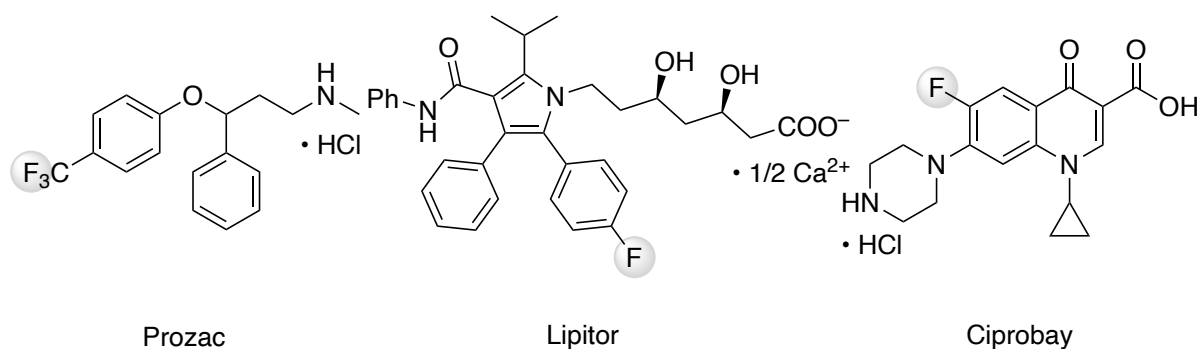


**Figure 2.** Representative examples of fluorine-containing drugs.

The role of fluorine in medicinal chemistry and drug design has been reviewed several times over the past few decades. The introduction of fluorine into pharmaceutical products is one of the most effective methods for improving pharmacological activity. The high electronegativity and small size of the fluorine atom, as well as its very different chemical reactivity from hydrogen, influence design considerations. Although fluorine (1.70 Å) is larger than hydrogen (1.20 Å), its van der Waals radius is closer to that of oxygen (1.52 Å), as is its electronegativity.<sup>23</sup> The strongly electron-withdrawing nature of a fluorine substituent is especially obvious in its effect on the acidity of neighboring functional groups.<sup>24</sup> Changes in *pK<sub>a</sub>* can also have effects on the number of different parameters in lead optimization including physicochemical properties, binding affinities, and absorption, distribution, metabolism, excretion (ADME), and safety issues. Beyond the expected inductive effects that fluorine may exert on neighboring functionalities to alter their physical properties or chemical reactivities, there is now greater interest in the role that a fluorine substituent may play in direct binding interactions. The interactions between fluorine and a protein may be bridged by a sphere of solvation or may occur due to a change in the conformation of the molecule.<sup>25b</sup>

In addition to achiral fluorinated compounds, optically active  $\alpha$ -fluorinated carbonyl compounds have received increased attention due to their widespread biological and therapeutic properties.<sup>25</sup> In a widely known embodiment, ( $\pm$ )-Thalidomide was released onto the market in 1956 as a sedative-hypnotic agent for the treatment of morning sickness (Fig. 3a). After unexpected severe birth defects were found in babies whose mothers had taken the drug, racemic thalidomide was withdrawn

from the market in 1962. This was one of the most notorious medical disasters of the 20th century. It has been suggested that while the (*R*)-enantiomer causes clinically effective sedative-hypnotic effects, the (*S*)-enantiomer is responsible for the teratogenic side effects. Thalidomide is known to rapidly epimerize under physiological conditions due to the presence of the acidic hydrogen atom on the stereogenic center adjacent to a carbonyl group. This undesirable racemization renders any bioassay of the individual enantiomers very difficult.<sup>26</sup> Replacement of this acidic hydrogen on the stereogenic center with fluorine blocks in vivo epimerization, allowing the synthesis and evaluation of both enantiomers (Fig. 3b). The (*S*)-fluorothalidomide analog was found to be a more active inhibitor of tumor necrosis factor- $\alpha$  (TNF- $\alpha$ ) which is implicated in the inflammatory process, than (*R*)-fluorothalidomide or the racemic fluorothalidomide.<sup>27</sup>

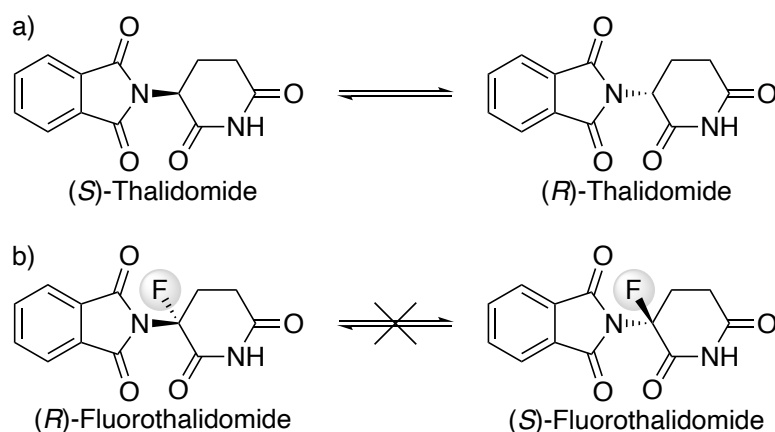


**Figure 3.** Strategy toward Thalidomide

In addition to the replacement of a hydrogen atom with a fluorine atom, many drugs contain fluorine atoms at a chiral carbon center. PF-06650833 inhibits IRAK-4 to block the production of inflammatory cytokines such as type I interferon and tumor necrosis factor, which are key drivers of autoimmune and inflammatory diseases (Figure 4a).<sup>28</sup> 7-F-PGI<sub>2</sub> is a potent platelet anti-aggregating and vasodilating agent and is more stable than 7-H-PGI<sub>2</sub> (Figure 4b).<sup>29</sup>

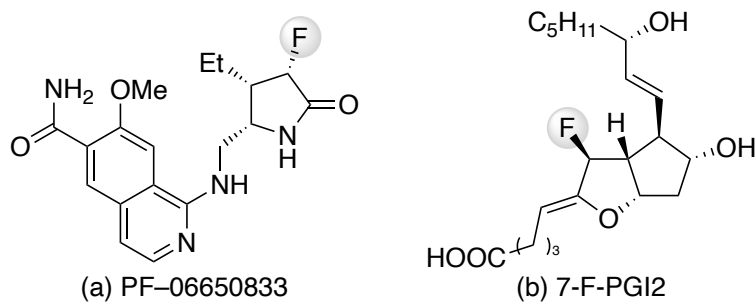


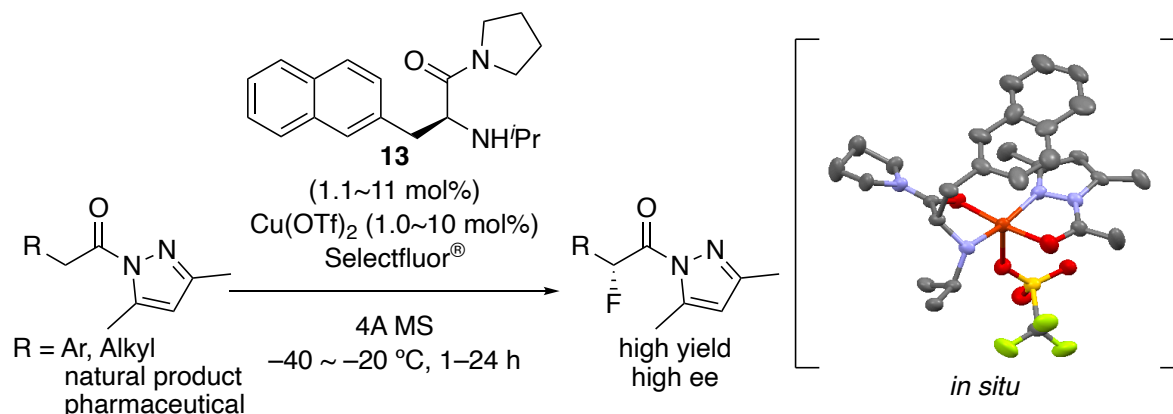
**Figure 4.** Examples of  $\alpha$ -fluorinated drugs.

Several drugs contain fluorine atoms on the chiral carbon center. Consequently, the introduction of various organofluorine compounds is one of the most significant tasks in synthetic organic chemistry, and mono-fluorination is a straightforward way to introduce a fluorine atom into various useful and bioactive compounds. One of the simplest methods for introducing fluorine atom is an  $\alpha$ -fluorination reaction of carbonyl compounds. Enantioselective  $\alpha$ -fluorination reactions of carbonyl compounds are among the most powerful and efficient methods for constructing optically active  $\alpha$ -fluorinated carbonyl derivatives, and great effort has been dedicated to the development of their catalytic versions.<sup>30</sup> Although there have been many reports on the  $\alpha$ -fluorination reaction, the carbonyl substrates are limited to aldehydes, ketones, 1,3-dicarbonyl compounds, and 3-substituted oxindoles which have relatively low  $pK_a$  values associated with the  $\alpha$ -hydrogen atoms (Chapter 1-1).

To address these problems, the development of a more sophisticated catalytic system is required. Chapter 2 describes  $\pi$ -Cu(II) complexes for the enantioselective  $\alpha$ -fluorination of *N*-Acyl-3,5-dimethylpyrazoles (Scheme 9).<sup>31</sup> With this catalytic system, the scope was greatly broadened to include substrates with an aliphatic side chain, and more complex molecules and products were obtained in high yield with high enantioselectivity. Moreover, structural characterization revealed the close contact between the naphthalene ring of the ligand and Cu(II), and this  $\pi$ -Cu(II) interaction was critical for increasing the reactivity and enantioselectivity.



### Scheme 8. $\pi$ -Cu(II) Complexes for Enantioselective $\alpha$ -Fluorination

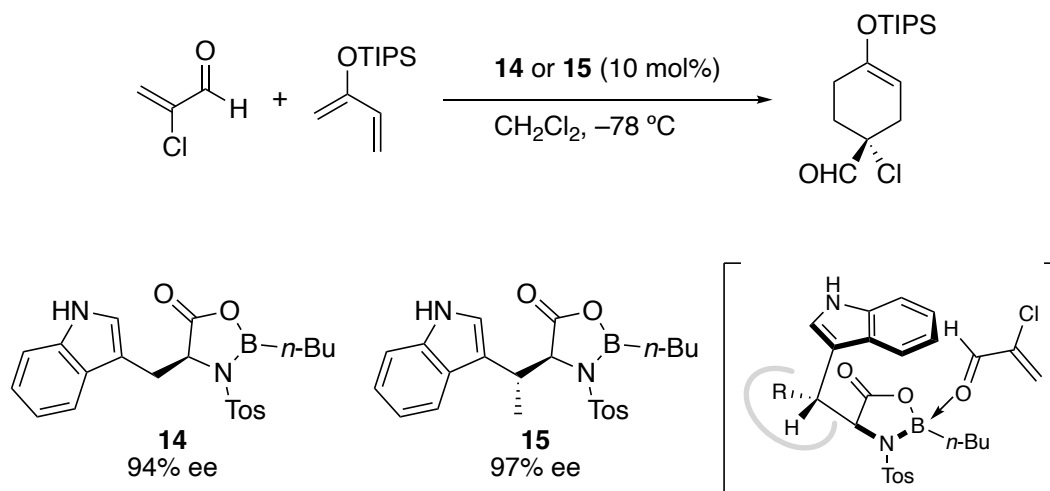


### 1-4. Thorpe-Ingold Effect and a High-Performance Chiral $\pi$ -Cu(II) Catalyst

The design of a chiral catalyst involving the Thorpe-Ingold effect<sup>32</sup> interlocking the chiral cavity is one of the most effective methods for inducing high enantioselectivity.

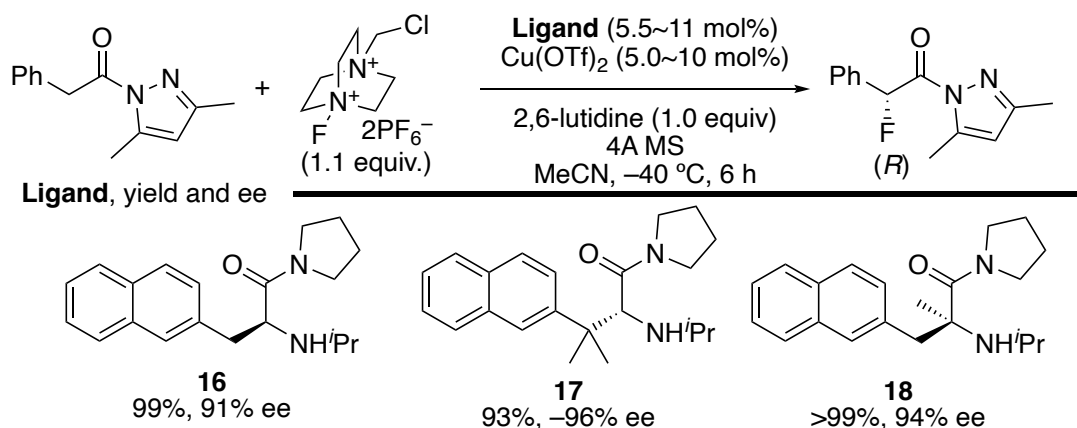
In particular, in 1992, Corey's group reported a catalytic enantioselective Diels-Alder reaction of 2-bromoacrolein and cyclopentadiene catalyzed by (*S*)-tryptophan-derived oxazaborolidine.<sup>33a,b</sup> They later discovered that (TIPSO)-1,3-butadiene reacted with 2-chloroacrolein with even higher enantioselectivity when catalyzed by **15** than by **14** (Scheme 9).<sup>33c</sup> The (*R*)- $\beta$ -methyl group of **15** may be important for creating a chiral atmosphere.

### Scheme 9. Effect of Methyl Substituents of the Catalyst for the Enantioselective Diels-Alder Reaction



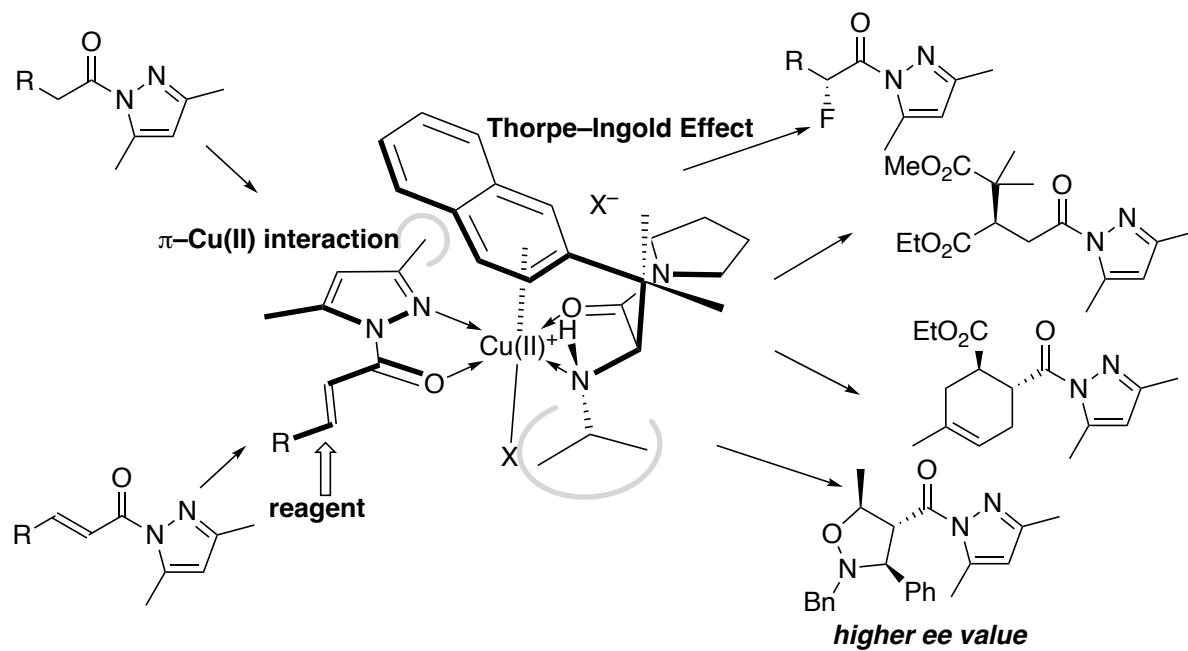
During the course of enantioselective  $\alpha$ -fluorination (Chapter 2), newly designed ligands **17** and **18** bearing methyl substituents gave higher enantioselectivity than **16** (Scheme 10). Methyl substituents of **17** and **18** may sterically stabilize transition-state assemblies folded by  $\pi$ -Cu(II) interaction due to the Thorpe–Ingold effect.

**Scheme 10.** Effect of Methyl Substituents of the Ligand for Enantioselective  $\alpha$ -Fluorination



Based on these promising results, the author envisioned that ligand **17** could be effective for other enantioselective reactions that our lab has previously developed.<sup>17</sup> Chapter 3 describes the enantioselective Mukaiyama–Michael reaction, Diels–Alder reactions, and 1,3-dipolar cycloaddition reactions with nitrones of **19** catalyzed by **17**-Cu(II) complex, which gave the corresponding products with higher enantioselectivity (Scheme 11).

**Scheme 11.** Thorpe–Ingold Effect for the  $\pi$ -Cu(II) Catalyst



## 1-5. A $\pi$ -Cu(II)- $\pi$ Complex as an Extremely Active Catalyst for the Enantioselective $\alpha$ -Halogenation of *N*-Acyl-3,5-dimethylpyrazoles

Enantioselective  $\alpha$ -halogenated compounds except for fluorine atom are some of the most useful synthetic intermediates for many organic reactions because halogens (Cl, Br, I) have a good leaving ability. Once these halogens are introduced to a chiral carbon center, halogens could be replaced by subsequent  $S_N2$ -type reactions to introduce new functional groups without a loss of enantiopurity in most cases. In addition, for the chemical synthesis of natural products and pharmaceuticals (Fig. 5), the enantioselective  $\alpha$ -halogenation of carbonyl compounds is an effective method for introducing halogen atoms. Many researchers have reported the enantioselective  $\alpha$ -chlorination of highly reactive 1,3-dicarbonyl compounds,<sup>8e,10a,d,34</sup> aldehydes,<sup>12a,b,e</sup> ketones,<sup>13a</sup> and silyl ketene acetals.<sup>35</sup> As for the chlorination of carboxylic acid derivatives, only a few successful methods have been reported using activated amides<sup>15a,b</sup> and acid chlorides.<sup>14,b</sup> Importantly, for the chlorination of activated amides, the use of highly toxic and reactive sulfonyl chloride in the presence of a stoichiometric base generates a “naked”  $Cl^+$  source. In addition, the substrates require an  $\alpha$ -aromatic or allyl group for activation of an  $\alpha$ -proton. It is difficult to generate enol species using substrates with an  $\alpha$ -chain.

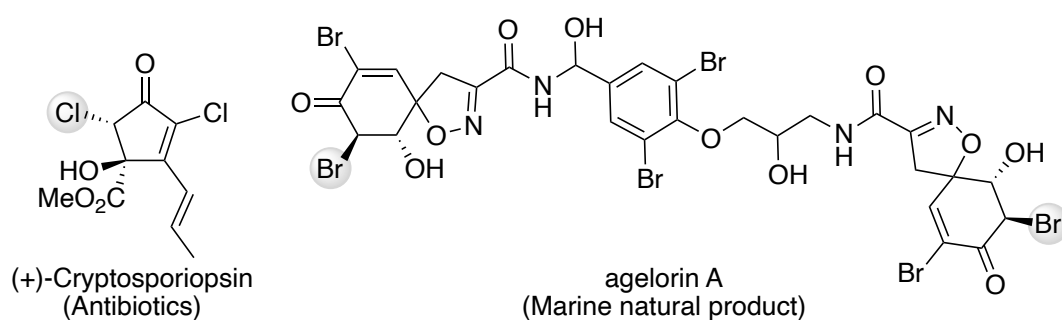
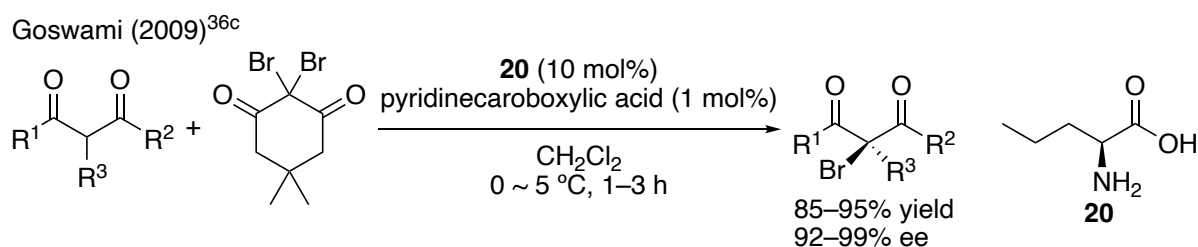


**Figure 5.** Representative  $\alpha$ -halogenated drug and natural product.

In this area, only a few asymmetric  $\alpha$ -bromination reactions of 1,3-dicarbonyl compounds<sup>36</sup> and aldehydes<sup>37</sup> have been developed, although they are reactive carbonyl compounds, probably due to undesired side reactions such as bromination of an amine catalyst. In 2009, Goswami developed

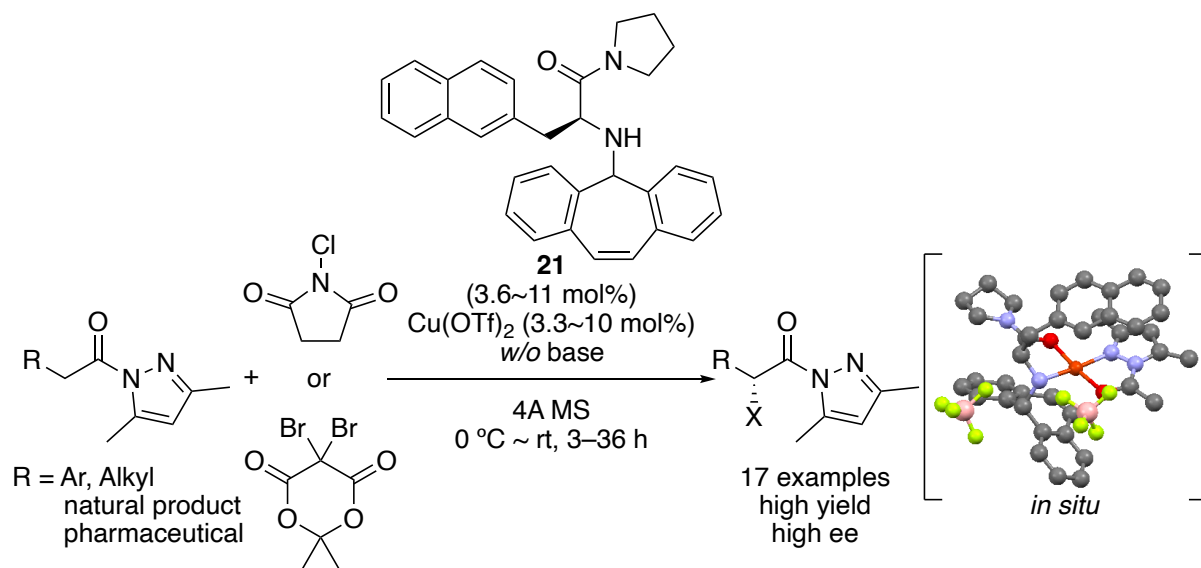
2,2-dibromodimedone as an organic mild brominating reagent for the asymmetric bromination of 1,3-dicarbonyl compounds (Scheme 12).<sup>36c</sup> In fact, there is competition for the background bromination of the enol even at low temperature, which affects the stereoselectivity, with the common bromination agent NBS. Regarding the bromination of carboxylic acid derivatives, to the best of our knowledge, only one successful example using acid chloride has been reported by Lectka.<sup>14b,38</sup> Examples of the enantioselective  $\alpha$ -bromination of activated amide have not yet been established.

**Scheme 12.** Highly Enantioselective  $\alpha$ -Bromination of 1,3-Dicarbonyl Compounds by a Mild Brominating Agent



To address these problems, the development of a more active catalytic system toward activated amide is required. Based on the results regarding enantioselective  $\alpha$ -fluorination by  $\pi$ -Cu(II) complexes (Chapter 2), the author envisioned that we could develop other halogenation reactions by the use of highly Lewis acidic  $\pi$ -Cu(II) complexes. In addition, the combination of a highly Lewis acidic  $\pi$ -Cu(II) complex and mild halogenating agents might be important for inducing high enantioselectivity. Chapter 4 describes the development of an extremely active catalyst for enantioselective  $\alpha$ -chlorination and bromination reactions. As a result of designing the  $\pi$ -Cu(II)- $\pi$  complex, the corresponding halogenated products were obtained in high yield with high enantioselectivity even in the absence of base (Scheme 13).

**Scheme 13.**  $\pi$ -Cu(II)- $\pi$  Complex for Enantioselective  $\alpha$ -Halogenation



## 1-6. Conclusion

In summary, the author has developed a highly enantio- and site-selective  $\alpha$ -halogenation of *N*-acyl-3,5-dimethylpyrazoles catalyzed by chiral  $\pi$ -Cu(II) or  $\pi$ -Cu(II)- $\pi$  complexes. This new catalytic method is far superior to those described in previous reports. The present catalysts are highly Lewis acidic, and thus the catalytic deprotonation of  $\alpha$ -C-H bonds proceeds smoothly. Characterization of the structures of  $\pi$ -Cu(II) and  $\pi$ -Cu(II)- $\pi$  complexes revealed the detailed transition states of these reactions. Furthermore, the generality of newly designed ligand **17** was investigated.

## 1-7. References

- (1) Bordwell, F. G. *Acc. Chem. Res.* **1988**, *21*, 456–463.
- (2) Bordwell, F. G.; Fried, H. E. *J. Org. Chem.* **1981**, *46*, 4327–4331.
- (3) Bordwell, F. G.; Harrelson, J. A. *Can. J. Chem.* **1990**, *68*, 1714–1718.
- (4) Olmstead, W. N.; Bordwell, F. G. *J. Org. Chem.* **1980**, *45*, 3299–3305.
- (5) Arnett, E. M.; Maroldo, S. G.; Schilling, S. L.; Harrelson, J. A. *J. Am. Chem. Soc.* **1984**, *106*, 6759–6767.
- (6) (a) R. E. Banks, S. N. Mohialdin-Khaffaf, G. S. Lal, I. Sharif, R. G. Syvret, *J. Chem. Soc. Chem. Commun.* **1992**, 595–597. (b) R. E. Banks, US5086178A.
- (7) Golebiewski, W. M.; Gucma, M. *Synthesis* **2007**, *23*, 3599–3619.
- (8) (a) Hintermann, L.; Togni, A. *Angew. Chem. Int. Ed.* **2000**, *39*, 4359–4362. (b) Hamashima, Y.; Yagi, K.; Takano, H.; Tamás, L.; Sodeoka, M. *J. Am. Chem. Soc.* **2002**, *124*, 14530–14531. (c) Frantz, R.; Hintermann, L.; Perseghini, M.; Broggini, D.; Togni, A. *Org. Lett.* **2003**, *5*, 1709–1712. (d) Ma, J.-A.; Cahard, D. *Tetrahedron: Asymmetry* **2004**, *15*, 1007–1011. (e) Frings, M.; Bolm, C. *Eur. J. Org. Chem.* **2009**, 4085–4090. (f) Hintermann, L.; Perseghini, M.; Togni, A. *Beilstein J. Org. Chem.* **2011**, *7*, 1421–1435. (g) Niu, T.; Han, X.; Huang, D.; Wang, K.-H.; Su, Y.; Hu, Y.; F, Y. *J. Fluor. Chem.* **2015**, *175*, 6–11. (h) Hayamizu, K.; Terayama, N.; Hashizume, D.; Dodo, K.; Sodeoka, M. *Tetrahedron* **2015**, *71*, 6594–6601.
- (9) (a) Kim, D. Y.; Park, E. *J. Org. Lett.* **2002**, *4*, 545–547. (b) Wang, X.; Lan, Q.; Shirakawa, S.; Maruoka, K. *Chem. Commun.* **2010**, *46*, 321–323. (c) Zhu, C.-L.; Fu, X.-Y.; Wei, A.-J.; Cahard, D.; Ma, J.-A. *J. Fluor. Chem.* **2013**, *150*, 60–66. (d) Novacek, J.; Waser, M. *Eur. J. Org. Chem.* **2014**, 802–809.
- (10) (a) Cai, Y.; Wang, W.; Shen, K.; Wang, J.; Hu, X.; Lin, L.; Liu, X.; Feng, X. *Chem. Commun.* **2010**, *46*, 1250–1252. (b) Yi, W.-B.; Zhang, Z.; Huang, X.; Tanner, A.; Cai, C.; Zhang, W. *RSC Adv.* **2013**, *3*, 18267–18270. (c) Novacek, J.; Waser, M. *Eur. J. Org. Chem.* **2014**, 802–809. (d) Guan, X.; An, D.; Liu, G.; Zhang, H.; Gao, J.; Zhou, T.; Zhang, G.; Zhang, S. *Tetrahedron Lett.* **2018**, *59*, 2418–2421.
- (11) List, B. *Tetrahedron* **2002**, *58*, 5573–5590.

- (12) (a) Halland, N.; Braunton, A.; Bachmann, S.; Marigo, M.; Jørgensen, K. A. *J. Am. Chem. Soc.* **2004**, *126*, 4790–4791. (b) Brochu, M. P.; Brown, S. P.; MacMillan, D. W. C. *J. Am. Chem. Soc.* **2004**, *126*, 4108–4109. (c) Li, F.; Wu, Z.; Wang, J. *Angew. Chem. Int. Ed.* **2015**, *54*, 656–659. (d) Shibatomi, K.; Kitahara, K.; Okimi, T.; Abe, Y.; Iwasa, S. *Chem. Sci.* **2016**, *7*, 1388–1392. (e) Hutchinson, G.; Alamillo-Ferrer, C.; Burés, J. *J. Am. Chem. Soc.* **2021**, *143*, 6805–6809.
- (13) (a) Marigo, M.; Bachmann, S.; Halland, N.; Braunton, A.; Jørgensen, K. A. *Angew. Chem. Int. Ed.* **2004**, *116*, 5623–5626. (b) Kwiatkowski, P.; Beeson, T. D.; Conrad, J. C.; MacMillan, D. W. C. *J. Am. Chem. Soc.* **2011**, *133*, 1738–1741.
- (14) (a) Wack, H.; Taggi, A. E.; Hafez, A. M.; Drury, W. J.; Lectka, T. *J. Am. Chem. Soc.* **2001**, *123*, 1531–1532. (b) France, S.; Wack, H.; Taggi, A. E.; Hafez, A. M.; Wagerle, T. R.; Shah, M. H.; Dusich, C. L.; Lectka, T. *J. Am. Chem. Soc.* **2004**, *126*, 4245–4255. (c) Lee, E. C.; MaCauley, K. M.; Fu, G. C. *Angew. Chem. Int. Ed.* **2007**, *46*, 977–979. (d) Douglas, J.; Ling, K. B.; Concellón, C.; Churchill, G.; Slawin, A. M.; Smith, A. D. *Eur. J. Org. Chem.* **2010**, 5863–5869. (e) Erbm J.; Alden-Danforth, E.; Kopf, N.; Scerba, M. T.; Lectka, T. *J. Org. Chem.* **2010**, *75*, 969–971. (f) Stockhammer, L.; Weinzierl, D.; Bögl, T.; Waser, M. *Org. Lett.* **2021**, *23*, 6143–6147.
- (15) (a) Suzuki, T.; Hamashima, Y.; Sodeoka, M. *Angew. Chem. Int. Ed.* **2007**, *46*, 5435–5439. (b) Hamashima, Y.; Nagi, T.; Shimizu, R.; Tsuchimoto, T.; Sodeoka, M. *Eur. J. Org. Chem.* **2011**, 3675–3678. (c) Xu, G.-Q.; Liang, H.; Fang, J.; Jia, Z.-L.; Chen, J.-Q.; Xu, P.-F. *Chem. Asian J.* **2016**, *11*, 3355–3358. (d) Grell, Y.; Xie, X.; Ivlev, S. I.; Meggers, E. *ACS Catal.* **2021**, *11*, 11396–11406.
- (16) (a) Davis, F. A.; Han, W. *Tetrahedron Lett.* **1992**, *33*, 1153–1156. (b) Davis, F. A.; Kasu, P. B. N. *Tetrahedron Lett.* **1998**, *39*, 6135–6138.
- (17) (a) Ishihara, K.; Fushimi, M. *Org. Lett.* **2006**, *8*, 1921–1924. (b) Ishihara, K.; Fushimi, M.; Akakura, M. *Acc. Chem. Res.* **2007**, *40*, 1049–1055. (c) Ishihara, K.; Fushimi, M. *J. Am. Chem. Soc.* **2008**, *130*, 7532–7533. (d) Sakakura, A.; Hori, M.; Fushimi, M.; Ishihara, K. *J. Am.*



- Chem. Soc.* **2010**, *132*, 15550–15552. (e) Sakakura, A.; Ishihara, K. *Chem. Soc. Rev.* **2011**, *40*, 163–172. (f) Hori, M.; Sakakura, A.; Ishihara, K. *J. Am. Chem. Soc.* **2014**, *136*, 13198–13201. (g) Yao, L.; Ishihara, K. *Chem. Sci.* **2019**, *10*, 2259–2263.
- (18) (a) Tan, B.; Hernández-Torres, G.; Barbas, C. F., III *Angew. Chem. Int. Ed.* **2012**, *51*, 5381–5385. (b) Li, T.-Z.; Wang, X.-B.; Sha, F.; Wu, X.-Y. *J. Org. Chem.* **2014**, *79*, 4332–4339. (c) Tokumatsu, K.; Yazaki, R.; Ohshima, T. *J. Am. Chem. Soc.* **2016**, *138*, 2664–2669. (d) Taninokichi, S.; Yazaki, R.; Ohshima, T. *Org. Lett.* **2017**, *19*, 3187–3190.
- (19) Harper, D. B.; O'Hagan, D.; Murphy, C. D., in *The Handbook of Environmental Chemistry*, vol. 3P, G. W. Gribble, Ed. (Springer, Heidelberg, Germany, 2003), pp. 141–169.
- (20) Heidelberger, C.; Chaudhuri, N. K.; Danneberg, P.; Mooren, D.; Griesbach, L.; Duschinsky, L.; Schnitzer, R. *J. Nature* **1957**, *179*, 663–666.
- (21) (a) Integrity (Proux Science, Barcelona, Spain, database analysis performed on 18 August 2006, [www.proux.com](http://www.proux.com)). (b) Bégué, J. P.; Bonnet-Delpon, D. *J. Fluorine Chem.* **2006**, *127*, 992–1012. (c) Isanbor, C.; O'Hagan, D. *J. Fluorine Chem.* **2006**, *127*, 303–319. (d) Kirk, K. L. *J. Fluorine Chem.* **2006**, *127*, 1013–1029.
- (22) (a) Wong, D. T.; Bymaster, F. P.; Engleman, E. A. *Life Sci.* **1995**, *57*, 411–441. (b) Roth, B. D., in *Progress in Medicinal Chemistry*, vol. 40, F. D. King, A. W. Oxford, Eds. (Elsevier, Amsterdam 2002), pp. 1–22. (c) Drlica, K.; Malik, M.; *Curr. Top. Med. Chem.* **2003**, *3*, 249.
- (23) Bondi, A. *J. Phys. Chem.* **1964**, *68*, 441–451.
- (24) (a) Morgenthaler, M.; Schweizer, E.; Hoffmann-Roder, A.; Benini, F.; Martin, R. E.; Jaeschke, G.; Wagner, B.; Fischer, H.; Bendels, S.; Zimmerli, D.; Schneider, J.; Diederich, F.; Kansy, M.; Müller, K. *ChemMedChem* **2007**, *2*, 1100–1115. (b) Lange's Handbook of Chemistry, 15th ed.; Dean, J. A., Ed.; McGrawHill Inc.: New York, 1999. (c) Brown, H. C.; In *Determination of Organic Structures by Physical Methods*; Braude, E. A., Nachod, F. C., Eds.; Academic Press; New York, 1955.
- (25) (a) Filler, R.; Kobayashi, Y.; Yugapolskii, L. M. *Organofluorine Compounds in Medicinal Chemistry and Biomedical Applications*; Elsevier: Amsterdam, 1993. (b) Müller, K.; Faeh,

- C.; Diederich, F. *Science* **2007**, *317*, 1881–1886. (c) Purser, S.; Moore, P. R.; Swallow, S.; Gouverneur, V. *Chem. Soc. Rev.* **2008**, *37*, 320–330. (d) Hagmann, W. K. *J. Med. Chem.* **2008**, *51*, 4359–4369. (e) Yamazaki, T.; Taguchi, T.; Ojima, I. *Fluorine in Medicinal Chemistry and Chemical Biology*; Wiley-Blackwell: Chichester, 2009. (f) Manteau, B.; Pazenok, S.; Vors, J.-P.; Leroux, F. R. *J. Fluor. Chem.* **2010**, *131*, 140–158. (g) Furuya, T.; Kamlet, A. S.; Ritter, T. *Nature* **2011**, *473*, 470–477.
- (26) Eriksson, T.; Björkman, S.; Roth, B.; Fyge, A.; Höglund, P. *Chirality* **1995**, *7*, 44–52.
- (27) Takeuchi, Y.; Shiragami, T.; Kimura, K.; Suzuki, E.; Shibata, N. *Org. Lett.* **1999**, *1*, 1571–1573.
- (28) Lee, K. L.; Ambler, C. M.; Anderson, D. R.; Boscoe, B. P.; Bree, A. G.; Brodfuehrer, J. I.; Chang, J. S.; Choi, C.; Chung, S.; Curran, K. J.; Day, J. E.; Dehnhardt, C. M.; Dower, K.; Drozda, S. E.; Frisbie, R. K.; Gavrin, L. K.; Goldberg, J. A.; Han, S.; Hegen, M.; Hepworth, D.; Hope, H. R.; Kamtekar, S.; Kilty, I. C.; Lee, A.; Lin, L. L.; Lovering, F. E.; Lowe, M. D.; Mathias, J. P.; Morgan, H. M.; Murphy, E. A.; Papaioannou, N.; Patny, A.; Pierce, B. S.; Rao, V. R.; Saiah, E.; Samardjiev, I. J.; Samas, B. M.; Shen, M. W. H.; Shin, J. H.; Soutter, H. H.; Strohbach, J. W.; Symanowicz, P. T.; Thomason, J. R.; Trzuppek, J. D. W.; Vargas, R.; Vincent, F.; Yan, J.; Zapf, C. W.; Wright, S. *J. Med. Chem.* **2017**, *60*, 5521–5542.
- (29) Mizuno, Y.; Ichikawa, A.; Tomita, K.; *Prostaglandins* **1983**, *26*, 785–795.
- (30) (a) Yang, X.; Wu, T.; Phippa, R. J.; Toste, F. D. *Chem. Rev.* **2015**, *115*, 826–870. (b) Champagne, P. A.; Desroches, J.; Hamel, J.-D.; Vandamme, M.; Paquin, J.-F. *Chem. Rev.* **2015**, *115*, 9073–9174.
- (31) Ishihara, K.; Nishimura, K.; Yamakawa, K. *Angew. Chem. Int. Ed.* **2020**, *59*, 17641–17647.
- (32) Beesley, R. M.; Ingold, C. K.; Thorpe, J. F. *J. Chem. Soc.* **1915**, *107*, 1080–1106.
- (33) (a) Corey, E. J.; Loh, T.-P. *J. Am. Chem. Soc.* **1991**, *113*, 8966–8967. (b) Corey, E. J.; Loh, T.-P.; Roper, T. D.; Azimioara, M. D.; Noe, M. C. *J. Am. Chem. Soc.* **1992**, *114*, 8290–8292. (c) Corey, E. J.; Guzman-Perez, A.; Loh, T.-P. *J. Am. Chem. Soc.* **1994**, *116*, 3611–3612.
- (34) (a) Bernardi, L.; Jørgensen, K. A. *Chem. Commun.* **2005**, 1324–1326. (b) Shibata, N.; Kohno, J.; Takai, K.; Ishimaru, T.; Nakamura, S.; Toru, T.; Kanemasa, S. *Angew. Chem. Int. Ed.* **2005**,

- 44, 4204–4207. (c) Jiang, J.-J.; Huang, J.; Wang, D.; Yuan, Z.-L.; Zhao, M.-X.; Wang, F.-J.; Shi, M. *Chirality* **2011**, *23*, 272–276. (d) Shibatomi, K.; Soga, Y.; Narayama, A.; Fujisawa, I.; Iwasa, S. *J. Am. Chem. Soc.* **2012**, *134*, 9836–9839. (e) Shibatomi, K.; Kitahara, K.; Sasaki, N.; Kawasaki, Y.; Fujisawa, I.; Iwasa, S. *Nat. Commun.* **2017**, *8*, 15600.
- (35) Liu, R. Y.; Wasa, M.; Jacobsen, E. N. *Tetrahedron Lett.* **2015**, *56*, 3428–3430.
- (36) (a) Hintermann, L.; Togni, A. *Helv. Chim. Acta.* **2000**, *83*, 2425–2435. (b) Bartoli, G.; Bosco, M.; Carlone, A.; Locatelli, M.; Melchiorre, P.; Sambri, L. *Angew. Chem. Int. Ed.* **2005**, *44*, 6219–6222. (c) Goswami, P.; Baruah, A.; Das, B. *Adv. Synth. Catal.* **2009**, *351*, 1483–1487.
- (37) (a) Bertelsen, S.; Halland, N.; Bachmann, S.; Marigo, M.; Braunton, A.; Jørgensen, K. A. *Chem. Commun.* **2005**, 4821–4823. (b) Kano, T.; Shirozu, F.; Maruoka, K. *Chem. Commun.* **2010**, *46*, 7590–7592. (c) Takeshima, A.; Shimogaki, M.; Kano, T.; Maruoka, K. *ACS Catal.* **2020**, *10*, 5959–5963.
- (38) Dogo-Isonagie, C.; Bekele, T.; France, S.; Wolfer, J.; Weatherwax, A.; Taggi, A. E.; Paull, D. H.; Dudding, T.; Lectka, T. *Eur. J. Org. Chem.* **2007**, 1091–1100.

## Chapter 2

### Enantio- and Site-selective $\alpha$ -Fluorination of *N*-Acyl-3,5-dimethylpyrazoles Catalyzed by Chiral $\pi$ -Cu(II) Catalyst

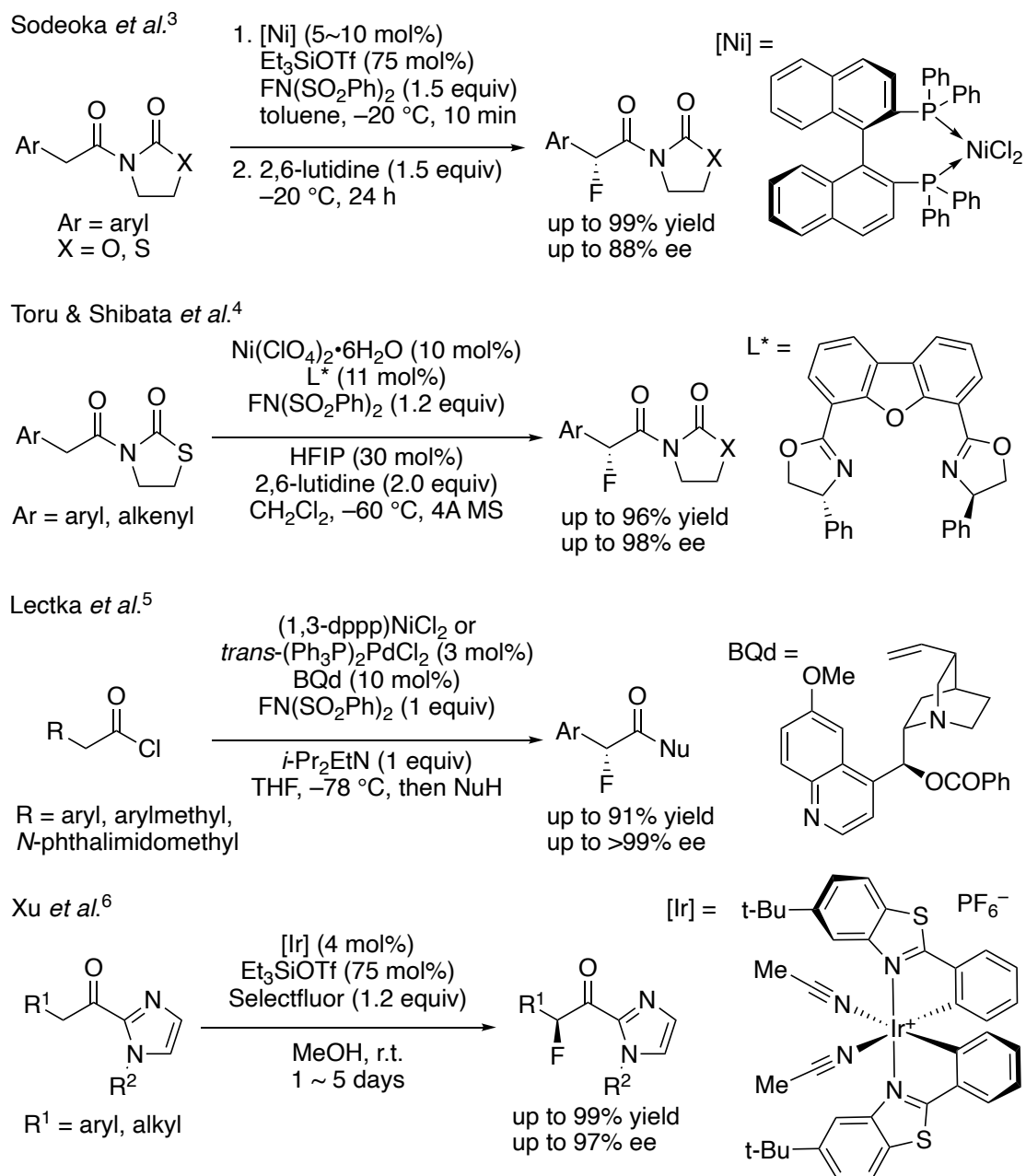
**Abstract:** Catalytic enantioselective  $\alpha$ -fluorination reactions of carbonyl compounds are among the most powerful and efficient synthetic methods for constructing optically active  $\alpha$ -fluorinated carbonyl compounds. Nevertheless,  $\alpha$ -fluorination of  $\alpha$ -nonbranched carboxylic acid derivatives is still a big challenge because of relatively high  $pK_a$  values of their  $\alpha$ -hydrogen atoms and difficulty of subsequent synthetic transformation without epimerization. Here we show that chiral Cu(II)-3-(2-naphthyl)-L-alanine-derived amide complexes are highly effective catalysts for the enantio- and site-selective  $\alpha$ -fluorination of *N*-( $\alpha$ -arylacetyl)- and *N*-( $\alpha$ -alkylacetyl)-3,5-dimethylpyrazoles. The substrate scope has been widely broadened (25 examples including quaternary  $\alpha$ -fluorinated  $\alpha$ -amino acid derivative).  $\alpha$ -Fluorinated products are converted to the corresponding esters, secondary amides, tertiary amides, ketones, and alcohols with almost no epimerization in quantitative yield.

## 2-1. Introduction

Optically active  $\alpha$ -fluorinated carbonyl compounds have received increased attention due to their widespread biological and therapeutic properties.<sup>1</sup> Enantioselective  $\alpha$ -fluorination reactions of carbonyl compounds are among the most powerful and efficient synthetic methods for constructing optically active target molecules, and great effort has been devoted to the development of their catalytic versions.<sup>8-12</sup> The carbonyl substrates for these are limited to aldehydes, ketones, 1,3-dicarbonyl compounds, and 3-substituted oxindoles that have relatively low  $pK_a$  values associated with the  $\alpha$ -hydrogen atoms.

In contrast,  $\alpha$ -fluorination of  $\alpha$ -nonbranched carboxylic acid derivatives is still a big challenge because of relatively high  $pK_a$  values of their  $\alpha$ -hydrogen atoms and difficulty of a synthetic transformation of  $\alpha$ -fluorinated products without epimerization. To the best of our knowledge, only a few successful examples of catalytic enantioselective  $\alpha$ -fluorination of carboxylic acid derivatives have been reported (Scheme 1).<sup>3-6</sup> In 2007, Sodeoka *et al.* developed the nickel(II)-catalyzed enantioselective fluorination of *N*-(arylacetyl)thioxazolidin-2-ones.<sup>3</sup> In this pioneering work, the substrates are limited to arylacetyl derivatives. In 2008 and 2009, Toru and Shibata *et al.* also reported a similar nickel(II)-catalyzed reaction.<sup>4</sup> In 2008, Lectka *et al.* reported nickel(II) or palladium(II) and chiral Lewis base cocatalyzed enantioselective  $\alpha$ -fluorination of highly reactive acid chlorides.<sup>5</sup> In 2016, Xu *et al.* reported the iridium(III)-catalyzed enantioselective  $\alpha$ -fluorination of 2-acylimidazoles.<sup>6</sup> Although the substrate scope is broadened to include aliphatic acyl derivatives, the reaction is very slow (reaction time: 1–5 days), and the removability of the imidazole moiety without epimerization has not been ascertained.<sup>6</sup> In view of these limitations, there has been a need for the development of a more efficient and practical asymmetric catalytic system. Very recently, Maulide *et al.* developed chemoselective fluorination to enolonium species generated from tertiary amides with nucleophilic fluorinating agents, but its asymmetric version has not been developed.<sup>7</sup>

**Scheme 1.** Previous Examples of Catalytic Enantioselective  $\alpha$ -Fluorination of Carboxylic Acid Derivatives



Our attention is focused on the use of  $\pi$ -Cu(II) complexes of CuX<sub>2</sub> with 3-aryl-L-alanine-derived amides as asymmetric catalysts. Since 2006, we have reported several  $\pi$ -Cu(II) complex-catalyzed enantioselective nucleophilic addition reactions to  $\alpha,\beta$ -unsaturated *N*-acylpyrazoles, which are appropriate as electrophiles because of the relatively low *pK*<sub>a</sub> values of *N*-acylpyrazoles<sup>8,9</sup> due to the electron-deficiency of the pyrazole moiety.<sup>10-16</sup> In addition, several groups have reported that *N*-acylpyrazoles are useful as amide pronucleophiles for the same reason.<sup>17-20</sup> Against this background,

here we describe the development of a highly efficient enantioselective  $\alpha$ -fluorination of *N*-acyl-3,5-dimethylpyrazoles catalyzed by chiral  $\pi$ -Cu(II) complexes.

## 2-2. Results and Discussion

Initially, to clarify the acidity of *N*-acylpyrazoles, we estimated the *pK*<sub>a</sub> value of *N*-acetyl-3,5-dimethylpyrazole (**1a**) based on its molecular electrostatic potential (MEP), because a linear relationship between MEP and *pK*<sub>a</sub> values had been established (Fig. 1).<sup>21</sup> The resonance and inductive effects from the pyrazole moiety to the *N*-acetyl moiety should be influenced by the difference in the rotational conformation of the amidyl C–N bond. Although the most stable conformer of **1a** is pseudo-*E* according to our theoretical calculation (Fig. 1A), the chelation of Cu(OTf)<sub>2</sub> to **1a** fixes the rotational conformation to pseudo-*Z* (Fig. 1B): *trans*-Cu(OTf)<sub>2</sub>•2[**1a**] is 23.18 kJ/mol more stable than *cis*-Cu(OTf)<sub>2</sub>•2[**1a**]. Thus, we realized that this chelation was highly significant for increasing the acidity of Ha: *pK*<sub>a</sub> of *cis*-Cu(OTf)<sub>2</sub>•2[**1a**] = 15.2; *pK*<sub>a</sub> of *trans*-Cu(OTf)<sub>2</sub>•2[**1a**] = 16.4 (Fig. 1C). This is one of the reasons why *N*-acetylpyrazole is more reactive than other esters and amides.

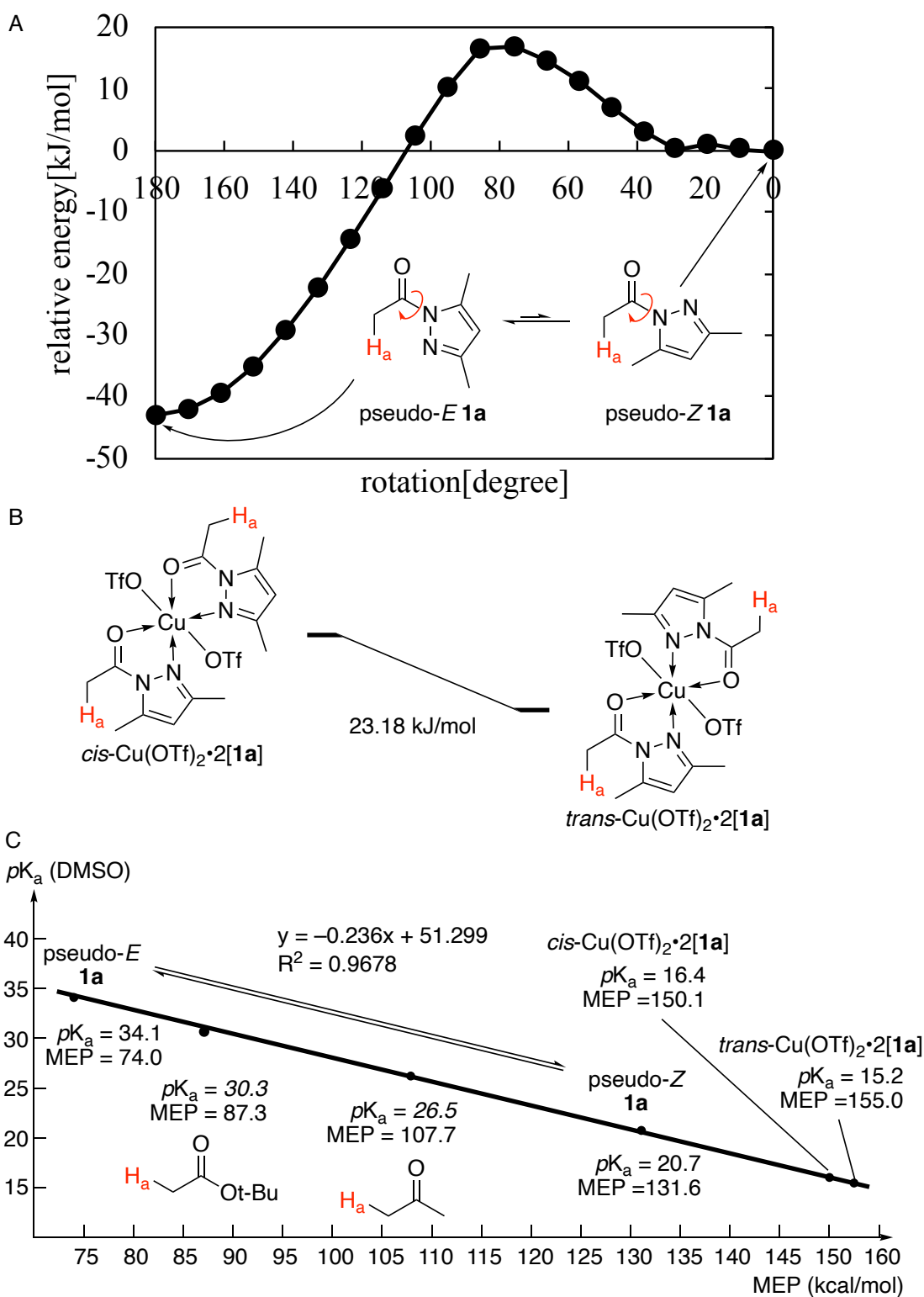


**Figure 1.** The  $pK_a$  values of **1a** and Cu(OTf)<sub>2</sub>·2[**1a**] Complexes.<sup>21</sup> (A) Relationship between relative energy and dihedral angle (N–N–C=O) of **1a**. Plotted dihedral angle (°) = 0.00, 9.47, 18.95, 28.42, 37.89, 47.37, 56.84, 66.32, 75.79, 85.26, 94.74, 104.21, 113.68, 123.16, 132.63, 142.11, 151.58, 161.05, 170.53, 180.00. (B) The thermal stability of Cu(OTf)<sub>2</sub>·2[**1a**]. (C) The linear relationship between  $pK_a$  (DMSO) and MEP values. Calculated  $pK_a$  values: plain numbers. Measured  $pK_a$



values: *Italic numbers*. The equation ( $y = -0.236x + 51.299$ ) was calculated based on the  $pK_a$  of known compounds and MEP values of these compounds calculated by us.

Next, we examined the enantioselective fluorination of **1b** in the presence of 10 mol% of  $\text{Cu}(\text{OTf})_2 \cdot 3$ -aryl-L-alanine-derived amide **L** under various conditions (Table 1). As expected, fluorinated product **2b** was obtained in 96% yield with 88% ee using Selectfluor **F1** in the presence of 10 mol% of  $\text{Cu}(\text{OTf})_2 \cdot 3$ -(2-naphthyl)-L-alanine-derived *N*-cyclopentylamide **L1**<sup>13</sup> and 2,6-lutidine in acetonitrile at  $-40\text{ }^\circ\text{C}$  for 6 h (entry 1). The addition of 1 equivalent of 2,6-lutidine was required to neutralize *in situ*-generated HX (entry 1 versus entry 2). Although  $\text{Cu}(\text{NTf}_2)_2$  was also examined in place of  $\text{Cu}(\text{OTf})_2$ , no difference was observed probably because of anion-exchange with  $\text{BF}_4^-$  of **F1** (footnote b, entry 1). Acetonitrile gave the best results as a solvent (entry 1 versus entries 3~5; entry 9 versus entries 10~12). Selectfluor analogue **F2** gave slightly higher enantioselectivity than **F1** (entry 1 versus entry 6). Although **F5** was also usable (entry 8), other fluorinating reagents **F3** and **F4** were inert (entry 7). *N*-Isopropylamide **L2** as well as **L1** were also effective as chiral ligands (entry 9). Thus, **2a** was obtained in 99% yield with 91% ee (entry 13). Surprisingly, this reaction completed within 1 h (footnote d).  $\text{Cu}(\text{OTf})_2$  and **L2** could be reduced to 1.0 mol% and 1.1 mol%, respectively, at a 20-times scale (6.0 mmol) of **1b** (entry 14). When *N*-(phenylacetyl)pyrazole (**1b'**) was used in place of **1b**, fluorinated product **2b'** was obtained in 38% yield with 81% ee because of the instability of amide bond of **1b'** and **2b'** (entry 15). When  $\alpha$ -methyl analogue **L3** was used in place of **L2**, **2b** was obtained in quantitative yield with 94% ee (entry 16). Furthermore, when 3,3-dimethyl analogue **L4** (5.5 mol%) was used, the enantioselectivity was increased to 96% ee (entry 17). Methyl substituents of **L3** and **L4** may sterically stabilize transition-state assemblies folded by  $\pi$ -Cu(II)-interaction due to the Ingold-Thorpe effect.<sup>22-25</sup>

**Table 1.** Optimization for the Enantioselective  $\alpha$ -Fluorination of **1b**<sup>a</sup>

**L1** (R<sup>1</sup> = *c*-C<sub>5</sub>H<sub>9</sub>)  
**L2** (R<sup>1</sup> = *i*-Pr)

**L3**

**L4**

**F1** (X = BF<sub>4</sub>)  
**F2** (X = PF<sub>6</sub>)

**F3**

**F4**

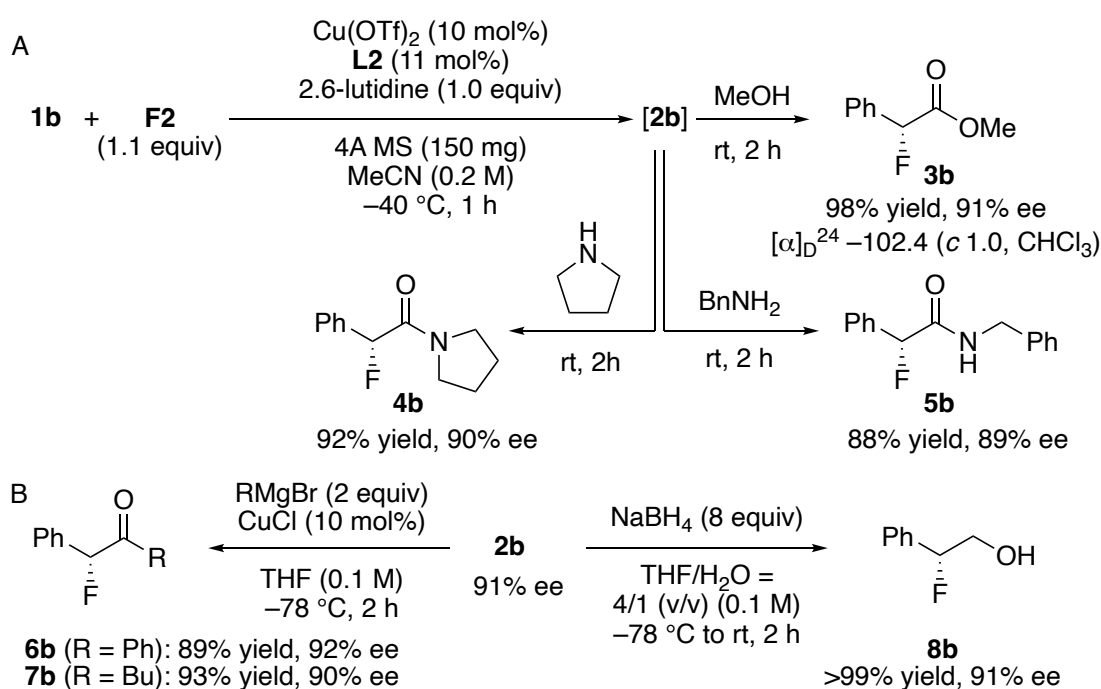
**F5**

Entry	L	F <sup>+</sup> reagent	Solvent	<b>2b</b>	
				Yield [%]	Ee [%]
1 <sup>b</sup>	L1	F1	MeCN	96	88
2 <sup>c</sup>	L1	F1	MeCN	24 <sup>d</sup>	87
3	L1	F1	EtCN	24	78
4	L1	F1	Acetone	87	85
5	L1	F1	THF	14	–
6	L1	F2	MeCN	85	90
7	L1	F3, F4	MeCN	0	–
8	L1	F5	MeCN	68	89
9	L2	F1	MeCN	91	89
10	L2	F1	PhCl <sup>e</sup>	<5 <sup>d</sup>	–
11	L2	F1	PhCl <sup>e</sup> /MeCN (1:2)	60	79
12	L2	F1	PhMe <sup>e</sup> /MeCN (1:2)	42	80
13	L2	F2	MeCN	99 (98) <sup>f</sup>	91 (89) <sup>f</sup>

14 <sup>g</sup>	<b>L2</b>	<b>F2</b>	MeCN	97	91
15 <sup>h</sup>	<b>L2</b>	<b>F2</b>	MeCN	38 <sup>i</sup>	81
16	<b>L3</b>	<b>F2</b>	MeCN	>99	94
17 <sup>j</sup>	<b>L4</b>	<b>F2</b>	MeCN	93	-96

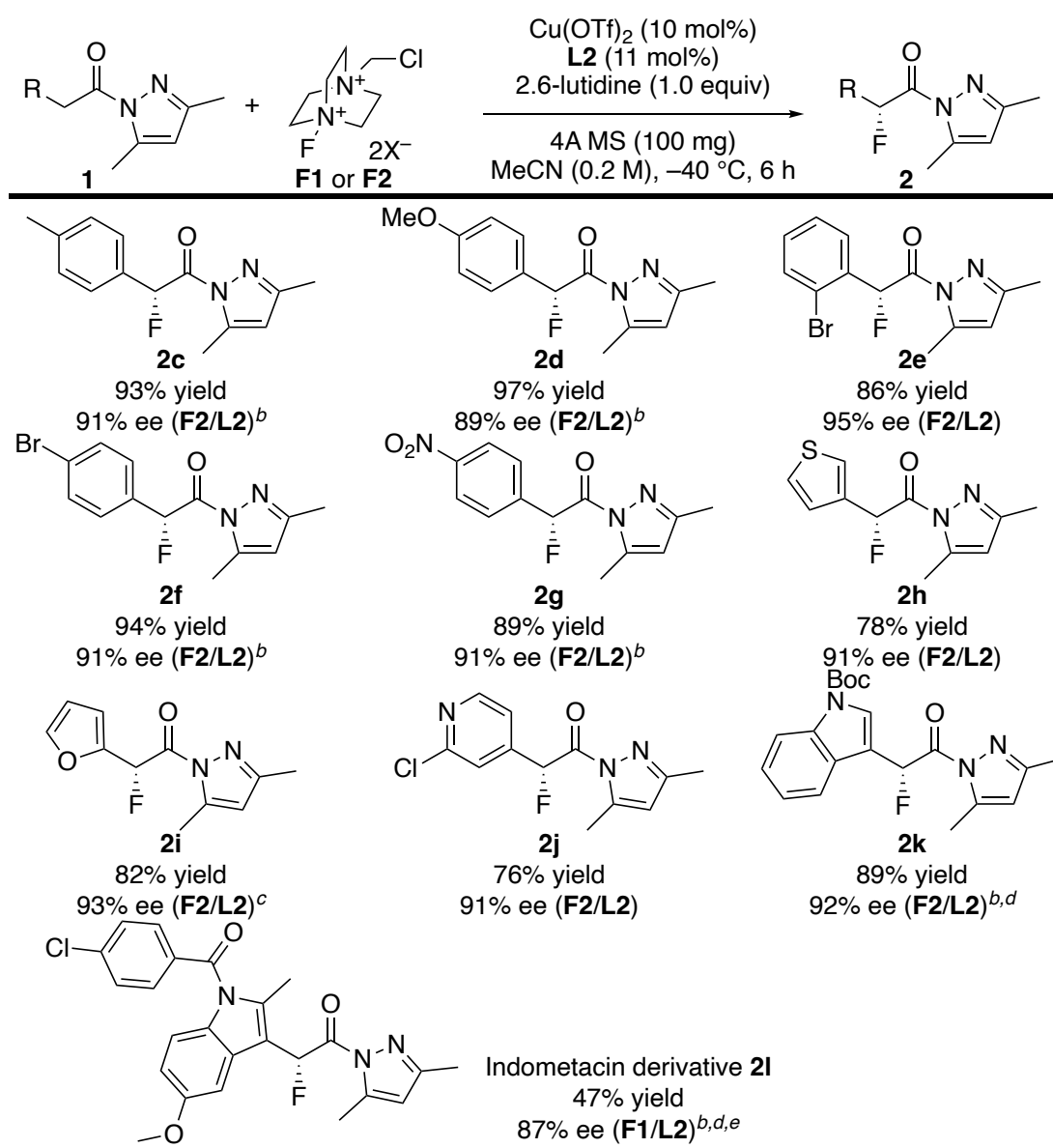
<sup>a</sup> Unless otherwise noted, **1b** (0.3 mmol), F<sup>+</sup> reagent (1.1 equiv), Cu(OTf)<sub>2</sub> (10 mol%), **L** (11 mol%), 2,6-lutidine (1.0 equiv), and 4A MS (powder, 100 mg) were added in solvent (1.5 mL). <sup>b</sup> When Cu(NTf<sub>2</sub>)<sub>2</sub> was used, the same results were obtained (96% yield, 88% ee). <sup>c</sup> Without 2,6-lutidine. <sup>d</sup> Any products except for **2b** were not observed. <sup>e</sup> **F1** did not dissolve in less polar solvents like chlorobenzene and toluene. <sup>f</sup> The results when the reaction was quenched after 1 h. <sup>g</sup> **1b** (6.0 mmol) was used in the presence of Cu(OTf)<sub>2</sub> (1.0 mol%), **L2** (1.1 mol%), and 4A MS (powder, 1.5 g). <sup>h</sup> **1b'** was used in place of **1b**. Yield and ee of **2b'** are shown. <sup>i</sup> **1b** was not recovered. <sup>j</sup> Cu(OTf)<sub>2</sub> (5 mol%) and **L4** (5.5 mol%) were used.

**Scheme 2.** Transformation of  $\alpha$ -Fluorinated Carboxamide **2b** (A) One-pot reaction from carboxamide **1b** to  $\alpha$ -fluorinated carboxylic ester **3b** and amides **4b** and **5b**. (B) Synthetic transformations from  $\alpha$ -fluorinated carboxamide **2b** to  $\alpha$ -fluoroalkanones **6b** and **7b** and  $\alpha$ -fluoroalkanol **8b**.



The absolute configuration of **2b** (entry 13, Table 1) was determined by comparison of the optical rotation with that of known methyl ester **3b**,<sup>26</sup> suggesting an *R* configuration (Scheme 2A). The transformation from **1b** to **3b** could be carried out by a one-pot procedure (Scheme 2A). In a similar manner, the corresponding tertiary amide **4b** and secondary amide **5b** were obtained with almost no epimerization.<sup>27</sup> Furthermore, transformations from **2b** to ketones **6b** and **7b** and alcohol **8b** also proceeded in good yield without epimerization (Scheme 2B).<sup>11,19,27</sup>

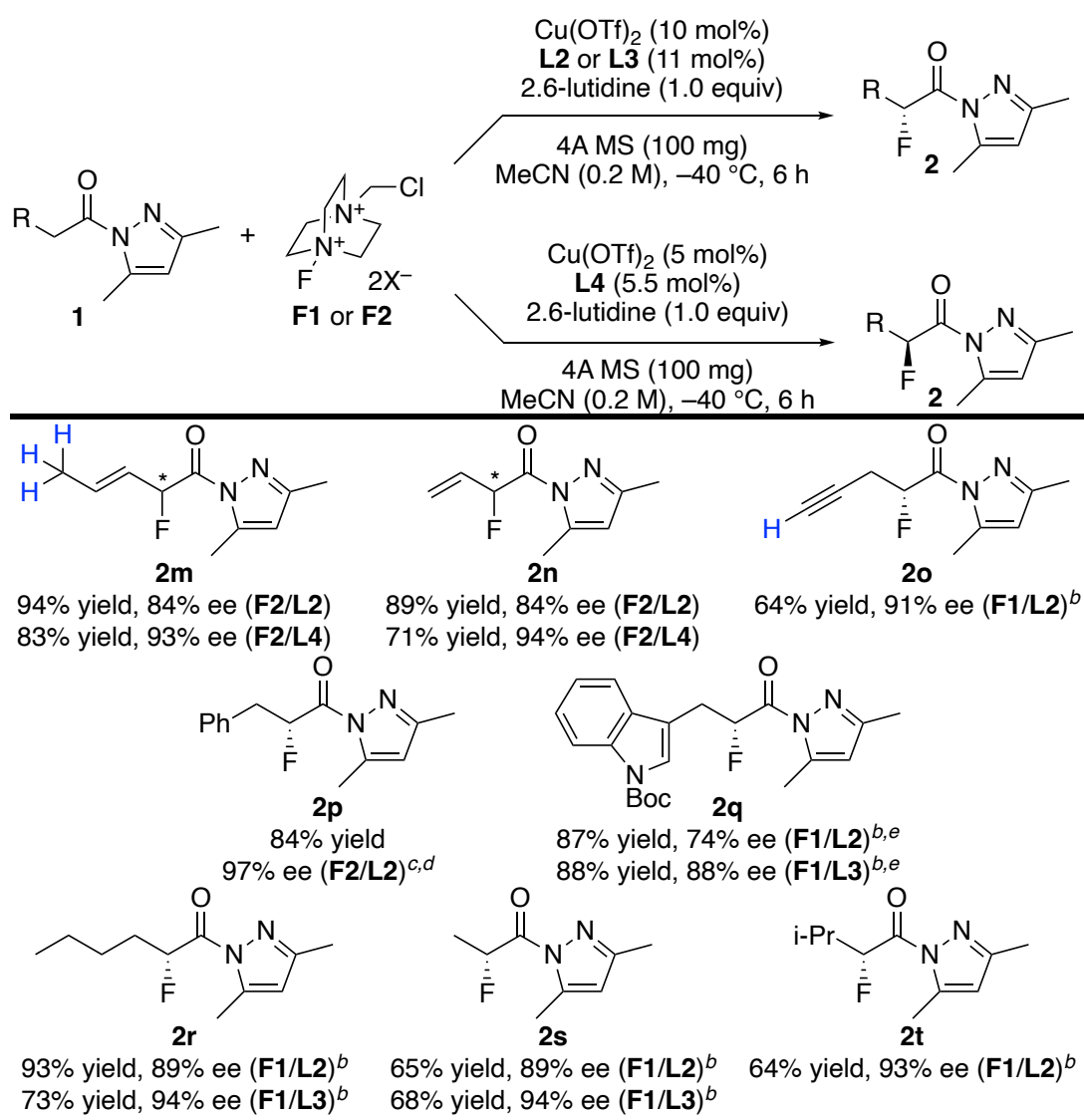
**Table 2.** The Enantioselective  $\alpha$ -Fluorination of  $\alpha$ -aryl- and  $\alpha$ -heteroarylacetamides<sup>a</sup>



<sup>a</sup> Unless otherwise noted, the reaction was carried out under the same conditions as for entry 13 in Table 1. <sup>b</sup> Solvent (0.1 M for **1**) was used. <sup>c</sup> Shortened to 1 h. <sup>d</sup> Acetone was used. <sup>e</sup> Shortened to 3 h.

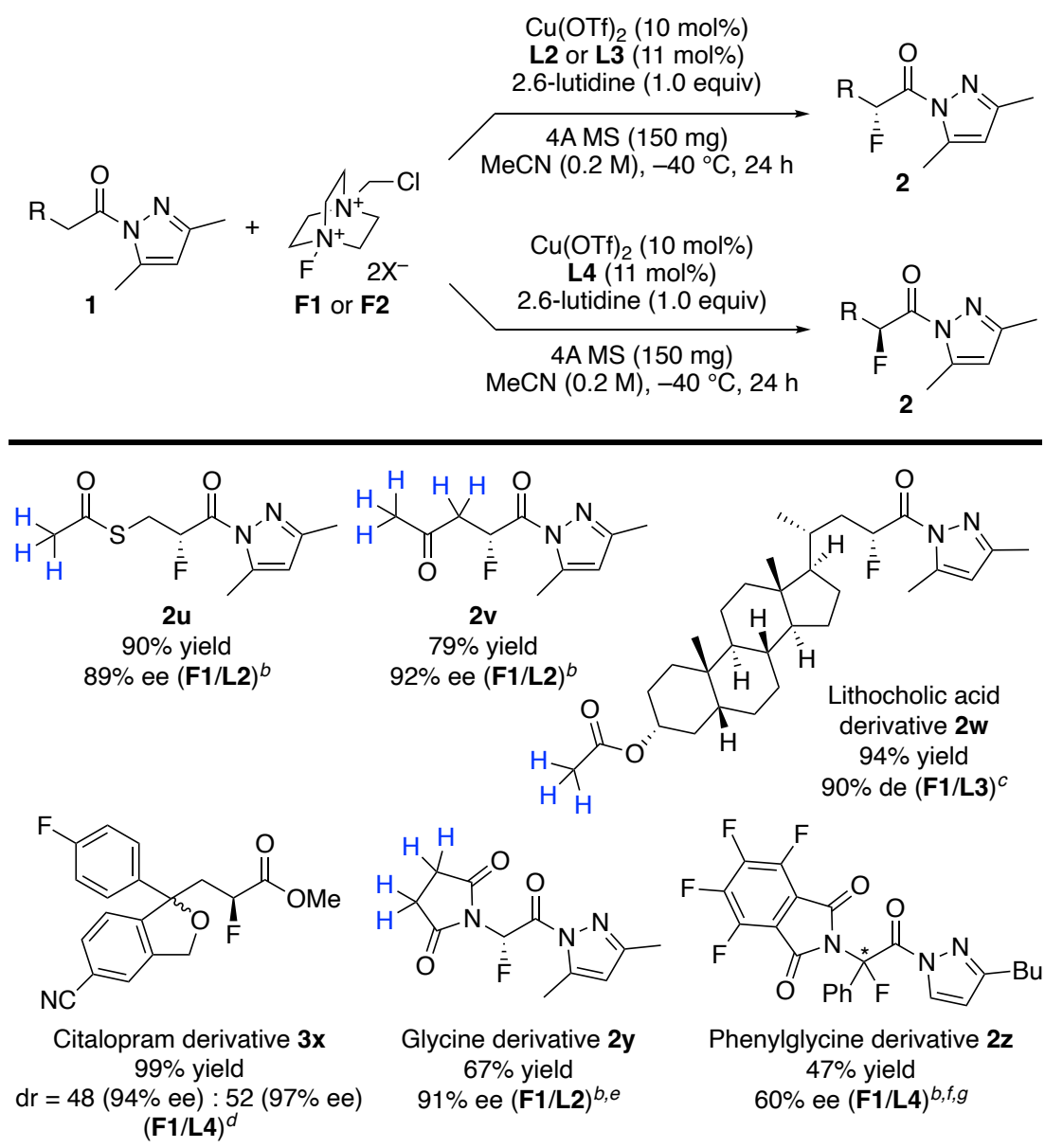
With the optimized reaction conditions in hand, we decided to explore the utility and applicability of our strategy by using differently substituted carboxamides **1** in the reaction with catalyst Cu(OTf)<sub>2</sub>•L2 (Tables 2–4). A variety of electron-withdrawing and electron-donating substituents were tolerated, independently of their position in the aromatic rings of  $\alpha$ -aryl- and  $\alpha$ -heteroarylacetamides **1c–1i** (Table 2).

**Table 3.** Site- and Enantioselective  $\alpha$ -Fluorination of  $\beta,\gamma$ - or  $\gamma,\delta$ -Unsaturated Carboxamides and Saturated Carboxamides<sup>a</sup>



<sup>a</sup> Unless otherwise noted, the reaction was carried out under the same conditions as for entry 13 in Table 1. <sup>b</sup> 150 mg of 4A MS (powder) was used. Changed to -20 °C. Extended to 24 h. <sup>c</sup> Solvent (0.1 M for **1**) was used. <sup>d</sup> Extended to 24 h. <sup>e</sup> Acetone was used.

**Table 4.** Site- and Enantioselective  $\alpha$ -Fluorination of Functionalized Carboxamides<sup>a</sup>



<sup>a</sup> Unless otherwise noted, the reaction was carried out under the same conditions as for entry 13 in Table 1. 150 mg of 4A MS (powder) was used. Extended to 24 h. <sup>b</sup> Changed to -20 °C. <sup>c</sup> Changed to -20 °C, and then elevated to 0 °C.

<sup>d</sup> **3x** was produced through one-pot procedure of enantioselective fluorination of **1x** and subsequent transesterification of **2x** (see Scheme 1A). <sup>e</sup> Solvent (0.3 M for **1**) was used. <sup>f</sup> Acetone was used. <sup>g</sup> Racemic 2-(2-(3-butyl-1*H*-pyrazol-1-yl)-2-oxo-1-phenylethyl)-4,5,6,7-tetrafluoroisindoline-1,3-dione **1z** was used in place of **1**.

Interestingly, site- and enantioselective  $\alpha$ -fluorination of  $\alpha,\beta$ -unsaturated carboxamides **1m** and **1n** proceeded in reasonable yield with good enantioselectivity, and no  $\alpha$ -fluorinated products were

observed (Table 3). The ee values of **2m** and **2n** were increased to 93 and 94 % by the use of **L4** (5 mol%). Saturated or  $\alpha,\beta$ -unsaturated carboxamides like **1o–1t** were also applicable as substrates, and highly enantioselective fluorination occurred at  $-20\text{ }^{\circ}\text{C}$  or  $-40\text{ }^{\circ}\text{C}$  in good yield (Table 3). The enantioselectivity was also increased by the use of **L3** (**1q–1s**). Lewis basic *N*-Boc, thioacetyl and acetyl substituents of **1** were tolerated (**1k** in Table 2, **1q** in Table 3, **1u** and **1v** in Table 4). The site- and enantioselective  $\alpha$ -fluorination of **1u**, **1v** and **1w** proceeded without  $\alpha$ -fluorination of their acetyl moieties (Table 4). In addition, dried molecular sieves 4A (powder) were effective for maintaining the catalytic activity, in particular, in the reaction of substrates with relatively low reactivities (**1o** and **1q–1t** in Table 3, **1u–1z** in Table 4). It is noteworthy that  $\alpha$ -fluorination of biologically important substrates such as Indometacin, Lithocholic acid, citalopram,<sup>7</sup> and glycine derivative proceeded with high enantioselectivity (**1l** in Table 2, **1w–1y** in Table 4). This method was applicable for enantioselective synthesis of quaternary  $\alpha$ -fluorinated  $\alpha$ -amino acid derivative **2z**, which is the first example of asymmetric catalysis to the best of our knowledge (Table 4).<sup>28,29</sup>

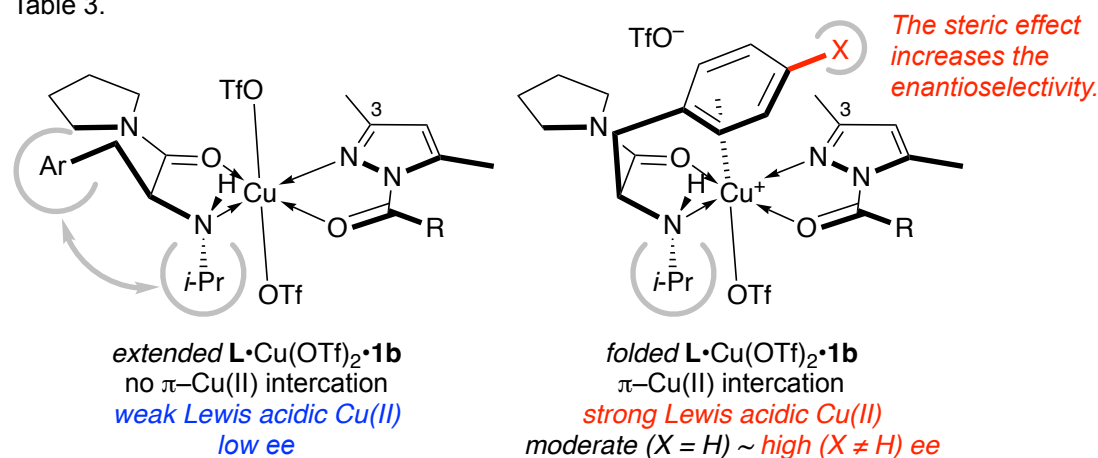
Finally, we turn our attention to mechanistic aspects. To ascertain the  $\pi$ -Cu(II) interaction of  $\text{Cu}(\text{OTf})_2\cdot\text{L2}$ , several aryl- and cyclohexyl-L-alanine amides **L5–L8** were examined for the enantioselective  $\alpha$ -fluorination of **1b** and **1p** under the same conditions using **L2** (Table 5). The use of **L6** gave **2b** in 91% yield with 55% ee while the use of **L5** gave **2b** in 43% yield with 30% ee. These results could be explained by assuming a folded cationic intermediate  $[\text{L6}\cdot\text{Cu}^+(\text{OTf})\cdot\text{1b}]^+[\text{OTf}]^-$  and an extended neutral intermediate  $[\text{L5}\cdot\text{Cu}(\text{OTf})_2\cdot\text{1b}]$ , respectively. The  $\pi$ -Cu(II) interaction between 3-phenyl moiety of **L6** and Cu(II) prefers the formation of a more active folded cationic intermediate  $[\text{L6}\cdot\text{Cu}(\text{II})^+(\text{OTf})\cdot\text{1b}]^+[\text{OTf}]^-$ , which promotes enolization and induces high enantioselectivity on  $\alpha$ -fluorination. In contrast, a nonpreferred extended complex  $[\text{L6}\cdot\text{Cu}(\text{OTf})_2\cdot\text{1b}]$  is a resting state. In a similar way, although  $\text{L2}\cdot\text{Cu}(\text{OTf})_2$  was quite effective for the enantioselective  $\alpha$ -fluorination of **1p**,  $\text{L5}\cdot\text{Cu}(\text{OTf})_2$  was almost inert. The use of  $\pi$ -electron poor **L7** decreased the reactivity (to 72% yield) but the enantioselectivity was still 65% ee. This lower reactivity could be explained by relatively weak  $\pi$ -Cu(II) interaction. The steric effect of *p*-trifluoromethyl group of **L7** might contribute to increase the enantioselectivity. In contrast, the use

of  $\pi$ -electron rich **L8** increased the reactivity (95% yield) and the enantioselectivity (69% ee). These results could be explained by stabilization of  $\pi$ -Cu(II) interaction and steric effect by *p*-methoxy group of **L8**. Ultimately, the use of **L2** increased the reactivity (91% yield) and the enantioselectivity (89% ee) by a synergistic effect of the  $\pi$ -Cu(II) interaction and steric effect of the 2-naphthyl group of **L2**.

**Table 5.** Ligand Effect of the Enantioselectivity and Reactivity

L: yield and ee of <b>2b</b> <sup>a</sup>	<b>L</b> ·Cu(OTf) <sub>2</sub> · <b>1b</b> <i>preferred conformation (extended/folded)</i>
<b>L5</b> (Ar = <i>o</i> -C <sub>6</sub> H <sub>11</sub> ): 42% yield, 30% ee <b>L6</b> (Ar = Ph): 91% yield, 55% ee <b>L7</b> (Ar = 4-CF <sub>3</sub> -C <sub>6</sub> H <sub>4</sub> ): 72% yield, 65% ee <b>L8</b> (Ar = 4-MeO-C <sub>6</sub> H <sub>4</sub> ): 95% yield, 69% ee cf. <b>L2</b> (Ar = 2-naphthyl): <sup>b</sup> 91% yield, 89% ee	extended ↑↓ folded
L: yield and ee of <b>2p</b> <sup>c</sup>	<b>L</b> ·Cu(OTf) <sub>2</sub> · <b>1p</b> <i>preferred conformation (extended/folded)</i>
<b>L5</b> (Ar = <i>o</i> -C <sub>6</sub> H <sub>11</sub> ): <5% yield, – cf. <b>L2</b> (Ar = 2-naphthyl): 84% yield, 97% ee	extended folded

<sup>a</sup> The same conditions with entry 9, Table 1. <sup>b</sup> Entry 9, Table 1. <sup>c</sup> For conditions, see: **2p** in Table 3.



The reactivity and the enantioselectivity in the  $\alpha$ -fluorination catalyzed by **L2**·Cu(OTf)<sub>2</sub> were



somewhat decreased in mixed solvents of acetonitrile and aromatic solvents like chlorobenzene and toluene (entry 9 versus entries 10~12 in Table 1). These results also suggest the existence of the  $\pi$ -Cu(II) interaction.

Furthermore, we succeeded in X-ray single-crystal diffraction analysis of the single-crystal structure of **L2**•Cu(OTf)<sub>2</sub>•**1a** as shown in Figure 2. The distance between C(33) of the 2-naphthyl moiety of **L2** and Cu(II) was 3.131 Å.<sup>30-33</sup> This result shows the  $\pi$ -cation interaction in the solid state of this complex. The pseudo-*trans* chelation of **1a** was preferred to avoid steric hindrance between the *N*-isopropyl group of **L2** and the 3-methyl group of **1a**. These results suggest that not only  $\pi$ -Cu(II) interaction but also the steric hindrance of *N*-isopropyl, pyrrolidinyl, 2-methyl, and 3-methyl groups for the 2-naphthylmethyl group of might be contributed to stabilizing its conformational folding.

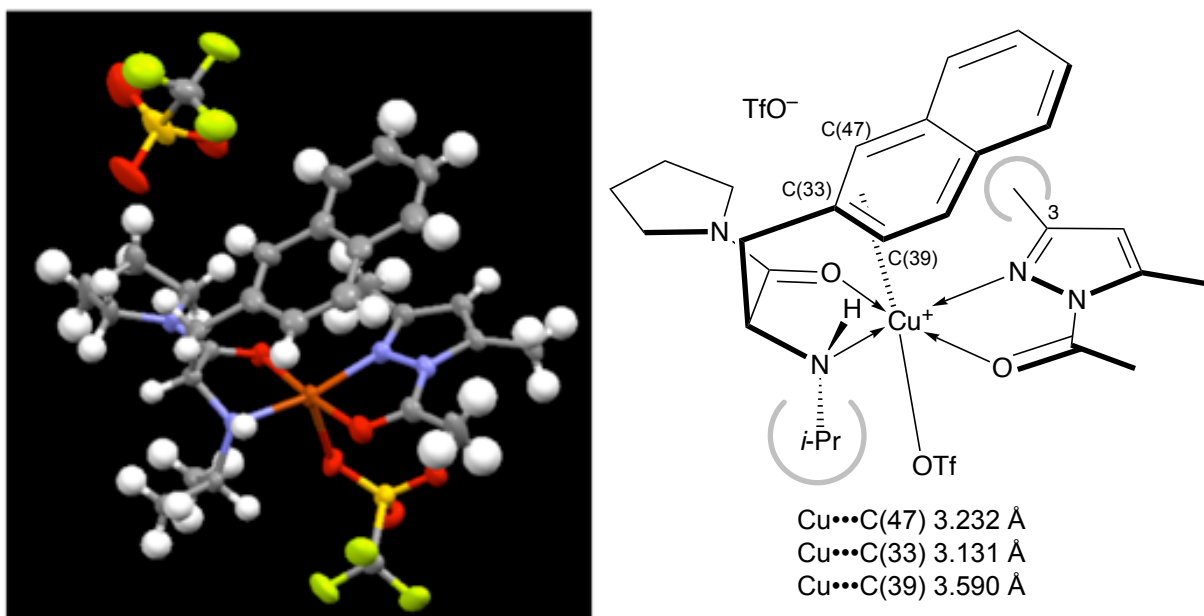


**Figure 2.** X-ray single-crystal diffraction analysis of a 1:1:1 complex of **L2**•Cu(OTf)<sub>2</sub>•**1a**.

In 2008, Takeuchi et al. reported the first UV spectral evidence for the  $\pi$ -cation interaction between the indolyl group of Tryptophan in peptides and Cu<sup>2+</sup>.<sup>30</sup> Based on Takeuchi's method,<sup>30</sup> the UV absorption difference spectrum between “a 1:1:1 complex of *N*-isopropyl-*L*-tryptophan pyrrolidine

amide **L9**•Cu(OTf)<sub>2</sub>•**1a**” and “**L9** and Cu(OTf)<sub>2</sub>•**1a**” in acetonitrile also exhibited a negative band at 226 nm and a weak positive band at 240 nm attributable to an indolyl π–Cu(II) interaction (Fig. 3). The enantioselective α-fluorination of **1b** using **L9** under the same conditions as for entry 13 in Table 1 gave **2b** with 58% ee in 70% yield. These results suggest the possibility of π–Cu(II) interaction of catalysts in an acetonitrile solution.

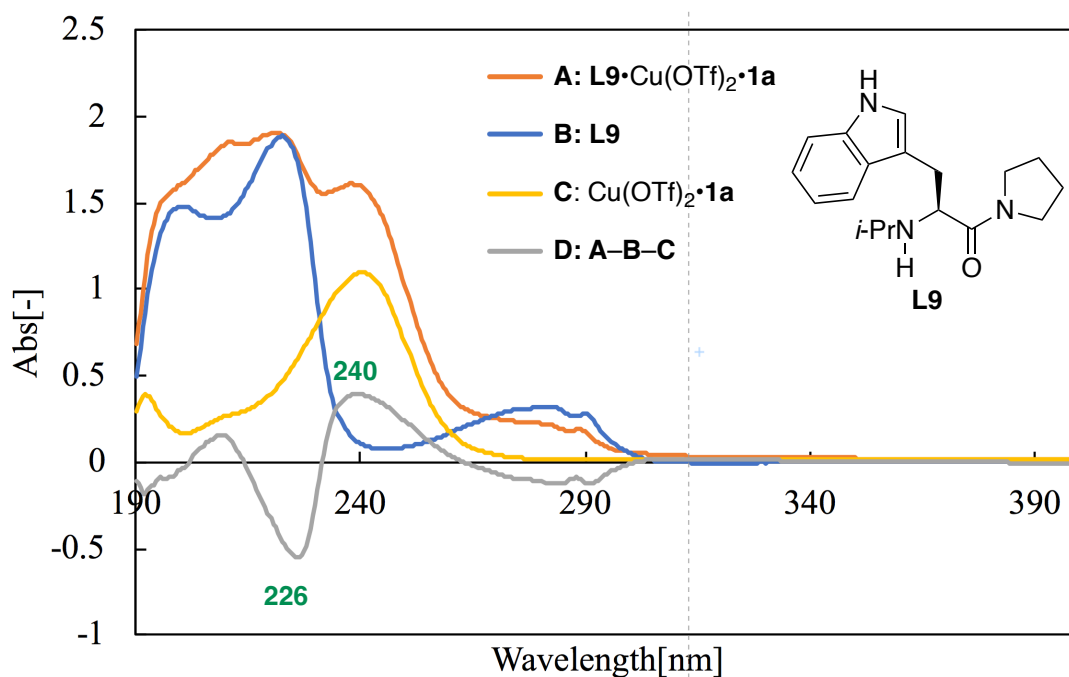


**Figure 3.** UV absorption spectra of **L9**, **1a**, and a 1:1:1 complex of **L9**•Cu(OTf)<sub>2</sub>•**1a**.

In addition, the difference of ESR spectra of **L2**•Cu(OTf)<sub>2</sub>•**1a** and **L5**•Cu(OTf)<sub>2</sub>•**1a** complexes mainly comes from the difference in the number of coordinated <sup>-</sup>OTf group (Fig. 4). When doubly coordinated <sup>-</sup>OTf groups reduced to single, distribution of unpaired electron on Cu(II) *d*-orbital should be changed with the changes of *g* tensors and hyperfine coupling constants of Cu(II).

Although there is no definite evidences of a very small electron donation from the naphthalene to Cu(II) *d*-orbital, the small donation may induce the distribution change of the unpaired electron in the Cu(II) *d*-orbital. These results may also suggest the possibility of the ligand exchange between a triflate anion and the 2-naphthyl moiety of **L2** at the apical position of **L2**•Cu(OTf)<sub>2</sub>•**1a** in a solution state.<sup>34</sup>

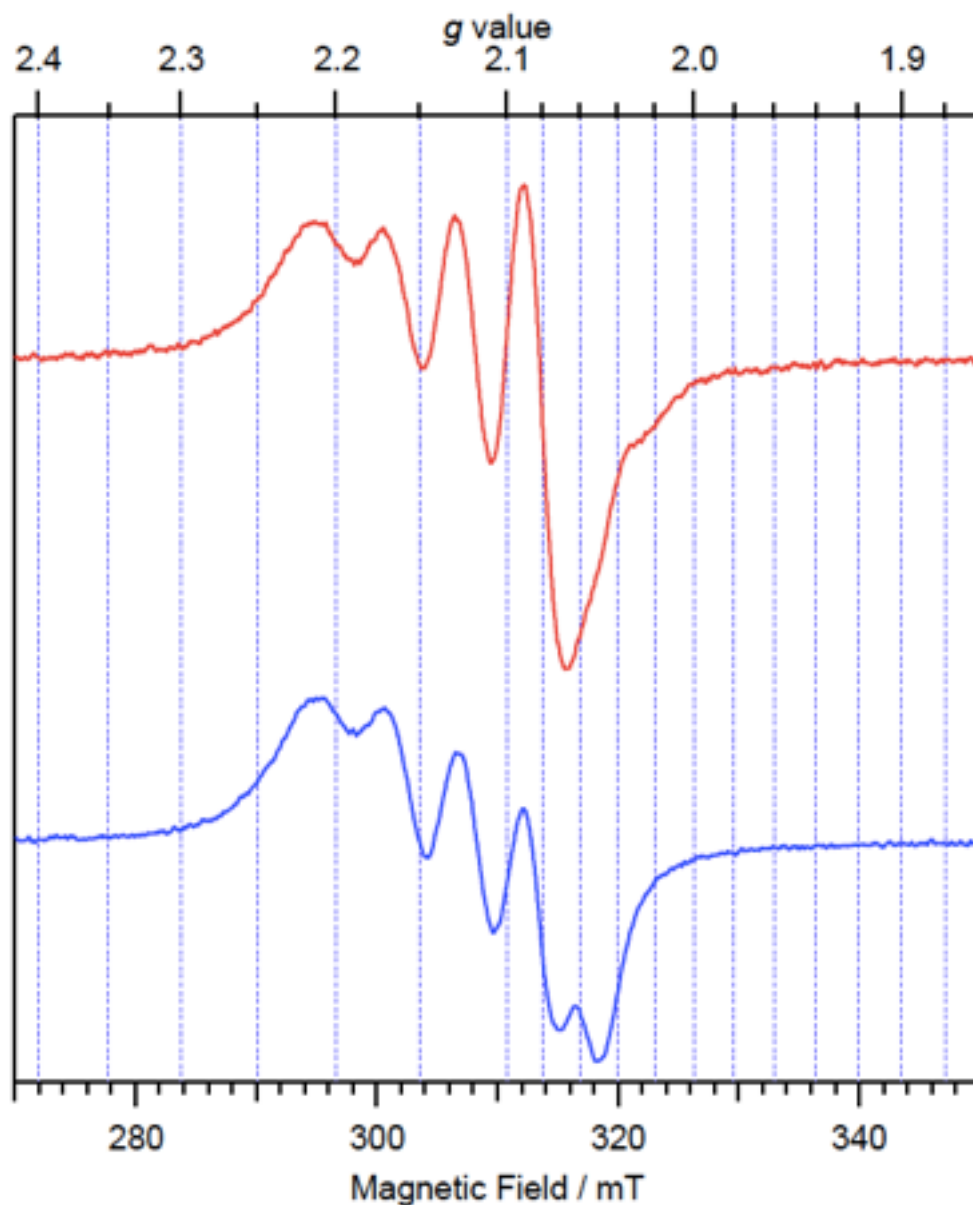
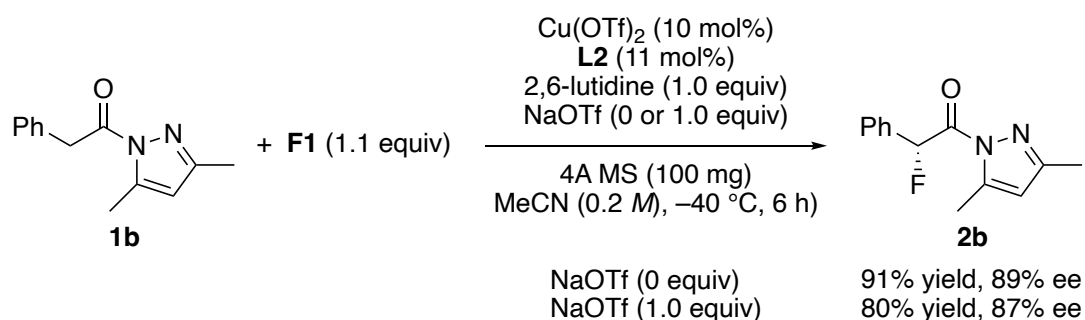


**Figure 4.** ESR spectra of **L2•Cu(OTf)<sub>2</sub>•1a** (red) and **L5•Cu(OTf)<sub>2</sub>•1a** (blue) at room temperature. The ESR sample tubes were set to an X-band ESR spectrometer (JEOL JES-RE1X). ESR parameters for the measurements at room temperature were microwave power of 1 mW, field modulation width of 0.1 mT at 100 kHz, the static magnetic field of  $310 \pm 40$  mT. Microwave frequency and magnetic field of the spectrometer were monitored using a microwave frequency counter (Hewlett-Packard, 53150A) and an NMR field meter (Echo Electronics Co. Ltd., EFM-2000AX), respectively.

The enantioselectivity was not influenced by the presence of excess NaOTf (Scheme 3). This

result suggests that the  $\pi$ -Cu(II) interaction was stable even in the presence of NaOTf. The bent conformation of **L2** might be stabilized by the  $\pi$ -Cu(II) electronic interaction and the steric effect of **L2**. The Lewis acidity of Cu(II) decreases due to strong  $\pi$ -Cu(II) electronic interaction but increases due to the release of its counter anion ( $^-$ OTf). Therefore, appropriate  $\pi$ -Cu(II) electronic interaction and the steric effect is important to appear Lewis acidity of Cu(II).

**Scheme 3.** The Influence of Sodium Triflate on the Enantioselective  $\alpha$ -Fluorination of **1b**



Based on these evidences of the  $\pi$ -Cu(II) interaction, the proposed (*Z*)-enol-type transition state assembly is shown in Figure 5. The 2-naphthalene ring of **L2** may effectively shield the *re*-face of the (*Z*)-enol form of **1b** through  $\pi$ -Cu(II) interaction. Thus,  $\text{F}^+$  reagent can approach the *si*-face of the (*Z*)-enol form of **1b** to give (*R*)-**2b**. In contrast, an (*E*)-enol-type transition state is disfavored due to the steric hindrance between the 5-methyl group and phenyl group. In this  $\alpha$ -fluorination, HX was produced together with (*R*)-**2b**, and was neutralized with 2,6-lutidine.

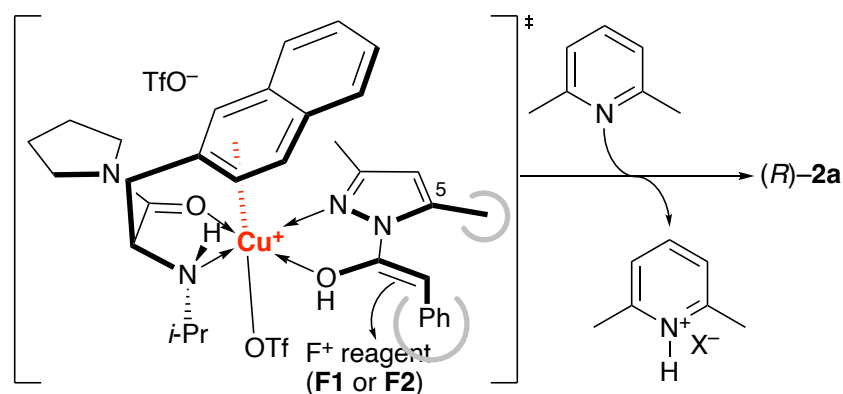


**Figure 4.** Proposed transition-state assembly.

## 2-3. Conclusion

In summary, we have developed a highly enantio-, and site-selective  $\alpha$ -fluorination of *N*-acyl-3,5-dimethylpyrazoles catalyzed by chiral  $\pi$ -Cu(II) catalysts. This new catalytic method is highly useful even compared to those described in previous reports:<sup>10-16</sup> (1) new chiral ligands **L3** and **L4** have been developed, (2) the pseudo-*Z* conformation of *N*-acylpyrazoles increases the acidity of  $\alpha$ -hydrogen atoms, (3) the substrate scope has been widely broadened, (4) the catalyst loading is reduced to 1.0~10 mol%, (5) the reaction is fast (1~24 h) and scalable (0.3~6.0 mmol), and (6)  $\alpha$ -fluorinated products are converted to the corresponding esters, secondary amides, tertiary amides, ketones, and alcohols with almost no epimerization. In addition, the  $\pi$ -Cu(II) interaction between 3-aryl-L-alanine amide and CuX<sub>2</sub> has been clarified by X-ray single-crystal analysis, the UV absorption difference spectral analysis, and ESR analysis.<sup>10-16,30-33</sup> The further application of these catalysts in other asymmetric reactions is underway.

## 2-3. References

- (1) (a) Manteau, B.; Pazenok, S.; Vors, J.-P.; Leroux, F. R. *J. Fluorine Chem.* **2010**, *131*, 140–158. (b) Furuya, T.; Kamlet, A. S.; Ritter, T. *Nature* **2011**, *473*, 470–477. (c) Gouverneur, V.; Müller, K. *Fluorine in Pharmaceutical and Medicinal Chemistry: From Biophysical Aspects to Clinical Applications*, Imperial College Press, London, **2012**. (d) Kirsch, P. *Modern Fluoroorganic Chemistry: Synthesis Reactivity, Applications*, 2nd ed., Wiley-VCH, Weinheim, **2013**.
- (2) (a) Yang, X.; Wu, T.; Phippa, R. J.; Toste, F. D. *Chem. Rev.* **2015**, *115*, 826–870. (b) Champagne, P. A.; Desroches, J.; Hamel, J.-D.; Vandamme, M.; Paquin, J.-F. *Chem. Rev.* **2015**, *115*, 9073–9174. (c) Kwiatkowski, P.; Beeson, T. D.; Conrad, J. C.; MacMillan, D. W. C. *J. Am. Chem. Soc.* **2011**, *133*, 1738–1741. (d) Beeson, T. D.; MacMillan, D. W. C. *J. Am. Chem. Soc.* **2005**, *127*, 8826–8828. (e) Marigo, M.; Fielenbach, D.; Branton, A.; Kjærsgaard, A.; Jørgensen, K. A. *Angew. Chem. Int. Ed.* **2005**, *44*, 3703–3706.
- (3) Suzuki, T.; Hamashima, Y.; Sodeoka, M. *Angew. Chem. Int. Ed.* **2007**, *46*, 5435–5439.
- (4) (a) Ishimaru, T.; Shibata, N.; Reddy, D. S.; Horikawa, T.; Nakamura, S.; Toru, T. *Beilstein J. Org. Chem.* **2008**, *4*, 1–5. (b) Reddy, D. S.; Shibata, N.; Horikawa, T.; Suzuki, S.; Nakamura, S.; Toru, T.; Shiro, M. *Chem. Asian J.* **2009**, *4*, 1411–1415.
- (5) Paull, D. H.; Scerba, M. T.; Alden-Danforth, E.; Widger, L. R.; Lectka, T. *J. Am. Chem. Soc.* **2008**, *130*, 17260–17261.
- (6) Xu, G.-Q.; Liang, H.; Fang, J.; Jia, Z.-L.; Chen, J.-Q.; Xu, P.-F. *Chem. Asian J.* **2016**, *11*, 3355–3358.
- (7) Adler, P.; Teskey, C. J.; Kaiser, D.; Holy, M.; Sitte, H. H.; Maulide, N. *Nat. Chem.* **2019**, *11*, 329–334.
- (8) Sibi, M.; Shay, J. J.; Ji, J. *Tetrahedron Lett.* **1997**, *34*, 5955–5958.
- (9) Sibi, M. P.; Itoh, K. *J. Am. Chem. Soc.* **2007**, *129*, 8064–8065.
- (10) Ishihara, K.; Fushimi, M. *Org. Lett.* **2006**, *8*, 1921–1924.
- (11) Ishihara, K.; Fushimi, M.; Akakura, M. *Acc. Chem. Res.* **2007**, *40*, 1049–1055.
- (12) Ishihara, K.; Fushimi, M. *J. Am. Chem. Soc.* **2008**, *130*, 7532–7533.

- (13) Sakakura, A.; Hori, M.; Fushimi, M.; Ishihara, K. *J. Am. Chem. Soc.* **2010**, *132*, 15550–15552.
- (14) Sakakura, A.; Ishihara, K. *Chem. Soc. Rev.* **2011**, *40*, 163–172.
- (15) Hori, M.; Sakakura, A.; Ishihara, K. *J. Am. Chem. Soc.* **2014**, *136*, 13198–13201.
- (16) Yao, L.; Ishihara, K. *Chem. Sci.* **2019**, *10*, 2259–2263.
- (17) Tan, B.; Hernández-Torres, G.; Barbas, C. F., III *Angew. Chem. Int. Ed.* **2012**, *51*, 5381–5385.
- (18) Li, T.-Z.; Wang, X.-B.; Sha, F.; Wu, X.-Y. *J. Org. Chem.* **2014**, *79*, 4332–4339.
- (19) Tokumatsu, K.; Yazaki, R.; Ohshima, T. *J. Am. Chem. Soc.* **2016**, *138*, 2664–2669.
- (20) Taninokichi, S.; Yazaki, R.; Ohshima, T. *Org. Lett.* **2017**, *19*, 3187–3190.
- (21) Theoretical calculations were performed using Spartan'16 and Spartan'18 for Macintosh from Wavefunction, Inc. The geometries of **1a** and Cu(OTf)<sub>2</sub>·2[**1a**] complexes were optimized with gradient-corrected density functional theory (DFT) calculations with B3LYP using 6–31+G\* basis set (gas) which authorizes for Cu(II), after MMFF (molecular mechanics) calculation. For 6–31+G\* basis set for atoms K through Zn, see: Rassolov, V. A.; Pople, J. A.; Ratner, M. A.; Windus, T. L. *J. Chem. Phys.* **1988**, *109*, 1223. For 6–31+G\* basis set for third-row atoms, see: Rassolov, V. A.; Ratner, M. A.; Pople, J. A.; Redfern, P. C.; Curtiss, L. A. *J. Comput. Chem.* **2001**, *22*, 976–984.
- (22) Parmee, E. R.; Tempkin, O.; Masamune, S. *J. Am. Chem. Soc.* **1991**, *113*, 9365–9366.
- (23) Corey, E. J.; Ishihara, K. *Tetrahedron Lett.* **1992**, *33*, 6807–6810.
- (24) Corey, E. J.; Loh, T.-P.; Roper, T. D.; Azimioara, M. D.; Noe, M. C. *J. Am. Chem. Soc.* **1992**, *114*, 8290–8292.
- (25) Hatano, M.; Yamashita, K.; Mizuno, M.; Ito, O.; Ishihara, K. *Angew. Chem. Int. Ed.* **2015**, *54*, 2707–2011.
- (26) Miyamoto, K.; Tsuchiya, S.; Ohta, H. *J. Fluor. Chem.* **1982**, *59*, 225–232.
- (27) Ding, X.; Tian, C.; Hu, Y.; Gong, L.; Meggers, E. *Eur. J. Org. Chem.* **2016**, 887–890.
- (28) Wei, Q.; Ma, Y.; Li, L.; Liu, Q.; Liu, Z.; Liu, G. *Org. Lett.* **2018**, *20*, 7100–7103.
- (29) Mohar, B.; Baudoux, J.; Plaquevent, J.-C. *Angew. Chem. Int. Ed.* **2001**, *40*, 4214–4216.
- (30) An analogous UV difference spectrum with a negative/positive band pair around 220/230 nm has

been observed for an indolyl model compound of the  $\pi$ -cation interaction. (a) Okada, A.; Miura, T.; Takeuchi, H. *Biochemistry* **2001**, *40*, 6053–6060. (b) Yorita, H.; Otomo, K.; Hiramatsu, H.; Toyama, A.; Miura, H.; Takeuchi, H. *J. Am. Chem. Soc.* **2008**, *130*, 15266–15267. For details of our UV spectral analysis, see Supporting Information.

(31) van der Helm, D.; Lawson, M. B.; Enwall, E. L. *Acta Crystallogr., Sect. B: Struct. Sci.* **1972**, *28*, 2307–2312.

(32) Muhonen, H.; Hämäläinen, R. *Finn. Chem. Lett.* **1983**, 120–124.

(33) Castiñeiras, A.; Sicilia-Zafra, A. G.; González-Pérez, J. M.; Choquesillo-Lazarte, D.; Niclós-Gutiérrez, J. *Inorg. Chem.* **2002**, *41*, 6956–6958.

(34) Buchanman, S. K.; Dismukes, G. C. *Biochemistry* **1987**, *26*, 5049–5055.



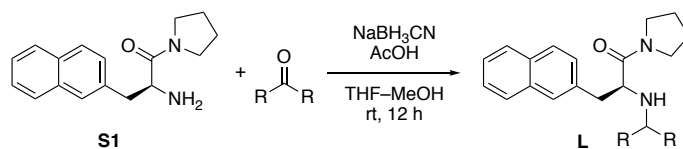
## 2-5. Experimental Section

### 2-5-1. General methods

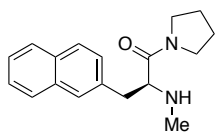
IR spectra were recorded on a JASCO FT/IR-460 plus spectrometer.  $^1\text{H}$  spectra were measured on a JEOL ECS-400 spectrometer (400 MHz) at ambient temperature. Chemical shift in ppm from internal tetramethylsilane (0.00 ppm) in  $\text{CDCl}_3$  or the solvent resonance (1.94 ppm) in acetonitrile- $d_3$  on the  $\delta$  scale, multiplicity (s = singlet; d = doublet; t = triplet; q = quartet, sep = septet, o = octet, m = multiplet, br = broad), coupling constant (Hz), integration, and assignment.  $^{13}\text{C}$  NMR spectra were measured on a JEOL ECS-400 spectrometer (100 MHz). Chemical shifts were recorded in ppm from the solvent resonance employed as the internal standard ( $\text{CDCl}_3$ : 77.16 ppm).  $^{19}\text{F}$  NMR spectra were measured on a JEOL ECS-400 spectrometer (376 MHz). Chemical shifts were recorded in ppm from the solvent resonance employed as the external standard ( $\text{CFCl}_3$  at 0 ppm). Optical rotations were measured on Rudolph Autopol IV digital polarimeter. High-performance liquid chromatography (HPLC) analysis was conducted using Shimadzu LC-10 AD coupled diode array-detector SPD-MA-10A-VP and chiral column of Daicel CHIRALCEL OD-3 (4.6 mm  $\times$  25 cm), Daicel CHIRALPAK AS-3 (4.6 mm  $\times$  25 cm), Daicel CHIRALPAK AD-3 (4.6 mm  $\times$  25 cm), Daicel CHIRALPAK OJ-H (4.6 mm  $\times$  25 cm), Daicel CHIRALPAK OB-H (4.6 mm  $\times$  25 cm), Daicel CHIRALPAK OD-H (4.6 mm  $\times$  25 cm), Daicel CHIRALPAK ID-3 (4.6 mm  $\times$  25 cm) or Daicel CHIRALPAK IC-3 (4.6 mm  $\times$  25 cm). For Thin-layer chromatography (TLC) analysis, Merck precoated TLC plates (silica gel 60 F<sub>254</sub> 0.25 mm) or silica gel 60 NH<sub>2</sub> F<sub>254S</sub> 0.20 mm) were used. Visualization was accomplished by UV light (254 nm). The products were purified by column chromatography on silica gel (E. Merck Art. 9385; Kanto Chemical Co., Inc. 37560; Fuji Silysia Chemical Ltd. Chromatorex<sup>®</sup> NH-DM1020). High resolution mass spectral analyses (HRMS) were performed at Chemical Instrument Facility, Nagoya University (Bruker Daltonics micrOTOF-QII (ESI), JEOL JMS-700 (FAB), JEOL JMS-T100GC (EI)). X-ray diffraction analysis was performed by Rigaku PILATUS-200K. Dry acetonitrile was distilled from  $\text{CaH}_2$  and dried over 4Å molecular sieves. Other materials were obtained from commercial supplies and used without further purification.

### 2-5-2. Preparation of *N*-alkyl-3-(2-naphthalenyl)-L-alanine amides **L**

#### 2-5-2-1. Method A: LS1, LS2, L1, L2, L5, L6, L7, L8, and L9

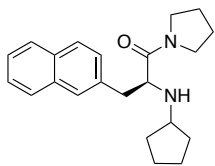


*N*-Alkyl-3-(2-naphthalenyl)-L-alanine amide **L** was prepared according to the following procedure.<sup>1,2</sup> To a solution of 3-(2-naphthalenyl)-L-alanine amide **S1**<sup>1</sup> (1.0 equiv) in a mixed solvent of MeOH and THF (v/v, 4/5, 0.06 M) were added the corresponding ketone (2.0 equiv), acetic acid (2.0 equiv) and NaBH<sub>3</sub>CN (2.0 equiv) at 0 °C. The mixture was stirred overnight at ambient temperature. The reaction was quenched with saturated aqueous NaHCO<sub>3</sub>. The reaction mixture was extracted with EtOAc, dried over Na<sub>2</sub>SO<sub>4</sub>, filtered, and concentrated *in vacuo*. Purification by column chromatography on Chromatorex<sup>®</sup> NH-DM1020 (*n*-hexane–EtOAc 10:1 to 7.5:1) afforded **L** as a colorless solid.



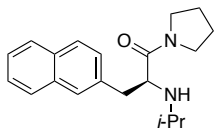
**(2S)-2-(1-Methylamino)-3-(2-naphthalenyl)-1-(1-pyrrolidinyl)-1-propanone (LS1)**<sup>2</sup> was

prepared followed by a literature procedure.<sup>2</sup>



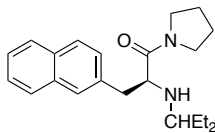
**(2S)-2-(Cyclopentylamino)-3-(2-naphthalenyl)-1-(1-pyrrolidinyl)-1-propanone (L1)**<sup>1</sup>

was prepared followed by a literature procedure.<sup>1</sup>



**(2S)-2-[(1-Methylethyl)amino]-3-(2-naphthalenyl)-1-(1-pyrrolidinyl)-1-propanone (L2)**<sup>1</sup>

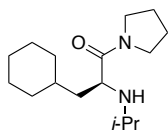
was prepared followed by a literature procedure.<sup>1</sup>



**(2S)-2-[(1-Ethylpropyl)amino]-3-(2-naphthalenyl)-1-(1-pyrrolidinyl)-1-propanone (LS2)**: 0.30 mmol scale, 41% yield as a colorless solid. TLC, *R*<sub>f</sub> = 0.18 (*n*-hexane:EtOAc = 3:1, NH silica); [α]<sup>26</sup><sub>D</sub>

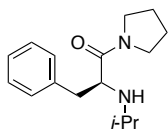
= 47.2 (*c* 1.00, CHCl<sub>3</sub>); <sup>1</sup>H NMR (400 MHz, CDCl<sub>3</sub>) δ 0.84 (t, *J* = 7.4 Hz, 3H), 0.91 (t, *J* = 7.4 Hz, 3H), 1.10–1.26 (m, 1H), 1.28–1.51 (m, 5H), 1.51–1.69 (m, 2H), 2.11 (s, 1H), 2.26–2.34 (m, 1H), 2.35–2.45 (m, 1H), 2.99 (dd, *J* = 12.8, 9.6 Hz, 1H), 3.05–3.16 (m, 2H), 3.26–3.36 (m, 1H), 3.36–3.47 (m, 1H), 3.70 (dd, *J* = 9.6, 5.5 Hz, 1H), 7.36 (dd, *J* = 8.7, 1.8 Hz, 1H), 7.38–7.48 (m, 2H), 7.66 (s, 1H), 7.70–7.82 (m, 3H); <sup>13</sup>C NMR (100 MHz, CDCl<sub>3</sub>) δ 9.6,

10.2, 24.0, 25.8 (2C), 26.7, 41.2, 45.6, 46.0, 58.0, 59.4, 125.5, 126.1, 127.6, 127.7, 127.7, 127.8, 128.0, 132.3, 133.5, 135.8, 173.3; IR (KBr) 3320, 3047, 2965, 2873, 1627, 1444  $\text{cm}^{-1}$ ; HRMS (ESI+) calcd for  $\text{C}_{22}\text{H}_{31}\text{N}_2\text{O}$   $[\text{M}+\text{H}]^+$  339.2431, found 339.2438.



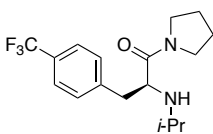
**(2S)-3-Cyclohexyl-2-[(propan-2-yl)amino]-1-(pyrrolidin-1-yl)propan-1-one (L5)** was prepared

from (2S)-3-cyclohexyl-2-amino-1-(pyrrolidin-1-yl)propan-1-one as well as **LS1**. 2.05 mmol scale, 90% yield as a colorless solid. TLC,  $R_f = 0.22$  (*n*-hexane:EtOAc = 3:1, NH silica);  $[\alpha]^{25}_{\text{D}} = -22.0$  (*c* 1.00,  $\text{CHCl}_3$ );  $^1\text{H}$  NMR (400 MHz,  $\text{CDCl}_3$ )  $\delta$  0.81–1.10 (m, 8H), 1.09–1.44 (m, 4H), 1.45–1.59 (m, 1H), 1.59–1.77 (m, 5H), 1.77–2.07 (m, 6H), 2.60 (sep,  $J = 6.0$  Hz, 1H), 3.36–3.60 (m, 5H);  $^{13}\text{C}$  NMR (100 MHz,  $\text{CDCl}_3$ )  $\delta$  22.4, 24.1, 24.2, 26.2 (2C), 26.2, 26.7, 32.8, 34.0, 34.4, 41.7, 45.8, 46.1, 46.9, 54.8, 174.9; IR (KBr) 3304, 2920, 2840, 1634, 1421, 1337  $\text{cm}^{-1}$ ; HRMS (ESI+) calcd for  $\text{C}_{16}\text{H}_{31}\text{N}_2\text{O}$   $[\text{M}+\text{H}]^+$  267.2431, found 267.2426.



**(2S)-3-phenyl-2-[(propan-2-yl)amino]-1-(pyrrolidin-1-yl)propan-1-one (L6)** was prepared from

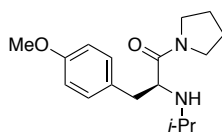
(2S)-3-phenyl-2-amino-1-(pyrrolidin-1-yl)propan-1-one as well as **LS1**.<sup>1,2</sup> 4.00 mmol scale, 63% yield as a colorless solid. TLC,  $R_f = 0.26$  (*n*-hexane:EtOAc = 3:1, NH silica);  $[\alpha]^{24}_{\text{D}} = 58.4$  (*c* 1.00,  $\text{CHCl}_3$ );  $^1\text{H}$  NMR (400 MHz,  $\text{CDCl}_3$ )  $\delta$  1.01 (d,  $J = 6.0$  Hz, 3H), 1.06 (d,  $J = 6.0$  Hz, 3H), 1.30–1.44 (m, 1H), 1.48–1.61 (m, 1H), 1.61–1.74 (m, 2H), 2.09 (brs, 1H), 2.31–2.42 (m, 1H), 2.73 (sep,  $J = 6.4$  Hz, 1H), 2.80 (dd,  $J = 12.4, 10.1$  Hz, 1H), 2.98 (dd,  $J = 12.4, 4.6$  Hz, 1H), 3.24–3.35 (m, 1H), 3.35–3.48 (m, 1H), 3.63 (dd,  $J = 10.1, 4.6$  Hz, 1H), 7.14–7.31 (m, 5H);  $^{13}\text{C}$  NMR (100 MHz,  $\text{CDCl}_3$ )  $\delta$  22.0, 23.7 (2C), 25.5, 40.7, 45.2, 45.6, 46.0, 126.3, 127.9 (2C), 129.1 (2C), 137.6, 172.7; IR (KBr) 3304, 2920, 1634, 1421, 1337, 1172  $\text{cm}^{-1}$ ; HRMS (ESI+) calcd for  $\text{C}_{16}\text{H}_{25}\text{N}_2\text{O}$   $[\text{M}+\text{H}]^+$  261.1961, found 261.1956.



**(2S)-2-[(propan-2-yl)amino]-1-(pyrrolidin-1-yl)-3-[4-(trifluoromethyl)phenyl]propan-1-**

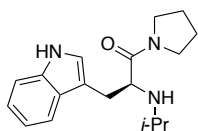
**one (L7)** was prepared from (2S)-3-[4-(trifluoromethyl)phenyl]-2-amino-1-(pyrrolidin-1-yl)propan-1-one as well as **LS1**.<sup>1,2</sup> 1.00 mmol scale, 35% yield as colorless solid. TLC,  $R_f = 0.26$  (*n*-hexane:EtOAc = 3:1, NH silica);  $[\alpha]^{24}_{\text{D}} = -40.4$  (*c* 1.00,  $\text{CHCl}_3$ );  $^1\text{H}$  NMR (400 MHz,  $\text{CDCl}_3$ )  $\delta$  1.00 (d,  $J = 6.4$  Hz, 3H), 1.06 (d,  $J = 6.0$  Hz, 3H), 1.38–1.51 (m, 1H), 1.54–1.65 (m, 1H), 1.65–1.80 (m, 2H), 2.10 (brs, 1H), 2.44–2.57 (m, 1H), 2.72 (sep,  $J = 6.4$  Hz,

1H), 2.82–2.92 (m, 1H), 2.95–3.06 (m, 1H), 3.13–3.24 (m, 1H), 3.24–3.36 (m, 1H), 3.58–3.67 (m, 1H), 7.35 (d,  $J = 7.8$  Hz, 2H), 7.52 (d,  $J = 8.3$  Hz, 2H);  $^{13}\text{C}$  NMR (100 MHz,  $\text{CDCl}_3$ )  $\delta$  22.3, 23.9, 24.0, 25.8, 40.5, 45.5, 56.0, 46.4, 58.9, 124.3 (q,  $J = 270.8$  Hz), 125.1 (d,  $J = 3.8$  Hz) (2C), 128.9 (d,  $J = 32.4$  Hz), 129.8, 142.3, 172.7;  $^{19}\text{F}$  NMR (376 MHz,  $\text{CDCl}_3$ )  $\delta$  –62.3 (s, 3F); IR (KBr) 3303, 2969, 1615, 1437, 1331, 1119  $\text{cm}^{-1}$ ; HRMS (FAB+) calcd for  $\text{C}_{17}\text{H}_{24}\text{F}_3\text{N}_2\text{O}$   $[\text{M}+\text{H}]^+$  329.1841, found 329.1846.



**(2S)-3-(4-Methoxyphenyl)-2-[(propan-2-yl)amino]-1-(pyrrolidin-1-yl)propan-1-one (L8)**

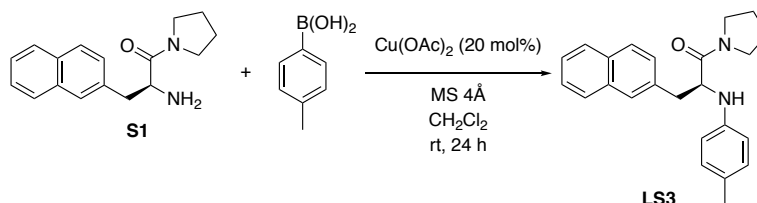
was prepared from (2S)-3-[4-(methoxy)phenyl]-2-amino-1-(pyrrolidin-1-yl)propan-1-one as well as **LS1**.<sup>1,2</sup> 1.00 mmol scale, 86% yield as a colorless solid. TLC,  $R_f = 0.26$  (*n*-hexane:EtOAc = 3:1, NH silica);  $[\alpha]_D^{23} = -50.4$  (*c* 1.00,  $\text{CHCl}_3$ );  $^1\text{H}$  NMR (400 MHz,  $\text{CDCl}_3$ )  $\delta$  1.01 (d,  $J = 6.4$  Hz, 3H), 1.06 (d,  $J = 6.0$  Hz, 3H), 1.37–1.51 (m, 1H), 1.52–1.76 (m, 3H), 2.06 (s, 1H), 2.40–2.50 (m, 1H), 2.66–2.79 (m, 2H), 2.91 (d,  $J = 12.8, 4.6$  Hz, 1H), 3.08–3.19 (m, 1H), 3.27–3.38 (m, 1H), 3.37–3.46 (m, 1H), 3.59 (dd,  $J = 10.1, 5.0$  Hz, 1H), 3.78 (s, 3H), 6.79 (d,  $J = 8.7$  Hz, 2H), 7.12 (d,  $J = 8.2$  Hz, 2H);  $^{13}\text{C}$  NMR (100 MHz,  $\text{CDCl}_3$ )  $\delta$  22.3, 24.0, 25.9, 40.1, 45.5, 45.9, 46.2, 55.4, 59.4, 113.6 (2C), 130.0, 130.3 (2C), 158.3, 173.2; IR (KBr) 2961, 1628, 1511, 1430, 1247, 1173  $\text{cm}^{-1}$ ; HRMS (FAB+) calcd for  $\text{C}_{17}\text{H}_{27}\text{N}_2\text{O}$   $[\text{M}+\text{H}]^+$  291.2073, found 291.2069.



**(2S)-3-(1H-Indol-3-yl)-2-[(propan-2-yl)amino]-1-(pyrrolidin-1-yl)propan-1-one (L9)**

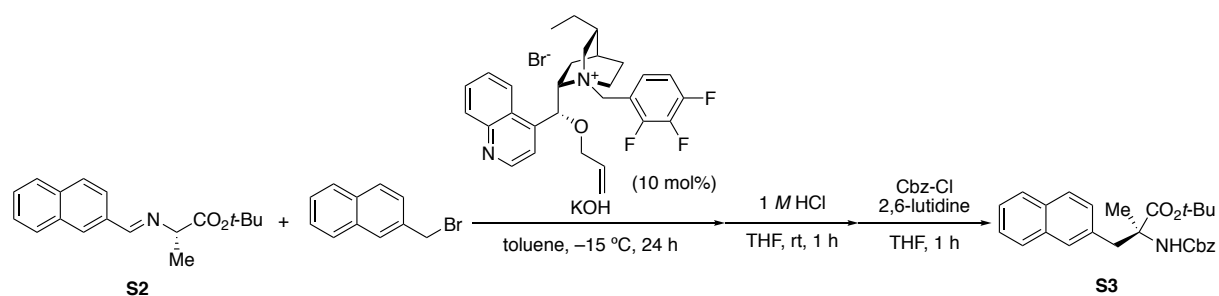
was prepared from (2S)-3-(1H-indol-3-yl)-2-amino-1-(pyrrolidin-1-yl)propan-1-one as well as **LS1**.<sup>1,2</sup> 2.89 mmol scale, 48% yield as colorless solid. TLC,  $R_f = 0.19$  (EtOAc, NH silica);  $[\alpha]_D^{23} = -54.8$  (*c* 1.00,  $\text{CHCl}_3$ );  $^1\text{H}$  NMR (400 MHz,  $\text{CDCl}_3$ )  $\delta$  1.01–1.17 (m, 7H), 1.29–1.42 (m, 1H), 1.47–1.70 (m, 2H), 2.13 (brs, 1H), 2.31–2.42 (m, 1H), 2.75 (sep,  $J = 6.4$  Hz, 1H), 3.01 (dd,  $J = 13.8, 10.1$  Hz, 1H), 3.06–3.09 (m, 1H), 3.15 (dd,  $J = 14.2, 4.6$  Hz, 1H), 3.18–3.28 (m, 1H), 3.31–3.41 (m, 1H), 3.74 (dd,  $J = 10.1, 4.6$  Hz, 1H), 7.05 (d,  $J = 2.3$  Hz, 1H), 7.10 (dt,  $J = 7.8, 0.9$  Hz, 1H), 7.17 (dt,  $J = 7.8, 0.9$  Hz, 1H), 7.34 (d,  $J = 7.8$  Hz, 1H), 7.62 (d,  $J = 7.8$  Hz, 1H), 8.07 (s, 1H);  $^{13}\text{C}$  NMR (100 MHz,  $\text{CDCl}_3$ )  $\delta$  22.3, 23.9, 24.0, 25.7, 30.3, 45.7, 46.0, 46.4, 58.6, 111.2, 111.9, 118.8, 119.3, 121.9, 122.9, 127.6, 136.2, 173.9; IR (KBr) 3305, 2975, 1949, 1628, 1441  $\text{cm}^{-1}$ ; HRMS (ESI+) calcd for  $\text{C}_{18}\text{H}_{26}\text{N}_3\text{O}$   $[\text{M}+\text{H}]^+$  300.2070, found 300.2079.

### 2-5-2-2. Method B: Preparation of (2S)-2-[(p-tolyl)amino]-3-(2-naphthalenyl)-1-(1-pyrrolidinyl)-1-propanone (LS3)



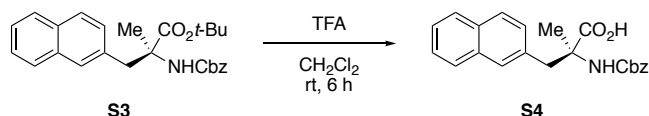
On the basis of a literature procedure,<sup>3</sup> a suspension of *p*-tolylboronic acid (136 mg, 1.00 mmol), Cu(OAc)<sub>2</sub> (18.2 mg, 0.10 mmol), and powdered 4 Å molecular sieves (400 mg) in CH<sub>2</sub>Cl<sub>2</sub> (4 mL) was stirred for 5 minutes at room temperature. To this stirring suspension was added **S1** (134 mg, 0.50 mmol). The reaction mixture was then sealed with a rubber septum, and stirred under an atmosphere of O<sub>2</sub>. Following a period of 24 h, the crude reaction mixture was filtered through a plug of celite to remove the molecular sieves and any insoluble byproducts and then concentrated *in vacuo* to afford the crude product mixture. The product was isolated by silica gel column chromatography on Chromatorex<sup>®</sup> NH-DM1020 (*n*-hexane–EtOAc 10:1 to 7.5:1) (eluting with *n*-hexane:EtOAc 9:1 to 3:1 gradient) to afford **LS3** (62.3 mg, 26% yield) as a colorless solid. TLC, *R<sub>f</sub>* = 0.15 (*n*-hexane:EtOAc = 3:1, NH silica); [α]<sub>D</sub><sup>26</sup> = −33.2 (*c* 1.00, CHCl<sub>3</sub>); <sup>1</sup>H NMR (400 MHz, CDCl<sub>3</sub>) δ 1.22–1.34 (m, 1H), 1.43–1.72 (m, 3H), 2.24 (s, 3H), 2.45–2.55 (m, 1H), 3.12 (dd, *J* = 12.8, 8.7 Hz, 1H), 3.18–3.32 (m, 2H), 3.32–3.50 (m, 2H), 4.42 (br, 2H), 6.60 (d, *J* = 8.3 Hz, 2H), 7.00 (d, *J* = 7.8 Hz, 2H), 7.38 (dd, *J* = 8.2, 1.8 Hz, 1H), 7.41–7.50 (m, 2H), 7.67 (s, 1H), 7.73–7.85 (m, 3H); <sup>13</sup>C NMR (100 MHz, CDCl<sub>3</sub>) δ 20.6, 24.0, 25.8, 39.8, 45.9, 46.3, 57.7, 114.2 (2C), 125.7, 126.3, 127.5, 127.6, 127.8, 127.8 (2C), 128.1, 130.0 (2C), 132.4, 133.6, 135.0, 144.4, 171.0; IR (KBr) 3403, 3328, 3049, 2969, 2921, 2865, 1634, 1523, 1448, 1309, 1280, 1137 cm<sup>−1</sup>; HRMS (ESI<sup>+</sup>) calcd for C<sub>24</sub>H<sub>27</sub>N<sub>2</sub>O [M+H]<sup>+</sup> 359.2118, found 359.2121.

### 2-5-3. Preparation of (2S)-2-methyl-3-(naphthalen-2-yl)-2-[(propan-2-yl)amino]-1-(pyrrolidin-1-yl)propan-1-one (L3)



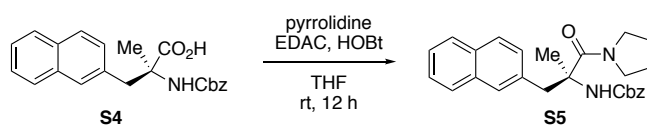
On the basis of a literature procedure,<sup>4</sup> to a cooled ( $-15\text{ }^{\circ}\text{C}$ ) mixture of *tert*-butyl (2*S*)-2-[(*E*)-[(naphthalen-2-yl)methylidene]amino]propanoate<sup>5</sup> **S2** (283 mg, 1.00 mmol), (5*R*)-5-ethyl-2-[(*R*)-(prop-2-en-1-yloxy)(quinolin-4-yl)methyl]-1-[(2,3,4-trifluorophenyl)methyl]-1-azabicyclo[2.2.2]octan-1-ium bromide<sup>6</sup> (56.1 mg, 0.10 mmol), and powdered potassium hydroxide (280.6 mg, 5.0 mmol) in toluene (4.0 mL) was added 2-(bromomethyl)naphthalene (1.1 g, 5.0 mmol). The reaction mixture was stirred vigorously at  $-15\text{ }^{\circ}\text{C}$  for 24 h. Then, water (5 mL) was added and the extraction was performed with dichloromethane (3 x 10 mL). The solvent was removed under reduced pressure, and the residue was dissolved in tetrahydrofuran (6.0 mL). Aqueous hydrochloric acid (1 *M*, 6.0 mL) was added, and the mixture washed with *n*-hexane (2 x 10 mL), and then the aqueous phase was basified with solid sodium bicarbonate and extracted with dichloromethane (3 x 10 mL). The dichloromethane extracts were dried ( $\text{MgSO}_4$ ) and concentrated under reduced pressure. Purification of the residue by column chromatography on silica gel (*n*-hexane: EtOAc = 1:2) gave amine as a colorless oil. The amine was dissolved in tetrahydrofuran (4.0 mL), and then, 2,6-lutidine (265  $\mu\text{L}$ , 2.28 mmol) and benzyl chloroformate (260  $\mu\text{L}$ , 1.85 mmol) were added successively. The reaction mixture was stirred at room temperature for 1 h. The resulting mixture was extracted with dichloromethane (3 x 10 mL), and the extracts were washed with water. The dichloromethane solution was then dried ( $\text{MgSO}_4$ ) and concentrated under reduced pressure. Purification of the residue by flash column chromatography on silica gel (*n*-hexane: EtOAc = 20:1) afforded the desired product **S3** (268 mg, 64% yield, 64% ee) as a colorless solid. Compound **S3** was recrystallized from EtOAc/*n*-hexane at room temperature (99% ee). TLC,  $R_f = 0.28$  (*n*-hexane:EtOAc = 20:1);  $[\alpha]_D^{25} = 60.8$  ( $c$  1.00,  $\text{CHCl}_3$ );  $^1\text{H NMR}$  (400 MHz,  $\text{CDCl}_3$ )  $\delta$  1.46 (s, 9H), 1.67 (s, 3H), 3.31 (d,  $J = 13.3$  Hz, 1H), 3.62 (d,  $J = 13.3$  Hz, 1H), 5.08 (d,  $J = 12.4$  Hz, 1H), 5.26 (d,  $J = 12.4$  Hz, 1H), 5.57 (s, 1H), 7.17 (dd,  $J = 8.7, 1.4$  Hz, 1H), 7.28–7.47 (m, 7H), 7.52 (s, 1H), 7.60–7.69 (m, 2H), 7.78 (dt,  $J = 9.2, 3.2$  Hz, 1H);  $^{13}\text{C NMR}$  (100 MHz,  $\text{CDCl}_3$ )  $\delta$  24.2, 28.0 (3C), 41.3, 61.1, 66.2, 82.6, 125.6, 126.0, 127.7 (3C), 128.2, 128.3 (2C), 128.5, 128.7 (2C), 128.9, 132.5, 133.3, 134.3, 137.0, 154.7, 172.6; IR (KBr) 3355, 2973,

1712, 1525, 1285, 1122, 1059  $\text{cm}^{-1}$ ; HRMS (ESI+) calcd for  $\text{C}_{26}\text{H}_{30}\text{NO}_4$   $[\text{M}+\text{H}]^+$  420.2169, found 420.2167; HPLC analysis; AD-3, *n*-hexane/*i*-PrOH = 50/1, 1.0 mL/min,  $t_{\text{R}} = 19.9$  min (minor),  $t_{\text{R}} = 22.8$  min (major).



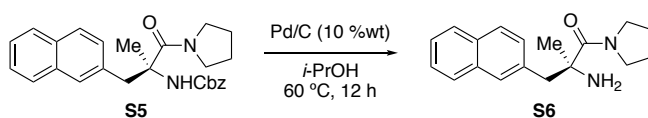
To a solution of **S3** (207 mg, 0.49 mmol, >99% ee) in dichloromethane (2.5 mL) was added trifluoroacetic acid (2.5 mL) at room temperature. The mixture was stirred at ambient temperature for 6 h. The reaction mixture was concentrated *in vacuo*. Purification of the residue by short flash column chromatography on silica gel ( $\text{CHCl}_3$ : MeOH = 20:1) afforded the desired product **S4** (178 mg, 100% yield) as a colorless solid. Purified product **S4** was washed with 1 M HCl (5 mL), extracted with dichloromethane ( $3 \times 10$  mL), dried over  $\text{Na}_2\text{SO}_4$ , filtered, and concentrated *in vacuo*.

**(2S)-2-[[ (Benzyloxy)carbonyl]amino]-2-methyl-3-(naphthalen-2-yl)propanoic acid (S4)**: TLC,  $R_f = 0.33$  ( $\text{CHCl}_3$ : MeOH = 30:1);  $[\alpha]_{\text{D}}^{28} = 110.7$  ( $c$  0.13,  $\text{CHCl}_3$ );  $^1\text{H}$  NMR (400 MHz,  $\text{CDCl}_3$ )  $\delta$  1.67 (s, 3H), 3.45 (d,  $J = 13.7$  Hz, 1H), 3.54 (d,  $J = 13.3$  Hz, 1H), 5.13 (d,  $J = 12.4$  Hz, 1H), 5.20 (d,  $J = 11.9$  Hz, 1H), 5.37 (s, 1H), 7.16 (d,  $J = 8.1$  Hz, 1H), 7.28–7.47 (m, 7H), 7.52 (s, 1H), 7.58–7.69 (m, 2H), 7.73–7.82 (m, 1H), 9.20–10.90 (brs, 1H);  $^{13}\text{C}$  NMR (100 MHz,  $\text{CDCl}_3$ )  $\delta$  23.8, 41.5, 60.6, 66.8, 125.9, 126.1, 127.7, 127.9, 128.0, 128.3, 128.4 (3C), 128.7 (3C), 129.1, 132.5, 133.4, 136.5, 155.1, 179.1; IR (KBr) 3409, 3324, 3057, 2940, 1716, 1508, 1456, 1284, 1230, 1061  $\text{cm}^{-1}$ ; HRMS (ESI+) calcd for  $\text{C}_{22}\text{H}_{22}\text{NO}_4$   $[\text{M}+\text{H}]^+$  364.1543, found 364.1540.



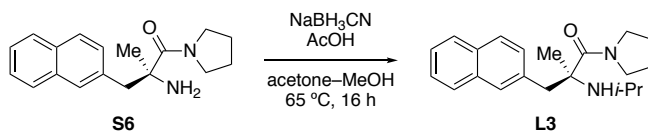
To a solution of **S4** in THF (6.0 mL) were added 1-hydroxybenzotriazole (HOBT, 329 mg, 2.15 mmol), pyrrolidine (330  $\mu\text{L}$ , 3.97 mmol) and *N*-(3-dimethylaminopropyl)-*N'*-ethylcarbodiimide hydrochloride (EDAC, 385 mg, 1.99 mmol) at ambient temperature. The mixture was stirred at ambient temperature for 12 h. The reaction was quenched by the addition of 1 M HCl (2 mL). The reaction mixture was extracted with EtOAc ( $3 \times 10$  mL), dried over  $\text{Na}_2\text{SO}_4$ , filtered, and concentrated *in vacuo*. Purification of the residue by flash column chromatography on silica gel (*n*-hexane:EtOAc = 1:1) afforded the desired product **S5** (458.9 mg, 66% yield) as a colorless solid.

**Benzyl *N*-[(2*S*)-2-methyl-3-(naphthalen-2-yl)-1-oxo-1-(pyrrolidin-1-yl)propan-2-yl]carbamate (S5):** TLC,  $R_f$  = 0.17 (*n*-hexane:EtOAc = 1:1);  $[\alpha]_D^{25} = -59.2$  ( $c$  1.00, CHCl<sub>3</sub>); <sup>1</sup>H NMR (400 MHz, MeCN-*d*<sub>3</sub>)  $\delta$  1.27 (s, 3H), 1.60–1.88 (m, 4H), 3.20–3.63 (m, 6H), 5.09 (d,  $J$  = 12.4 Hz, 1H), 5.14 (d,  $J$  = 12.4 Hz, 1H), 5.89 (s, 1H), 7.17 (d,  $J$  = 8.2 Hz, 1H), 7.31–7.49 (m, 7H), 7.52 (s, 1H), 7.66–7.79 (m, 2H), 7.80–7.88 (m, 1H); <sup>13</sup>C NMR (100 MHz, CDCl<sub>3</sub>)  $\delta$  22.4, 22.9, 27.2, 41.1, 47.3, 48.4, 60.1, 66.4, 125.6, 125.9, 127.5 (2C), 127.6 (2C), 128.2, 128.5 (3C), 128.7, 129.1, 132.3, 134.3, 136.7, 154.4, 170.8; IR (KBr) 3247, 3033, 2966, 2879, 1714, 1602, 1539, 1427, 1266, 1104, 1058 cm<sup>-1</sup>; HRMS (ESI+) calcd for C<sub>26</sub>H<sub>29</sub>N<sub>2</sub>O<sub>3</sub> [M+H]<sup>+</sup> 417.2173, found 417.2173.



To a solution of **S5** (459 mg, 1.10 mmol) in *i*-PrOH (14 mL) was added 10% Pd/C (46.0 mg), and the mixture was stirred at 60 °C for 12 h under H<sub>2</sub> atmosphere. The reaction mixture was filtrated through Celite<sup>®</sup> and the filtrate was concentrated under reduced pressure. Purification of the residue by flash column chromatography on Chromatorex<sup>®</sup> NH-DM1020 (CHCl<sub>3</sub>) afforded the desired product **S6** (286 mg, 92% yield) as a yellow oil.

**(2*S*)-2-Amino-2-methyl-3-(naphthalen-2-yl)-1-(pyrrolidin-1-yl)propan-1-one (S6):** TLC,  $R_f$  = 0.60 (CHCl<sub>3</sub>, broad, NH silica);  $[\alpha]_D^{23} = -22.4$  ( $c$  1.00, CHCl<sub>3</sub>); <sup>1</sup>H NMR (400 MHz, CDCl<sub>3</sub>)  $\delta$  1.47 (s, 3H), 1.65–1.82 (m, 4H), 3.00 (d,  $J$  = 13.3 Hz, 1H), 3.15 (d,  $J$  = 13.3 Hz, 1H), 3.37–3.62 (broad, 4H), 7.30 (dd,  $J$  = 8.3, 1.8 Hz, 1H), 7.41–7.49 (m, 2H), 7.64 (s, 1H), 7.73–7.83 (m, 3H); <sup>13</sup>C NMR (100 MHz, CDCl<sub>3</sub>)  $\delta$  23.0, 26.5, 27.1, 47.4, 48.1, 48.4, 59.4, 125.5, 125.9, 127.5, 127.5 (2C), 128.6, 128.8, 132.2, 133.2, 134.6, 174.4; IR (neat) 2967, 2926, 1541, 1027, 797 cm<sup>-1</sup>; HRMS (ESI+) calcd for C<sub>18</sub>H<sub>23</sub>N<sub>2</sub>O [M+H]<sup>+</sup> 283.1805, found 283.1806.

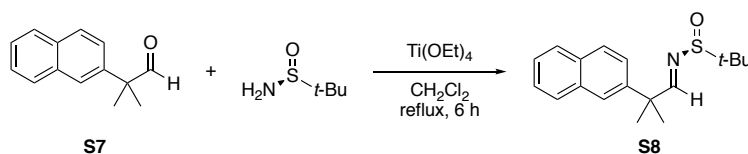


To a solution of **S6** (286 mg, 1.01 mmol) in a mixture of acetone (4.0 mL) and MeOH (5.0 mL) were added acetic acid (280  $\mu$ L, 5.07 mmol) and NaBH<sub>3</sub>CN (635 mg, 10.1 mmol) at room temperature. The mixture was stirred at 65 °C for 16 h. The reaction was cooled to room temperature and quenched with saturated aqueous NaHCO<sub>3</sub>. The reaction mixture was extracted with EtOAc, dried over Na<sub>2</sub>SO<sub>4</sub>, filtered, and concentrated *in vacuo*. Purification of the residue by flash column chromatography on Chromatorex<sup>®</sup> NH-DM1020 (*n*-hexane:EtOAc = 5:1) afforded the desired product **L3** (289 mg, 88% yield) as a colorless solid.



**(2S)-2-Methyl-3-(naphthalen-2-yl)-2-[(propan-2-yl)amino]-1-(pyrrolidin-1-yl)propan-1-one (L3):** TLC,  $R_f = 0.13$  (*n*-hexane:EtOAc = 5:1, NH silica);  $[\alpha]_D^{24} = 9.2$  (*c* 1.00, CHCl<sub>3</sub>); <sup>1</sup>H NMR (400 MHz, CDCl<sub>3</sub>)  $\delta$  0.99 (d,  $J = 2.3$  Hz, 3H), 1.00 (d,  $J = 2.3$  Hz, 3H), 1.36 (s, 3H), 1.61–1.84 (m, 4H), 3.02 (sep,  $J = 6.4$  Hz, 1H), 3.12 (d,  $J = 13.3$  Hz, 1H), 3.16 (d,  $J = 13.3$  Hz, 1H), 3.51 (t,  $J = 6.4$  Hz, 2H), 3.73–3.90 (m, 2H), 7.29 (dd,  $J = 8.2, 1.8$  Hz, 1H), 7.41–7.50 (m, 2H), 7.60 (s, 1H), 7.72–7.84 (m, 3H); <sup>13</sup>C NMR (100 MHz, CDCl<sub>3</sub>)  $\delta$  22.6, 23.2, 23.7, 24.8, 26.9, 44.4, 44.8, 48.0, 48.3, 62.9, 125.5, 126.0, 127.6 (3C), 129.2 (2C), 129.2, 132.2, 133.3, 134.7, 174.4; IR (KBr) 3293, 2957, 2852, 1611, 1409, 1364, 1184 cm<sup>-1</sup>; HRMS (ESI+) calcd for C<sub>21</sub>H<sub>29</sub>N<sub>2</sub>O [M+H]<sup>+</sup> 325.2274, found 325.2266.

#### 2-5-4. Preparation of (2S)-3-methyl-3-(naphthalen-2-yl)-2-[(propan-2-yl)amino]-1-(pyrrolidin-1-yl)butan-1-one (L4)

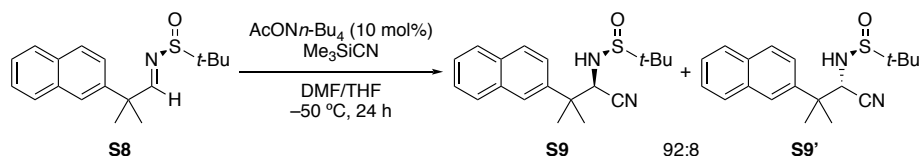


**S7** was prepared followed by a literature procedure.<sup>7,8</sup> Characterization data corresponded to the literature values.<sup>7</sup> <sup>1</sup>H NMR (400 MHz, CDCl<sub>3</sub>)  $\delta$  1.57 (s, 3H), 7.37 (dd,  $J = 8.7, 2.3$  Hz, 1H), 7.44–7.53 (m, 2H), 7.74 (d,  $J = 1.4$  Hz, 1H), 7.79–7.89 (m, 3H), 9.57 (s, 1H); <sup>13</sup>C NMR (100 MHz, CDCl<sub>3</sub>)  $\delta$  22.6 (2C), 50.7, 124.9, 125.6, 126.3, 126.5, 127.6, 128.1, 128.7, 132.5, 133.5, 138.7, 202.3; IR (neat) 3421, 3058, 2979 cm<sup>-1</sup>; HRMS (FAB+) calcd for C<sub>14</sub>H<sub>14</sub>NaO [M+Na]<sup>+</sup> 221.0942, found 221.0944.

**S8** was prepared followed by a literature procedure.<sup>9</sup> To a solution of aldehyde **S7** (240 mg, 1.23 mmol) and (*S*)-(-)-*tert*-butylsulfonamide (307 mg, 1.47 mmol) in CH<sub>2</sub>Cl<sub>2</sub> (10 mL) was added Ti(OEt)<sub>4</sub> (1.3 mL, 6.15 mmol). The mixture was refluxed and monitored by TLC. After completion, the reaction mixture was quenched at 0 °C by addition of H<sub>2</sub>O (10 mL). The solution was filtered through Celite<sup>®</sup>, and the filter cake was washed with CH<sub>2</sub>Cl<sub>2</sub> (3 × 20 mL). The aqueous phase was extracted with CH<sub>2</sub>Cl<sub>2</sub> (2 × 10 mL), and the combined organic portions were dried over Na<sub>2</sub>SO<sub>4</sub>, concentrated, and purified by Chromatorex<sup>®</sup> NH-DM1020 (*n*-hexane:EtOAc = 10:1) to give the afforded the desired product **S8** (351 mg, 95% yield) as a colorless solid.

**(S)-2-methyl-N-[(1E)-2-methyl-2-(naphthalen-2-yl)propylidene]propane-2-sulfonamide (S8):** TLC,  $R_f = 0.22$  (*n*-hexane:EtOAc = 10:1, NH silica);  $[\alpha]_D^{28} = 273.9$  (*c* 1.00, CHCl<sub>3</sub>); <sup>1</sup>H NMR (400 MHz, CDCl<sub>3</sub>)  $\delta$  1.22 (s, 9H),

1.65 (s, 6H), 7.43 (dd,  $J = 8.7, 1.8$  Hz, 1H), 7.45–7.51 (m, 2H), 7.74 (s, 1H), 7.76–7.84 (m, 1H), 8.13 (s, 1H);  $^{13}\text{C}$  NMR (100 MHz,  $\text{CDCl}_3$ )  $\delta$  22.6 (3C), 25.9, 26.1, 45.4, 57.1, 124.8, 125.0, 126.1, 126.3, 127.6, 128.1, 128.4, 132.3, 133.4, 141.6, 173.8; IR (KBr) 2056, 2972, 1622, 1363, 1085  $\text{cm}^{-1}$ ; HRMS (FAB+) calcd for  $\text{C}_{18}\text{H}_{24}\text{NOS}$   $[\text{M}+\text{H}]^+$  302.1579, found 302.1587.

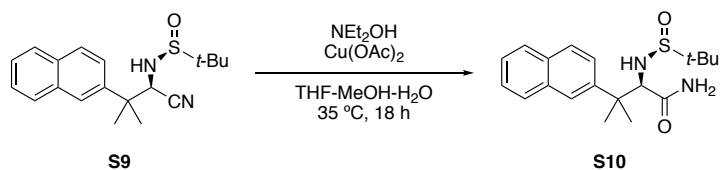


**S9** was prepared followed by a literature procedure.<sup>10</sup> To a stirred solution of tetrabutylammonium acetate (15.1 mg, 0.050 mmol) in THF (1.0 mL) were added successively a solution of trimethylsilyl cyanide (80  $\mu\text{L}$ , 0.60 mmol) in DMF (1.0 mL) and a solution of freshly prepared *N*-sulfinimine **S8** (151 mg, 0.50 mmol) in DMF (1.0 mL) at  $-50$   $^{\circ}\text{C}$ . After completion, the reaction mixture was quenched with a saturated solution of  $\text{NH}_4\text{Cl}$  and the resultant mixture was extracted three times with ethyl acetate, and combined organic layer was wash with sat.  $\text{NaHCO}_3$  and brine successively. The resulting organic layers were dried over  $\text{Na}_2\text{SO}_4$ . The organic layer was concentrated under reduced pressure, and the resultant crude mixture was purified by silica gel column chromatography (*n*-hexane/ $\text{EtOAc} = 3/1$  to  $1/1$ ) to give the desired  $\alpha$ -amino nitrile **S9** and **S9'** (156 mg, 95% yield, 92/8 dr) as colorless solids. The diastereomeric mixture was separated into individual diastereomers by Chromatorex<sup>®</sup> NH-DM1020 ( $\text{CHCl}_3$ :*n*-hexane = 1:3 to 1:1) to give afford **S9** and **S9'** respectively. The diastereoselectivity was determined by  $^1\text{H}$  NMR.

**(S)-N-[(1R)-1-Cyano-2-methyl-2-(naphthalen-2-yl)propyl]-2-methylpropane-2-sulfinamide (S9) (major product):** TLC,  $R_f = 0.61$  ( $\text{CHCl}_3$ , NH silica);  $[\alpha]_D^{22} = 66.0$  ( $c$  1.00,  $\text{CHCl}_3$ );  $^1\text{H}$  NMR (400 MHz,  $\text{CDCl}_3$ )  $\delta$  1.08 (s, 9H), 1.68 (s, 3H), 1.72 (s, 3H), 3.16 (d,  $J = 5.0$  Hz, 1H), 4.47 (d,  $J = 5.0$  Hz, 1H), 7.25–7.53 (m, 2H), 7.55 (dd,  $J = 9.2, 2.3$  Hz, 1H), 7.82–7.87 (m, 3H), 7.90 (d,  $J = 8.7$  Hz, 1H);  $^{13}\text{C}$  NMR (100 MHz,  $\text{CDCl}_3$ )  $\delta$  22.3 (3C), 24.1, 26.7, 42.3, 56.9, 57.7, 112.7, 123.9, 126.0, 126.7, 126.8, 127.7, 128.3, 129.3, 132.6, 133.3, 139.1; IR (neat) 2976, 1074, 819  $\text{cm}^{-1}$ ; HRMS (FAB+) calcd for  $\text{C}_{19}\text{H}_{25}\text{N}_2\text{OS}$   $[\text{M}+\text{H}]^+$  329.1688, found 329.1679.

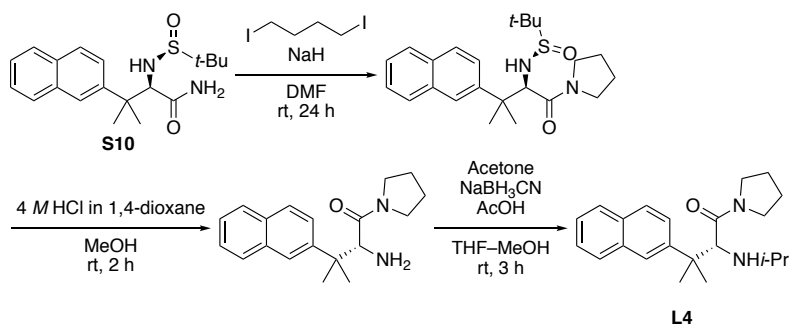
**(S)-N-[(1S)-1-Cyano-2-methyl-2-(naphthalen-2-yl)propyl]-2-methylpropane-2-sulfinamide (S9') (minor product):** TLC,  $R_f = 0.29$  ( $\text{CHCl}_3$ , NH silica);  $^1\text{H}$  NMR (400 MHz,  $\text{CDCl}_3$ )  $\delta$  1.05 (s, 9H), 1.62 (s, 3H), 1.68 (s, 3H), 3.42 (d,  $J = 9.6$  Hz, 1H), 4.31 (d,  $J = 9.6$  Hz, 1H), 7.25–7.52 (m, 2H), 7.54 (dd,  $J = 8.7, 1.8$  Hz, 1H), 7.81–7.88 (m,

4H);  $^{13}\text{C}$  NMR (100 MHz,  $\text{CDCl}_3$ )  $\delta$  22.5 (3C), 24.8, 25.9, 42.6, 56.9, 57.5, 118.3, 124.2, 126.1, 126.5, 126.6, 127.6, 128.2, 128.6, 132.5, 133.3, 139.6.



**S10** was prepared followed by a literature procedure.<sup>11</sup> To a solution of **S10** (886 mg, 2.70 mmol) in a mixed solvent of THF, MeOH and  $\text{H}_2\text{O}$  (v/v, 2/1/1, 0.15 M) were added  $\text{Cu}(\text{OAc})_2$  (245 mg, 1.35 mmol) and *N,N*-diethylhydroxylamine (2.76 mL, 27.0 mmol) at 35 °C for 18 h. The reaction mixture was filtered through silica gel short column ( $\text{CHCl}_3/\text{MeOH} = 5/1$ ) until the product was completely recovered. The combined solvent was concentrated *in vacuo* and purified by silica gel column chromatography ( $\text{CHCl}_3/\text{MeOH} = 20/1$ ) to give the desired product **S10** (981 mg, >99% yield) as a colorless solid.

**(2R)-3-methyl-2-[(S)-2-methylpropane-2-sulfinyl]amino-3-(naphthalen-2-yl)butanamide (S10):** TLC,  $R_f = 0.33$  ( $\text{CHCl}_3/\text{MeOH} = 20/1$ );  $[\alpha]_{\text{D}}^{28} = 13.6$  ( $c$  0.50,  $\text{CHCl}_3$ );  $^1\text{H}$  NMR (400 MHz,  $\text{CDCl}_3$ )  $\delta$  1.09 (s, 9H), 1.56 (s, 3H), 1.62 (s, 3H), 4.05 (d,  $J = 5.0$  Hz, 1H), 4.15 (d,  $J = 5.0$  Hz, 1H), 5.32 (brs, 1H), 5.55 (brs, 1H), 7.45–7.53 (m, 2H), 7.59 (dd,  $J = 8.7, 1.8$  Hz, 1H), 7.78–7.85 (m, 3H), 7.88 (d,  $J = 8.7$  Hz, 1H);  $^{13}\text{C}$  NMR (100 MHz,  $\text{CDCl}_3$ )  $\delta$  22.3 (3C), 24.9, 25.7, 42.3, 56.6, 66.2, 124.5, 125.5, 126.4, 126.6, 127.7, 128.2, 129.0, 132.3, 133.3, 142.8, 172.5; IR (KBr) 3382, 3310, 3190, 2965, 1682, 1066  $\text{cm}^{-1}$ ; HRMS (FAB+) calcd for  $\text{C}_{19}\text{H}_{27}\text{N}_2\text{O}_2\text{S}$   $[\text{M}+\text{H}]^+$  347.1793, found 347.1778.



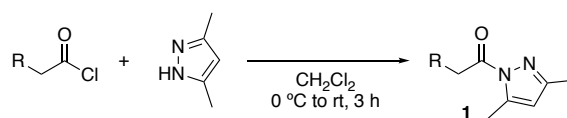
To a solution of **S10** (2.83 g, 8.64 mmol) in DMF (86 mL) and 1,4-diiodobutane (1.71 mL, 13.0 mmol) was added NaH (60% in oil) (864 mg, 21.6 mmol) and stirred at room temperature for 24 h. The reaction mixture was quenched with water, extracted three times with EtOAc, dried over  $\text{Na}_2\text{SO}_4$ , and concentrated *in vacuo*. The crude mixture was filtered through silica short column chromatography on Chromatorex<sup>®</sup> NH-DM1020 (EtOAc). To

the product in MeOH (40 mL) was added 4 M HCl in 1,4-dioxane (4.57 mL, 18.3 mmol) at ambient temperature and stirred for 2 h and then volatiles were removed under reduced pressure. The residue was diluted with DCM and washed with saturated NaHCO<sub>3</sub> aqueous solution. The organic layers were dried over Na<sub>2</sub>SO<sub>4</sub> and then concentrated under reduced pressure. The crude mixture was filtered through Chromatorex<sup>®</sup> NH-DM1020 (CHCl<sub>3</sub>/MeOH = 20/1). To a solution the product in a mixed solvent of MeOH (21.0 mL) and THF (17 mL) were added acetone (903 μL, 12.2 mmol), acetic acid (673 μL, 12.2 mmol) and NaBH<sub>3</sub>CN (765 mg, 12.2 mmol) at room temperature. The mixture was stirred for 3 hours at ambient temperature. The reaction was quenched with saturated aqueous NaHCO<sub>3</sub> then organic solvent was removed under reduced pressure. The mixture was extracted with EtOAc, dried over Na<sub>2</sub>SO<sub>4</sub>, filtered, and concentrated *in vacuo*. Purification by column chromatography on Chromatorex<sup>®</sup> NH-DM1020 (*n*-hexane–EtOAc 10:1 to 7.5:1) afforded **L4** (1.36 g, 43% yield, 3 steps from **S10** as a colorless solid.

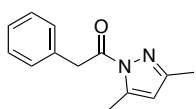
**(2R)-3-Methyl-3-(naphthalen-2-yl)-2-[(propan-2-yl)amino]-1-(pyrrolidin-1-yl)butan-1-one (L4):** TLC,  $R_f = 0.30$  (*n*-hexane:EtOAc = 5:1, NH silica);  $[\alpha]_D^{28} = -60.0$  ( $c$  0.50, CHCl<sub>3</sub>, 100% ee); <sup>1</sup>H NMR (400 MHz, CDCl<sub>3</sub>)  $\delta$  0.85–0.98 (m, 1H), 0.96 (d,  $J = 6.4$  Hz, 3H), 1.02 (d,  $J = 6.4$  Hz, 3H), 1.16–1.28 (m, 1H), 1.38–1.55 (m, 2H), 1.50 (s, 3H), 1.63 (s, 3H), 1.90 (brs, 1H), 2.16–2.25 (m, 1H), 2.54 (sep,  $J = 6.4$  Hz, 1H), 2.91–3.00 (m, 1H), 3.04–3.14 (m, 1H), 3.30 (s, 1H), 3.30–3.39 (m, 1H), 7.39–7.47 (m, 2H), 7.60 (dd,  $J = 8.7, 1.8$  Hz, 1H), 7.73 (d,  $J = 8.7$  Hz, 1H), 7.75–7.83 (m, 2H), 7.86 (d,  $J = 1.4$  Hz, 1H); <sup>13</sup>C NMR (100 MHz, CDCl<sub>3</sub>)  $\delta$  22.6, 22.8, 23.8, 24.3, 25.7, 26.6, 41.9, 45.4, 46.3, 47.5, 65.8, 125.5, 125.6, 125.8, 125.9, 126.9, 127.3, 128.1, 132.0, 133.2, 144.9, 173.4; IR (KBr) 2960, 1775, 1611, 1427, 1075 cm<sup>-1</sup>; HRMS (FAB+) calcd for C<sub>22</sub>H<sub>31</sub>N<sub>2</sub>O [M+H]<sup>+</sup> 339.2436, found 339.2437; HPLC analysis: IC-3, *n*-hexane/*i*-PrOH = 9/1, 1.0 mL/min,  $t_R = 8.5$  min (minor),  $t_R = 14.7$  min (major).

## 2-5-5. Preparation of *N*-acylpyrazoles **1**

### 2-5-5-1. Method A

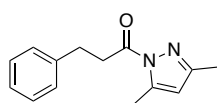


To a solution of 3,5-dimethylpyrazole (2.0 equiv) in dry  $\text{CH}_2\text{Cl}_2$  (0.3 *M*) was added the corresponding acid chloride (1.0 equiv) at 0 °C under nitrogen atmosphere. The suspended reaction mixture was stirred under ambient temperature for 3 h. The reaction was quenched with 1 *M* HCl. The resultant mixture was extracted three times with ethyl acetate, and combined organic layer was wash with sat.  $\text{NaHCO}_3$  and brine successively. The resulting organic layers were dried over  $\text{Na}_2\text{SO}_4$ . The organic layer was concentrated under reduced pressure, and the resultant crude mixture was purified by silica gel column chromatography (*n*-hexane/EtOAc = 30/1 to 20/1) to give the desired *N*-acylpyrazole **1**.



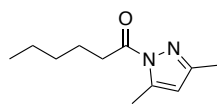
**1-(3,5-Dimethyl-1*H*-pyrazol-1-yl)-2-phenylethan-1-one (1b):** 10 mmol scale, 100% yield as a

colorless solid.  $^1\text{H}$  NMR (400 MHz,  $\text{CDCl}_3$ )  $\delta$  2.27 (s, 3H), 2.51 (s, 3H), 4.43 (s, 2H), 5.97 (s, 1H), 7.25–7.35 (m, 5H);  $^{13}\text{C}$  NMR (100 MHz,  $\text{CDCl}_3$ )  $\delta$  14.0, 14.7, 41.9, 111.5, 127.2, 128.6 (2C), 130.1 (2C), 134.2, 144.5, 152.2, 172.0; IR (KBr) 3110, 3030, 1733, 1582, 1358, 1244, 962, 715  $\text{cm}^{-1}$ ; HRMS (ESI+) calcd for  $\text{C}_{13}\text{H}_{14}\text{N}_2\text{NaO}$   $[\text{M}+\text{Na}]^+$  237.0998, found 237.0997.



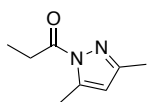
**1-(3,5-Dimethyl-1*H*-pyrazol-1-yl)-3-phenylpropan-1-one (1p):** 10 mmol scale, 90% yield as

a colorless solid.  $^1\text{H}$  NMR (400 MHz,  $\text{CDCl}_3$ )  $\delta$  2.22 (s, 3H), 2.53 (s, 3H), 3.06 (t,  $J$  = 8.2 Hz, 2H), 3.44 (t,  $J$  = 6.9 Hz, 2H), 5.94 (s, 1H), 7.17–7.31 (m, 5H);  $^{13}\text{C}$  NMR (100 MHz,  $\text{CDCl}_3$ )  $\delta$  13.9, 14.7, 30.4, 37.1, 111.1, 126.3, 128.5 (2C), 128.6 (2C), 140.9, 141.1, 152.0, 173.2; IR (KBr) 3028, 2927, 1731, 1579, 1330, 1229, 960, 734  $\text{cm}^{-1}$ ; HRMS (ESI+) calcd for  $\text{C}_{14}\text{H}_{16}\text{N}_2\text{NaO}$   $[\text{M}+\text{Na}]^+$  251.1155, found 251.1152.



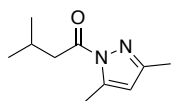
**1-(3,5-Dimethyl-1*H*-pyrazol-1-yl)hexan-1-one (1r):** 10 mmol scale, >99% yield as a colorless

oil.  $^1\text{H}$  NMR (400 MHz,  $\text{CDCl}_3$ )  $\delta$  0.87–0.96 (m, 3H), 1.30–1.43 (m, 4H), 1.66–1.80 (m, 2H), 2.24 (s, 3H), 2.54 (s, 3H), 3.09 (t,  $J$  = 7.3 Hz, 2H), 5.95 (s, 1H);  $^{13}\text{C}$  NMR (100 MHz,  $\text{CDCl}_3$ )  $\delta$  14.0, 14.1, 14.8, 22.6, 24.1, 31.4, 35.3, 110.0, 144.1, 151.8, 174.4; IR (neat) 2930, 2871, 1731, 1582, 1339, 960  $\text{cm}^{-1}$ ; HRMS (FAB+) calcd for  $\text{C}_{11}\text{H}_{19}\text{N}_2\text{O}$   $[\text{M}+\text{H}]^+$  195.1497, found 195.1498.



**1-(3,5-Dimethyl-1H-pyrazol-1-yl)propan-1-one (1s):** 10 mmol scale, 87% yield as a colorless oil.

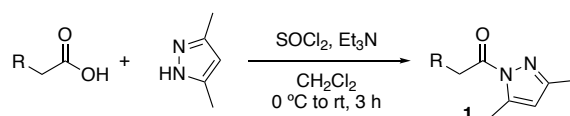
$^1\text{H}$  NMR (400 MHz,  $\text{CDCl}_3$ )  $\delta$  1.23 (t,  $J = 7.6$  Hz, 3H), 2.24 (s, 3H), 2.54 (s, 3H), 3.12 (q,  $J = 7.3$  Hz, 2H), 5.95 (s, 1H);  $^{13}\text{C}$  NMR (100 MHz,  $\text{CDCl}_3$ )  $\delta$  8.3, 13.7, 14.4, 28.6, 110.8, 143.8, 151.6, 174.7; IR (neat) 2980, 2931, 1731, 1250, 947  $\text{cm}^{-1}$ ; HRMS (FAB+) calcd for  $\text{C}_8\text{H}_{13}\text{N}_2\text{O}$   $[\text{M}+\text{H}]^+$  153.1028, found 153.1023.



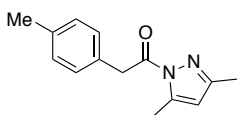
**1-(3,5-Dimethyl-1H-pyrazol-1-yl)-3-methylbutan-1-one (1t):** 6 mmol scale, 96% yield as a colorless oil.

$^1\text{H}$  NMR (400 MHz,  $\text{CDCl}_3$ )  $\delta$  1.02 (d,  $J = 6.9$  Hz, 6H), 2.24 (s, 3H), 2.28 (sep,  $J = 6.9$  Hz, 1H), 2.54 (s, 3H), 2.99 (d,  $J = 6.8$  Hz, 2H), 5.95 (s, 1H);  $^{13}\text{C}$  NMR (100 MHz,  $\text{CDCl}_3$ )  $\delta$  13.8, 14.7, 22.6 (2C), 25.0, 43.8, 111.0, 143.9, 151.6, 173.4; IR (neat) 2959, 2872, 1730, 1582, 1377, 963, 746  $\text{cm}^{-1}$ ; HRMS (ESI+) calcd for  $\text{C}_{10}\text{H}_{17}\text{N}_2\text{O}$   $[\text{M}+\text{H}]^+$  181.1335, found 181.1347.

## 2-5-5-2. Method B



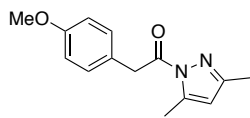
To a solution of 3,5-dimethylpyrazole (1.0 equiv) and triethylamine (4.0 equiv) in dry toluene (0.3 M) were added thionyl chloride (1.3 equiv) and the corresponding carboxylic acid (1.3 equiv) at 0 °C under nitrogen atmosphere. The suspended reaction mixture was stirred under ambient temperature for 3 h. The reaction was quenched with 1 M HCl. The resultant mixture was extracted three times with ethyl acetate, and combined organic layer was wash with sat.  $\text{NaHCO}_3$  and brine successively. The resulting organic layers were dried over  $\text{Na}_2\text{SO}_4$ . The organic layer was concentrated under reduced pressure, and the resultant crude mixture was purified by silica gel column chromatography ( $n$ -hexane/EtOAc = 30/1 to 20/1) to give the desired  $N$ -acylpyrazole **1**.



**1-(3,5-Dimethyl-1H-pyrazol-1-yl)-2-(p-tolyl)ethan-1-one (1c):** 5 mmol scale, 86% yield as a yellow solid.

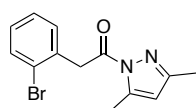
$^1\text{H}$  NMR (400 MHz,  $\text{CDCl}_3$ )  $\delta$  2.27 (s, 3H), 2.33 (s, 3H), 2.51 (s, 3H), 4.39 (s, 2H), 5.96 (s, 1H), 7.14 (d,  $J = 7.8$  Hz, 2H), 7.23 (d,  $J = 7.8$  Hz, 2H);  $^{13}\text{C}$  NMR (100 MHz,  $\text{CDCl}_3$ )  $\delta$  14.0, 14.7, 21.2, 41.4, 111.4,

129.3 (2C), 129.9 (2C), 131.1, 136.8, 144.5, 152.2, 172.2; IR (KBr) 2934, 1721, 1582, 1351, 1026, 963, 776  $\text{cm}^{-1}$ ;  
HRMS (ESI+) calcd for  $\text{C}_{14}\text{H}_{16}\text{N}_2\text{NaO}$   $[\text{M}+\text{Na}]^+$  251.1155, found 251.1152.



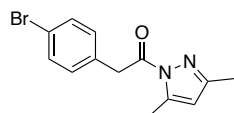
**1-(3,5-Dimethyl-1H-pyrazol-1-yl)-2-(p-methoxyphenyl)ethan-1-one (1d):** 5 mmol scale,

81% yield as a yellow solid.  $^1\text{H}$  NMR (400 MHz,  $\text{CDCl}_3$ )  $\delta$  2.27 (s, 3H), 2.51 (s, 3H), 3.79 (s, 3H), 4.37 (s, 2H), 5.97 (s, 1H), 6.88 (d,  $J = 8.7$  Hz, 2H), 7.27 (d,  $J = 9.2$  Hz, 2H);  $^{13}\text{C}$  NMR (100 MHz,  $\text{CDCl}_3$ )  $\delta$  14.0, 14.7, 41.0, 55.4, 111.5, 114.1 (2C), 126.2, 131.1 (2C), 144.5, 152.2, 158.8, 172.3; IR (KBr) 2934, 2841, 1719, 1609, 1581, 1247, 1034  $\text{cm}^{-1}$ ; HRMS (FAB+) calcd for  $\text{C}_{14}\text{H}_{16}\text{N}_2\text{O}_2$   $[\text{M}+\text{H}]^+$  245.1290, found 245.1281.



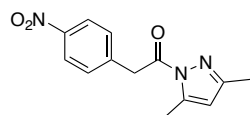
**1-(3,5-Dimethyl-1H-pyrazol-1-yl)-2-(o-bromophenyl)ethan-1-one (1e):** 5 mmol scale, 78%

yield as a red solid.  $^1\text{H}$  NMR (400 MHz,  $\text{CDCl}_3$ )  $\delta$  2.29 (s, 3H), 2.53 (s, 3H), 4.62 (s, 2H), 6.00 (s, 1H), 7.14–7.21 (m, 1H), 7.28–7.31 (m, 2H), 7.61 (d,  $J = 7.8$  Hz, 1H);  $^{13}\text{C}$  NMR (100 MHz,  $\text{CDCl}_3$ )  $\delta$  14.0, 14.6, 42.8, 111.4, 125.6, 127.6, 129.1, 132.1, 132.9, 134.6, 144.5, 152.4, 170.1; IR (KBr) 2925, 1733, 1581, 1357, 986, 960, 739  $\text{cm}^{-1}$ ; HRMS (ESI+) calcd for  $\text{C}_{13}\text{H}_{13}\text{BrN}_2\text{NaO}$   $[\text{M}+\text{Na}]^+$  315.0103, found 315.0100.



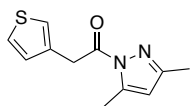
**1-(3,5-Dimethyl-1H-pyrazol-1-yl)-2-(p-bromophenyl)ethan-1-one (1f):** 5 mmol scale, 73%

yield as a red solid.  $^1\text{H}$  NMR (400 MHz,  $\text{CDCl}_3$ )  $\delta$  2.26 (s, 3H), 2.51 (s, 3H), 4.38 (s, 2H), 5.98 (s, 1H), 7.23 (d,  $J = 8.2$  Hz, 2H), 7.46 (d,  $J = 8.7$  Hz, 2H);  $^{13}\text{C}$  NMR (100 MHz,  $\text{CDCl}_3$ )  $\delta$  14.0, 14.6, 41.3, 111.7, 121.3, 131.7 (2C), 131.8 (2C), 133.2, 144.6, 152.4, 171.4; IR (KBr) 2975, 1721, 1585, 1372, 963  $\text{cm}^{-1}$ ; HRMS (ESI+) calcd for  $\text{C}_{13}\text{H}_{13}\text{BrN}_2\text{NaO}$   $[\text{M}+\text{Na}]^+$  315.0103, found 315.0100.



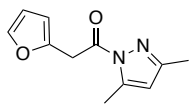
**1-(3,5-Dimethyl-1H-pyrazol-1-yl)-2-(p-nitrophenyl)ethan-1-one (1g):** 5 mmol scale, 57%

yield as a light green solid.  $^1\text{H}$  NMR (400 MHz,  $\text{CDCl}_3$ )  $\delta$  2.27 (s, 3H), 2.52 (s, 3H), 4.54 (s, 2H), 6.01 (s, 1H), 7.53 (d,  $J = 8.7$  Hz, 2H), 8.20 (d,  $J = 8.7$  Hz, 2H);  $^{13}\text{C}$  NMR (100 MHz,  $\text{CDCl}_3$ )  $\delta$  14.0, 14.6, 41.8, 111.9, 123.8 (2C), 131.0 (2C), 141.8, 144.6, 147.3, 152.8, 170.5; IR (KBr) 2925, 1726, 1589, 1514, 1358, 965, 726  $\text{cm}^{-1}$ ; HRMS (ESI+) calcd for  $\text{C}_{13}\text{H}_{13}\text{N}_3\text{NaO}_3$   $[\text{M}+\text{Na}]^+$  282.0849, found 282.0841.



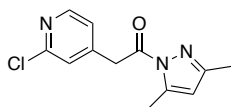
**1-(3,5-Dimethyl-1H-pyrazol-1-yl)-2-(3-thienyl)ethan-1-one (1h):** 2.27 mmol scale, 41% yield

as a brown oil.  $^1\text{H NMR}$  (400 MHz,  $\text{CDCl}_3$ )  $\delta$  2.27 (s, 3H), 2.53 (s, 3H), 4.47 (s, 2H), 5.98 (s, 1H), 7.11 (dd,  $J = 5.0, 1.4$  Hz, 1H), 7.21–7.24 (m, 1H), 7.30 (dd,  $J = 5.0, 3.2$  Hz, 1H);  $^{13}\text{C NMR}$  (100 MHz,  $\text{CDCl}_3$ )  $\delta$  14.0, 14.7, 36.5, 111.5, 123.6, 125.6, 129.1, 133.7, 144.5, 152.3, 171.4; IR (neat) 3104, 2927, 1728, 1584, 1350, 963, 746  $\text{cm}^{-1}$ ; HRMS (FAB+) calcd for  $\text{C}_{11}\text{H}_{13}\text{N}_2\text{OS}$   $[\text{M}+\text{H}]^+$  221.0749, found 221.0751.



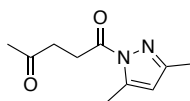
**1-(3,5-Dimethyl-1H-pyrazol-1-yl)-2-(furan-2-yl)ethan-1-one (1i):** 7.93 mmol scale, 64% yield

as a colorless solid.  $^1\text{H NMR}$  (400 MHz,  $\text{CDCl}_3$ )  $\delta$  2.21 (s, 3H), 2.26 (s, 3H), 2.53 (s, 3H), 4.50 (s, 2H), 5.98 (s, 1H), 6.29 (d,  $J = 3.2$  Hz, 1H), 6.33–6.39 (m, 1H), 7.37–7.42 (m, 1H);  $^{13}\text{C NMR}$  (100 MHz,  $\text{CDCl}_3$ )  $\delta$  14.0, 14.6, 35.0, 108.8, 110.6, 111.6, 142.4, 144.6, 147.9, 152.5, 169.7; IR (KBr) 3113, 2928, 2894, 1736, 1585, 1170  $\text{cm}^{-1}$ ; HRMS (FAB+) calcd for  $\text{C}_{11}\text{H}_{13}\text{N}_2\text{O}_2$   $[\text{M}+\text{H}]^+$  205.0977, found 205.0967.



**2-(2-Chloropyridin-4-yl)-1-(3,5-dimethyl-1H-pyrazol-1-yl)ethan-1-one (1j):** 6.41 mmol

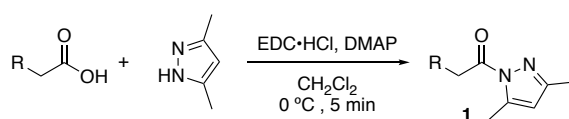
scale, 52% yield as a colorless solid.  $^1\text{H NMR}$  (400 MHz,  $\text{CDCl}_3$ )  $\delta$  2.26 (s, 3H), 2.52 (s, 3H), 4.43 (s, 2H), 7.23 (d,  $J = 5.0$  Hz, 1H), 7.33–7.38 (m, 1H), 8.35 (d,  $J = 5.5$  Hz, 1H);  $^{13}\text{C NMR}$  (100 MHz,  $\text{CDCl}_3$ )  $\delta$  13.9, 14.5, 40.9, 112.0, 124.0, 125.7, 144.6, 146.4, 149.7, 151.8, 152.9, 169.6; IR (KBr) 2929, 1712, 1598, 1550, 1383  $\text{cm}^{-1}$ ; HRMS (FAB+) calcd for  $\text{C}_{12}\text{H}_{13}\text{ClN}_3\text{O}$   $[\text{M}+\text{H}]^+$  250.0747, found 250.0747.



**1-(3,5-Dimethyl-1H-pyrazol-1-yl)pentan-1,4-dione (1v):** 5 mmol scale, 80% yield as a yellow

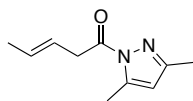
solid.  $^1\text{H NMR}$  (400 MHz,  $\text{CDCl}_3$ )  $\delta$  2.24 (s, 3H), 2.25 (s, 3H), 2.50 (s, 3H), 2.85 (t,  $J = 6.0$  Hz, 2H), 3.39 (t,  $J = 5.5$  Hz, 2H), 5.95 (s, 1H);  $^{13}\text{C NMR}$  (100 MHz,  $\text{CDCl}_3$ )  $\delta$  13.9, 14.5, 29.6, 30.0, 37.4, 111.1, 144.1, 152.1, 172.9, 206.8; IR (KBr) 3412, 3118, 2925, 1718, 1587, 1375, 1316, 1161  $\text{cm}^{-1}$ ; HRMS (FAB+) calcd for  $\text{C}_{10}\text{H}_{15}\text{N}_2\text{O}_2$   $[\text{M}+\text{H}]^+$  195.1134, found 195.1129.

### 2-5-5-3. Method C



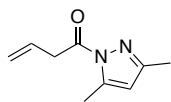


On the basis of a literature procedure,<sup>12</sup> to the mixture of carboxylic acid (1.1 equiv) and 3,5-dimethylpyrazole (1.0 equiv) in dry dichloromethane (0.5 M) was added EDC•HCl (1.1 equiv) and DMAP (0.001 equiv) at 0 °C. After stirring for 5 minutes, it was quenched by saturated brine. The organic layer was separated and the aqueous phase was extracted twice with CH<sub>2</sub>Cl<sub>2</sub>. The organic layer was concentrated under reduced pressure, and the resultant crude mixture was purified by silica gel column chromatography (*n*-hexane/EtOAc = 30/1 to 20/1) to give the desired *N*-acylpyrazole **1**.



**(3E)-1-(3,5-Dimethyl-1H-pyrazol-1-yl)-3-penten-1-one (1m):** 5 mmol scale, 75% yield as a

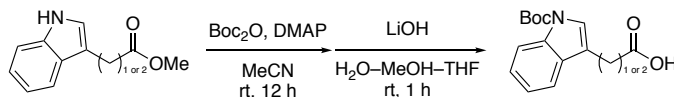
colorless oil. <sup>1</sup>H NMR (400 MHz, CDCl<sub>3</sub>) δ 1.73 (d, *J* = 4.1 Hz, 3H), 2.24 (s, 3H), 2.53 (s, 3H), 3.81 (d, *J* = 4.6 Hz, 2H), 5.59–5.65 (m, 2H), 5.95 (s, 1H); <sup>13</sup>C NMR (100 MHz, CDCl<sub>3</sub>) δ 14.0, 14.7, 18.2, 39.2, 111.1, 122.8, 130.1, 144.3, 152.1, 172.8; IR (neat) 2929, 1730, 1583, 1378, 1359, 963 cm<sup>-1</sup>; HRMS (ESI+) calcd for C<sub>10</sub>H<sub>14</sub>N<sub>2</sub>NaO [M+Na]<sup>+</sup> 201.0998, found 201.0991.



**1-(3,5-Dimethyl-1H-pyrazol-1-yl)-3-buten-1-one (1n):**<sup>12</sup> 5 mmol scale, 84% yield as a colorless

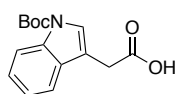
oil. <sup>1</sup>H NMR (400 MHz, CDCl<sub>3</sub>) δ 2.24 (s, 3H), 2.54 (s, 3H), 3.89 (ddd, *J* = 6.9, 1.4, 1.4 Hz, 2H), 5.21–5.24 (m, 1H), 5.24–5.29 (m, 1H), 5.96 (s, 1H), 6.08 (dddd, *J* = 17.4, 10.6, 6.9, 6.9 Hz, 1H); <sup>13</sup>C NMR (100 MHz, CDCl<sub>3</sub>) δ 13.7, 14.4, 40.0, 111.1, 118.9, 130.3, 144.0, 152.0, 171.8

#### 2-5-5-4. Method D

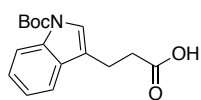


On the basis of a literature,<sup>13</sup> the corresponding methyl ester (56.0 mmol, 1.0 equiv) was dissolved in acetonitrile (45 mL) and di-*tert*-butyl dicarbonate (37.4 g, 171 mmol, 3.0 equiv) and DMAP (1.34 g, 11.0 mmol, 0.2 equiv) were added. The mixture was stirred for 2 h after which the solvent was removed under reduced pressure. The residue was dissolved in EtOAc (500 mL) and subsequently washed with saturated aqueous NH<sub>4</sub>Cl (300 mL), saturated aqueous NaHCO<sub>3</sub> (300 mL) and brine (150 mL). After drying over MgSO<sub>4</sub>, the solvent was removed *in vacuo* and the crude product purified by flash chromatography on silica gel (EtOAc/*n*-hexane; gradient

1:10 to 1:2) to give *N*-Boc protected ester as a colorless solid. A solution of lithium hydroxide (LiOH•H<sub>2</sub>O, 6.00 g, 143 mmol, 3.0 equiv) in H<sub>2</sub>O (250 mL) was added to a solution of ester (1.0 equiv) in THF (350 mL) and MeOH (150 mL). After stirring for 18 h, the mixture was concentrated *in vacuo* and a 10% aqueous solution of citric acid (300 mL) was added. The aqueous layer was extracted with EtOAc (3 × 200 mL) and the combined organic layers were washed with water (200 mL) and brine (200 mL) and dried over MgSO<sub>4</sub>. The solvent was removed under reduced pressure and the residue purified by flash chromatography on silica gel (EtOAc/*n*-hexane gradient 1:10 to 1:1, 1% AcOH) yielding corresponding carboxylic acid as a colorless solid.

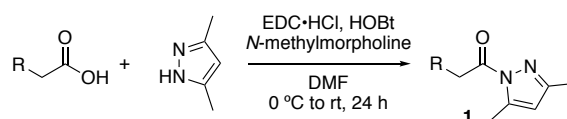


**2-(1-(*tert*-Butoxycarbonyl)-1*H*-indol-3-yl)acetic acid:**<sup>13</sup> 70% yield for 2 steps.

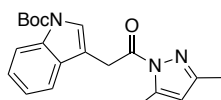


**3-(1-(*tert*-Butoxycarbonyl)-1*H*-indol-3-yl)propanoic acid:**<sup>14</sup> quantitative yield for 2 steps.

#### 2-5-5-5. Method E



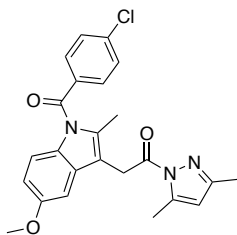
On the basis of a literature procedure,<sup>15</sup> the round bottom flask equipped with a magnetic stirring bar and 3-way glass stopcock was evacuated and filled with argon (three cycles). To the solution of carboxylic acid (1.0 equiv) in dry DMF (1.0 *M*) was added EDC•HCl (1.2 equiv), HOBT (1.2 equiv), 3,5-dimethylpyrazole (1.1 equiv) and *N*-methylmorpholine (2.0 equiv) at 0 °C. After stirring for 24 h at room temperature, it was quenched by 1 *M* HCl or 10% citric acid aq. The resultant mixture was extracted with EtOAc, and combined organic layer was washed with sat. NaHCO<sub>3</sub> solution and brined successively. The resulting organic layers were dried over Na<sub>2</sub>SO<sub>4</sub>. After removal of solvent under reduced pressure, the crude mixture was purified by silica gel column chromatography (*n*-hexane/EtOAc = 30/1 to 20/1) to afford desired *N*-acylpyrazole **1**.



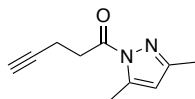
**1-(3,5-Dimethyl-1*H*-pyrazol-1-yl)-2-[*N*-(*tert*-butoxycarbonyl)-3-indolyl]- ethan-1-one**

**(1k):** 1.4 mmol scale, 83% yield as a colorless solid. <sup>1</sup>H NMR (400 MHz, CDCl<sub>3</sub>) δ 1.66 (s, 9H), 2.29 (s, 3H), 2.52 (s, 3H), 4.53 (s, 2H), 6.00 (s, 1H), 7.20–7.35 (m, 2H), 7.59 (d, *J* = 7.8 Hz, 1H), 7.63 (s, 1H), 8.14 (br, 1H); <sup>13</sup>C

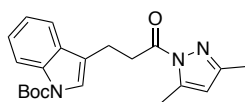
NMR (100 MHz, CDCl<sub>3</sub>) δ 14.0, 14.7, 28.3 (3C), 31.8, 83.6, 111.6, 113.3, 115.4, 119.4, 122.7, 124.6, 125.2, 130.6, 135.5, 144.5, 149.8, 152.3, 171.1; IR (KBr) 2977, 1716, 1587, 1407, 1164, 1079, 962 cm<sup>-1</sup>; HRMS (FAB+) calcd for C<sub>20</sub>H<sub>23</sub>N<sub>3</sub>NaO<sub>3</sub> [M+Na]<sup>+</sup> 376.1637, found 376.1629.



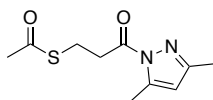
**2-[1-(4-Chlorobenzoyl)-5-methoxy-2-methyl-1H-indol-3-yl]-1-(3,5-dimethyl-1H-pyrazol-1-yl)ethan-1-one (11):**<sup>16</sup> 5 mmol scale, 84% yield as a yellow solid. <sup>1</sup>H NMR (400 MHz, CDCl<sub>3</sub>) δ 2.29 (s, 3H), 2.44 (s, 3H), 2.52 (s, 3H), 3.82 (s, 3H), 4.48 (s, 2H), 6.00 (s, 1H), 6.65 (dd, *J* = 9.2, 2.8 Hz, 1H), 6.87 (d, *J* = 8.7 Hz, 1H), 7.07 (d, *J* = 2.8 Hz, 1H), 7.43–7.49 (m, 2H), 7.63–7.71 (m, 2H); <sup>13</sup>C NMR (100 MHz, CDCl<sub>3</sub>) δ 13.8, 14.0, 14.7, 31.2, 55.8, 101.7, 111.6, 111.7, 112.8, 115.0, 129.2, 130.9, 131.1, 131.3, 134.1, 136.7, 139.3, 144.6, 152.3, 156.1, 168.4, 170.9.



**1-(3,5-Dimethyl-1H-pyrazol-1-yl)-4-pentyn-1-one (10):** 5 mmol scale, 90% yield as a colorless solid. <sup>1</sup>H NMR (400 MHz, CDCl<sub>3</sub>) δ 1.99 (t, *J* = 2.8 Hz, 1H), 2.24 (s, 3H), 2.54 (s, 3H), 2.62 (td, *J* = 7.8, 2.8 Hz, 2H), 3.37 (t, *J* = 7.3 Hz, 2H), 5.96 (s, 1H); <sup>13</sup>C NMR (100 MHz, CDCl<sub>3</sub>) δ 13.7, 13.9, 14.6, 34.5, 69.0, 82.9, 111.2, 144.2, 152.3, 172.0; IR (KBr) 3417, 3242, 3134, 2931, 2117, 1720, 1587, 1389, 1333, 1233 cm<sup>-1</sup>; HRMS (ESI+) calcd for C<sub>10</sub>H<sub>12</sub>N<sub>2</sub>NaO<sub>2</sub> [M+Na]<sup>+</sup> 199.0842, found 199.0845.

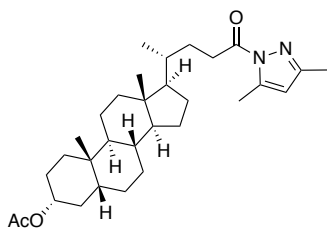


**1-(3,5-Dimethyl-1H-pyrazol-1-yl)-3-[N-(tert-butoxycarbonyl)-3-indolyl]-propan-1-one (1q):** 2.0 mmol scale, quantitative yield as a colorless solid. <sup>1</sup>H NMR (400 MHz, CDCl<sub>3</sub>) δ 1.66 (s, 9H), 2.23 (s, 3H), 2.55 (d, *J* = 0.9 Hz, 3H), 3.10–3.18 (m, 2H), 3.47–3.55 (m, 2H), 5.96 (s, 1H), 7.25 (td, *J* = 7.8, 0.9 Hz, 1H), 7.45 (br, 1H), 7.60 (d, *J* = 7.4 Hz, 1H), 8.11 (br, 1H); <sup>13</sup>C NMR (100 MHz, CDCl<sub>3</sub>) δ 13.9, 14.7, 19.9, 28.3 (3C), 35.1, 83.5, 111.2, 115.3, 119.1, 119.7, 122.5, 122.8, 124.5, 130.5, 135.6, 144.1, 149.9, 152.1, 173.3; IR (KBr) 3428, 3142, 3053, 2980, 2925, 1725, 1581, 1451, 1385, 1331, 1249, 1156, 1091 cm<sup>-1</sup>; HRMS (FAB+) calcd for C<sub>21</sub>H<sub>26</sub>N<sub>3</sub>O<sub>3</sub> [M+H]<sup>+</sup> 368.1974, found 368.1975.

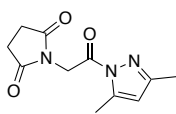


**1-(3,5-Dimethyl-1H-pyrazol-1-yl)-3-thioacetylpropan-1-one (1u):** 6.75 mmol scale, 94% yield as a colorless solid. <sup>1</sup>H NMR (400 MHz, CDCl<sub>3</sub>) δ 2.21 (s, 3H), 2.33 (s, 3H), 2.54 (s, 3H), 3.23 (t, *J* = 6.9

Hz, 2H), 3.43 (t,  $J = 6.9$  Hz, 2H), 5.96 (s, 1H);  $^{13}\text{C}$  NMR (100 MHz,  $\text{CDCl}_3$ )  $\delta$  13.8, 14.5, 23.6, 30.5, 35.7, 111.2, 144.1, 152.3, 172.0, 195.6; IR (KBr) 3420, 3358, 3114, 2984, 2927, 1721, 1693, 1377, 1341, 1138  $\text{cm}^{-1}$ ; HRMS (ESI+) calcd for  $\text{C}_{10}\text{H}_{14}\text{N}_2\text{NaO}_2\text{S}$   $[\text{M}+\text{Na}]^+$  249.0668, found 249.0675.

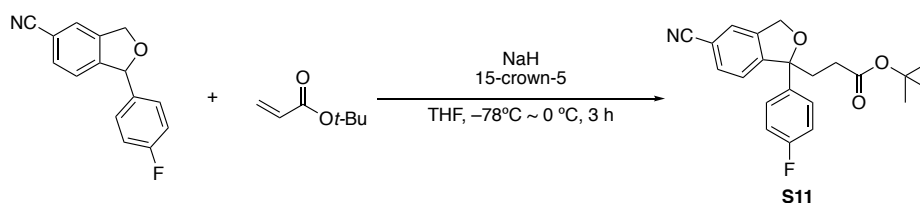


**(1R,3aS,3bR,5aR,7R,9aS,9bS,11aR)-1-[(2R,4R)-5-(3,5-Dimethyl-1H-pyrazol-1-yl)-4-fluoro-5-oxopentan-2-yl]-9a,11a-dimethyl-hexadecahydro-1H-cyclopenta[a]phenanthren-7-yl acetate (1w):**<sup>16</sup> Amidation (Method E) was conducted after *O*-acetylation of lithocholic acid, prepared followed by a literature procedure.<sup>17</sup> 5 mmol scale, 70% yield over 2 steps as a colorless solid.  $^1\text{H}$  NMR (400 MHz,  $\text{CDCl}_3$ )  $\delta$  0.65 (s, 3H), 0.93 (s, 3H), 0.98 (d,  $J = 6.4$  Hz, 3H), 1.00–1.72 (m, 20H), 1.74–1.99 (m, 6H), 2.03 (s, 3H), 2.24 (s, 3H), 2.53 (s, 3H), 2.99–3.15 (m, 2H), 4.69–4.74 (m, 1H), 5.94 (s, 1H);  $^{13}\text{C}$  NMR (100 MHz,  $\text{CDCl}_3$ )  $\delta$  12.2, 14.0, 14.8, 18.7, 21.0, 21.6, 23.5, 24.3, 26.5, 26.8, 27.2, 28.3, 30.5, 32.3, 32.4, 34.7, 35.2, 35.5, 35.9, 40.2, 40.5, 42.0, 42.9, 56.1, 56.6, 74.5, 111.0, 144.1, 151.8, 170.8, 174.8.



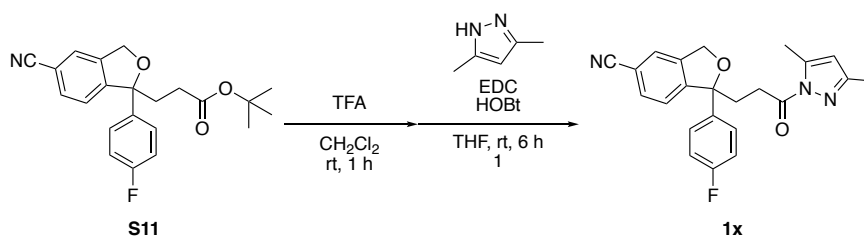
**1-[2-(3,5-Dimethyl-1H-pyrazol-1-yl)-2-oxoethyl]pyrrolidine-2,5-dione (1y):** Amidation (Method E) was conducted after *N*-protection of glycine, prepared followed by a literature procedure.<sup>18</sup> 5 mmol scale, 82% yield over 2 steps as a colorless solid.  $^1\text{H}$  NMR (400 MHz,  $\text{CDCl}_3$ )  $\delta$  2.25 (s, 3H), 2.50 (d,  $J = 0.9$  Hz, 3H), 2.85 (s, 4H), 5.06 (s, 2H), 5.99 (d,  $J = 0.9$  Hz, 1H);  $^{13}\text{C}$  NMR (100 MHz,  $\text{CDCl}_3$ )  $\delta$  13.9, 14.1, 28.5 (2C), 41.8, 111.7, 144.6, 153.6, 165.9, 176.8 (2C); IR (KBr) 3476, 3117, 3004, 2955, 1709, 1417, 1327, 1173  $\text{cm}^{-1}$ ; HRMS (FAB+) calcd for  $\text{C}_{11}\text{H}_{14}\text{N}_3\text{O}$   $[\text{M}+\text{H}]^+$  236.1035, found 236.1033.

#### 2-5-5-6. Preparation of 1-(3-(3,5-dimethyl-1H-pyrazol-1-yl)-3-oxopropyl)-1-(4-fluorophenyl)-1,3-dihydroisobenzofuran-5-carbonitrile (1x)



**tert-butyl 3-(5-cyano-1-(4-fluorophenyl)-1,3-dihydroisobenzofuran-1-yl)propanoate (S11):** On the basis of a literature procedure,<sup>21</sup> to a solution of 1-(4-fluorophenyl)-1,3-dihydroisobenzofuran-5-carbonitrile (1.08 g, 4.54 mmol, 1.00 equiv) in dry THF (11 mL) were added sodium hydride (60%, 182 mg, 4.54 mmol, 1.00 equiv) and 15-

crown-5 (990  $\mu\text{L}$ , 4.99 mmol, 1.10 equiv) and the resulting mixture was stirred at  $-78\text{ }^\circ\text{C}$  for 5 minutes. After the elevation of the reaction flask to  $0\text{ }^\circ\text{C}$ , *tert*-butyl acrylate (1.16 mL, 6.80 mmol, 1.5 equiv) was added and stirred for 3 h. The reaction was quenched by 1 M HCl. The mixture was extracted with ethyl acetate three times and the combined organic extracts were dried over  $\text{Na}_2\text{SO}_4$ . After removal of solvent under reduced pressure, the crude mixture was purified by silica gel column chromatography (*n*-hexane/EtOAc = 5/1 to 3/1) to afford desired product **S10** in quantitative yield as a colorless oil. TLC,  $R_f = 0.30$  (*n*-hexane/EtOAc = 3/1).  $^1\text{H}$  NMR (400 MHz,  $\text{CDCl}_3$ )  $\delta$  1.39 (s, 9H), 2.07–2.25 (m, 2H), 2.36–2.45 (m, 1H), 2.46–2.56 (m, 1H), 5.13 (d,  $J = 12.8$  Hz, 1H), 5.19 (d,  $J = 13.3$  Hz, 1H), 6.98–7.07 (m, 2H), 7.37–7.46 (m, 3H), 7.51 (s, 1H), 7.61 (dd,  $J = 7.3, 0.9$  Hz, 1H);  $^{13}\text{C}$  NMR (100 MHz,  $\text{CDCl}_3$ )  $\delta$  28.1 (3C), 30.6, 36.2, 71.4, 80.6, 90.6, 112.0, 115.6 (d,  $J = 21.0$  Hz, 2C), 118.7, 123.0, 125.4, 126.9 (d,  $J = 8.6$  Hz, 2C), 132.1, 139.1, 140.4, 148.8, 162.2 (d,  $J = 246$  Hz), 172.5;  $^{19}\text{F}$  (376 MHz,  $\text{CDCl}_3$ )  $\delta$   $-115.0$ – $-114.9$  (m, 1F); IR (KBr) 2230, 1724, 1508, 1152  $\text{cm}^{-1}$ ; HRMS (ESI+) calcd for  $\text{C}_{22}\text{H}_{22}\text{FNNaN}_3\text{O}_3$   $[\text{M}+\text{Na}]^+$  390.1476, found 390.1479.

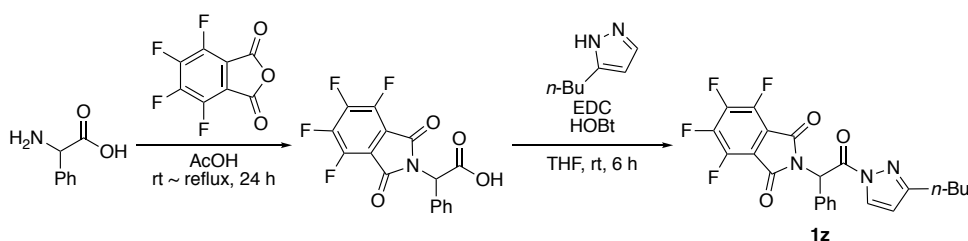


To a solution of **S10** (1.668 g, 4.54 mmol) was added in dichloromethane (5 mL) was added trifluoroacetic acid (2.5 mL) at room temperature. The mixture was stirred at ambient temperature for 1 h. The reaction mixture was concentrated *in vacuo* to afford the corresponding carboxylic acid as a colorless oil. To the mixture of carboxylic acid (1.0 equiv) and 3,5-dimethylpyrazole (1.31 g, 13.6 mmol, 3.0 equiv) in dry THF (9 mL) was added EDC•HCl (846 mg, 5.45 mmol, 1.2 equiv) and HOBT (834 mg, 5.45 mmol, 1.2 equiv) at room temperature. After stirring for 6 hours, it was quenched by saturated brine. The organic layer was separated and the aqueous phase was extracted three times with EtOAc. The organic layer was dried over  $\text{Na}_2\text{SO}_4$  and concentrated under reduced pressure. The resultant crude mixture was purified by silica gel column chromatography (*n*-hexane/EtOAc = 5/1 to 3/1) to give the desired *N*-acylpyrazole **1?** in 55% yield over 2 steps as a colorless solid.

**1-(3-(3,5-dimethyl-1H-pyrazol-1-yl)-3-oxopropyl)-1-(4-fluorophenyl)-1,3-dihydroisobenzofuran-2-carbonitrile**

**furan-5-carbonitrile (1x):** TLC,  $R_f = 0.29$  (*n*-hexane/EtOAc = 3/1).  $^1\text{H}$  NMR (400 MHz,  $\text{CDCl}_3$ )  $\delta$  2.18 (s, 3H), 2.47 (d,  $J = 0.9$  Hz, 3H), 2.53–2.63 (m, 1H), 2.64–2.74 (m, 1H), 3.03–3.10 (m, 2H), 5.14 (d,  $J = 12.8$  Hz, 1H), 5.19 (d,  $J = 12.8$  Hz, 1H), 5.92 (d,  $J = 0.9$  Hz, 1H), 6.98–7.05 (m, 2H), 7.40–7.51 (m, 4H), 7.57–7.63 (m, 1H);  $^{13}\text{C}$  NMR (100 MHz,  $\text{CDCl}_3$ )  $\delta$  13.7, 14.5, 30.4, 35.7, 71.3, 90.5, 111.1, 111.8, 115.4 (d,  $J = 21.0$  Hz, 2C), 118.6, 122.9, 125.3, 126.8 (d,  $J = 8.6$  Hz, 2C), 131.8, 139.1 (d,  $J = 2.9$  Hz), 140.4, 143.8, 148.7, 151.8, 162.1 (d,  $J = 245$  Hz), 173.4;  $^{19}\text{F}$  (376 MHz,  $\text{CDCl}_3$ )  $\delta$  -115.0– -114.9 (m, 1F); IR (KBr) 2230, 1721, 1507, 1336, 1225  $\text{cm}^{-1}$ ; HRMS (ESI+) calcd for  $\text{C}_{23}\text{H}_{20}\text{FN}_3\text{NaO}_2$   $[\text{M}+\text{Na}]^+$  412.1432, found 412.1435.

### 2-5-5-7. Preparation of 2-(2-(3-butyl-1H-pyrazol-1-yl)-2-oxo-1-phenylethyl)-4,5,6,7-tetrafluoro-isoindoline-1,3-dione (1z)

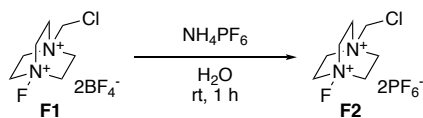


Amidation with 5-butyl-1H-pyrazole<sup>20</sup> was conducted after *N*-protection of phenylglycine,<sup>18</sup> the dried two-necked flask equipped with a magnetic stirring bar was charged with phenylglycine (1.51 g, 10.0 mmol, 1.0 equiv) and tetrafluorophthalic anhydride (2.20 g, 10.0 mmol, 1.0 equiv). Then acetic acid (10.0 mL) was added to the flask and the reaction mixture was refluxed at 130 °C. After 24 hours, evaporation of the organic solvent under reduced pressure gave a yellow solid, followed by addition of 10 mL of water and the mixture was extracted three times with  $\text{CH}_3\text{Cl}$ . The combined organic extracts were dried over  $\text{Na}_2\text{SO}_4$ . After removal of solvent under reduced pressure, the crude mixture was recrystallized from  $\text{CH}_3\text{Cl}/n$ -hexane at room temperature to give 2-phenyl-2-(4,5,6,7-tetrafluoro-1,3-dioxoisoindolin-2-yl)acetic acid in 88% yield as a colorless solid. To the mixture of carboxylic acid (1.06 g, 3.00 mmol, 1.00 equiv) and 5-butyl-1H-pyrazole (447 mg, 3.60 mmol, 1.20 equiv) in dry THF (6 mL) was added EDC•HCl (559 mg, 3.60 mmol, 1.20 equiv) and HOBt (551 mg, 3.60 mmol, 1.20 equiv) at room temperature. After stirring for 6 hours, it was quenched by saturated brine. The organic layer was separated and the aqueous phase was extracted three times with EtOAc. The organic layer was dried over  $\text{Na}_2\text{SO}_4$  and concentrated under reduced pressure. The resultant crude mixture was purified by silica gel column chromatography (*n*-hexane/EtOAc = 5/1 to 3/1) to give the mixture containing the desired *N*-acylpyrazole, which was recrystallized in  $\text{CHCl}_3/n$ -hexane and precipitate was washed three times with *n*-hexane to provide **1y** (1.18 g) in 86% yield as a yellow solid.

**2-(2-(3-butyl-1H-pyrazol-1-yl)-2-oxo-1-phenylethyl)-4,5,6,7-tetrafluoroisoindoline-1,3-dione (1z):** TLC,  $R_f = 0.50$  (*n*-hexane/EtOAc = 5/1);  $^1\text{H}$  NMR (400 MHz,  $\text{CDCl}_3$ )  $\delta$  0.78 (t,  $J = 7.3$  Hz, 3H), 1.04–1.19 (m, 2H), 1.30–1.51 (m, 2H), 2.47 (t,  $J = 7.8$  Hz, 3H), 6.22 (t,  $J = 2.7$  Hz, 2H), 6.81 (s, 1H), 7.31–7.41 (m, 3H), 7.42–7.51 (m, 2H), 8.16 (d,  $J = 2.9$  Hz, 1H);  $^{13}\text{C}$  NMR (100 MHz,  $\text{CDCl}_3$ )  $\delta$  13.8, 22.1, 28.1, 28.0, 30.2, 57.0, 110.3, 113.8 (2C), 128.8 (2C), 129.0, 129.7 (2C), 129.8, 133.3, 142.3 (m), 143.8 (m), 145.0 (m), 146.5 (m), 159.2, 161.6, 164.9;  $^{19}\text{F}$  (376 MHz,

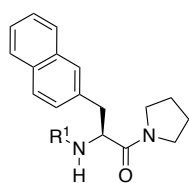
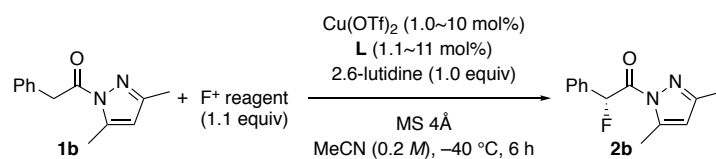
CDCl<sub>3</sub>) δ -141.9– -141.6 (m, 2F), -135.1– -134.8 (m, 2F); IR (KBr) 1717, 1515, 1411 cm<sup>-1</sup>; HRMS (ESI+) calcd for C<sub>23</sub>H<sub>17</sub>F<sub>4</sub>N<sub>3</sub>NaO<sub>3</sub> [M+Na]<sup>+</sup> 482.1098, found 482.1102.

### 2-5-6. Synthesis of Selectfluor analogue F2 (X = PF<sub>6</sub>)



**1-Chloromethyl-4-fluoro-1,4-diazoniabicyclo[2.2.2]octane bis(hexafluorophosphate) (F2):** On the basis of a literature procedure,<sup>22</sup> to 1-chloromethyl-4-fluoro-1,4-diazoniabicyclo[2.2.2]octane bis(tetrafluoroborate) **F1** (1.06 g, 3.00 mmol, 1.00 equiv) in H<sub>2</sub>O (9.0 mL) at 23 °C was added ammonium hexafluorophosphate (2.93 g, 18.0 mmol, 6.00 equiv). After stirring for 1 h, the suspension was filtered off and washed with H<sub>2</sub>O (5 × 5 mL) and Et<sub>2</sub>O (10 mL) to afford 1.43 g of **F2** as a colorless solid (quantitative yield).

### 2-5-7. Table S1. Optimization of the conditions for the enantioselective fluorination of 1b<sup>a</sup>



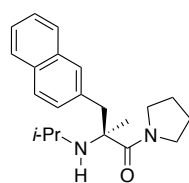
**L1** (R<sup>1</sup> = *c*-C<sub>5</sub>H<sub>9</sub>)

**L2** (R<sup>1</sup> = *i*-Pr)

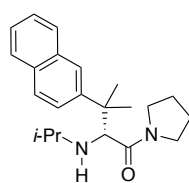
**LS1** (R<sup>1</sup> = Me)

**LS2** (R<sup>1</sup> = CHEt<sub>2</sub>)

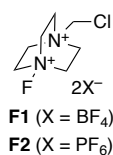
**LS3** (R<sup>1</sup> = 4-MeC<sub>6</sub>H<sub>4</sub>)



**L3**

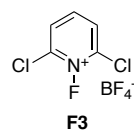


**L4**

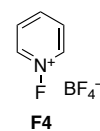


**F1** (X = BF<sub>4</sub>)

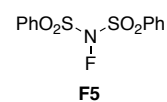
**F2** (X = PF<sub>6</sub>)



**F3**



**F4**



**F5**

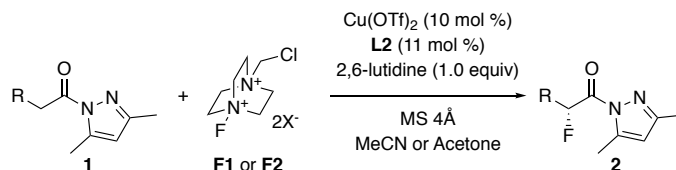
Entry	L	F <sup>+</sup> reagent	Solvent	2b	
				Yield (%)	Ee (%)

1	LS1	F1	MeCN	79	82
			MeCN		
2 <sup>b</sup>	L1	F1	MeCN	96	88
3 <sup>c</sup>	L1	F1	Acetone	24	87
			EtCN		
4	L1	F1	THF	87	85
5 <sup>d</sup>	L1	F1	MeCN	24	78
			MeCN		
6	L1	F1	MeCN	14	–
7	L1	F2	MeCN	85	90
			PhCl <sup>e</sup>		
8	L1	F3–F4	PhCl <sup>e</sup> /MeCN (1:2)	0	–
9	L1	F5	PhMe <sup>e</sup> /MeCN (1:2)	68	89
10	L2	F1	MeCN	91	89
11	L2	F1	MeCN	91	89
12	L2	F1	MeCN	<5	–
			MeCN		
13	L2	F1	MeCN	60	79
14 <sup>g</sup>	L2	F1	MeCN	42	80
			MeCN		
15 <sup>h</sup>	L2	F2		99 (98) <sup>f</sup>	91 (89) <sup>f</sup>
16	L2	F2		97	91
17	L2	F2		38	81
18	L3	F2		>99	94
	L4				
19		F2		93	–96
21	LS2	F1		89	74
	LS3	F1		74	85

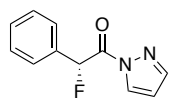
<sup>a</sup> Unless otherwise noted, **1b** (0.3 mmol), F<sup>+</sup> reagent (1.1 equiv), Cu(OTf)<sub>2</sub> (10 mol%), **L** (11 mol%), 2,6-lutidine (1.0 equiv), and MS 4Å (100 mg) were added in MeCN (1.5 mL). <sup>b</sup> When Cu(NTf<sub>2</sub>)<sub>2</sub> was used, the same results were obtained (96% yield, 88% ee). <sup>c</sup> 2,6-Lutidine was not added. <sup>d</sup> The reaction was carried out at –60 °C for 24 h. <sup>e</sup> Selectfluor **F1** did not dissolve in less polar solvents like chlorobenzene and toluene. <sup>f</sup> The results when the reaction was quenched after 1 h. <sup>g</sup> **1b** (6.0 mmol) was used in the presence of Cu(OTf)<sub>2</sub> (1.0 mol%), **L2** (1.1 mol%), and MS 4Å (1.5 g). <sup>h</sup> The yield and ee of **2b'** are shown when *N*-(phenylacetyl)pyrazole **1b'** was used in the presence of MS 4Å (150 mg).



## 2-5-8. General procedure for the enantioselective $\alpha$ -fluorination reaction of **1** (Tables 1–4)

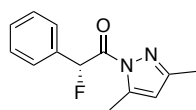


A mixture of **L2** and copper(II) triflate (10.9 mg, 0.030 mmol, in an inert atmosphere (Ar) of glove box) and 4Å pellet or powdered molecular sieves (100–150 mg) in 20 mL shlenk flask were dissolved in acetonitrile (1.5 mL, freshly distilled from calcium hydride and dried over activated molecular sieves 4Å) or acetone (1.5 mL). To a solution of the mixture were added **1**, **F1** (117 mg, 0.33 mmol) or **F2** (155 mg, 0.33 mmol) and 2,6-lutidine (35  $\mu\text{L}$ , 0.30 mmol) at  $-40\text{ }^\circ\text{C}$  or  $-20\text{ }^\circ\text{C}$ . The mixture was stirred at the same temperature for 6 ~ 24 h. The reaction mixture was filtered through neutral silica short column (*n*-hexane/EtOAc = 1/1). After evaporation of the organic solvent under reduced pressure, the crude mixture was purified by neutral silica gel column chromatography (*n*-hexane/EtOAc = 30/1 to 9/1) to give the desired product **2**. The enantiomeric excess (ee) was determined through chiral HPLC analysis.



**(2R)-2-Fluoro-2-phenyl-1-(1H-pyrazol-1-yl)ethan-1-one (2b')**: entry 12 in Table 1, 38% yield as

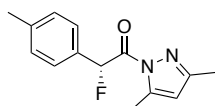
a colorless solid. TLC,  $R_f = 0.17$  (*n*-hexane:EtOAc = 10:1);  $[\alpha]_D^{29} = -2.0$  ( $c$  1.00,  $\text{CHCl}_3$ , 81% ee);  $^1\text{H}$  NMR (400 MHz,  $\text{CDCl}_3$ )  $\delta$  6.45 (dd,  $J = 2.8, 1.4$  Hz, 1H), 7.05 (d,  $J = 47.7$  Hz, 1H), 7.34–7.42 (m, 3H), 7.58–7.66 (m, 2H), 7.71 (s, 1H), 8.24 (d,  $J = 3.2$  Hz, 1H);  $^{13}\text{C}$  NMR (100 MHz,  $\text{CDCl}_3$ )  $\delta$  88.8 (d,  $J = 179.3$  Hz), 110.6, 128.0 (d,  $J = 4.8$  Hz, 2C), 128.9, 129.1, 130.0 (2C), 133.7 (d,  $J = 21.0$  Hz), 145.0, 166.6 (d,  $J = 27.7$  Hz);  $^{19}\text{F}$  (376 MHz,  $\text{CDCl}_3$ )  $\delta$  -179.1 (d,  $J = 27.7$  Hz); IR (KBr) 3154, 1743, 1390, 1058  $\text{cm}^{-1}$ ; HRMS (ESI+) calcd for  $\text{C}_{11}\text{H}_9\text{FN}_2\text{NaO}$   $[\text{M}+\text{Na}]^+$  227.0591, found 227.0591; HPLC analysis; OD-3, *n*-hexane/*i*-PrOH = 99/1, 1.0 mL/min,  $t_R = 12.5$  min (minor),  $t_R = 19.8$  min (major).



**(R)-1-(3,5-Dimethyl-1H-pyrazol-1-yl)-2-fluoro-2-phenylethan-1-one (2b)**: entry 10 in Table 1,

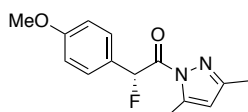
99% yield as a colorless oil. TLC,  $R_f = 0.17$  (*n*-hexane:EtOAc = 20:1);  $[\alpha]_D^{26} = 62.4$  ( $c$  1.00,  $\text{CHCl}_3$ , 91% ee);  $^1\text{H}$  NMR (400 MHz,  $\text{CDCl}_3$ )  $\delta$  2.20 (s, 3H), 2.53 (s, 3H), 5.94 (s, 1H), 7.06 (d,  $J = 48.6$  Hz, 1H), 7.36–7.38 (m, 3H),

7.62–7.64 (m, 2H);  $^{13}\text{C}$  NMR (100 MHz,  $\text{CDCl}_3$ )  $\delta$  13.9, 14.9, 88.7 (d,  $J = 177.3$  Hz), 111.8, 127.9, 128.0, 128.7, 129.5, 134.5 (d,  $J = 21.0$  Hz), 153.2, 168.0 (d,  $J = 27.7$  Hz);  $^{19}\text{F}$  (376 MHz,  $\text{CDCl}_3$ )  $\delta$  -178.4 (d,  $J = 49.1$  Hz); IR (neat) 2929, 1741, 1588, 1382, 962, 747  $\text{cm}^{-1}$ ; HRMS (ESI+) calcd for  $\text{C}_{13}\text{H}_{13}\text{FN}_2\text{NaO}$   $[\text{M}+\text{Na}]^+$  255.0904, found 255.0904; HPLC analysis; OD-3, *n*-hexane/*i*-PrOH = 99/1, 1.0 mL/min,  $t_{\text{R}} = 6.3$  min (minor),  $t_{\text{R}} = 9.1$  min (major).



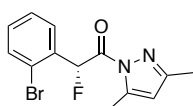
**(R)-1-(3,5-Dimethyl-1H-pyrazol-1-yl)-2-fluoro-2-(*p*-tolyl)ethan-1-one (2c):** entry 1 in Table

2, 93% yield as a yellow solid. TLC,  $R_f = 0.24$  (*n*-hexane:EtOAc = 20:1);  $[\alpha]_{\text{D}}^{27} = -12.8$  ( $c$  1.00,  $\text{CHCl}_3$ , 91% ee);  $^1\text{H}$  NMR (400 MHz,  $\text{CDCl}_3$ )  $\delta$  2.19 (s, 3H), 2.34 (s, 3H), 2.53 (s, 3H), 5.93 (s, 1H), 7.01 (d,  $J = 48.6$  Hz, 1H), 7.18 (d,  $J = 7.8$  Hz, 2H), 7.51 (d,  $J = 7.8$  Hz, 2H);  $^{13}\text{C}$  NMR (100 MHz,  $\text{CDCl}_3$ )  $\delta$  14.0, 14.2, 21.4, 88.8 (d,  $J = 10.2$  Hz), 111.8, 128.0 (d,  $J = 5.7$  Hz, 2C), 129.4 (2C), 131.6 (d,  $J = 21.0$  Hz), 139.6, 144.8, 153.2, 168.2 (d,  $J = 28.6$  Hz);  $^{19}\text{F}$  (376 MHz,  $\text{CDCl}_3$ )  $\delta$  -176.0 (d,  $J = 52.0$  Hz); IR (KBr) 3113, 2940, 1741, 1589, 1380, 1346, 962  $\text{cm}^{-1}$ ; HRMS (FAB+) calcd for  $\text{C}_{14}\text{H}_{15}\text{FN}_2\text{NaO}$   $[\text{M}+\text{Na}]^+$  269.1066, found 269.1064; HPLC analysis: OD-3, *n*-hexane/*i*-PrOH = 99/1, 1.0 mL/min,  $t_{\text{R}} = 5.7$  min (minor),  $t_{\text{R}} = 6.9$  min (major).



**(R)-1-(3,5-Dimethyl-1H-pyrazol-1-yl)-2-fluoro-2-(4-methoxy-phenyl)ethan-1-one (2d):**

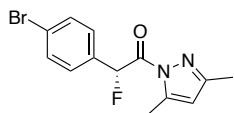
entry 2 in Table 2, 97% yield as a colorless solid. TLC,  $R_f = 0.18$  (*n*-hexane:EtOAc = 20:1);  $[\alpha]_{\text{D}}^{27} = 42.4$  ( $c$  1.00,  $\text{CHCl}_3$ , 89% ee);  $^1\text{H}$  NMR (400 MHz,  $\text{CDCl}_3$ )  $\delta$  2.19 (s, 3H), 2.53 (s, 3H), 3.80 (s, 3H), 5.93 (s, 1H), 6.89 (d,  $J = 8.7$  Hz, 2H), 6.99 (d,  $J = 48.7$  Hz, 1H), 7.55 (d,  $J = 8.7$  Hz, 2H);  $^{13}\text{C}$  NMR (100 MHz,  $\text{CDCl}_3$ )  $\delta$  13.9, 14.1, 55.4, 88.5 (d,  $J = 177.3$  Hz), 111.7, 114.1 (2C), 126.5 (d,  $J = 20.0$  Hz), 129.6 (2C), 144.7, 153.1, 160.6, 168.2 (d,  $J = 28.6$  Hz);  $^{19}\text{F}$  (376 MHz,  $\text{CDCl}_3$ )  $\delta$  -175.1 (d,  $J = 57.8$  Hz); IR (KBr) 3116, 2934, 2843, 1736, 1610, 1513, 1385, 1303, 1251, 1174, 1029  $\text{cm}^{-1}$ ; HRMS (FAB+) calcd for  $\text{C}_{14}\text{H}_{15}\text{FN}_2\text{NaO}_2$   $[\text{M}+\text{Na}]^+$  285.1015, found 285.1013; HPLC analysis: OD-3, *n*-hexane/*i*-PrOH = 99/1, 1.0 mL/min,  $t_{\text{R}} = 7.8$  min (minor),  $t_{\text{R}} = 10.2$  min (major).



**(R)-2-(2-Bromophenyl)-1-(3,5-dimethyl-1H-pyrazol-1-yl)-2-fluoroethan-1-one (2e):** entry 3

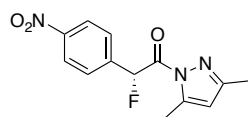
in Table 2, 86% yield as a colorless solid. TLC,  $R_f = 0.33$  (*n*-hexane:EtOAc = 20:1);  $[\alpha]_{\text{D}}^{27} = -227.5$  ( $c$  1.00,  $\text{CHCl}_3$ , 95% ee);  $^1\text{H}$  NMR (400 MHz,  $\text{CDCl}_3$ )  $\delta$  2.16 (s, 3H), 2.58 (s, 3H), 5.95 (s, 1H), 7.21–7.36 (m, 3H), 7.52 (d,  $J = 8.2$  Hz, 1H), 7.63 (d,  $J = 2.0$  Hz, 2H);  $^{13}\text{C}$  NMR (100 MHz,  $\text{CDCl}_3$ )  $\delta$  13.9, 14.0, 88.6 (d,  $J = 178.3$  Hz), 111.9,

124.7 (d,  $J = 4.8$  Hz), 127.9, 129.1, 131.2, 133.5, 133.8 (d,  $J = 73.4$  Hz), 144.5, 153.5, 167.5 (d,  $J = 26.7$  Hz);  $^{19}\text{F}$  (376 MHz,  $\text{CDCl}_3$ )  $\delta -176.0$  (d,  $J = 57.8$  Hz); IR (KBr) 3125, 2927, 1736, 1386, 1066, 963, 846, 758  $\text{cm}^{-1}$ ; HRMS (ESI) calcd for  $\text{C}_{13}\text{H}_{12}\text{BrFN}_2\text{NaO}$   $[\text{M}+\text{Na}]^+$  333.0001, found 333.0009; HPLC analysis: OD-3, *n*-hexane/*i*-PrOH = 99/1, 1.0 mL/min,  $t_{\text{R}} = 8.9$  min (minor),  $t_{\text{R}} = 12.1$  min (major).



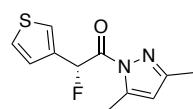
**(R)-2-(4-Bromophenyl)-1-(3,5-dimethyl-1H-pyrazol-1-yl)-2-fluoro-ethan-1-one (2f):**

entry 4 in Table 2, 94% yield as a yellow solid. TLC,  $R_f = 0.33$  (*n*-hexane:EtOAc = 20:1);  $[\alpha]_{\text{D}}^{27} = 46.0$  ( $c$  1.00,  $\text{CHCl}_3$ , 91% ee);  $^1\text{H}$  NMR (400 MHz,  $\text{CDCl}_3$ )  $\delta$  2.21 (s, 3H), 2.52 (s, 3H), 5.96 (s, 1H), 7.01 (d,  $J = 48.1$  Hz, 1H), 7.50 (s, 4H);  $^{13}\text{C}$  NMR (100 MHz,  $\text{CDCl}_3$ )  $\delta$  14.0, 14.1, 88.2 (d,  $J = 178.3$  Hz), 112.0, 123.9, 129.6 (d,  $J = 5.7$  Hz, 2C), 131.9, 133.5 (d,  $J = 21.0$ ), 144.9, 153.5, 167.5 (d,  $J = 26.7$  Hz);  $^{19}\text{F}$  (376 MHz,  $\text{CDCl}_3$ )  $\delta -179.4$  (d,  $J = 49.1$  Hz); IR (KBR) 3463, 3073, 2979, 2937, 1749, 1587, 1489, 1379, 1301, 1194, 1012  $\text{cm}^{-1}$ ; HRMS (ESI+) calcd for  $\text{C}_{13}\text{H}_{12}\text{BrFN}_2\text{NaO}$   $[\text{M}+\text{Na}]^+$  333.0001, found 333.0009; HPLC analysis: ID-3, *n*-hexane/*i*-PrOH = 99/1, 1.0 mL/min,  $t_{\text{R}} = 7.6$  min (minor),  $t_{\text{R}} = 8.2$  min (major).



**(R)-1-(3,5-Dimethyl-1H-pyrazol-1-yl)-2-fluoro-2-(4-nitrophenyl)-ethan-1-one (2g):**

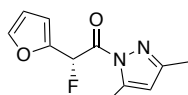
entry 5 in Table 2, 89% yield as a yellow solid. TLC,  $R_f = 0.25$  (*n*-hexane:EtOAc = 9:1);  $[\alpha]_{\text{D}}^{27} = -96.7$  ( $c$  1.00,  $\text{CHCl}_3$ , 91% ee);  $^1\text{H}$  NMR (400 MHz,  $\text{CDCl}_3$ )  $\delta$  2.24 (s, 3H), 2.53 (s, 3H), 6.00 (s, 1H), 7.16 (d,  $J = 48.1$  Hz, 1H), 7.84 (d,  $J = 8.7$  Hz, 2H), 8.23 (d,  $J = 8.2$  Hz, 2H);  $^{13}\text{C}$  NMR (100 MHz,  $\text{CDCl}_3$ )  $\delta$  14.0, 14.0, 87.7 (d,  $J = 179.3$  Hz), 112.3, 123.9 (2C), 128.7 (d,  $J = 5.7$  Hz, 2C), 141.2 (d,  $J = 21.0$  Hz), 145.1, 148.5, 153.9, 166.6 (d,  $J = 26.7$  Hz);  $^{19}\text{F}$  (376 MHz,  $\text{CDCl}_3$ )  $\delta -182.1$  (d,  $J = 46.2$  Hz); IR (KBr) 3115, 1740, 1525, 1388, 1346, 1069, 961, 827, 740  $\text{cm}^{-1}$ ; HRMS (FAB+) calcd for  $\text{C}_{13}\text{H}_{13}\text{FN}_3\text{O}_3$   $[\text{M}+\text{H}]^+$  278.0941, found 278.0948; HPLC analysis: OD-3, *n*-hexane/*i*-PrOH = 99/1, 1.0 mL/min,  $t_{\text{R}} = 14.0$  min (minor),  $t_{\text{R}} = 15.8$  min (major).



**(R)-1-(3,5-Dimethyl-1H-pyrazol-1-yl)-2-fluoro-2-(thiophen-3-yl)ethan-1-one (2h):** entry 6 in

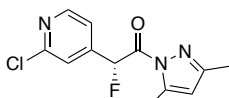
Table 2, 78% yield as a brown solid. TLC,  $R_f = 0.20$  (*n*-hexane:EtOAc = 20:1);  $[\alpha]_{\text{D}}^{27} = 62.0$  ( $c$  1.00,  $\text{CHCl}_3$ , 91% ee);  $^1\text{H}$  NMR (400 MHz,  $\text{CDCl}_3$ )  $\delta$  2.22 (s, 3H), 2.55 (s, 3H), 5.97 (s, 1H), 7.15 (d,  $J = 48.6$  Hz, 1H), 7.25–7.33 (m, 3H), 7.55 (s, 1H);  $^{13}\text{C}$  NMR (100 MHz,  $\text{CDCl}_3$ )  $\delta$  13.9, 14.1, 85.1 (d,  $J = 176.4$  Hz), 111.9, 125.7 (d,  $J = 6.7$  Hz),

126.3, 126.6 (d,  $J = 2.9$  Hz), 135.1 (d,  $J = 22.9$  Hz), 144.8, 153.8, 167.5 (d,  $J = 27.7$  Hz);  $^{19}\text{F}$  (376 MHz,  $\text{CDCl}_3$ )  $\delta$  -172.4 (d,  $J = 46.2$  Hz); IR (KBr) 3120, 2975, 2928, 2855, 1734, 1590, 1381, 1303, 1230, 1146  $\text{cm}^{-1}$ ; HRMS (FAB+) calcd for  $\text{C}_{11}\text{H}_{11}\text{FN}_2\text{NaOS}$   $[\text{M}+\text{Na}]^+$  261.0474, found 261.0471; HPLC analysis: OD-3, *n*-hexane/*i*-PrOH = 99/1, 1.0 mL/min,  $t_{\text{R}} = 8.5$  min (minor),  $t_{\text{R}} = 10.0$  min (major).



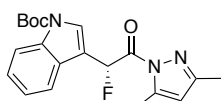
**(R)-1-(3,5-Dimethyl-1H-pyrazol-1-yl)-2-fluoro-2-(furan-2-yl)ethan-1-one (2i):** entry 7 in Table

2, 82% yield as a colorless oil. TLC,  $R_f = 0.21$  (*n*-hexane:EtOAc = 20:1);  $[\alpha]_{\text{D}}^{24} = 3.2$  ( $c$  1.00,  $\text{CHCl}_3$ , 93% ee);  $^1\text{H}$  NMR (400 MHz,  $\text{CDCl}_3$ )  $\delta$  2.15 (s, 3H), 2.59 (d,  $J = 0.9$  Hz, 3H), 5.96 (s, 1H), 6.36–6.43 (m, 1H), 6.56–6.63 (m, 1H), 7.04 (d,  $J = 50.0$  Hz, 1H), 7.43–7.48 (m, 1H);  $^{13}\text{C}$  NMR (100 MHz,  $\text{CDCl}_3$ )  $\delta$  13.9, 14.1, 81.7 (d,  $J = 178.3$  Hz), 111.1 (d,  $J = 3.8$  Hz), 111.9, 112.4 (d,  $J = 5.7$  Hz), 144.3 (d,  $J = 3.8$  Hz), 144.7, 147.3 (d,  $J = 21.9$  Hz), 153.5, 165.5 (d,  $J = 28.6$  Hz);  $^{19}\text{F}$  (376 MHz,  $\text{CDCl}_3$ )  $\delta$  -173.2–-173.1 (m, 1F); IR (KBr) 1744, 1587, 1378, 962  $\text{cm}^{-1}$ ; HRMS (ESI+) calcd for  $\text{C}_{11}\text{H}_{11}\text{FN}_2\text{NaO}_2$   $[\text{M}+\text{Na}]^+$  245.0697, found 245.0697; HPLC analysis: OD-3, *n*-hexane/*i*-PrOH = 99/1, 1.0 mL/min,  $t_{\text{R}} = 8.3$  min (minor),  $t_{\text{R}} = 10.5$  min (major).



**(R)-2-(2-Chloropyridin-4-yl)-1-(3,5-dimethyl-1H-pyrazol-1-yl)-2-fluoroethan-1-one (2j):**

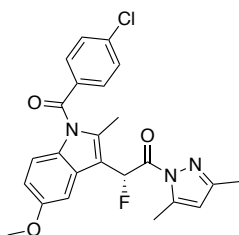
entry 8 in Table 2, 76% yield as a colorless oil. TLC,  $R_f = 0.38$  (*n*-hexane:EtOAc = 3:1);  $[\alpha]_{\text{D}}^{25} = 105.2$  ( $c$  1.00,  $\text{CHCl}_3$ , 91% ee);  $^1\text{H}$  NMR (400 MHz,  $\text{CDCl}_3$ )  $\delta$  2.26 (s, 3H), 2.54 (d,  $J = 0.9$  Hz, 3H), 6.03 (s, 1H), 7.08 (d,  $J = 48.6$  Hz, 1H), 7.46–7.52 (m, 1H), 7.62 (d,  $J = 0.9$  Hz, 1H), 8.41 (d,  $J = 5.5$  Hz, 1H);  $^{13}\text{C}$  NMR (100 MHz,  $\text{CDCl}_3$ )  $\delta$  14.0 (2C), 86.7 (d,  $J = 181.2$  Hz), 112.5, 120.6 (d,  $J = 6.7$  Hz), 122.7 (d,  $J = 5.7$  Hz), 145.1, 146.2 (d,  $J = 21.9$  Hz), 150.1, 152.0, 154.2, 165.8 (d,  $J = 25.8$  Hz);  $^{19}\text{F}$  (376 MHz,  $\text{CDCl}_3$ )  $\delta$  -186.8 (d,  $J = 49.1$  Hz, 1F); IR (KBr) 1737, 1594, 1384, 1079  $\text{cm}^{-1}$ ; HRMS (FAB+) calcd for  $\text{C}_{12}\text{H}_{12}\text{ClFN}_3\text{O}$   $[\text{M}+\text{H}]^+$  268.0653, found 268.0642; HPLC analysis: AS-3, *n*-hexane/*i*-PrOH = 9/1, 1.0 mL/min,  $t_{\text{R}} = 7.0$  min (minor),  $t_{\text{R}} = 16.5$  min (major).



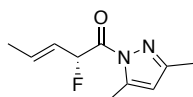
**tert-Butyl (R)-3-(2-(3,5-dimethyl-1H-pyrazol-1-yl)-1-fluoro-2-oxoethyl)-1H-indole-1-**

**carboxylate (2k):** entry 9 in Table 2. Acetone was used as solvent. 89% yield as a colorless solid. TLC,  $R_f = 0.16$  (*n*-hexane:EtOAc = 20:1);  $[\alpha]_{\text{D}}^{27} = -28.8$  ( $c$  1.00,  $\text{CHCl}_3$ , 92% ee);  $^1\text{H}$  NMR (400 MHz,  $\text{CDCl}_3$ )  $\delta$  1.67 (s, 9H), 2.17 (s, 3H), 2.55 (d,  $J = 0.9$  Hz, 3H), 5.93 (s, 1H), 7.22–7.39 (m, 3H), 7.92 (dd,  $J = 7.8, 0.9$  Hz, 1H), 8.12 (br, 1H).  $^{13}\text{C}$  NMR (100 MHz,  $\text{CDCl}_3$ )  $\delta$  14.2, 14.5, 28.6 (3C), 82.9, 84.7 (d,  $J = 11.4$  Hz), 112.1, 114.7 (d,  $J = 23.8$  Hz), 115.6, 120.9, 123.5, 125.3, 127.3 (d,  $J = 8.6$  Hz), 128.5, 135.8, 145.1, 149.8, 153.5, 167.8 (d,  $J = 28.6$  Hz);  $^{19}\text{F}$  (376 MHz,  $\text{CDCl}_3$ )  $\delta$  -179.6 (d,  $J = 57.8$  Hz); IR (KBR) 3116, 3059, 2977, 2932, 1751, 1455, 1386, 1238, 1155, 1089

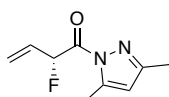
cm<sup>-1</sup>; HRMS (FAB<sup>+</sup>) calcd for C<sub>20</sub>H<sub>22</sub>FN<sub>3</sub>NaO<sub>3</sub> [M+Na]<sup>+</sup> 394.1543, found 394.1540; HPLC analysis: AS-3, *n*-hexane/*i*-PrOH = 99/1, 1.0 mL/min, *t*<sub>R</sub> = 9.2 min (minor), *t*<sub>R</sub> = 17.7 min (major).



**(R)-2-[1-(4-Chlorobenzoyl)-5-methoxy-2-methyl-1H-indol-3-yl]-1-(3,5-dimethyl-1H-pyrazol-1-yl)-2-fluoroethan-1-one (2l):** entry 10 in Table 2, 47% yield as a yellow solid. TLC, *R*<sub>f</sub> = 0.34 (*n*-hexane:EtOAc = 5:1); [α]<sub>D</sub><sup>26</sup> = -20.0 (*c* 1.00, CHCl<sub>3</sub>, 87% ee); <sup>1</sup>H NMR (400 MHz, CDCl<sub>3</sub>) δ 2.17 (s, 3H), 2.55 (s, 3H), 2.60 (d, *J* = 3.2 Hz, 3H), 3.87 (s, 3H), 5.93 (s, 1H), 6.67 (dd, *J* = 9.2, 2.3 Hz, 1H), 6.84 (d, *J* = 8.7 Hz, 1H), 7.16 (d, *J* = 46.7 Hz, 1H), 7.40 (d, *J* = 2.3 Hz, 1H) 7.42–7.49 (m, 2H), 7.59–7.68 (m, 2H); <sup>13</sup>C NMR (100 MHz, CDCl<sub>3</sub>) δ 13.9, 13.9, 14.2, 55.8, 83.9 (d, *J* = 174.5 Hz), 102.5, 111.6, 112.4 (d, *J* = 23.8 Hz), 112.7, 114.7, 128.3, 129.3, 130.9, 131.5, 133.5, 139.0 (d, *J* = 8.6 Hz), 140.0, 144.8, 152.9, 156.2, 167.3 (d, *J* = 30.5 Hz), 168.5; <sup>19</sup>F (376 MHz, CDCl<sub>3</sub>) δ -182.2 (d, *J* = 49.2 Hz, 1F); IR (KBr) 2927, 1744, 1692, 1591, 1476, 1377, 1308, 1217 cm<sup>-1</sup>; HRMS (FAB<sup>+</sup>) calcd for C<sub>24</sub>H<sub>21</sub>ClFN<sub>3</sub>O<sub>3</sub> [M]<sup>+</sup> 453.1255, found 453.1255; HPLC analysis: AS-3, *n*-hexane/*i*-PrOH = 9/1, 1.0 mL/min, *t*<sub>R</sub> = 11.2 min (minor), *t*<sub>R</sub> = 17.1 min (major).

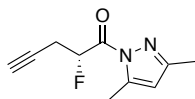


**(R,E)-1-(3,5-Dimethyl-1H-pyrazol-1-yl)-2-fluoropent-3-en-1-one (2m):** entry 1 in Table 3, 94% yield as a colorless solid. TLC, *R*<sub>f</sub> = 0.25 (*n*-hexane:EtOAc = 20:1); [α]<sub>D</sub><sup>27</sup> = 77.2 (*c* 1.00, CHCl<sub>3</sub>, 84% ee); <sup>1</sup>H NMR (400 MHz, CDCl<sub>3</sub>) δ 1.71–1.79 (m, 3H), 2.21 (s, 3H), 2.56 (s, 3H), 5.72–5.85 (m, 1H), 5.99 (s, 1H), 6.05–6.17 (m, 1H), 6.33–6.51 (m, 1H); <sup>13</sup>C NMR (100 MHz, CDCl<sub>3</sub>) δ 13.9, 14.1, 87.9 (d, *J* = 177.4 Hz), 111.7, 123.8 (d, *J* = 19.1 Hz), 132.9 (d, *J* = 11.4 Hz), 144.8, 153.3, 168.2 (d, *J* = 26.7 Hz); <sup>19</sup>F (376 MHz, CDCl<sub>3</sub>) δ -185.4 (d, *J* = 34.7 Hz); IR (KBR) 2966, 2925, 2863, 1747, 1585, 1387, 1321, 1130, 1091 cm<sup>-1</sup>; HRMS (FAB<sup>+</sup>) calcd for C<sub>10</sub>H<sub>13</sub>FN<sub>2</sub>NaO [M+Na]<sup>+</sup> 219.0910, found 219.0911; HPLC analysis: AS-3, *n*-hexane/*i*-PrOH = 99/1, 1.0 mL/min, *t*<sub>R</sub> = 5.8 min (minor), *t*<sub>R</sub> = 12.2 min (major).



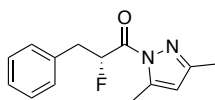
**(R)-1-(3,5-dimethyl-1H-pyrazol-1-yl)-2-fluorobut-3-en-1-one (2n):** entry 2 in Table 3, 89% yield as a yellow oil. TLC, *R*<sub>f</sub> = 0.20 (*n*-hexane:EtOAc = 20:1); [α]<sub>D</sub><sup>26</sup> = 135.6 (*c* 1.00, CHCl<sub>3</sub>, 84% ee). <sup>1</sup>H NMR (400 MHz, CDCl<sub>3</sub>) δ 2.23 (s, 3H), 2.56 (d, *J* = 0.9 Hz, 3H), 5.35–5.43 (m, 1H), 5.68 (ddd, *J* = 17.4, 2.8, 1.8 Hz, 1H), 6.00 (s, 1H), 6.19 (dddd, *J* = 18.3, 17.4, 10.5, 4.6 Hz, 1H), 6.48 (ddt, *J* = 48.6, 5.0, 1.8 Hz, 1H); <sup>13</sup>C NMR (100 MHz, CDCl<sub>3</sub>) δ 13.9, 14.1, 88.1 (d, *J* = 179.3 Hz), 111.7, 119.1 (d, *J* = 11.4 Hz), 130.8 (d, *J* = 19.1 Hz), 144.8,

153.5, 167.5 (d,  $J = 25.7$  Hz);  $^{19}\text{F}$  (376 MHz,  $\text{CDCl}_3$ )  $\delta$  -193.1– -193.0 (m, 1F); IR (neat) 2931, 1748, 1384, 986, 858  $\text{cm}^{-1}$ ; HRMS (EI) calcd for  $\text{C}_9\text{H}_{11}\text{FN}_2\text{O}$   $[\text{M}]^+$  182.0855, found 182.0850; HPLC analysis: AS-3, *n*-hexane/*i*-PrOH = 99/1, 1.0 mL/min,  $t_{\text{R}} = 5.5$  min (minor),  $t_{\text{R}} = 8.7$  min (major).



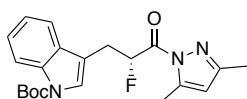
**(R)-1-(3,5-Dimethyl-1H-pyrazol-1-yl)-2-fluoro-4-pentyn-1-one (2o):** entry 3 in Table 3, 64%

yield as a colorless solid. TLC,  $R_f = 0.20$  (*n*-hexane:EtOAc = 20:1);  $[\alpha]_{\text{D}}^{24} = 73.6$  ( $c$  1.00,  $\text{CHCl}_3$ , 91% ee).  $^1\text{H}$  NMR (400 MHz,  $\text{CDCl}_3$ )  $\delta$  2.12 (t,  $J = 0.9$  Hz, 1H), 2.23 (s, 3H), 2.57 (d,  $J = 0.9$  Hz, 3H), 3.01–3.06 (m, 1H), 3.10 (dd,  $J = 5.0, 2.3$  Hz, 1H), 6.01 (s, 1H), 6.07 (dt,  $J = 48.6, 5.0$  Hz, 1H);  $^{13}\text{C}$  NMR (100 MHz,  $\text{CDCl}_3$ )  $\delta$  13.9, 14.1, 23.4, 23.6, 71.9, 86.8 (d,  $J = 183.1$  Hz), 111.8, 144.9, 153.7, 167.3 (d,  $J = 22.9$  Hz);  $^{19}\text{F}$  (376 MHz,  $\text{CDCl}_3$ )  $\delta$  -191.3– -191.1 (m, 1F); IR (KBr) 3264, 1743, 1586, 1401, 1088, 963, 698  $\text{cm}^{-1}$ ; HRMS (ESI+) calcd for  $\text{C}_{10}\text{H}_{11}\text{FN}_2\text{NaO}$   $[\text{M}+\text{Na}]^+$  217.0748, found 217.0754; HPLC analysis: AD-3, *n*-hexane/*i*-PrOH = 99/1, 1.0 mL/min,  $t_{\text{R}} = 12.0$  min (major),  $t_{\text{R}} = 14.0$  min (minor).



**(R)-1-(3,5-Dimethyl-1H-pyrazol-1-yl)-2-fluoro-3-phenylpropan-1-one (2p):** entry 4 in Table

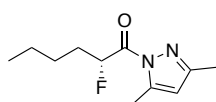
3, 84% yield as a colorless oil. TLC,  $R_f = 0.25$  (*n*-hexane:EtOAc = 20:1);  $[\alpha]_{\text{D}}^{26} = 16.8$  ( $c$  1.00,  $\text{CHCl}_3$ , 97% ee);  $^1\text{H}$  NMR (400 MHz,  $\text{CDCl}_3$ )  $\delta$  2.26 (s, 3H), 2.53 (s, 3H), 3.21 (ddd,  $J = 23.2, 14.8, 8.2$  Hz, 1H), 3.43 (ddd,  $J = 33.4, 14.6, 3.8$  Hz, 1H), 6.01 (s, 1H), 6.12 (ddd,  $J = 52.7, 8.2, 2.7$  Hz, 1H), 7.26–7.34 (m, 5H);  $^{13}\text{C}$  NMR (100 MHz,  $\text{CDCl}_3$ )  $\delta$  14.0, 14.1, 39.1 (d,  $J = 21.0$  Hz), 89.8 (d,  $J = 181.2$  Hz), 111.6, 127.2, 128.6 (2C), 129.5 (2C), 136.1, 144.8, 153.4, 168.9 (d,  $J = 95.3$  Hz);  $^{19}\text{F}$  (376 MHz,  $\text{CDCl}_3$ )  $\delta$  -192.2– -191.9 (m, 1F); IR (neat) 2928, 1746, 1389, 1327, 962  $\text{cm}^{-1}$ ; HRMS (FAB+) calcd for  $\text{C}_{14}\text{H}_{15}\text{FN}_2\text{NaO}$   $[\text{M}+\text{Na}]^+$  269.1066, found 269.1064; HPLC analysis: ID-3, *n*-hexane/*i*-PrOH = 99/1, 1.0 mL/min,  $t_{\text{R}} = 9.1$  min (minor),  $t_{\text{R}} = 10.1$  min (major).



**tert-Butyl (R)-3-(3-(3,5-dimethyl-1H-pyrazol-1-yl)-2-fluoro-3-oxopropyl)- 1H-indole-1-**

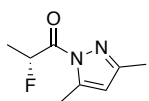
**carboxylate (2q):** entry 5 in Table 3, 86% yield as a colorless solid. TLC,  $R_f = 0.19$  (*n*-hexane:EtOAc = 20:1);  $[\alpha]_{\text{D}}^{27} = -2.0$  ( $c$  1.00,  $\text{CHCl}_3$ , 88% ee);  $^1\text{H}$  NMR (400 MHz,  $\text{CDCl}_3$ ) (ppm)  $\delta$  1.67 (s, 9H), 2.31 (s, 3H), 2.51 (d,  $J = 0.9$  Hz, 3H), 3.33 (ddd,  $J = 23.4, 15.1, 8.3$  Hz, 1H), 3.54 (dddd,  $J = 32.5, 15.1, 2.8, 0.9$  Hz, 1H), 6.03 (s, 1H), 6.24 (ddd,  $J = 49.9, 8.2, 1.8$  Hz, 1H), 7.23 (td,  $J = 7.8, 0.9$  Hz), 7.32 (td,  $J = 7.4, 1.4$  Hz, 1H), 7.52 (s, 1H), 7.60 (d,  $J =$

7.8 Hz, 1H), 8.14 (br, 1H);  $^{13}\text{C}$  NMR (100 MHz,  $\text{CDCl}_3$ )  $\delta$  14.0, 14.1, 28.3 (3C), 29.1 (d,  $J = 21.9$  Hz), 83.7, 88.5 (d,  $J = 180.0$  Hz), 111.6, 114.7, 115.4, 119.2, 122.6, 124.6, 130.3, 135.6, 145.0, 149.8, 153.5, 168.9 (d,  $J = 23.8$  Hz);  $^{19}\text{F}$  (376 MHz,  $\text{CDCl}_3$ )  $\delta$  -191.2–-191.0 (m, 1F); IR (KBr) 3135, 3050, 2972, 2928, 1734, 1457, 1372, 1157, 1088  $\text{cm}^{-1}$ ; HRMS (FAB+) calcd for  $\text{C}_{21}\text{H}_{25}\text{FN}_3\text{O}_3$   $[\text{M}+\text{H}]^+$  386.1880, found 386.1891; HPLC analysis: AD-3, *n*-hexane/*i*-PrOH = 50/1, 1.0 mL/min,  $t_{\text{R}} = 8.0$  min (minor),  $t_{\text{R}} = 8.9$  min (major).



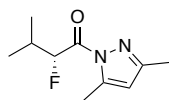
**(R)-1-(3,5-Dimethyl-1H-pyrazol-1-yl)-2-fluorohexan-1-one (2r):** entry 6 in Table 3, 93%

yield as a colorless oil.  $[\alpha]_{\text{D}}^{27} = 57.3$  ( $c$  1.00,  $\text{CHCl}_3$ , 89% ee). TLC,  $R_f = 0.26$  (*n*-hexane:EtOAc = 30:1);  $^1\text{H}$  NMR (400 MHz,  $\text{CDCl}_3$ )  $\delta$  0.92 (t,  $J = 7.3$  Hz, 3H), 1.31–1.62 (m, 4H), 2.22 (s, 3H), 2.56 (s, 3H), 5.98 (s, 1H), 6.00 (ddd,  $J = 50.4, 8.2, 3.6$  Hz, 1H);  $^{13}\text{C}$  NMR (100 MHz,  $\text{CDCl}_3$ )  $\delta$  13.9 (2C), 14.3, 22.3, 26.9, 32.4 (d,  $J = 21.0$  Hz), 89.2 (d,  $J = 176.4$  Hz), 111.5, 144.7, 153.2, 170.1 (d,  $J = 22.9$  Hz);  $^{19}\text{F}$  (376 MHz,  $\text{CDCl}_3$ )  $\delta$  -194.3–-194.0 (m, 1F); IR (neat) 2959, 1747, 1586, 1389, 1326, 961  $\text{cm}^{-1}$ ; HRMS (EI) calcd for  $\text{C}_{11}\text{H}_{17}\text{FN}_2\text{O}$   $[\text{M}]^+$  212.1325, found 212.1325; HPLC analysis: OB-H, *n*-hexane/*i*-PrOH = 99/1, 6.6 mL/min,  $t_{\text{R}} = 7.8$  min (minor),  $t_{\text{R}} = 8.7$  min (major).



**(R)-1-(3,5-Dimethyl-1H-pyrazol-1-yl)-2-fluoropropan-1-one (2s):** entry 7 in Table 3, 68% yield as

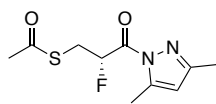
a colorless oil.  $[\alpha]_{\text{D}}^{23} = 73.2$  ( $c$  1.00,  $\text{CHCl}_3$ , 94% ee). TLC,  $R_f = 0.26$  (*n*-hexane:EtOAc = 20:1);  $^1\text{H}$  NMR (400 MHz,  $\text{CDCl}_3$ )  $\delta$  1.72 (dd,  $J = 23.8, 6.9$  Hz, 3H), 2.23 (s, 3H), 2.57 (s, 3H), 6.00 (s, 1H), 6.09 (dq,  $J = 49.5, 6.9$  Hz, 1H);  $^{13}\text{C}$  NMR (100 MHz,  $\text{CDCl}_3$ )  $\delta$  13.9, 14.2, 86.0 (d,  $J = 174.5$  Hz), 111.6, 144.8, 153.3, 170.4 (d,  $J = 22.9$  Hz);  $^{19}\text{F}$  (376 MHz,  $\text{CDCl}_3$ )  $\delta$  -185.7–-186.0 (m, 1F); IR (neat) 3398, 2984, 1746, 1584, 1417, 1298  $\text{cm}^{-1}$ ; HRMS (EI) calcd for  $\text{C}_8\text{H}_{11}\text{FN}_2\text{O}$   $[\text{M}]^+$  170.0855, found 170.0855; HPLC analysis: AD-3, *n*-hexane/*i*-PrOH = 99/1, 1.0 mL/min,  $t_{\text{R}} = 5.7$  min (minor),  $t_{\text{R}} = 9.7$  min (major).



**(R)-1-(3,5-Dimethyl-1H-pyrazol-1-yl)-2-fluoro-4-methylpentan-1-one (2t):** Entry 8 in Table 3,

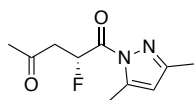
64% yield as a colorless oil.  $[\alpha]_{\text{D}}^{26} = 23.2$  ( $c$  1.00,  $\text{CHCl}_3$ , 93% ee); TLC,  $R_f = 0.24$  (*n*-hexane:EtOAc = 30:1);  $^1\text{H}$  NMR (400 MHz,  $\text{CDCl}_3$ )  $\delta$  0.97 (d,  $J = 7.3$ , 3H), 1.13 dd,  $J = 6.9$  Hz, 3H), 2.22 (s, 3H), 2.46 (do,  $J = 28.4, 3.6$  Hz, 1H), 2.57 (s, 1H), 5.87 (dd,  $J = 49.5, 3.2$  Hz, 1H), 5.99 (s, 1H);  $^{13}\text{C}$  NMR (100 MHz,  $\text{CDCl}_3$ )  $\delta$  13.9, 14.3, 15.7 (d,  $J = 4.8$  Hz), 19.0 (d,  $J = 3.8$  Hz), 31.3 (d,  $J = 20.0$  Hz), 92.7 (d,  $J = 179.3$  Hz), 111.5, 144.6, 153.0, 169.5 (d,  $J =$

23.8 Hz);  $^{19}\text{F}$  (376 MHz,  $\text{CDCl}_3$ )  $\delta$  -205.5– -205.3 (m, 1F); IR (neat) 2970, 1744, 1587, 1387, 1140, 923  $\text{cm}^{-1}$ ; HRMS (ESI+) calcd for  $\text{C}_{10}\text{H}_{15}\text{FN}_2\text{NaO}$   $[\text{M}+\text{Na}]^+$  221.1067, found 221.1067; HPLC analysis: OB-H, *n*-hexane/*i*-PrOH = 99/1, 1.0 mL/min,  $t_{\text{R}}$  = 5.7 min (minor),  $t_{\text{R}}$  = 9.7 min (major).



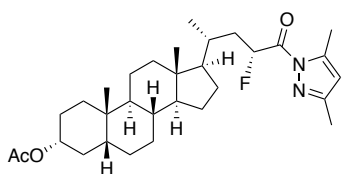
**(R)-1-(3,5-Dimethyl-1H-pyrazol-1-yl)-2-fluoro-3-thioacetylpropan-1-one (2u):** entry 1 in

Table 4, 90% yield as a colorless oil.  $[\alpha]_{\text{D}}^{26} = 27.6$  ( $c$  1.00,  $\text{CHCl}_3$ , 89% ee); TLC,  $R_f = 0.26$  (*n*-hexane:EtOAc = 10:1).  $^1\text{H}$  NMR (400 MHz,  $\text{CDCl}_3$ )  $\delta$  2.25 (s, 3H), 2.34 (s, 3H), 3.58–3.62 (m, 1H), 6.02 (s, 1H), 6.12 (dt,  $J = 49.0$ , 5.0 Hz, 1H);  $^{13}\text{C}$  NMR (100 MHz,  $\text{CDCl}_3$ )  $\delta$  13.9, 14.3, 15.7 (d,  $J = 4.8$  Hz), 31.3 (d,  $J = 20.0$  Hz), 92.7 (d,  $J = 179.3$  Hz), 111.5, 144.6, 153.0, 169.5 (d,  $J = 23.8$  Hz);  $^{19}\text{F}$  (376 MHz,  $\text{CDCl}_3$ )  $\delta$  -190.1– -189.9 (m, 1F); IR (neat) 2930, 1746, 1698, 1388, 1321, 1132, 961  $\text{cm}^{-1}$ ; HRMS (ESI+) calcd for  $\text{C}_{10}\text{H}_{13}\text{FN}_2\text{NaO}_2\text{S}$   $[\text{M}+\text{Na}]^+$  267.0574, found 267.0580; HPLC analysis: OD-3, *n*-hexane/*i*-PrOH = 99/1, 1.0 mL/min,  $t_{\text{R}}$  = 17.7 min (minor),  $t_{\text{R}}$  = 19.2 min (major).



**(R)-1-(3,5-Dimethyl-1H-pyrazol-1-yl)-2-fluoropentane-1,4-dione (2v):** entry 2 in Table 4, 79%

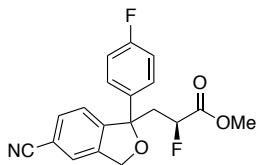
yield, 92% ee as a colorless solid. TLC,  $R_f = 0.13$  (*n*-hexane:EtOAc = 5:1). >99% ee after recrystallization with  $\text{CHCl}_3$  and *n*-hexane.  $[\alpha]_{\text{D}}^{26} = 10.9$  ( $c$  0.70,  $\text{CHCl}_3$ , >99% ee);  $^1\text{H}$  NMR (400 MHz,  $\text{CDCl}_3$ )  $\delta$  2.21 (s, 3H), 2.26 (s, 3H), 2.56 (s, 3H), 3.15 (ddd,  $J = 20.2$ , 17.4, 7.8 Hz, 1H), 3.26 (ddd,  $J = 30.7$ , 17.4, 3.2, 1H), 6.00 (s, 1H), 6.36 (ddd,  $J = 48.1$ , 7.8, 3.2 Hz, 1H);  $^{13}\text{C}$  NMR (100 MHz,  $\text{CDCl}_3$ )  $\delta$  13.9, 14.1, 46.0 (d,  $J = 22.9$  Hz), 85.3 (d,  $J = 177.3$  Hz), 111.7, 144.9, 153.6, 168.5 (d,  $J = 22.9$  Hz), 203.3;  $^{19}\text{F}$  (376 MHz,  $\text{CDCl}_3$ )  $\delta$  -191.4– -191.2 (m, 1F); IR (KBr) 3109, 2989, 2963, 2934, 1747, 1714, 1363, 1325, 1087  $\text{cm}^{-1}$ ; HRMS (EI) calcd for  $\text{C}_{10}\text{H}_{13}\text{FN}_2\text{O}_2$   $[\text{M}]^+$  212.0961, found 212.0961; HPLC analysis: AD-3, *n*-hexane/*i*-PrOH = 4/1, 1.0 mL/min,  $t_{\text{R}}$  = 5.8 min (major),  $t_{\text{R}}$  = 6.4 min (minor).



**(1R,3aS,3bR,5aR,7R,9aS,9bS,11aR)-1-[(2R,4R)-5-(3,5-Dimethyl-1H-pyrazol-1-yl)-4-fluoro-5-oxopentan-2-yl]-9a,11a-dimethyl-hexadecahydro-1H-cyclopenta[a]phenanthren-7-yl acetate (2w):** entry 3 in Table 4, 94% yield, 90% de as a colorless oil. TLC,  $R_f = 0.25$  (*n*-hexane:EtOAc = 10:1);  $^1\text{H}$  NMR (400 MHz,  $\text{CDCl}_3$ )  $\delta$  0.68 (s, 3H), 0.93 (s, 3H), 0.94–1.90 (m, 29H, overlapped with  $\text{H}_2\text{O}$ ), 2.03 (s, 3H), 2.22 (s,

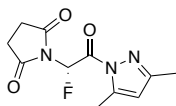


3H), 2.56 (s, 3H), 4.63–4.78 (m, 1H), 5.98 (s, 1H), 6.10 (ddd,  $J = 51.3, 10.5, 1.4$  Hz, 1H);  $^{13}\text{C}$  NMR (100 MHz,  $\text{CDCl}_3$ )  $\delta$  12.2, 14.0, 14.2, 18.3, 21.0, 23.5, 26.4, 26.8, 27.1, 28.4, 32.4, 33.0, 34.7, 35.2, 35.9, 38.9 (d,  $J = 21.0$  Hz), 40.3, 40.5, 42.0, 43.1, 56.4, 56.7, 74.5, 87.6 (d,  $J = 176.4$  Hz), 111.4, 144.7, 153.0, 170.7 (d,  $J = 22.9$  Hz), 170.8;  $^{19}\text{F}$  (376 MHz,  $\text{CDCl}_3$ )  $\delta$  -194.0–-193.7 (m, 1F); IR (KBr) 2933, 1738, 1382, 1260  $\text{cm}^{-1}$ ; HRMS (ESI+) calcd for  $\text{C}_{31}\text{H}_{47}\text{FN}_2\text{NaO}_3$   $[\text{M}+\text{Na}]^+$  537.3463, found 537.3463.



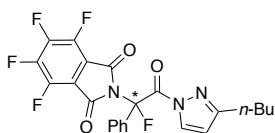
**methyl (2S)-3-(5-cyano-1-(4-fluorophenyl)-1,3-dihydroisobenzofuran-1-yl)-2-**

**fluoropropanoate (3x):** entry 4 in Table 4, 99% yield after one-pot esterification, dr = 48 (94% ee) / 52 (97% ee) as a colorless oil. Diastereomeric mixture is reported. TLC,  $R_f = 0.19$  (*n*-hexane:EtOAc = 3:1);  $^1\text{H}$  NMR (400 MHz,  $\text{CDCl}_3$ )  $\delta$  2.71–2.91 (m, 2H), 3.76 (s, 3H), 4.88–5.29 (m, 3H), 6.98–7.08 (m, 2H), 7.38–7.50 (m, 3H), 7.52 (s, 1H), 7.62 (d,  $J = 7.8$  Hz, 1H); Two isomers were determined by NMR analysis of racemic product **3x'** (dr = 64/36). Major diastereomer:  $^{13}\text{C}$  NMR (100 MHz,  $\text{CDCl}_3$ )  $\delta$  43.2 (d,  $J = 19.1$  Hz), 52.4, 71.4, 86.0 (d,  $J = 185.0$  Hz), 88.8, 112.1, 115.5 (d,  $J = 21.0$  Hz), 118.6, 123.1, 123.5, 125.4, 126.6 (d,  $J = 8.6$  Hz, 2C), 131.9, 138.9, 139.9, 148.1, 162.2 (d,  $J = 246.0$  Hz), 169.9 (d,  $J = 23.8$  Hz). Minor diastereomer:  $^{13}\text{C}$  NMR (100 MHz,  $\text{CDCl}_3$ )  $\delta$  43.5 (d,  $J = 20.0$  Hz), 52.6, 71.6, 85.9 (d,  $J = 186.1$  Hz), 88.8, 112.0, 115.6 (d,  $J = 21.9$  Hz), 118.6, 123.1, 123.5, 125.3, 126.6 (d,  $J = 8.6$  Hz, 2C), 131.8, 138.8, 139.9, 147.8, 162.2 (d,  $J = 246.0$  Hz), 169.9 (d,  $J = 23.8$  Hz);  $^{19}\text{F}$  (376 MHz,  $\text{CDCl}_3$ )  $\delta$  -189.8–-189.6 (m, major diastereomer), -188.4–-188.2 (m, minor diastereomer), -114.4–-114.2 (m); IR (neat) 2230, 1759, 1507, 1226, 1072  $\text{cm}^{-1}$ ; HRMS (ESI+) calcd for  $\text{C}_{19}\text{H}_{15}\text{F}_2\text{NNaO}_3$   $[\text{M}+\text{Na}]^+$  366.0912, found 366.0922. HPLC analysis: IC-3, *n*-hexane/EtOAc = 5/1, 1.0 mL/min, major diastereomer:  $t_R = 12.9$  min (minor),  $t_R = 46.4$  min (major), minor diastereomer:  $t_R = 13.8$  min (major),  $t_R = 18.7$  min (minor).



**1-[(1S)-2-(3,5-Dimethyl-1H-pyrazol-1-yl)-1-fluoro-2-oxoethyl]pyrrolidine-2,5-**

**dione (2y):** entry 5 in Table 4, 67% yield, 91% ee as a colorless solid.  $[\alpha]_D^{26} = -191.6$  (*c* 1.00,  $\text{CHCl}_3$ , 91% ee); TLC,  $R_f = 0.31$  (*n*-hexane:EtOAc = 1:1);  $^1\text{H}$  NMR (400 MHz,  $\text{CDCl}_3$ )  $\delta$  2.12 (s, 3H), 2.59 (s, 3H), 2.69–2.84 (m, 4H), 5.97 (s, 2H), 6.78 (d,  $J = 49.9$  Hz, 1H);  $^{13}\text{C}$  NMR (100 MHz,  $\text{CDCl}_3$ )  $\delta$  13.8, 13.9, 28.1 (2C), 82.3 (d,  $J = 205.9$  Hz), 111.5, 141.2, 153.8, 162.0 (d,  $J = 30.5$  Hz), 174.5 (2C);  $^{19}\text{F}$  (376 MHz,  $\text{CDCl}_3$ )  $\delta$  -160.8 (d,  $J = 52.0$  Hz); IR (KBr) 3499, 3102, 2985, 2941, 1721, 1380  $\text{cm}^{-1}$ ; HRMS (FAB+) calcd for  $\text{C}_{11}\text{H}_{13}\text{FN}_3\text{O}_2$   $[\text{M}+\text{H}]^+$  254.0941, found 254.0946. HPLC analysis: OD-3, *n*-hexane/*i*-PrOH = 4/1, 1.0 mL/min,  $t_R = 17.1$  min (major),  $t_R = 29.1$  min (minor).

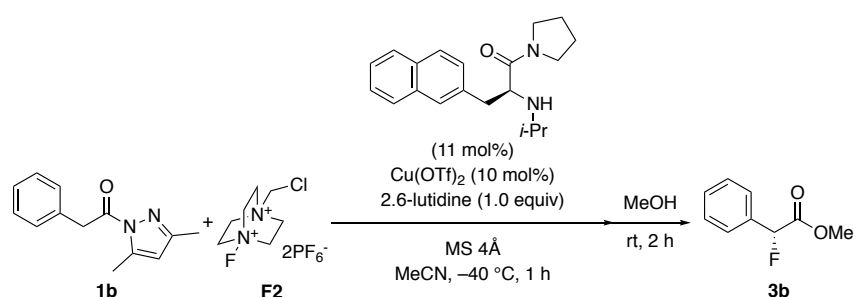


**(S)-2-(2-(3-butyl-1H-pyrazol-1-yl)-1-fluoro-2-oxo-1-phenylethyl)-4,5,6,7-**

**tetrafluoroisoindoline-1,3-dione (2z):** entry 6 in Table 4, 47% yield, -60% ee as a colorless solid.  $[\alpha]_D^{26} = -105.2$  (*c* 1.00,  $\text{CHCl}_3$ , >99% ee); TLC,  $R_f = 0.48$  (*n*-hexane:EtOAc = 5:1);  $^1\text{H}$  NMR (400 MHz,  $\text{CDCl}_3$ )  $\delta$  0.80 (t,  $J = 7.3$  Hz, 3H), 1.09–1.29 (m, 2H), 2.52 (t,  $J = 7.3$  Hz, 2H), 6.22 (d,  $J = 2.8$  Hz, 1H), 7.33–7.45 (m, 2H), 8.16 (d,  $J$

= 3.2 Hz, 1H);  $^{13}\text{C}$  NMR (100 MHz,  $\text{CDCl}_3$ )  $\delta$  13.2, 22.1, 28.1, 30.4, 95.8 (d,  $J = 216.4$  Hz), 110.1, 113.8 (2C), 127.0 (d,  $J = 8.6$  Hz, 2C), 128.4 (2C), 130.2 (2C), 131.0 (d,  $J = 8.6$  Hz), 131.9, 142.6 (m), 144.2 (m), 145.2 (m), 146.9 (m), 159.5, 160.2, 161.1 (d,  $J = 8.6$  Hz);  $^{19}\text{F}$  (376 MHz,  $\text{CDCl}_3$ )  $\delta$  -140.3 (d,  $J = 8.6$  Hz, 2F), -134.0 (d,  $J = 8.6$  Hz, 2F), -116.7; IR (KBr) 1742, 1595, 1516, 1474, 1402  $\text{cm}^{-1}$ ; HRMS (ESI+) calcd for  $\text{C}_{23}\text{H}_{17}\text{F}_5\text{N}_3\text{O}_3$   $[\text{M}+\text{H}]^+$  478.1185, found 478.1177. HPLC analysis: OD-3, *n*-hexane/*i*-PrOH = 4/1, 1.0 mL/min,  $t_R = 21.5$  min (minor),  $t_R = 24.6$  min (major).

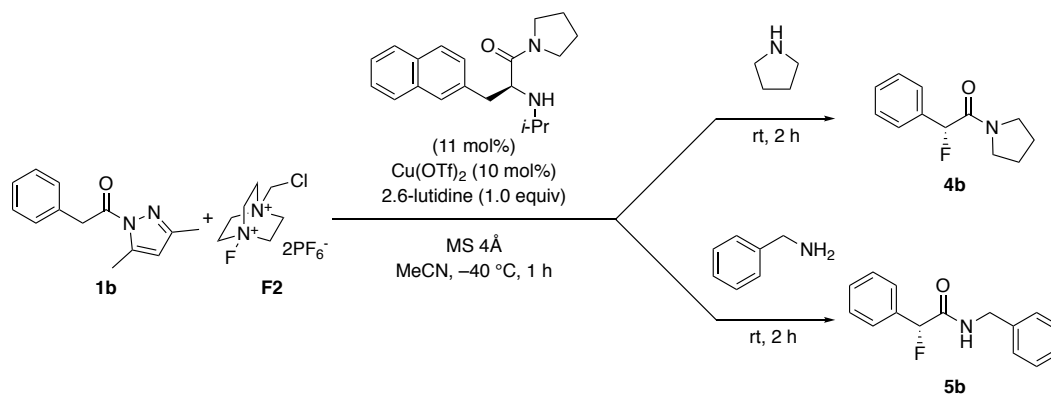
### 2-5-9. Procedure for the one-pot transformation of **1b** to **3b** (Scheme 2)



A mixture of **L2** (10.2 mg, 0.033 mmol) and copper(II) triflate (10.9 mg, 0.030 mmol, in an inert atmosphere (Ar) of glove box) and powdered molecular sieves (150 mg) in 20 mL shlenk flask were dissolved in acetonitrile (1.5 mL, freshly distilled from calcium hydride and dried over activated molecular sieves 4Å). To a solution of the mixture were added **1b** (64.3 mg, 0.30 mmol), 2,6-lutidine (35  $\mu\text{L}$ , 0.30 mmol) and **F2** (155 mg, 0.33 mmol) at  $-40$  °C. The mixture was stirred at the same temperature for 1 h. To a reaction mixture was added dry methanol (1.5 mL) and the reaction mixture was stirred at the room temperature for 2 h. The reaction mixture was filtered through neutral silica short column (*n*-hexane/EtOAc = 10/1). After evaporation of the organic solvent under reduced pressure, the crude mixture was purified by neutral silica gel column chromatography (*n*-hexane/EtOAc = 20/1) to give the desired product **3b** (49.4 mg, 98% yield) as a colorless oil.<sup>23,24</sup>  $[\alpha]_D^{24} = -102.4$  ( $c$  1.00,  $\text{CHCl}_3$ , 91% ee) [lit.<sup>23</sup>  $[\alpha]_D = -116$  ( $c$  1.00,  $\text{CHCl}_3$ , 95% ee for *R* enantiomer)]; TLC,  $R_f = 0.16$  (*n*-hexane:EtOAc = 20:1);  $^1\text{H}$  NMR (400 MHz,  $\text{CDCl}_3$ )  $\delta$  3.79 (s, 3H), 5.80 (d,  $J = 47.6$  Hz, 1H), 7.37–7.48 (m, 5H);  $^{13}\text{C}$  NMR (100 MHz,  $\text{CDCl}_3$ )  $\delta$  52.8, 89.5 (d,  $J = 184$  Hz), 126.8 (d,  $J = 5.7$  Hz, 2C), 128.9, 129.8 (2C), 134.2 (d,  $J = 21.0$  Hz), 169.1 (d,  $J = 27.7$  Hz);  $^{19}\text{F}$  (376 MHz,  $\text{CDCl}_3$ )  $\delta$  -179.8 (d,  $J = 46.2$  Hz, 1F); HRMS (EI) calcd for  $\text{C}_9\text{H}_9\text{FO}_2$   $[\text{M}]^+$  168.0587,

found 168.0591; IR (neat) 2956, 1766, 1285, 1058  $\text{cm}^{-1}$ ; HPLC analysis: OJ-H, *n*-hexane/*i*-PrOH = 50/1, 1.0 mL/min,  $t_R = 22.0$  min (major),  $t_R = 25.9$  min (minor).

## 2-5-10. Procedure for the one-pot transformation of **1b** to **4b** or **5b** (Scheme 2)



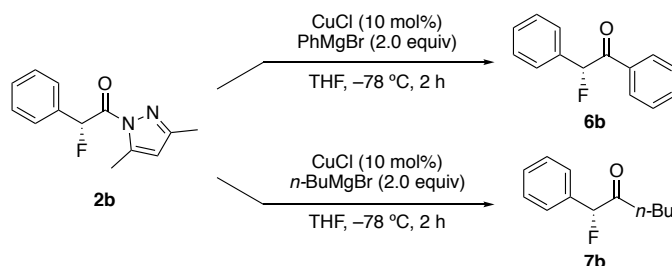
A mixture of **L2** (10.2 mg, 0.033 mmol, 11 mol%) and copper(II) triflate (10.9 mg, 0.030 mmol, in an inert atmosphere (Ar) of glove box) and powdered molecular sieves (150 mg) in 20 mL shlenk flask were dissolved in acetonitrile (1.5 mL, freshly distilled from calcium hydride and dried over activated molecular sieves 4Å). To a solution of the mixture were added **1b** (64.3 mg, 0.30 mmol, 1.0 equiv), 2,6-lutidine (35  $\mu\text{L}$ , 0.30 mmol, 1.0 equiv) and **F2** (155 mg, 0.33 mmol, 1.1 equiv) at  $-40^\circ\text{C}$ . The mixture was stirred at the same temperature for 1 h. To a reaction mixture was slowly added pyrrolidine (246  $\mu\text{L}$ , 3.0 mmol, 10 equiv) or benzylamine (328  $\mu\text{L}$ , 3.0 mmol, 10 equiv) and the reaction mixture was stirred at the room temperature for 2 h. The reaction mixture was diluted with 5 mL of  $\text{CHCl}_3$  filtered through neutral silica short column (*n*-hexane/EtOAc = 1/1). After evaporation of the organic solvent under reduced pressure, the crude mixture was purified by neutral silica gel column chromatography (*n*-hexane/EtOAc = 3/1 to 1/1) to give the desired products **4b** (57.0 mg, 92% yield) as a colorless solid or **5b** (69.6 mg, 95% yield).

**(R)-2-fluoro-2-phenyl-1-(pyrrolidin-1-yl)ethan-1-one (4b)**: TLC,  $R_f = 0.54$  (EtOAc);  $[\alpha]_D^{24} = -44.4$  ( $c$  1.00,  $\text{CHCl}_3$ , 90% ee);  $^1\text{H}$  NMR (400 MHz,  $\text{CDCl}_3$ )  $\delta$  1.70–1.93 (m, 4H), 3.23–3.33 (m, 1H), 3.38–3.63 (m, 3H), 5.92 (d,  $J = 49.0$  Hz, 1H), 7.36–7.52 (m, 5H);  $^{13}\text{C}$  NMR (100 MHz,  $\text{CDCl}_3$ )  $\delta$  23.4, 26.3, 45.9 (d,  $J = 3.8$  Hz), 46.7, 90.9 (d,  $J = 183.1$  Hz), 127.2 (d,  $J = 5.9$  Hz, 2C), 128.9 (2C), 129.5 (d,  $J = 2.9$  Hz), 134.4 (d,  $J = 20.0$  Hz), 166.5 (d,  $J = 23.8$  Hz);  $^{19}\text{F}$  (376 MHz,  $\text{CDCl}_3$ )  $\delta$   $-174.3$ – $-174.1$  (m, 1F); HRMS (ESI+) calcd for  $\text{C}_{12}\text{H}_{14}\text{FNNaO}$   $[\text{M}+\text{Na}]^+$

230.0952, found 230.0952; IR (KBr) 1653, 1440, 1027  $\text{cm}^{-1}$ ; HPLC analysis: OD-3, *n*-hexane/*i*-PrOH = 1/1, 1.0 mL/min,  $t_R = 5.7$  min (minor),  $t_R = 6.3$  min (major).

**(*R*)-*N*-benzyl-2-fluoro-2-phenylacetamide (**5b**)**<sup>25</sup>: TLC,  $R_f = 0.27$  (*n*-hexane:EtOAc = 3:1);  $[\alpha]_D^{25} = -54.4$  (*c* 1.00,  $\text{CHCl}_3$ , 89% ee);  $^1\text{H}$  NMR (400 MHz,  $\text{CDCl}_3$ )  $\delta$  4.42–4.57 (m, 2H), 5.81 (d,  $J = 48.6$  Hz, 1H), 6.84 (brs, 1H), 7.24–7.49 (m, 5H);  $^{13}\text{C}$  NMR (100 MHz,  $\text{CDCl}_3$ )  $\delta$  43.3, 92.0 (d,  $J = 186.9$  Hz), 126.7 (d,  $J = 6.7$  Hz, 2C), 127.9, 128.0 (2C), 128.8 (2C), 128.9 (2C), 129.6 (d,  $J = 2.9$  Hz), 134.9 (d,  $J = 19.1$  Hz), 137.6, 168.5 (d,  $J = 21.9$  Hz);  $^{19}\text{F}$  (376 MHz,  $\text{CDCl}_3$ )  $\delta$  -177.6 (d,  $J = 49.1$  Hz, 1F); HRMS (ESI+) calcd for  $\text{C}_{15}\text{H}_{14}\text{FNNaO}$   $[\text{M}+\text{Na}]^+$  266.0952, found 266.0952; HPLC analysis: OD-H, *n*-hexane/*i*-PrOH = 4/1, 1.0 mL/min,  $t_R = 9.5$  min (minor),  $t_R = 10.4$  min (major).

### 2-5-11. Procedure for the transformation of **2b** to **6b** or **7b** (Scheme 2)



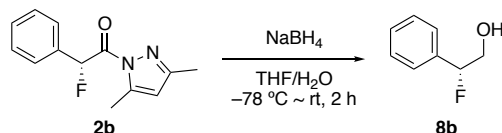
The dried shlenk flask equipped with a magnetic stirring bar and 3-way glass stopcock was charged with CuCl (3.0 mg, 0.03 mmol, 10 mol%) and **2b** (69.7 mg, 0.30 mmol, 1.00 equiv). Then dry THF (3.0 mL) was added to the shlenk flask and the reaction mixture was cooled to  $-78$  °C. To the solution was added 1.0 *M* RMgBr in THF solution (600  $\mu\text{L}$ , 0.60 mmol, 2.00 equiv) and the reaction mixture was stirred for 2 h. After quenching with 1 *M* HCl, the resultant mixture was extracted with EtOAc. The combined organic layer was washed with brine, and dried over  $\text{Na}_2\text{SO}_4$ . After evaporation of the organic solvent under reduced pressure, the crude mixture was purified by neutral silica gel column chromatography to give the product **6b** (57.2 mg, 89% yield) or **7b** (54.4 mg, 93% yield) as a colorless solid.

**(*R*)-2-fluoro-1,2-diphenylethan-1-one (**6b**)**<sup>27</sup>: TLC,  $R_f = 0.23$  (*n*-hexane:EtOAc = 20:1);  $[\alpha]_D^{23} = -93.2$  (*c* 1.00,  $\text{CHCl}_3$ , 92% ee);  $^1\text{H}$  NMR (400 MHz,  $\text{CDCl}_3$ )  $\delta$  6.52 (d,  $J = 48.6$  Hz, 1H), 7.34–7.59 (m, 8H), 7.91–7.98 (m, 2H);  $^{13}\text{C}$  NMR (100 MHz,  $\text{CDCl}_3$ )  $\delta$  94.4 (d,  $J = 184.0$  Hz), 127.5 (d,  $J = 5.7$  Hz, 2C), 128.8 (2C), 129.2 (2C), 129.8 (d,  $J = 2.9$  Hz), 133.9 (2C), 134.1, 134.3 (d,  $J = 19.1$  Hz), 194.3 (d,  $J = 21.0$  Hz);  $^{19}\text{F}$  (376 MHz,  $\text{CDCl}_3$ )  $\delta$  -175.7 (d,  $J = 49.1$  Hz, 1F); HPLC analysis: OD-3, *n*-hexane/*i*-PrOH = 50/1, 1.0 mL/min,  $t_R = 12.1$  min (minor),  $t_R = 17.3$  min (major).

**(*R*)-1-fluoro-1-phenylhexan-2-one (**7b**)**: TLC,  $R_f = 0.50$  (*n*-hexane:EtOAc = 20:1);  $[\alpha]_D^{26} = -4.8$  (*c* 1.00,  $\text{CHCl}_3$ , 90% ee);  $^1\text{H}$  NMR (400 MHz,  $\text{CDCl}_3$ )  $\delta$  0.85 (t,  $J = 7.3$  Hz, 1H), 1.20–1.30 (m, 2H), 1.48–1.60 (m, 2H), 2.48–2.67 (m, 2H), 5.70 (d,  $J = 48.6$  Hz, 1H), 7.36–7.43 (m, 5H);  $^{13}\text{C}$  NMR (100 MHz,  $\text{CDCl}_3$ )  $\delta$  13.9, 22.3, 25.0, 37.3, 95.9

(d,  $J = 187.7$  Hz), 126.2 (d,  $J = 6.7$  Hz, 2C), 129.0 (2C), 129.4, 134.3 (d,  $J = 21.0$  Hz), 206.9 (d,  $J = 24.8$  Hz);  $^{19}\text{F}$  (376 MHz,  $\text{CDCl}_3$ )  $\delta -184.3$  (d,  $J = 49.1$  Hz, 1F); HRMS (ESI+) calcd for  $\text{C}_{12}\text{H}_{15}\text{FNaO}$   $[\text{M}+\text{Na}]^+$  217.0999, found 217.0997; IR (neat) 2960, 1727, 1454, 1026  $\text{cm}^{-1}$ ; HPLC analysis: OD-3, *n*-hexane/*i*-PrOH = 99/1, 1.0 mL/min,  $t_R = 5.9$  min (minor),  $t_R = 6.4$  min (major).

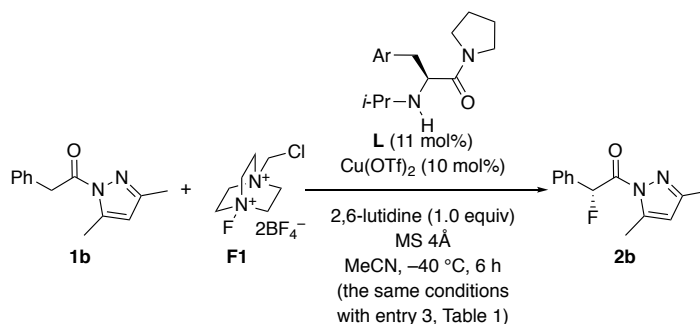
## 2-5-12. Procedure for the transformation of 2b to 8b (Scheme 2)



The shlenk flask equipped with a magnetic stirring bar and 3-way glass stopcock was charged with **2b** (69.7 mg, 0.30 mmol, 1.00 equiv). Then THF (2.4 mL) and  $\text{H}_2\text{O}$  (0.6 mL) were added to the shlenk flask and the reaction mixture was cooled to  $-78$   $^\circ\text{C}$ . To the solution was added  $\text{NaBH}_4$  (90.8 mg, 2.40 mmol, 8.00 equiv) and the reaction flask was removed from acetone bath and stirred for 2 h at room temperature. After quenching with 1 M HCl, the resultant mixture was extracted with  $\text{CHCl}_3$ . The combined organic layer was washed with brine, and dried over  $\text{Na}_2\text{SO}_4$ . After evaporation of the organic solvent under reduced pressure, the crude mixture was purified by neutral silica gel column chromatography (*n*-hexane/EtOAc = 5/1 to 1/1) to give the product **8b** (42.6 mg, >99% yield) as a colorless oil.

**(R)-2-fluoro-2-phenylethan-1-ol (8b)**<sup>27</sup>: TLC,  $R_f = 0.16$  (*n*-hexane:EtOAc = 3:1);  $[\alpha]_D^{26} = -93.2$  ( $c$  0.70,  $\text{CHCl}_3$ , 91% ee);  $^1\text{H}$  NMR (400 MHz,  $\text{CDCl}_3$ )  $\delta$  2.24 (brs, 1H), 3.71–4.01 (m, 2H), 2.26 (ddd,  $J = 48.6, 7.3, 2.8$  Hz, 1H), 7.27–7.48 (m, 5H);  $^{13}\text{C}$  NMR (100 MHz,  $\text{CDCl}_3$ )  $\delta$  66.7 (d,  $J = 23.9$  Hz), 95.0 (d,  $J = 170.7$  Hz), 125.8 (d,  $J = 7.6$  Hz, 2C), 128.7 (2C), 128.9, 136.5 (d,  $J = 20.0$  Hz);  $^{19}\text{F}$  (376 MHz,  $\text{CDCl}_3$ )  $\delta -187.0$  (ddd,  $J = 49.1, 28.9, 17.3$  Hz, 1F); HPLC analysis: AS-3, *n*-hexane/*i*-PrOH = 9/1, 1.0 mL/min,  $t_R = 10.9$  min (minor),  $t_R = 12.0$  min (major).

## 2-5-13. Stereoelectronic effect on 3-aryl moiety of 3-aryl-L-alanine-derived amide L for the enantioselective fluorination of 1b (See Table 5)



**L5** (Ar = *o*- $\text{C}_6\text{H}_{11}$ ): 43% yield, 30% ee  
**L6** (Ar = Ph): 91% yield, 55% ee  
**L7** (Ar = 4- $\text{CF}_3$ - $\text{C}_6\text{H}_4$ ): 72% yield, 65% ee  
**L8** (Ar = 4-MeO- $\text{C}_6\text{H}_4$ ): 95% yield, 69% ee  
**L2** (Ar = 2-naphthyl): 91% yield, 89% ee (entry 3, Table 1)

These results can be explained by steric effect and electronic effect of 3-aryl moiety of 3-aryl-L-alanine-derived amide **L** (Figure S1). We expected that the  $\pi$ -Cu(II) interaction between 3-aryl moiety of **L** and Cu(II) increases the Lewis acidity of Cu(II) and enantioselectivity by releasing a triflate anion. The use of **L6** gave **2b** in 91% yield with 55% ee. In contrast, the use of **L5** gave **2b** in 43% yield with 30% ee. These results could be explained by the  $\pi$ -Cu(II) interaction between phenyl moiety of **L6** and Cu(II). The use of **L8** increased the reactivity (to 95% yield) and the enantioselectivity (to 69% ee). These results could be explained by stabilization of  $\pi$ -Cu(II) interaction and steric effect by *p*-methoxy group of **L8**. In contrast, the use of **L7** decreased the reactivity (to 72% yield) but the enantioselectivity was still 65% ee. These results could be explained by destabilization of  $\pi$ -Cu(II) interaction and steric effect by *p*-trifluoromethyl group of **L7** under equilibrium between the active  $\pi$ -Cu(II) complex and the low active extended Cu(II) complex. The use of **L2** increased the reactivity (to 91% yield) and the enantioselectivity (to 89% ee) by synergistic effect of the  $\pi$ -Cu(II) interaction and steric effect of 2-naphthyl group of **L2**.

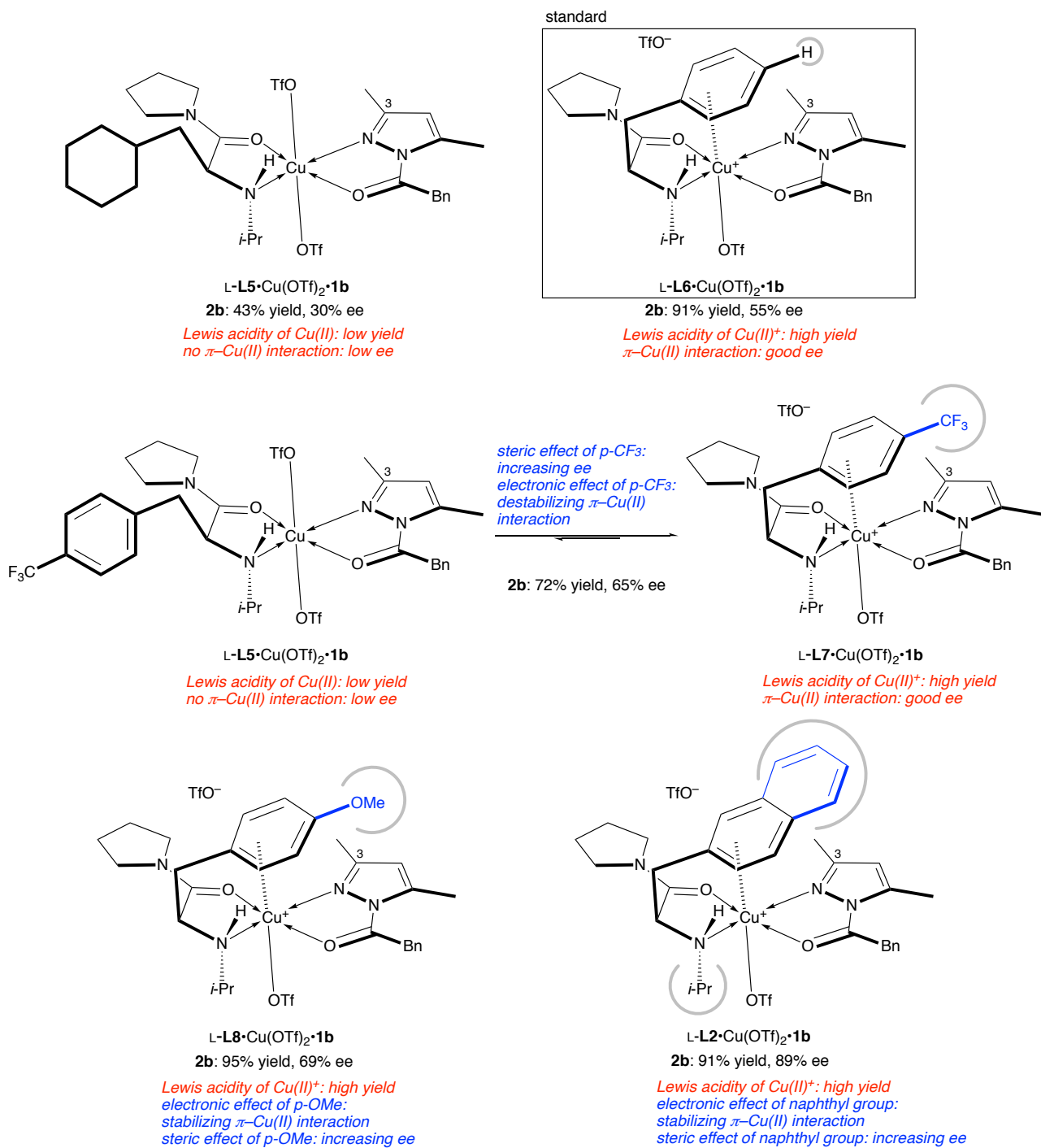
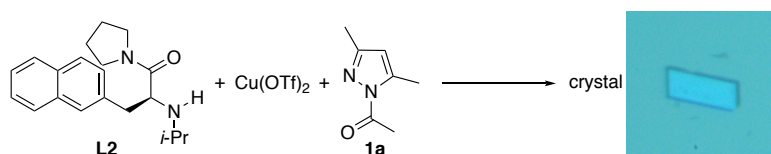


Figure S1. Proposed intermediates.

## 2-5-14. X-ray diffraction analysis of L-L2/Cu(OTf)<sub>2</sub>/1r complex (Figure 2)



**Preparation of a crystal sample:** L-L2 (62.1 mg, 0.20 mmol), Cu(OTf)<sub>2</sub> (72.3 mg, 0.20 mmol), and **1a** (61.4 mg, 0.20 mmol) were placed in a Schlenk test tube under argon atmosphere and dissolved in dry acetonitrile (1 mL). Then the solution was stirred for 1 h at room temperature. The volatiles were removed *in vacuo*, and then ethyl acetate (1 mL) and *n*-hexane (0.5 mL) were added at room temperature. And the solution passed through a membrane filter (0.50 μm pore size). The solution was settled at room temperature, and a single crystal was obtained within a week.

**Crystal data of L-L2/Cu(OTf)<sub>2</sub>/1a complex (Figure 2):** Formula C<sub>29</sub>H<sub>36</sub>CuN<sub>4</sub>O<sub>8</sub>S<sub>2</sub>, pale blue, triclinic, space group *P*1, *a* = 9.3546(16) Å, *b* = 9.4927(18) Å, *c* = 10.407(2) Å, α = 103.763(4)°, β = 92.537(3)°, γ = 97.847(3)°, *V* = 8864.4(3) Å<sup>3</sup>, *Z* = 1, ρ<sub>calc</sub> = 1.518 g/cm<sup>3</sup>, λ(MoKα) = 0.71075 Å, *T* = 123 K. 5452 reflections collected, and 460 parameters were used for the solution of the structure. *R*<sub>1</sub> = 0.0546 and *wR*<sub>2</sub> = 0.1395. GOF = 1.022. Flack *x* parameter = 0.025(11). Crystallographic data (excluding structure factors) for the structure reported in this paper have been deposited with the Cambridge Crystallographic Data Centre as supplementary publication no. CCDC-1815795. Copies of the data can be obtained free of charge on application to CCDC, 12 Union Road, Cambridge CB2 1EZ, UK [Fax: int. code + 44(1223)336-033; E-mail: deposit@ccdc.cam.ac.uk; Web page: <http://www.ccdc.cam.ac.uk/pages/Home.aspx>].

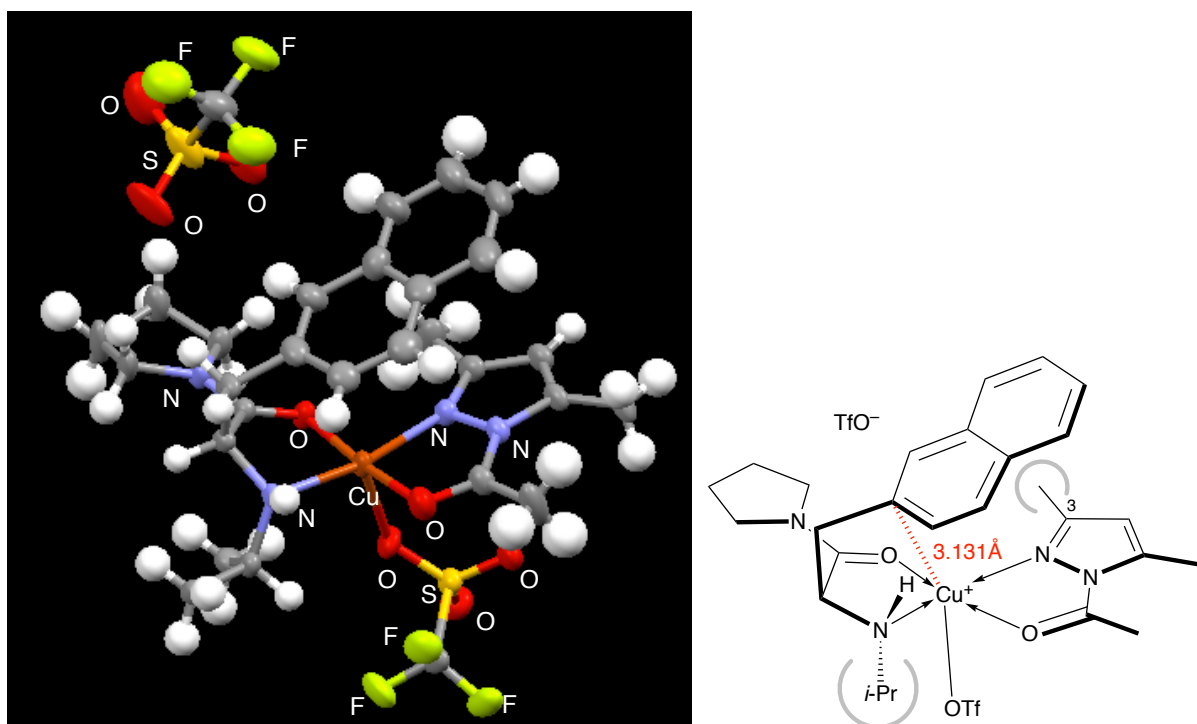


**Figure 2.** X-ray diffraction analysis of a 1:1:1 complex of L-L2/Cu(OTf)<sub>2</sub>/1a (ORTEP Drawing)



### 2-5-15. UV absorption difference spectral analyses of L-L9/Cu(OTf)<sub>2</sub> and L-L9/Cu(OTf)<sub>2</sub>/1a complexes (Figure 3)

*N*-Isopropyl-L-tryptophan pyrrolidine amide L-**L9** (0.10 mmol, 29.9 mg), Cu(OTf)<sub>2</sub> (0.10 mmol, 36.1 mg) and **1a** (0.10 mmol, 13.8 mg) were dissolved in 10 mL of acetonitrile (dried over activated molecular sieves 4Å)(1 x 10<sup>-2</sup> M) in the presence of 4Å pellet molecular sieves (100 mg) in 20 mL shlenk flask. A 0.5 mL of solution (1 x 10<sup>-2</sup> M) was diluted with 4.5 mL of acetonitrile in the presence of 4Å pellet molecular sieves (100 mg) to give a 1 x 10<sup>-3</sup> M solution, 0.5 mL of which was further diluted with 4.5 mL of acetonitrile (dried over activated molecular sieves 4Å) to prepare a 1 x 10<sup>-4</sup> M solution. This 1.0 x 10<sup>-4</sup> M solution was passed through a membrane filter (0.50 μm pore size), and added in a 10 mm cell, and the UV spectrum was measured at 20 °C. Other samples were also prepared in the same way.

According to Figure S2, the UV absorption difference spectrum “a 1:1:1 complex of L-**L9**/Cu(OTf)<sub>2</sub>/**1a**” minus “L-**L9** and **1a**” in acetonitrile revealed a negative band at 226 nm and a weak positive band at 240 nm attributable to an indolyl π–Cu(II) interaction (Figure S2). The enantioselective α-fluorination of **1b** using **L9** in place of **L2** under the same conditions with entry 4 in Table 1 gave **2b** with 58% ee in 70% yield (Scheme S1). According to Figure S3 as well as Figure S2, the UV absorption difference spectrum “a 1:1 complex of L-**L9**/Cu(OTf)<sub>2</sub>” minus “L-**L9**” in acetonitrile revealed a negative band at 227 nm and a weak positive band at 237 nm attributable to an indolyl π–Cu(II) interaction (Figure S3). These results suggest the possibility of π–Cu(II) interaction of catalysts in an acetonitrile solution.<sup>28</sup>

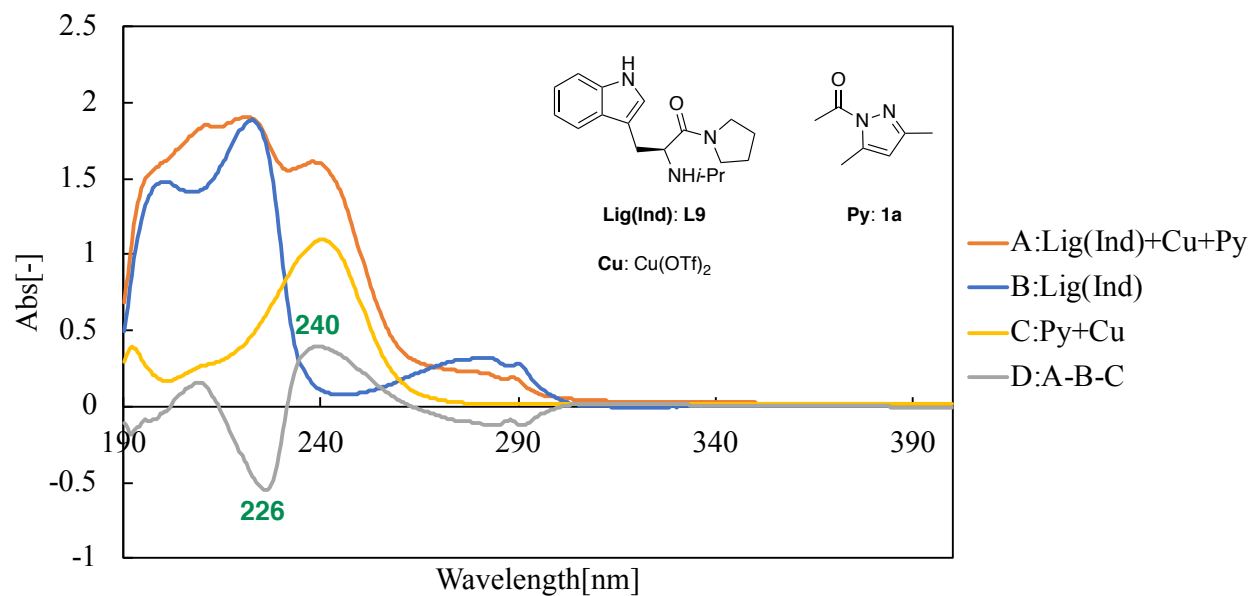


**Figure S2.** UV Absorption spectra of L-L9, 1a, and a 1:1:1 complex of L-L9/Cu(OTf)<sub>2</sub>/1a.

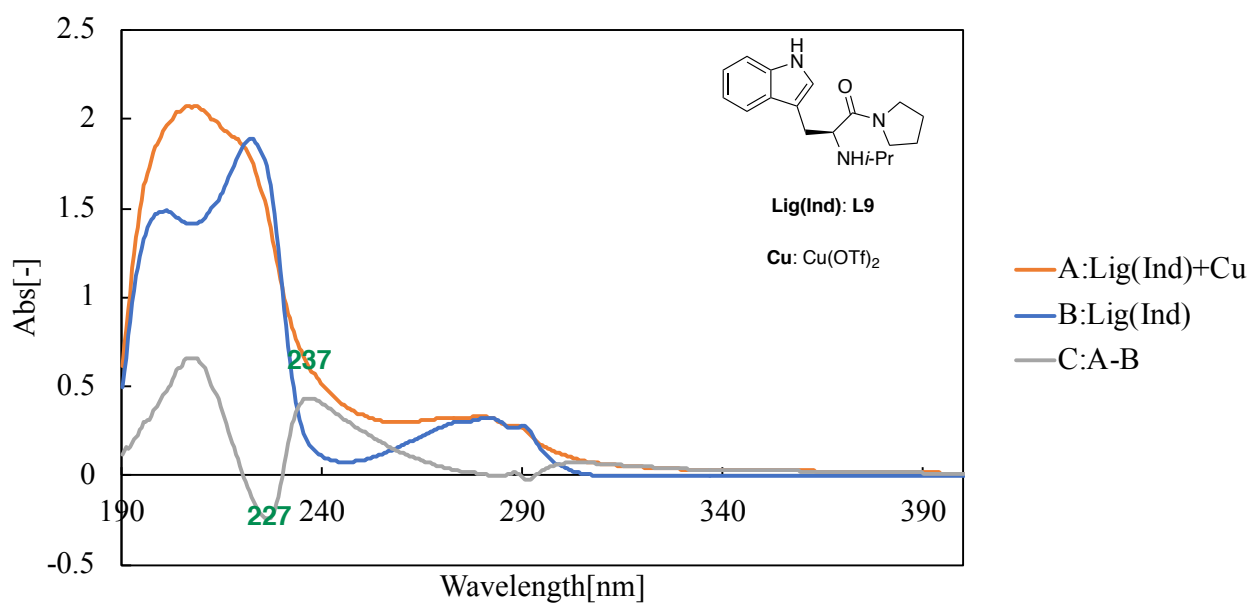
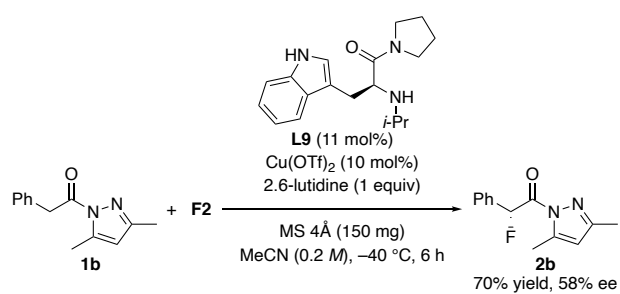


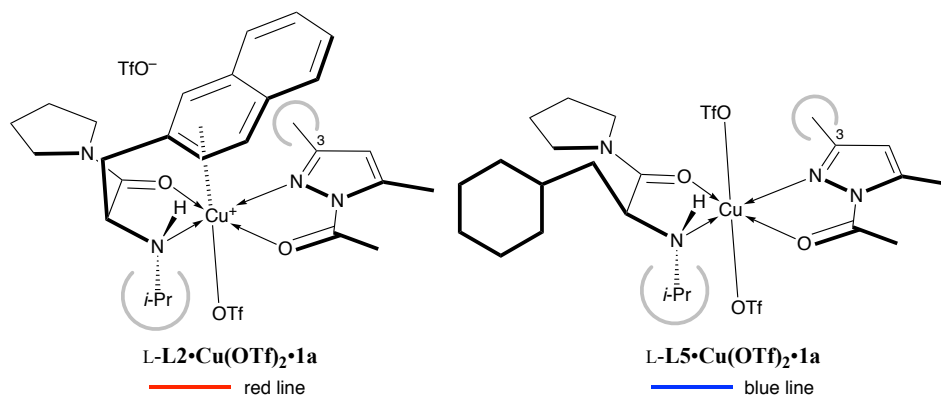
**Figure S3.** UV Absorption spectra of L-L9, and a 1:1 complex of L-L9/Cu(OTf)<sub>2</sub>.



**Scheme S1.** Enantioselective  $\alpha$ -Fluorination of **1b** with **F2** Catalyzed by L-L9/Cu(OTf)<sub>2</sub>

**2-5-16. ESR spectral analyses of L-L2•Cu(OTf)<sub>2</sub>•1a and L-L5•Cu(OTf)<sub>2</sub>•1a complexes (Figure 4)**

In the presence of heat-gun-dried pellet molecular sieves 4Å (100 mg), L-L2 (0.033 mmol, 10.2 mg) or L-L5 (0.033 mmol, 8.8 mg), Cu(OTf)<sub>2</sub> (0.030 mmol, 10.9 mg) and **1a** (0.3 mmol, 41.4 mg) were dissolved in 1.5 mL of acetonitrile (dried over activated molecular sieves 4Å). The solution was stirred for 10 min under N<sub>2</sub> and carefully poured into the ESR sample tube (Figure S4). Appearance of hyperfine structure by protons of the naphthalene of L-L2 on Cu(II) signal was expected when the naphthalene of L-L2 interacted with Cu(II) center as donating small part of its electron to the center to produce unpaired spin density in the molecule, but it never be observed even the field modulation width was reduced to 0.005 mT for the ESR measurement.<sup>29</sup> The difference of the both spectra of L-L2•Cu(OTf)<sub>2</sub>•1a and L-L5•Cu(OTf)<sub>2</sub>•1a complexes mainly comes from the difference in the number of coordinated <sup>-</sup>OTf group. When doubly coordinated <sup>-</sup>OTf groups reduced to single, distribution of unpaired electron on Cu(II) *d*-orbital should be changed with the changes of *g* tensors and hyperfine coupling constants of Cu(II). Although there is no definite evidences of a very small electron donation from the naphthalene to Cu(II) *d*-orbital, the small donation may induce the distribution change of the unpaired electron in the Cu(II) *d*-orbital.



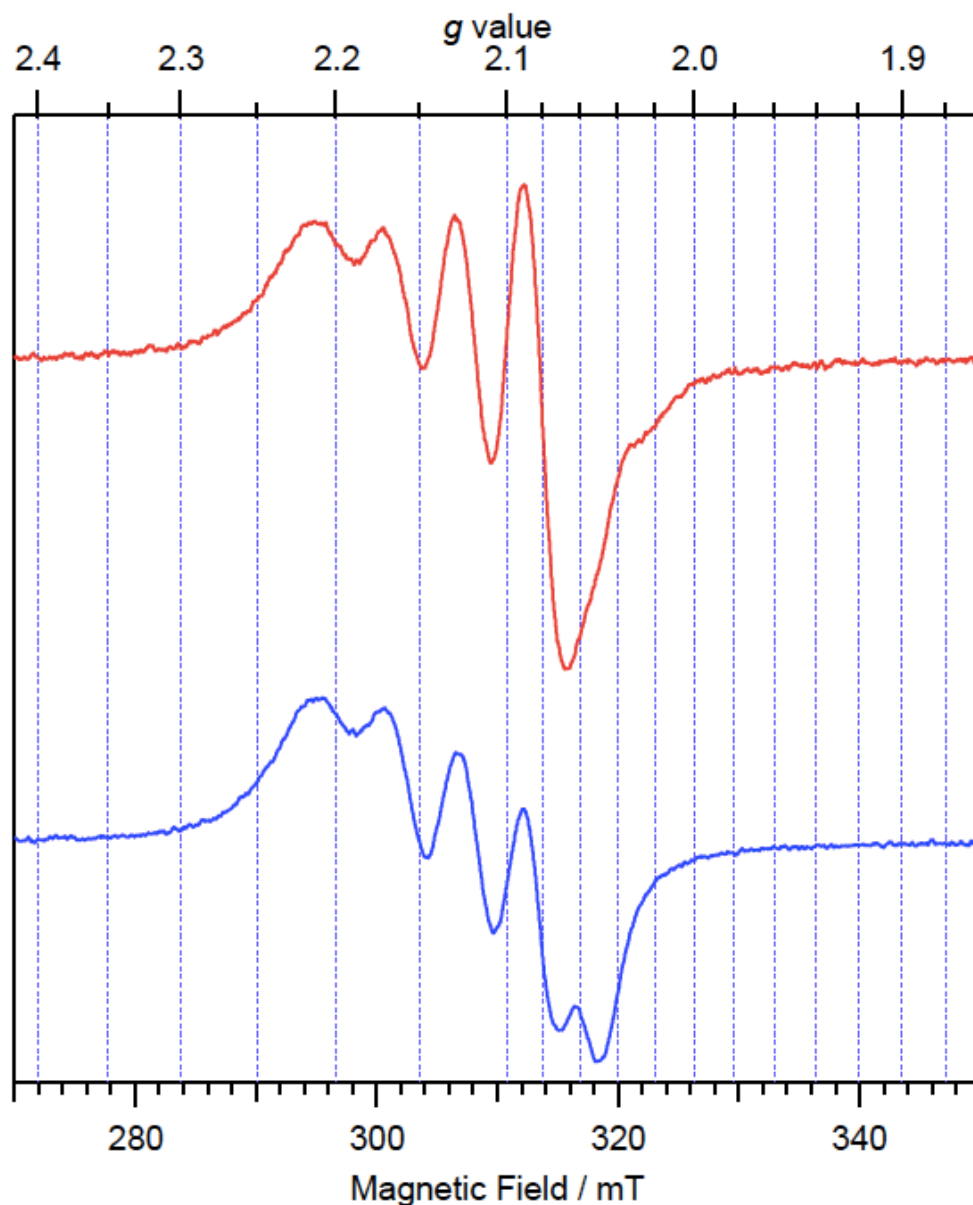
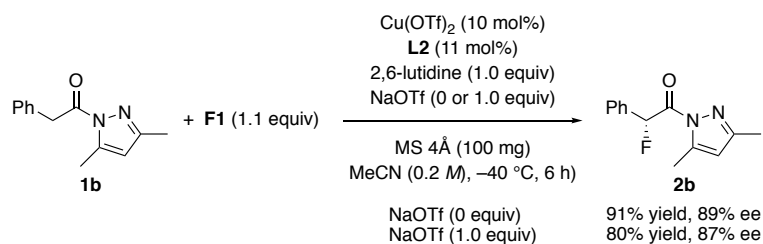


**Figure S4.** ESR spectra of L-L2•Cu(OTf)<sub>2</sub>•1a (red) and L-L5•Cu(OTf)<sub>2</sub>•1a (blue) at room temperature. The ESR sample tubes were set to an X-band ESR spectrometer (JEOL JES-RE1X). ESR parameters for the measurements at room temperature were microwave power of 1 mW, field modulation width of 0.1 mT at 100 kHz, static magnetic field of 310 ± 40 mT. Microwave frequency and magnetic field of the spectrometer were monitored using a microwave frequency counter (Hewlett-Packard, 53150A) and an NMR field meter (Echo Electronics Co. Ltd., EFM-2000AX), respectively.

**2-5-17. Influence of NaOTf for  $\pi$ -Cu(II) interaction of Cu(OTf)<sub>2</sub>•L2 (Scheme 3)**

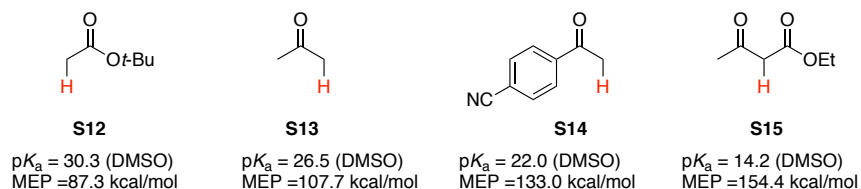
The effect of NaOTf (100 mol%) was examined in the enantioselective fluorination of **1b** in the presence of 10 mol% of Cu(OTf)<sub>2</sub>•**L2**. The enantioselectivity was not influenced in the presence of excess NaOTf. This result suggests that the π–Cu interaction between **L2** and Cu(OTf)<sub>2</sub> was stable even in the presence of NaOTf.

The bended conformation of **L2** might be stabilized by the π–Cu(II) electronic interaction and the steric effect of **L2**. Strong π–Cu(II) electronic interaction decreases the Lewis acidity of Cu(II). Therefore, appropriate π–Cu(II) electronic interaction and steric effect is important to appear Lewis acidity of Cu(II).



## 2-5-18. Calculation of the electrostatic potential of *N*-acylpyrazoles (Figure 1c)

An effective approach to estimating molecular p*K*<sub>a</sub> values from simple density functional calculations has been developed by Liu.<sup>30</sup> Various compounds show a strong correlation between experimental p*K*<sub>a</sub> values and molecular electrostatic potential (MEP). As a result of their research, a linear relationship between the MEP and experimental p*K*<sub>a</sub> values has been established. Therefore, we performed preliminary theoretical calculations using Spartan'16 and Spartan'18 for Macintosh from Wavefunction, Inc. (Figures S5 and S6).<sup>31</sup> The geometries of **S12**–**S15** and **1a** and **1v** were optimized with gradient-corrected density functional theory (DFT) calculations with B3LYP using 6-31+G\* basis set, after MMFF (molecular mechanics) calculation.



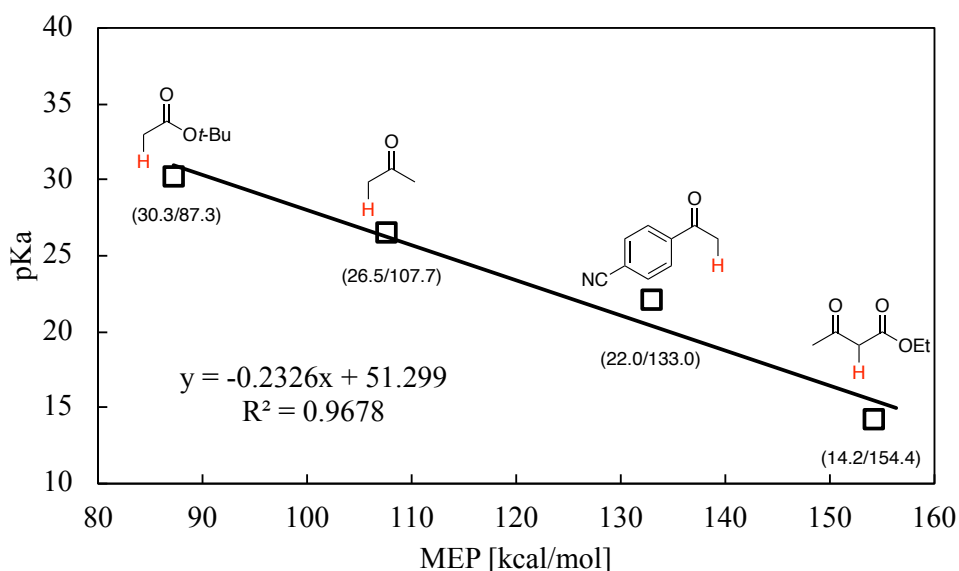


**Figure S5.** The linear relationship between  $pK_a$  (DMSO) and MEP values.

We first investigated the MEP values of commercially available compounds **S12** [ $pK_a$  (DMSO) = 30.3<sup>32</sup>], **S13** [ $pK_a$  (DMSO) = 26.5<sup>33</sup>], **S14** [ $pK_a$  (DMSO) = 22.0<sup>34</sup>], and **S15** [ $pK_a$  (DMSO) = 14.2<sup>33</sup>], which have known  $pK_a$  values. Our preliminary calculations for these model compounds certainly support a linear relationship between  $pK_a$  and MEP values. The following linear regression equation was calculated by the least-squares method: “ $y = -0.2326x + 51.299$ ” ( $x = \text{MEP value (kcal/mol)}$ ,  $y = pK_a$  (DMSO),  $R^2 = 0.9678$ ) (Figure S5). A linear regression of measured  $pK_a$  values and predicted MEP values yielded an  $R^2$  of 0.9678, indicating a reasonable agreement.

Next, predicted  $pK_a$  values (DMSO) of **1a**, **1v**, and their complexes of  $\text{CuCl}_2$  were calculated based on the linear regression equation in Figure S5. Interestingly,  $H_b$  ( $pK_a = 34.1$ ) is more acidic than  $H_a$  ( $pK_a = 26.7$ ) in the *pseudo-E* geometry of *N*-acetyl-3,5-dimethylpyrazole **1a**. In contrast,  $H_a$  ( $pK_a = 20.7$ ) is more acidic than  $H_b$  ( $pK_a = 24.7$ ) in the *pseudo-Z* geometry of **1a**. It is noted that the resonance and inductive effects from the electron-deficient pyrazole moiety to the *N*-acyl moiety are influenced by the difference of the rotational conformation of the amidyl C–N bond. The chelation of  $\text{CuCl}_2$  to *N*-acetyl-3,5-dimethylpyrazole fixes the rotational conformation to **1a** $\cdot\text{CuCl}_2$ . This chelation is highly effective to increase the acidity of  $H_a$  ( $pK_a = 17.3$ ). This is the reason why *N*-acylpyrazole is more reactive than other esters and amides.

In addition, we calculated predicted  $pK_a$  values of 1-(3,5-dimethyl-1*H*-pyrazol-1-yl)pentan-1,4-dione (**1s**) (Figure S6). Interestingly,  $H_d$  ( $pK_a = 27.0$ ) is the most acidic in the *pseudo-E* geometry of **1v**, and  $H_a$  ( $pK_a = 38.0$ )

is less acidic than H<sub>b</sub> (pK<sub>a</sub> = 30.5) and H<sub>c</sub> (pK<sub>a</sub> = 28.4). In contrast, H<sub>a</sub> is (pK<sub>a</sub> = 24.9) the most acidic in the *pseudo-Z* geometry. The 1:1:1 complex of **1v**, CuCl<sub>2</sub>, and **1a** fixes the rotational conformation to the *pseudo-Z* geometry. This chelation is highly effective to increase the acidity of H<sub>a</sub> (pK<sub>a</sub> = 22.4). These results support the site-selective fluorination of **1v**.

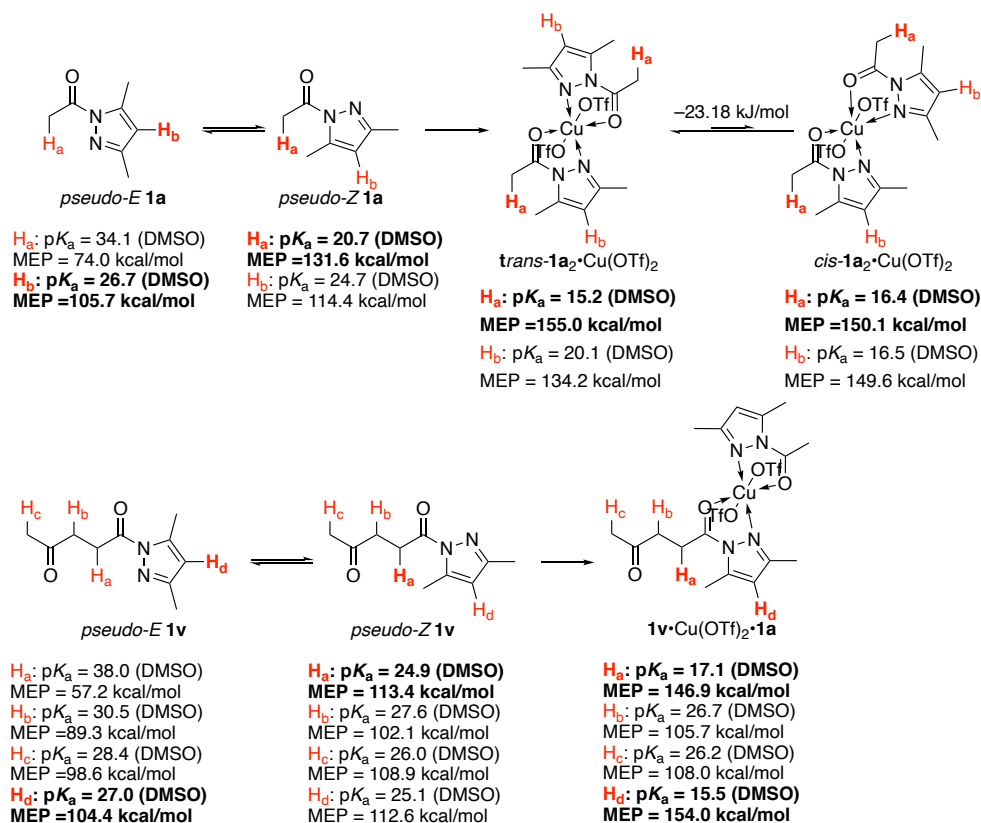
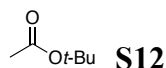


**Figure S6.** Calculation of electrostatic potential (kcal/mol) and predicted pK<sub>a</sub> values (DMSO) based on the linear regression equation in Figure S5.

**Table S2.** Summary of DFT calculation of **S12–S15** and **1a** and **1s** by using B3LYP/6-31+G\*



MacSPARTAN '16 MECHANICS PROGRAM: (x86/Darwin) build 1.1.2

Frequency Calculation

Adjusted 1 (out of 60) low frequency modes

Reason for exit: Successful completion

Mechanics CPU Time : .04

Mechanics Wall Time: .04

MacSPARTAN '16 Quantum Mechanics Program: (x86/Darwin) build 1.1.2

Job type: Geometry optimization.

Method: RB3LYP

Basis set: 6-31+G\*

Number of basis functions: 176

Number of electrons: 64

Parallel Job: 2 threads

SCF model:

A restricted hybrid HF-DFT SCF calculation will be  
performed using Pulay DIIS + Geometric Direct Minimization

Optimization:

Step Energy Max Grad. Max Dist.

1 -386.351323 0.009721 0.090000

2 -386.352997 0.005168 0.090000

3 -386.353606 0.000652 0.006857

4 -386.353612 0.000512 0.031268

5 -386.353623 0.000146 0.001528

6 -386.353623 0.000046 0.000274

Reason for exit: Successful completion

Quantum Calculation CPU Time : 3:09.09

Quantum Calculation Wall Time: 1:39.60

MacSPARTAN '16 Properties Program: (x86/Darwin) build 1.1.2

Reason for exit: Successful completion

Properties CPU Time : .32

Properties Wall Time: .33

MacSPARTAN '16 Properties Program: (x86/Darwin) build 1.1.2



Use of molecular symmetry enabled

Cartesian Coordinates (Angstroms)

Atom X Y Z

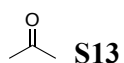
-----  
1 H H1 1.4084374 -0.8824249 2.8878214  
2 C C1 0.7595322 0.0000000 2.9037514  
3 H H2 1.4084374 0.8824249 2.8878214  
4 H H3 0.1567395 0.0000000 3.8133417  
5 C C2 -0.1524687 0.0000000 1.6956707  
6 O O1 -1.3668215 0.0000000 1.7524211  
7 O O2 0.5735819 0.0000000 0.5579953  
8 C C3 -0.0521720 0.0000000 -0.7840210  
9 C C4 1.1631648 0.0000000 -1.7151022  
10 H H5 1.7818340 -0.8880482 -1.5455412  
11 H H7 1.7818340 0.8880482 -1.5455412  
12 H H8 0.8363073 0.0000000 -2.7609474  
13 C C5 -0.8849013 1.2726993 -0.9737392  
14 H H6 -1.7610766 1.2764284 -0.3225189  
15 H H9 -1.2231852 1.3321819 -2.0150485  
16 H H10 -0.2800400 2.1620239 -0.7625284  
17 C C6 -0.8849013 -1.2726993 -0.9737392  
18 H H4 -0.2800400 -2.1620239 -0.7625284  
19 H H11 -1.2231852 -1.3321819 -2.0150485  
20 H H12 -1.7610766 -1.2764284 -0.3225189

Point Group = CS Order = 1 Nsymop = 2

Reason for exit: Successful completion

Properties CPU Time : .31

Properties Wall Time: 1.52



MacSPARTAN '16 MECHANICS PROGRAM: (x86/Darwin) build 1.1.2

Frequency Calculation

Adjusted 2 (out of 30) low frequency modes

Reason for exit: Successful completion

Mechanics CPU Time : .04

Mechanics Wall Time: .04

MacSPARTAN '16 Quantum Mechanics Program: (x86/Darwin) build 1.1.2

Job type: Geometry optimization.

Method: RB3LYP

Basis set: 6-31+G\*

Number of basis functions: 88

Number of electrons: 32

Parallel Job: 4 threads

SCF model:

A restricted hybrid HF-DFT SCF calculation will be

performed using Pulay DIIS + Geometric Direct Minimization

Optimization:

Step Energy Max Grad. Max Dist.

1 -193.165250 0.016605 0.075950

2 -193.166242 0.002865 0.007883

3 -193.166260 0.000542 0.002453

4 -193.166261 0.000204 0.001248

5 -193.166261 0.000005 0.000033

Reason for exit: Successful completion

Quantum Calculation CPU Time : 30.36

Quantum Calculation Wall Time: 9.80

MacSPARTAN '16 Properties Program: (x86/Darwin) build 1.1.2

Reason for exit: Successful completion

Properties CPU Time : .11

Properties Wall Time: .12

MacSPARTAN '16 Properties Program: (x86/Darwin) build 1.1.2

Use of molecular symmetry enabled

Cartesian Coordinates (Angstroms)

Atom X Y Z

-----  
1 C C1 0.0000000 0.0000000 -0.6407364

2 O O1 0.0000000 0.0000000 -1.8596125

3 C C2 -1.2937888 0.0000000 0.1552873

4 H H2 -1.3411722 0.8813930 0.8081279

5 H H1 -1.3411722 -0.8813930 0.8081279

6 H H4 -2.1512217 0.0000000 -0.5213687

7 C C3 1.2937888 0.0000000 0.1552873

8 H H3 1.3411722 0.8813930 0.8081279

9 H H5 2.1512217 0.0000000 -0.5213687

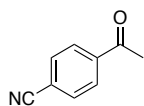
10 H H6 1.3411722 -0.8813930 0.8081279

Point Group = CNV Order = 2 Nsymop = 4

Reason for exit: Successful completion

Properties CPU Time : .10

Properties Wall Time: .11



**S14**

MacSPARTAN '16 Quantum Mechanics Program: (x86/Darwin) build 1.1.2

Job type: Geometry optimization.

Method: RB3LYP

Basis set: 6-31+G\*

Number of basis functions: 223

Number of electrons: 76

Parallel Job: 4 threads

SCF model:

A restricted hybrid HF-DFT SCF calculation will be  
performed using Pulay DIIS + Geometric Direct Minimization

Optimization:

Step Energy Max Grad. Max Dist.

1 -477.155538 0.006864 0.017467

2 -477.155789 0.001754 0.004053

3 -477.155801 0.000386 0.001405

4 -477.155801 0.000175 0.000435

Reason for exit: Successful completion

Quantum Calculation CPU Time : 4:05.45

Quantum Calculation Wall Time: 1:07.31

MacSPARTAN '16 Properties Program: (x86/Darwin) build 1.1.2

Use of molecular symmetry enabled

Cartesian Coordinates (Angstroms)

Atom X Y Z

-----  
1 C C1 -0.4149882 -0.0000001 -2.0638391

2 O O1 -1.5193454 -0.0000003 -2.5878379

3 C C2 0.8446410 0.0000001 -2.9089405

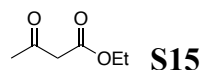
4 H H1 1.4601853 0.8844757 -2.7021895  
5 H H3 0.5598054 -0.0000002 -3.9627556  
6 H H4 1.4601856 -0.8844753 -2.7021893  
7 C C3 -0.2913548 0.0000001 -0.5634367  
8 C C4 -0.1629189 0.0000000 2.2393069  
9 C C5 0.9507541 0.0000000 0.0912858  
10 C C6 -1.4690413 0.0000001 0.2027857  
11 C C7 -1.4125452 0.0000001 1.5911985  
12 C C8 1.0206108 -0.0000001 1.4826598  
13 H H2 1.8741908 0.0000001 -0.4788949  
14 H H6 -2.4235513 0.0000002 -0.3134771  
15 H H5 -2.3236696 0.0000001 2.1814612  
16 H H7 1.9821500 -0.0000002 1.9863660  
17 C C9 -0.0954929 -0.0000001 3.6730854  
18 N N1 -0.0396155 -0.0000001 4.8354113

Point Group = CS Order = 1 Nsymop = 2

Reason for exit: Successful completion

Properties CPU Time : .43

Properties Wall Time: .44



SPARTAN '18 MECHANICS PROGRAM: (x86/Darwin) build 1.3.0

Frequency Calculation

Adjusted 4 (out of 57) low frequency modes

Reason for exit: Successful completion

Mechanics CPU Time : .05

Mechanics Wall Time: .05

SPARTAN '18 Quantum Mechanics Program: (x86/Darwin) build 1.3.0

Job type: Geometry optimization.

Method: RB3LYP

Basis set: 6-31+G\*

Number of basis functions: 191

Number of electrons: 70

Parallel Job: 4 threads

SCF model:

A restricted hybrid HF-DFT SCF calculation will be  
performed using Pulay DIIS + Geometric Direct Minimization

Optimization:

Step Energy Max Grad. Max Dist.

1 -460.335797 0.025682 0.111746 2

2 -460.339636 0.004278 0.067713 1

3 -460.339737 0.000546 0.001569

4 -460.339738 0.000445 0.007695

Reason for exit: Successful completion

Quantum Calculation CPU Time : 3:13.51

Quantum Calculation Wall Time: 50.53

SPARTAN '18 Properties Program: (x86/Darwin) build 1.3.0

Use of molecular symmetry disabled

Cartesian Coordinates (Angstroms)

Atom X Y Z

-----  
1 H H1 0.9207417 0.9517384 0.3443017

2 C C1 0.7821192 -0.0314476 -0.1273270

3 C C2 2.1209097 -0.7815242 -0.0047050

4 C C3 0.1818522 0.1677570 -1.5178661  
5 O O1 2.7455280 -1.2330440 -0.9368864  
6 O O2 0.6703666 -0.2162591 -2.5477659  
7 O O4 -0.9934112 0.8656490 -1.5795799  
8 C C4 2.6166061 -0.9147524 1.4294830  
9 H H3 2.7610556 0.0739479 1.8843296  
10 H H5 3.5627093 -1.4601144 1.4374341  
11 H H6 1.8828457 -1.4488110 2.0472124  
12 C C5 -1.7966944 1.2254436 -0.4375867  
13 H H4 -1.1690621 1.4682503 0.4259646  
14 H H8 -2.3016695 2.1446346 -0.7471181  
15 C C6 -2.8133955 0.1386423 -0.1096191  
16 H H7 -3.4728694 0.4722494 0.7010588  
17 H H9 -2.3263032 -0.7897607 0.2105282  
18 H H10 -3.4277482 -0.0852596 -0.9874569  
19 H H13 0.0564192 -0.5473395 0.5155987

Point Group = C1 Order = 1 Nsymop = 1

Reason for exit: Successful completion

Properties CPU Time : .33

Properties Wall Time: 1.33

SPARTAN '18 Graphics Program: (x86/Darwin) build 1.3.0

Graphics requests:

2: volume=potential resolution=low pending

1: volume=density resolution=low pending

Surface Type Property S.mo P.mo Resolution Value Size Time

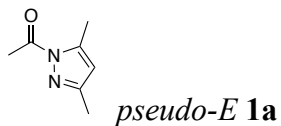
1 Elpot 0.700 -5.000 3.000 2.42

2 Density 0.700 0.002 2.000 0.33

Reason for exit: Successful completion

Graphics Program CPU Time : 2.79

Graphics Program Wall Time: 3.79



MacSPARTAN '16 MECHANICS PROGRAM: (x86/Darwin) build 1.1.2

Frequency Calculation

Adjusted 1 (out of 60) low frequency modes

Reason for exit: Successful completion

Mechanics CPU Time : .04

Mechanics Wall Time: .04

MacSPARTAN '16 Quantum Mechanics Program: (x86/Darwin) build 1.1.2

Job type: Geometry optimization.

Method: RB3LYP

Basis set: 6-31+G\*

Number of basis functions: 210

Number of electrons: 74

Parallel Job: 2 threads

SCF model:

A restricted hybrid HF-DFT SCF calculation will be

performed using Pulay DIIS + Geometric Direct Minimization

Optimization:

Step Energy Max Grad. Max Dist.

1 -457.513081 0.016836 0.082615

2 -457.515241 0.006679 0.016868

3 -457.515413 0.000944 0.003750

4 -457.515421 0.000334 0.001874



5 -457.515422 0.000086 0.000309

Reason for exit: Successful completion

Quantum Calculation CPU Time : 4:25.66

Quantum Calculation Wall Time: 2:17.76

MacSPARTAN '16 Properties Program: (x86/Darwin) build 1.1.2

Reason for exit: Successful completion

Properties CPU Time : .41

Properties Wall Time: .42

MacSPARTAN '16 Graphics Program: (x86/Darwin) build 1.1.2

Graphics requests:

1: volume=homo resolution=med pending

2: volume=lumo resolution=med pending

3: volume=density resolution=med pending

4: volume=potential resolution=med pending

5: volume=ionization resolution=med pending

Surface Type Property S.mo P.mo Resolution Value Size Time

1 MO 37 0.500 0.032 2.000 0.03

2 MO 38 0.500 0.032 2.000 0.03

3 Density 0.500 0.002 2.000 0.72

4 Elpot 0.500 -5.000 3.000 6.85

5 Local1 0.500 12.000 2.000 2.87

Reason for exit: Successful completion

Graphics Program CPU Time : 10.54

Graphics Program Wall Time: 11.55

SPARTAN '18 Properties Program: (x86/Darwin) build 1.3.0

Use of molecular symmetry enabled

Cartesian Coordinates (Angstroms)

Atom X Y Z

-----

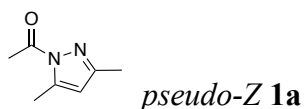
1 C C1 1.1439597 0.0000000 1.2724095  
2 C C2 1.2277643 0.0000000 -0.0994665  
3 C C3 -0.2463275 0.0000000 1.5936167  
4 N N1 -0.9867906 0.0000000 0.4977604  
5 N N2 -0.0888560 0.0000000 -0.5461210  
6 C C4 -0.5620838 0.0000000 -1.8771434  
7 O O1 0.2223857 0.0000000 -2.8088908  
8 C C5 -2.0625461 0.0000000 -2.0394063  
9 C C7 -0.8776913 0.0000000 2.9549767  
10 C C8 2.4339447 0.0000000 -0.9826101  
11 H H2 1.9767065 0.0000000 1.9634327  
12 H H3 -1.5106299 -0.8838108 3.0949252  
13 H H5 -1.5106299 0.8838108 3.0949252  
14 H H7 -0.1122757 0.0000000 3.7369053  
15 H H8 3.3321100 0.0000000 -0.3570721  
16 H H4 2.4579671 -0.8775299 -1.6366783  
17 H H9 2.4579671 0.8775299 -1.6366783  
18 H H6 -2.5051244 0.8777754 -1.5584944  
19 H H1 -2.5051244 -0.8777754 -1.5584944  
20 H H10 -2.2847256 0.0000000 -3.1078961

Point Group = CS Order = 1 Nsymop = 2

Reason for exit: Successful completion

Properties CPU Time : .40

Properties Wall Time: .41



MacSPARTAN '16 MECHANICS PROGRAM: (x86/Darwin) build 1.1.2

Frequency Calculation

Adjusted 2 (out of 60) low frequency modes

Reason for exit: Successful completion

Mechanics CPU Time : .04

Mechanics Wall Time: .04

MacSPARTAN '16 Quantum Mechanics Program: (x86/Darwin) build 1.1.2

Job type: Geometry optimization.

Method: RB3LYP

Basis set: 6-31+G\*

Number of basis functions: 210

Number of electrons: 74

SCF model:

A restricted hybrid HF-DFT SCF calculation will be

performed using Pulay DIIS + Geometric Direct Minimization

Optimization:

Step Energy Max Grad. Max Dist.

1 -457.496841 0.022157 0.076060

2 -457.499854 0.006368 0.020861

3 -457.500026 0.001463 0.003642

4 -457.500037 0.000815 0.001864

4 -457.500037 0.000312 0.004155 Switching to cartesian

5 -457.500038 0.000071 0.000994

Reason for exit: Successful completion

Quantum Calculation CPU Time : 5:31.76

Quantum Calculation Wall Time: 5:42.86

MacSPARTAN '16 Properties Program: (x86/Darwin) build 1.1.2

Reason for exit: Successful completion

Properties CPU Time : .40

Properties Wall Time: 1.41

MacSPARTAN '16 Graphics Program: (x86/Darwin) build 1.1.2

Graphics requests:

1: volume=homo resolution=med pending

2: volume=lumo resolution=med pending

3: volume=density resolution=med pending

4: volume=potential resolution=med pending

5: volume=ionization resolution=med pending

Surface Type Property S.mo P.mo Resolution Value Size Time

1 MO 37 0.500 0.032 2.000 0.03

2 MO 38 0.500 0.032 2.000 0.02

3 Density 0.500 0.002 2.000 0.73

4 Elpot 0.500 -5.000 3.000 6.92

5 LocalI 0.500 12.000 2.000 2.86

Reason for exit: Successful completion

Graphics Program CPU Time : 10.59

Graphics Program Wall Time: 11.60

SPARTAN '18 Properties Program: (x86/Darwin) build 1.3.0

Use of molecular symmetry enabled

Cartesian Coordinates (Angstroms)

Atom X Y Z

-----

1 C C1 0.7770233 0.0000000 1.4096658

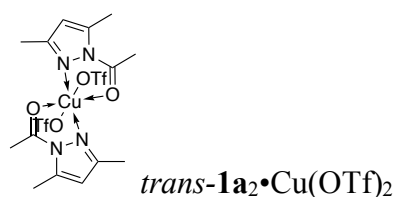
2 C C2 0.7680003 0.0000000 0.0363938  
 3 C C3 -0.5876879 0.0000000 1.8211905  
 4 N N1 -1.3963107 0.0000000 0.7785630  
 5 N N2 -0.5810840 0.0000000 -0.3283849  
 6 C C4 -1.2318339 0.0000000 -1.6005942  
 7 O O1 -2.4401939 0.0000000 -1.6667285  
 8 C C5 -0.3652111 0.0000000 -2.8431370  
 9 C C7 -1.1327770 0.0000000 3.2195911  
 10 C C8 1.9652038 0.0000000 -0.8660358  
 11 H H2 1.6563866 0.0000000 2.0408791  
 12 H H3 -1.7569542 -0.8833029 3.3958102  
 13 H H5 -1.7569542 0.8833029 3.3958102  
 14 H H7 -0.3215712 0.0000000 3.9543291  
 15 H H8 2.8617576 0.0000000 -0.2395271  
 16 H H4 2.0158153 -0.8852544 -1.5094408  
 17 H H9 2.0158153 0.8852544 -1.5094408  
 18 H H6 0.2752715 -0.8859859 -2.8942387  
 19 H H1 0.2752715 0.8859860 -2.8942387  
 20 H H10 -1.0399670 0.0000000 -3.7004661

Point Group = CS Order = 1 Nsymop = 2

Reason for exit: Successful completion

Properties CPU Time : .40

Properties Wall Time: .41



SPARTAN '18 MECHANICS PROGRAM: (x86/Darwin) build 1.3.0

Frequency Calculation

Adjusted 11 (out of 171) low frequency modes

Reason for exit: Successful completion

Mechanics CPU Time : .09

Mechanics Wall Time: .16

SPARTAN '18 Quantum Mechanics Program: (x86/Darwin) build 1.3.0

Job type: Geometry optimization.

Method: UB3LYP

Basis set: 6-31+G\*

Number of basis functions: 761

Number of electrons: 323 (1 unpaired)

Parallel Job: 4 threads

SCF model:

An unrestricted hybrid HF-DFT SCF calculation will be  
performed using Pulay DIIS + Geometric Direct Minimization

Optimization:

Step Energy Max Grad. Max Dist.

1 -4478.309237 0.059175 0.119375

2 -4478.335820 0.024282 0.087579

3 -4478.345399 0.007531 0.094833

4 -4478.349733 0.003973 0.084114

5 -4478.350979 0.002490 0.113948

6 -4478.351691 0.002308 0.147439

7 -4478.352175 0.001998 0.150682

8 -4478.352508 0.001495 0.140402

9 -4478.352786 0.000675 0.127927

10 -4478.352922 0.000816 0.083775

11 -4478.352971 0.000740 0.032876

12 -4478.353001 0.000729 0.036842

13 -4478.353010 0.000388 0.033897

Reason for exit: Successful completion

Quantum Calculation CPU Time : 27:15:41.31

Quantum Calculation Wall Time: 6:51:26.01

SPARTAN '18 Properties Program: (x86/Darwin) build 1.3.0

Use of molecular symmetry disabled

Cartesian Coordinates (Angstroms)

Atom X Y Z

-----  
1 C C1 -3.9063218 0.5369078 1.6157358

2 C C2 -4.1875045 0.2093970 0.3117571

3 C C3 -2.5001798 0.4283703 1.7789195

4 N N1 -1.9525536 0.0458503 0.6371405

5 N N2 -2.9684297 -0.1052897 -0.2753035

6 C C4 -2.5899483 -0.5003478 -1.5833325

7 O O1 -1.4146229 -0.7446715 -1.7956100

8 C C5 -3.6343966 -0.5911370 -2.6577354

9 C C7 -1.6831150 0.7017521 3.0000417

10 C C8 -5.5288574 0.1803288 -0.3494803

11 H H2 -4.6246429 0.8284762 2.3695502

12 H H3 -1.1858502 1.6752607 2.9193182

13 H H5 -0.9048606 -0.0551259 3.1255518

14 H H7 -2.3217787 0.7116952 3.8877476

15 H H8 -6.2757739 0.5044165 0.3797994

16 H H4 -5.5820384 0.8572300 -1.2076693

17 H H9 -5.8078135 -0.8242957 -0.6860242  
18 H H6 -4.0336023 0.4062586 -2.8680582  
19 H H1 -4.4568599 -1.2569593 -2.3847767  
20 H H10 -3.1421732 -0.9708457 -3.5537610  
21 C C6 3.8507974 -0.4267570 -1.6131508  
22 C C9 4.1280655 -0.0357714 -0.3274813  
23 C C10 2.4392151 -0.5042680 -1.7347047  
24 N N3 1.8808463 -0.1604982 -0.5830862  
25 N N4 2.8984945 0.1416349 0.2947838  
26 C C11 2.5231772 0.5011866 1.6102038  
27 O O2 1.3407999 0.6695742 1.8556097  
28 C C12 3.5859142 0.6462688 2.6630668  
29 C C13 1.6399330 -0.9020468 -2.9303408  
30 C C14 5.4770992 0.1758503 0.2827034  
31 H H11 4.5756881 -0.6493020 -2.3835372  
32 H H12 1.0645997 -0.0483274 -3.3054855  
33 H H13 0.9412217 -1.7051716 -2.6774996  
34 H H14 2.3062199 -1.2539970 -3.7225286  
35 H H15 6.2310912 -0.0408400 -0.4784209  
36 H H16 5.6307973 1.2082945 0.6149667  
37 H H17 5.6599653 -0.4905389 1.1315376  
38 H H18 4.3250406 1.4095166 2.4050514  
39 H H19 4.0987704 -0.3087771 2.8141866  
40 H H20 3.0843780 0.9326580 3.5882674  
41 Cu Cu1 -0.0290826 -0.0727338 0.0362612  
42 O O3 -0.0141075 -1.9068602 0.8219267  
43 S S1 1.1060737 -2.9383083 0.8853022



44 O O4 1.3733918 -3.5981154 -0.3977189

45 O O5 2.2628147 -2.4920115 1.6829531

46 O O6 -0.1013800 1.8586440 -0.5020658

47 S S2 -0.6700256 2.5266936 -1.7430090

48 O O7 0.1273485 2.3054271 -2.9556868

49 O O8 -2.1349425 2.3944284 -1.8547427

50 C C15 -0.3792406 4.3213478 -1.2727736

51 C C16 0.2566413 -4.2323112 1.9505881

52 F F1 -1.0340644 4.6299911 -0.1398909

53 F F2 0.9297210 4.5569542 -1.0833293

54 F F3 -0.8189876 5.1283257 -2.2504397

55 F F4 -0.0840809 -3.7204870 3.1466121

56 F F5 -0.8567097 -4.6890672 1.3543489

57 F F6 1.0858392 -5.2678766 2.1537119

Point Group = C1 Order = 1 Nsymop = 1

Reason for exit: Successful completion

Properties CPU Time : 13.87

Properties Wall Time: 14.97

SPARTAN '18 Graphics Program: (x86/Darwin) build 1.3.0

Graphics requests:

3: volume=density resolution=med pending

4: volume=potential resolution=med pending

5: volume=ionization resolution=med pending

2: volume=lumo resolution=med pending

1: volume=homo resolution=med pending

Surface Type Property S.mo P.mo Resolution Value Size Time

1 Density 0.500 0.002 2.000 43.52

2 Elpot 0.500 -5.000 3.000 128.62

3 LocalI 0.500 12.000 2.000 63.29

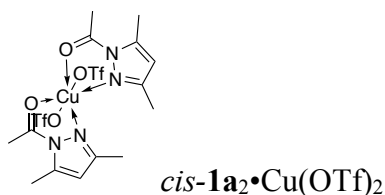
4 Alpha MO 163 0.500 0.032 2.000 0.39

5 Alpha MO 162 0.500 0.032 2.000 0.38

Reason for exit: Successful completion

Graphics Program CPU Time : 3:56.74

Graphics Program Wall Time: 3:57.91



SPARTAN '18 MECHANICS PROGRAM: (x86/Darwin) build 1.3.0

Frequency Calculation

Adjusted 11 (out of 171) low frequency modes

Reason for exit: Successful completion

Mechanics CPU Time : .13

Mechanics Wall Time: .13

SPARTAN '18 Quantum Mechanics Program: (x86/Darwin) build 1.3.0

Job type: Geometry optimization.

Method: UB3LYP

Basis set: 6-31+G\*

Number of basis functions: 761

Number of electrons: 323 (1 unpaired)

SCF model:

An unrestricted hybrid HF-DFT SCF calculation will be

performed using Pulay DIIS + Geometric Direct Minimization

Optimization:

Step Energy Max Grad. Max Dist.

1 -4478.300204 0.060816 0.129454  
2 -4478.326259 0.022966 0.078907  
3 -4478.334052 0.007404 0.127599  
4 -4478.336591 0.004303 0.133995  
5 -4478.338204 0.002816 0.132098  
6 -4478.339401 0.003742 0.117530  
7 -4478.340378 0.004305 0.115566  
8 -4478.341252 0.003812 0.093934  
9 -4478.341978 0.002513 0.101648  
10 -4478.342408 0.002545 0.126363  
11 -4478.342687 0.003089 0.187342  
12 -4478.342913 0.002631 0.180741  
13 -4478.343120 0.001847 0.130558  
14 -4478.343339 0.001500 0.128414  
15 -4478.343523 0.001294 0.160616  
16 -4478.343727 0.001875 0.176900  
17 -4478.343870 0.002370 0.062224  
18 -4478.343953 0.001317 0.045571  
19 -4478.344007 0.000696 0.042685  
20 -4478.344052 0.000565 0.104713  
21 -4478.344131 0.000756 0.126969  
22 -4478.344076 0.001121 0.086050  
23 -4478.344179 0.000868 0.052867  
24 -4478.344181 0.000694 0.045855

Reason for exit: Successful completion

Quantum Calculation CPU Time : 38:23:05.19

Quantum Calculation Wall Time: 38:33:35.12

SPARTAN '18 Properties Program: (x86/Darwin) build 1.3.0

Use of molecular symmetry disabled

Cartesian Coordinates (Angstroms)

Atom X Y Z

```
-----  
1 C C1 3.3983596 0.6805054 2.5374028  
2 C C2 3.7413407 1.4240398 1.4347800  
3 C C3 2.2511479 -0.0789693 2.1841949  
4 N N1 1.9182336 0.1770810 0.9280312  
5 N N2 2.8204754 1.0961883 0.4502347  
6 C C4 2.6567757 1.4868369 -0.9077108  
7 O O1 1.7380312 0.9924611 -1.5316005  
8 C C5 3.6127568 2.4718897 -1.5160021  
9 C C7 1.4750196 -1.0151412 3.0533976  
10 C C8 4.8660041 2.4024997 1.3114194  
11 H H2 3.9052054 0.6846743 3.4927823  
12 H H3 0.8345891 -1.6812894 2.4716065  
13 H H5 0.8488112 -0.4504980 3.7562230  
14 H H7 2.1587041 -1.6321429 3.6463373  
15 H H8 5.3807456 2.4550568 2.2742814  
16 H H4 5.6023393 2.1071148 0.5565000  
17 H H9 4.5086230 3.4076047 1.0658335  
18 H H6 4.6496368 2.1281956 -1.4584241  
19 H H1 3.5246613 3.4418857 -1.0182384  
20 H H10 3.3259094 2.5875179 -2.5618989  
21 Cu Cu1 0.1420736 -0.1181258 -0.0923825  
22 H H11 -2.9965919 -0.6164993 -4.2607622
```

23 C C6 -2.1516575 -1.2334966 -3.9417541  
24 H H12 -1.3451537 -1.1392631 -4.6699814  
25 H H16 -2.4742074 -2.2782088 -3.8943120  
26 C C9 -1.5995610 -0.7867850 -2.6164987  
27 O O2 -0.4531198 -0.4165440 -2.4737263  
28 N N3 -2.4431331 -0.8146454 -1.4692628  
29 N N4 -1.8495655 -0.5122966 -0.2696630  
30 C C11 -3.7833133 -1.1078738 -1.2778316  
31 C C12 -4.0147491 -0.9761626 0.0708287  
32 H H19 -4.9579635 -1.1321594 0.5756955  
33 C C10 -2.7842460 -0.6076091 0.6672624  
34 C C13 -4.7715684 -1.4856061 -2.3351175  
35 H H13 -4.4949867 -2.4132419 -2.8461951  
36 H H15 -4.8976023 -0.7012595 -3.0887578  
37 H H17 -5.7411480 -1.6441566 -1.8560431  
38 C C14 -2.4898341 -0.3961364 2.1160567  
39 H H14 -2.1151995 -1.3282751 2.5564504  
40 H H18 -3.3996663 -0.1055077 2.6495470  
41 H H20 -1.7418676 0.3894654 2.2518944  
42 O O3 -0.6801323 -3.3502897 1.3107210  
43 S S1 -0.1483039 -3.2683180 -0.0601481  
44 O O4 -1.0537702 -3.6024782 -1.1686563  
45 O O5 0.6780254 -2.0100513 -0.2963211  
46 C C15 1.2287053 -4.5437472 -0.1371287  
47 F F1 0.7283282 -5.7637565 0.1113226  
48 F F2 1.8028502 -4.5544910 -1.3485003  
49 F F3 2.1730828 -4.2751500 0.7821112

50 O O6 -0.3527131 1.6845721 0.6034756

51 S S2 -0.4130482 3.0450578 -0.0857199

52 O O7 0.8913538 3.7297581 -0.0953133

53 O O8 -1.2182681 3.0576423 -1.3095636

54 C C16 -1.4299285 3.9715763 1.1938955

55 F F4 -1.5704981 5.2524100 0.8215899

56 F F5 -2.6534763 3.4250631 1.3132469

57 F F6 -0.8365157 3.9410781 2.4003918

Point Group = C1 Order = 1 Nsymop = 1

Reason for exit: Successful completion

Properties CPU Time : 12.83

Properties Wall Time: 13.87

SPARTAN '18 Graphics Program: (x86/Darwin) build 1.3.0

Graphics requests:

3: volume=density resolution=med pending

4: volume=potential resolution=med pending

5: volume=ionization resolution=med pending

2: volume=lumo resolution=med pending

1: volume=homo resolution=med pending

Surface Type Property S.mo P.mo Resolution Value Size Time

1 Density 0.500 0.002 2.000 43.63

2 Elpot 0.500 -5.000 3.000 124.47

3 LocalI 0.500 12.000 2.000 60.38

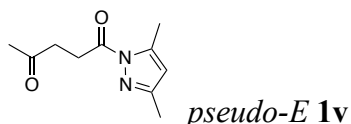
4 Alpha MO 163 0.500 0.032 2.000 0.38

5 Alpha MO 162 0.500 0.032 2.000 0.37

Reason for exit: Successful completion

Graphics Program CPU Time : 3:49.76

Graphics Program Wall Time: 3:50.82



MacSPARTAN '16 MECHANICS PROGRAM: (x86/Darwin) build 1.1.2

Frequency Calculation

Adjusted 4 (out of 84) low frequency modes

Reason for exit: Successful completion

Mechanics CPU Time : .04

Mechanics Wall Time: .05

MacSPARTAN '16 Quantum Mechanics Program: (x86/Darwin) build 1.1.2

Job type: Geometry optimization.

Method: RB3LYP

Basis set: 6-31+G\*

Number of basis functions: 294

Number of electrons: 104

SCF model:

A restricted hybrid HF-DFT SCF calculation will be

performed using Pulay DIIS + Geometric Direct Minimization

Optimization:

Step Energy Max Grad. Max Dist.

1 -649.473623 0.017568 0.090000

2 -649.476798 0.004107 0.060426

2 -649.476798 0.006156 0.031881 Switching to cartesian

3 -649.477079 0.001979 0.009266

4 -649.477092 0.000295 0.002446

5 -649.477093 0.000078 0.001067

Reason for exit: Successful completion

Quantum Calculation CPU Time : 13:24.67

Quantum Calculation Wall Time: 13:47.90

MacSPARTAN '16 Properties Program: (x86/Darwin) build 1.1.2

Reason for exit: Successful completion

Properties CPU Time : .87

Properties Wall Time: 1.89

MacSPARTAN '16 Graphics Program: (x86/Darwin) build 1.1.2

Graphics requests:

1: volume=homo resolution=med pending

2: volume=lumo resolution=med pending

3: volume=density resolution=med pending

4: volume=potential resolution=med pending

5: volume=ionization resolution=med pending

Surface Type Property S.mo P.mo Resolution Value Size Time

1 MO 52 0.500 0.032 2.000 0.05

2 MO 53 0.500 0.032 2.000 0.06

3 Density 0.500 0.002 2.000 1.89

4 Elpot 0.500 -5.000 3.000 13.81

5 Local1 0.500 12.000 2.000 6.83

Reason for exit: Successful completion

Graphics Program CPU Time : 22.68

Graphics Program Wall Time: 23.88

SPARTAN '18 Properties Program: (x86/Darwin) build 1.3.0

Use of molecular symmetry enabled

Cartesian Coordinates (Angstroms)

Atom X Y Z

-----



1 C C1 0.0476140 0.0000000 3.4282226  
2 H H2 -0.1084097 0.0000000 4.4989430  
3 C C2 -0.9321139 0.0000000 2.4646936  
4 C C3 1.2967918 0.0000000 2.7369769  
5 N N1 1.1144095 0.0000000 1.4276784  
6 N N2 -0.2508224 0.0000000 1.2511781  
7 C C4 -0.7885614 0.0000000 -0.0530981  
8 O O1 -1.9968308 0.0000000 -0.2191751  
9 C C5 0.2230836 0.0000000 -1.1815572  
10 H H1 0.8872054 0.8637120 -1.0690679  
11 H H6 0.8872054 -0.8637120 -1.0690679  
12 C C6 -0.4599639 0.0000000 -2.5461867  
13 H H3 -1.1245422 0.8684282 -2.6520279  
14 H H7 -1.1245422 -0.8684282 -2.6520279  
15 C C7 2.6777904 0.0000000 3.3241357  
16 H H5 2.6351888 0.0000000 4.4175760  
17 H H8 3.2408644 0.8833848 3.0022487  
18 H H9 3.2408644 -0.8833848 3.0022487  
19 C C8 -2.4192024 0.0000000 2.6156993  
20 H H4 -2.8750835 0.8776889 2.1462686  
21 H H10 -2.6680393 0.0000000 3.6816752  
22 H H12 -2.8750835 -0.8776889 2.1462686  
23 C C9 0.5184946 0.0000000 -3.7133758  
24 O O2 1.7268891 0.0000000 -3.5486854  
25 C C10 -0.0951624 0.0000000 -5.1029510  
26 H H11 -0.7353515 -0.8812636 -5.2385652  
27 H H13 0.6926593 0.0000000 -5.8594620

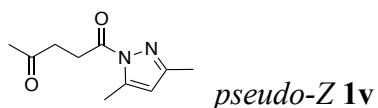
28 H H14 -0.7353515 0.8812636 -5.2385652

Point Group = CS Order = 1 Nsymop = 2

Reason for exit: Successful completion

Properties CPU Time : .90

Properties Wall Time: 1.92



MacSPARTAN '16 MECHANICS PROGRAM: (x86/Darwin) build 1.1.2

Frequency Calculation

Adjusted 4 (out of 84) low frequency modes

Reason for exit: Successful completion

Mechanics CPU Time : .06

Mechanics Wall Time: .06

MacSPARTAN '16 Quantum Mechanics Program: (x86/Darwin) build 1.1.2

Job type: Geometry optimization.

Method: RB3LYP

Basis set: 6-31+G\*

Number of basis functions: 294

Number of electrons: 104

SCF model:

A restricted hybrid HF-DFT SCF calculation will be

performed using Pulay DIIS + Geometric Direct Minimization

Optimization:

Step Energy Max Grad. Max Dist.

1 -649.459097 0.020569 0.090000

2 -649.462744 0.008691 0.068537

3 -649.463194 0.001374 0.003938

4 -649.463208 0.000232 0.001349

5 -649.463208 0.000109 0.000241

Reason for exit: Successful completion

Quantum Calculation CPU Time : 13:19.85

Quantum Calculation Wall Time: 13:43.39

MacSPARTAN '16 Properties Program: (x86/Darwin) build 1.1.2

Reason for exit: Successful completion

Properties CPU Time : .86

Properties Wall Time: 1.87

MacSPARTAN '16 Graphics Program: (x86/Darwin) build 1.1.2

Graphics requests:

1: volume=homo resolution=med pending

2: volume=lumo resolution=med pending

3: volume=density resolution=med pending

4: volume=potential resolution=med pending

5: volume=ionization resolution=med pending

Surface Type Property S.mo P.mo Resolution Value Size Time

1 MO 52 0.500 0.032 2.000 0.05

2 MO 53 0.500 0.032 2.000 0.05

3 Density 0.500 0.002 2.000 1.84

4 Elpot 0.500 -5.000 3.000 13.84

5 LocalI 0.500 12.000 2.000 6.76

Reason for exit: Successful completion

Graphics Program CPU Time : 22.58

Graphics Program Wall Time: 23.70

SPARTAN '18 Properties Program: (x86/Darwin) build 1.3.0

Use of molecular symmetry enabled

Cartesian Coordinates (Angstroms)

Atom X Y Z

-----  
1 C C1 1.0170471 0.0000000 3.1106681  
2 H H2 1.8837173 0.0000000 3.7591639  
3 C C2 1.0369246 0.0000000 1.7376755  
4 C C3 -0.3554262 0.0000000 3.4952849  
5 N N1 -1.1436658 0.0000001 2.4374396  
6 N N2 -0.3060762 0.0000001 1.3458226  
7 C C4 -0.9370226 0.0000001 0.0646505  
8 O O1 -2.1460500 0.0000000 -0.0166188  
9 C C5 -0.0414000 0.0000000 -1.1626477  
10 H H1 0.6207865 0.8719984 -1.1434854  
11 H H6 0.6207866 -0.8719984 -1.1434854  
12 C C6 -0.8565967 -0.0000001 -2.4538476  
13 H H3 -1.5280094 0.8682204 -2.4914479  
14 H H7 -1.5280094 -0.8682205 -2.4914479  
15 C C7 -0.9276221 0.0000000 4.8828827  
16 H H5 -0.1306962 -0.0000001 5.6330314  
17 H H8 -1.5550879 -0.8833384 5.0469744  
18 H H9 -1.5550879 0.8833384 5.0469744  
19 C C8 2.2535037 0.0000000 0.8613473  
20 H H4 2.3191224 -0.8836834 0.2176957  
21 H H10 3.1357419 -0.0000001 1.5077949  
22 H H12 2.3191225 0.8836834 0.2176957  
23 C C9 0.0133671 0.0000000 -3.7031396  
24 O O2 1.2325806 0.0000000 -3.6411052

25 C C10 -0.7157159 0.0000000 -5.0339082

26 H H11 -1.3653564 -0.8810106 -5.1144755

27 H H13 0.0044788 0.0000001 -5.8550171

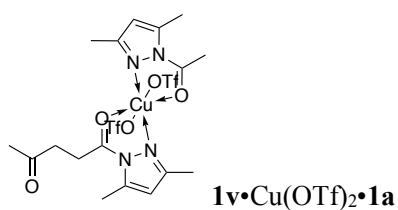
28 H H14 -1.3653564 0.8810106 -5.1144754

Point Group = CS Order = 1 Nsymop = 2

Reason for exit: Successful completion

Properties CPU Time : .89

Properties Wall Time: 1.91



SPARTAN '18 MECHANICS PROGRAM: (x86/Darwin) build 1.3.0

Frequency Calculation

Adjusted 15 (out of 186) low frequency modes

Reason for exit: Successful completion

Mechanics CPU Time : .11

Mechanics Wall Time: .11

SPARTAN '18 Quantum Mechanics Program: (x86/Darwin) build 1.3.0

Job type: Geometry optimization.

Method: UB3LYP

Basis set: 6-31+G\*

Number of basis functions: 822

Number of electrons: 345 (1 unpaired)

Parallel Job: 2 threads

SCF model:

An unrestricted hybrid HF-DFT SCF calculation will be

performed using Pulay DIIS + Geometric Direct Minimization

Optimization:

Step Energy Max Grad. Max Dist.

1 -4630.947526 0.057206 0.113722

2 -4630.974868 0.025105 0.072148

3 -4630.985331 0.010203 0.072086

4 -4630.990251 0.004823 0.074321

5 -4630.992273 0.003417 0.086559

6 -4630.993254 0.002794 0.080410

7 -4630.993614 0.001882 0.091211

8 -4630.994004 0.001255 0.088523

9 -4630.994325 0.001311 0.131596

10 -4630.994530 0.001291 0.144593

11 -4630.994901 0.001453 0.152708

12 -4630.995054 0.001527 0.160809

13 -4630.995121 0.001159 0.042579

14 -4630.995165 0.000811 0.039000

15 -4630.995188 0.000854 0.070128

16 -4630.995210 0.000801 0.019354

17 -4630.995216 0.000422 0.006503

Reason for exit: Successful completion

Quantum Calculation CPU Time : 31:52:30.97

Quantum Calculation Wall Time: 16:00:26.98

SPARTAN '18 Properties Program: (x86/Darwin) build 1.3.0

Use of molecular symmetry disabled

Cartesian Coordinates (Angstroms)

Atom X Y Z

-----  
1 C C1 2.2728545 0.6603521 -3.8970669  
2 H H2 3.2662417 0.7393535 -4.3154980  
3 C C2 1.0904946 0.6388136 -4.5901805  
4 N N2 0.0939818 0.5244274 -3.6348925  
5 C C4 -1.2837542 0.4998501 -3.8093107  
6 O O1 -2.0640483 0.3880662 -2.8869140  
7 C C8 0.8123839 0.7249501 -6.0557887  
8 H H4 0.2600546 -0.1482363 -6.4223814  
9 H H10 1.7600948 0.7722677 -6.5979745  
10 H H12 0.2381789 1.6256176 -6.3036997  
11 Cu Cu1 -0.5959532 0.4080306 -0.7888111  
12 C C11 -3.5742580 0.0056667 2.1727285  
13 H H15 -4.5872392 -0.0189349 2.5500744  
14 C C12 -2.4382568 -0.3056077 2.8811045  
15 C C13 -3.1655549 0.3665893 0.8625333  
16 N N3 -1.8470897 0.2871590 0.7771585  
17 N N6 -1.3771643 -0.1185036 2.0029905  
18 C C14 0.0324267 -0.2334672 2.1302946  
19 O O3 0.7239695 0.1412869 1.1967184  
20 C C19 0.6009271 -0.8166442 3.3956389  
21 C C16 2.1060191 -1.0488440 3.2870480  
22 C C17 -4.0141922 0.7697034 -0.2997736  
23 H H20 -4.9921009 1.1137081 0.0488313  
24 H H21 -4.1678722 -0.0770837 -0.9787414  
25 H H22 -3.5362650 1.5691988 -0.8713666  
26 C C18 -2.3506857 -0.7390849 4.3097193

27 H H23 -1.9410121 -1.7490718 4.4129095  
28 H H24 -3.3612098 -0.7448678 4.7265841  
29 H H25 -1.7415264 -0.0643219 4.9196201  
30 C C15 2.7035181 -1.5595046 4.5916301  
31 O O4 2.0519193 -1.6041327 5.6228393  
32 H H31 2.3277003 -1.7585504 2.4806727  
33 H H32 2.6279089 -0.1219608 3.0131996  
34 H H33 0.3828123 -0.1568876 4.2434228  
35 H H34 0.0955968 -1.7644332 3.6001909  
36 C C20 4.1494574 -2.0097805 4.5380383  
37 H H16 4.5157156 -2.2170040 5.5459615  
38 H H17 4.7802341 -1.2505683 4.0591905  
39 H H18 4.2285245 -2.9199962 3.9289981  
40 N N1 0.6288119 0.4933104 -2.3721007  
41 C C3 1.9452158 0.5722235 -2.5128046  
42 C C7 2.8689454 0.5668517 -1.3419017  
43 H H5 2.7425269 -0.3572264 -0.7678105  
44 H H8 2.6543609 1.4199681 -0.6895186  
45 H H9 3.9057902 0.6372172 -1.6806787  
46 H H19 -1.5880878 0.5808577 -4.8604899  
47 O O2 -0.8011484 2.3757562 -0.6653223  
48 O O5 -0.1576190 -2.8970069 1.0552796  
49 S S1 0.1558985 -2.6902886 -0.3709036  
50 O O6 -0.6689517 -1.5851390 -1.0090022  
51 O O7 1.5748373 -2.6728798 -0.7533997  
52 S S2 -0.1666726 3.4818876 -1.5069174  
53 O O8 1.2531438 3.7003093 -1.2041906



54 O O9 -0.5716776 3.4396171 -2.9213050

55 C C5 -1.0748727 4.9559749 -0.7770696

56 C C6 -0.5849265 -4.1729086 -1.2536194

57 F F1 -2.4024411 4.8300724 -0.9483931

58 F F2 -0.8257641 5.0673747 0.5370375

59 F F3 -0.6724563 6.0820752 -1.3851745

60 F F4 -1.9013150 -4.2658815 -1.0082680

61 F F5 -0.4055063 -4.0716244 -2.5816080

62 F F6 0.0090766 -5.2980958 -0.8275367

Point Group = C1 Order = 1 Nsymop = 1

Reason for exit: Successful completion

Properties CPU Time : 17.45

Properties Wall Time: 18.51

SPARTAN '18 Graphics Program: (x86/Darwin) build 1.3.0

Graphics requests:

3: volume=density resolution=med pending

4: volume=potential resolution=med pending

5: volume=ionization resolution=med pending

2: volume=lumo resolution=med pending

1: volume=homo resolution=med pending

Surface Type Property S.mo P.mo Resolution Value Size Time

1 Density 0.500 0.002 2.000 61.98

2 Elpot 0.500 -5.000 3.000 164.40

3 LocalI 0.500 12.000 2.000 70.51

4 Alpha MO 174 0.500 0.032 2.000 0.49

5 Alpha MO 173 0.500 0.032 2.000 0.50

Reason for exit: Successful completion

Graphics Program CPU Time : 4:58.51

Graphics Program Wall Time: 4:59.64

## 2-5-19. Conformational stability of *pseudo-E/Z* 1a and *pseudo-E/Z* S16 (Figure 1A)

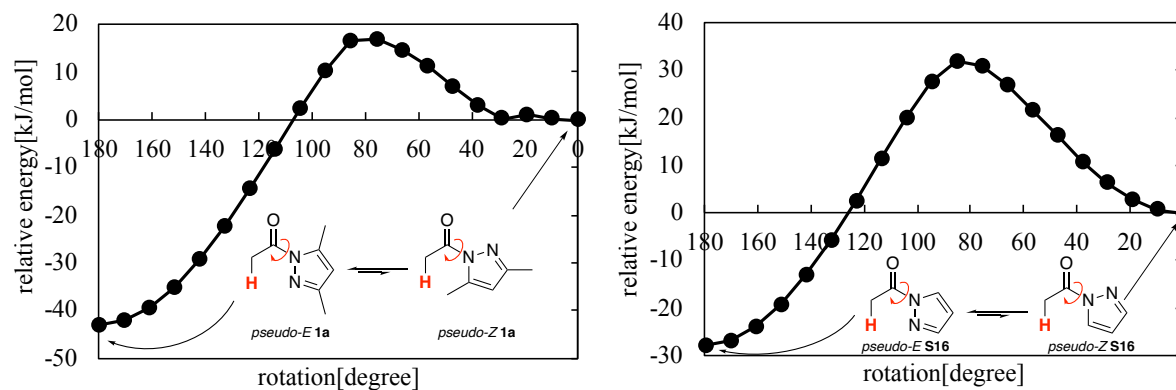
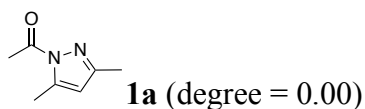


**Figure S7.** Relationship between relative energy and dihedral angle of **1a** (a) and **S16** (b).

**Table S3.** Summary of DFT calculation of **1a** (degree = 0.00 to 180.00) and **S16** (degree = 0.00 to 180.00) by using B3LYP/6-31+G\*



SPARTAN '18 MECHANICS PROGRAM: (x86/Darwin) build 1.3.0

Frequency Calculation

Adjusted 2 (out of 60) low frequency modes

Reason for exit: Successful completion

Mechanics CPU Time : .05

Mechanics Wall Time: .05

SPARTAN '18 Quantum Mechanics Program: (x86/Darwin) build 1.3.0

Job type: Geometry optimization.

Method: RB3LYP

Basis set: 6-31+G\*

Number of basis functions: 210

Number of electrons: 74

Parallel Job: 4 threads

SCF model:

A restricted hybrid HF-DFT SCF calculation will be performed using Pulay DIIS + Geometric Direct Minimization

Optimization:

Step Energy Max Grad. Max Dist.

1 -457.496842 0.022155 0.076043

2 -457.499855 0.006366 0.020853

3 -457.500026 0.001459 0.004249

4 -457.500037 0.000705 0.001252

5 -457.500038 0.000182 0.000268

Reason for exit: Successful completion

Quantum Calculation CPU Time : 5:52.87

Quantum Calculation Wall Time: 1:31.36

SPARTAN '18 Properties Program: (x86/Darwin) build 1.3.0

Use of molecular symmetry disabled

Cartesian Coordinates (Angstroms)

Atom X Y Z

-----  
1 C C1 0.7747914 0.0000000 1.4109744

2 C C2 0.7680045 0.0000000 0.0376909

3 C C3 -0.5906000 0.0000000 1.8202708

4 N N1 -1.3975208 0.0000000 0.7763314

5 N N2 -0.5804864 0.0000000 -0.3292838

6 C C4 -1.2291877 0.0000000 -1.6025368

7 O O1 -2.4374437 0.0000000 -1.6705932

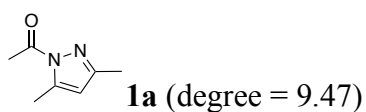
8 C C5 -0.3606298 0.0000000 -2.8437153  
9 H H2 1.6531288 0.0000000 2.0436135  
10 H H6 0.2799244 -0.8859891 -2.8938634  
11 H H1 0.2799244 0.8859891 -2.8938634  
12 H H10 -1.0340283 0.0000000 -3.7020496  
13 C C6 1.9665937 0.0000000 -0.8629027  
14 H H3 2.8622132 0.0000000 -0.2350977  
15 H H4 2.0181159 0.8852438 -1.5062532  
16 H H5 2.0181159 -0.8852438 -1.5062532  
17 C C7 -1.1379891 0.0000000 3.2177743  
18 H H7 -0.3280013 0.0000000 3.9538452  
19 H H8 -1.7624625 -0.8833032 3.3929559  
20 H H9 -1.7624625 0.8833032 3.3929559

Point Group = C1 Order = 1 Nsymop = 1

Reason for exit: Successful completion

Properties CPU Time : .40

Properties Wall Time: 1.40



SPARTAN '18 MECHANICS PROGRAM: (x86/Darwin) build 1.3.0

Frequency Calculation

Adjusted 2 (out of 60) low frequency modes

Reason for exit: Successful completion

Mechanics CPU Time : .05

Mechanics Wall Time: .05

SPARTAN '18 Quantum Mechanics Program: (x86/Darwin) build 1.3.0

Job type: Geometry optimization.

Method: RB3LYP

Basis set: 6-31+G\*

Number of basis functions: 210

Number of electrons: 74

Parallel Job: 4 threads

SCF model:

A restricted hybrid HF-DFT SCF calculation will be performed using Pulay DIIS + Geometric Direct Minimization

Optimization:

Step Energy Max Grad. Max Dist.

1 -457.499858 0.001764 0.016643

2 -457.499884 0.001495 0.070707

3 -457.499943 0.000401 0.004550

4 -457.499946 0.000337 0.023813

Reason for exit: Successful completion

Quantum Calculation CPU Time : 4:36.86

Quantum Calculation Wall Time: 1:11.86

SPARTAN '18 Properties Program: (x86/Darwin) build 1.3.0

Use of molecular symmetry disabled

Cartesian Coordinates (Angstroms)

Atom X Y Z

-----  
1 C C1 0.7740452 -0.0134718 1.4108334  
2 C C2 0.7668739 -0.0130175 0.0373799  
3 C C3 -0.5912103 0.0004200 1.8201990  
4 N N1 -1.3982505 0.0093754 0.7760455  
5 N N2 -0.5806935 0.0048338 -0.3289291

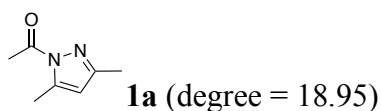
6 C C4 -1.2270068 0.0159129 -1.6034380  
7 O O1 -2.4204292 0.2005285 -1.6796301  
8 C C5 -0.3734354 -0.2223959 -2.8322406  
9 H H2 1.6524846 -0.0168678 2.0433115  
10 H H6 0.1620226 -1.1759982 -2.7749610  
11 H H1 0.3633190 0.5732042 -2.9767787  
12 H H10 -1.0474658 -0.2399867 -3.6898690  
13 C C6 1.9631249 -0.0002056 -0.8663296  
14 H H3 2.8605453 0.0047969 -0.2411460  
15 H H4 2.0047321 0.8904034 -1.5038414  
16 H H5 2.0202309 -0.8803288 -1.5156325  
17 C C7 -1.1385791 -0.0013978 3.2177500  
18 H H7 -0.3285504 -0.0102669 3.9537319  
19 H H8 -1.7696348 -0.8806183 3.3899498  
20 H H9 -1.7562916 0.8859588 3.3962881

Point Group = C1 Order = 1 Nsymop = 1

Reason for exit: Successful completion

Properties CPU Time : .41

Properties Wall Time: .42



SPARTAN '18 MECHANICS PROGRAM: (x86/Darwin) build 1.3.0

Frequency Calculation

Adjusted 2 (out of 60) low frequency modes

Reason for exit: Successful completion

Mechanics CPU Time : .06

Mechanics Wall Time: .06

SPARTAN '18 Quantum Mechanics Program: (x86/Darwin) build 1.3.0

Job type: Geometry optimization.

Method: RB3LYP

Basis set: 6-31+G\*

Number of basis functions: 210

Number of electrons: 74

Parallel Job: 4 threads

SCF model:

A restricted hybrid HF-DFT SCF calculation will be  
performed using Pulay DIIS + Geometric Direct Minimization

Optimization:

Step Energy Max Grad. Max Dist.

1 -457.499430 0.004428 0.125122

2 -457.499543 0.001243 0.001767

3 -457.499548 0.001209 0.003534

4 -457.499558 0.001141 0.049512

5 -457.499630 0.000643 0.062420

6 -457.499640 0.000432 0.043505

Reason for exit: Successful completion

Quantum Calculation CPU Time : 6:48.71

Quantum Calculation Wall Time: 1:45.81

SPARTAN '18 Properties Program: (x86/Darwin) build 1.3.0

Use of molecular symmetry disabled

Cartesian Coordinates (Angstroms)

Atom X Y Z

-----

1 C C1 0.7715195 -0.0448629 1.4125919

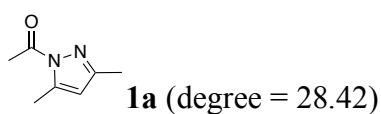
2 C C2 0.7646166 -0.0330212 0.0383789  
3 C C3 -0.5930372 0.0054628 1.8210980  
4 N N1 -1.3989310 0.0529698 0.7758467  
5 N N2 -0.5790053 0.0289890 -0.3267049  
6 C C4 -1.2172110 0.0487127 -1.6058125  
7 O O1 -2.3631401 0.4225704 -1.7092145  
8 C C5 -0.4154958 -0.4362866 -2.7964762  
9 H H2 1.6489335 -0.0713128 2.0458928  
10 H H6 0.0538982 -1.4060666 -2.6032289  
11 H H1 0.3711513 0.2743097 -3.0696809  
12 H H10 -1.1076204 -0.5253010 -3.6354079  
13 C C6 1.9528534 -0.0076712 -0.8754472  
14 H H3 2.8569945 0.0257779 -0.2608526  
15 H H4 1.9650038 0.8772129 -1.5228601  
16 H H5 2.0224855 -0.8931779 -1.5158750  
17 C C7 -1.1418903 -0.0050475 3.2180796  
18 H H7 -0.3322642 -0.0020443 3.9545709  
19 H H8 -1.7584981 -0.8947339 3.3896416  
20 H H9 -1.7739069 0.8719838 3.3970060

Point Group = C1 Order = 1 Nsymop = 1

Reason for exit: Successful completion

Properties CPU Time : .42

Properties Wall Time: .43



SPARTAN '18 MECHANICS PROGRAM: (x86/Darwin) build 1.3.0

Frequency Calculation



Adjusted 2 (out of 60) low frequency modes

Reason for exit: Successful completion

Mechanics CPU Time : .06

Mechanics Wall Time: .06

SPARTAN '18 Quantum Mechanics Program: (x86/Darwin) build 1.3.0

Job type: Geometry optimization.

Method: RB3LYP

Basis set: 6-31+G\*

Number of basis functions: 210

Number of electrons: 74

Parallel Job: 4 threads

SCF model:

A restricted hybrid HF-DFT SCF calculation will be

performed using Pulay DIIS + Geometric Direct Minimization

Optimization:

Step Energy Max Grad. Max Dist.

1 -457.498801 0.007332 0.085462

2 -457.498952 0.002142 0.013547

3 -457.498963 0.001706 0.016008

4 -457.498975 0.001327 0.160890

5 -457.499084 0.002262 0.171300

6 -457.499158 0.005367 0.157684

7 -457.499228 0.007562 0.156809

8 -457.499313 0.008749 0.150015

9 -457.499429 0.008687 0.158297

10 -457.499610 0.005623 0.185487

11 -457.499835 0.001402 0.164971

12 -457.499942 0.000668 0.047412

13 -457.499965 0.003073 0.098566

14 -457.499978 0.000705 0.053965

15 -457.499986 0.000174 0.016862

Reason for exit: Successful completion

Quantum Calculation CPU Time : 17:39.87

Quantum Calculation Wall Time: 4:32.79

SPARTAN '18 Properties Program: (x86/Darwin) build 1.3.0

Use of molecular symmetry disabled

Cartesian Coordinates (Angstroms)

Atom X Y Z

-----

1 C C1 0.7662326 -0.1368144 1.4185314

2 C C2 0.7616409 -0.0978296 0.0450534

3 C C3 -0.5928386 0.0101972 1.8267246

4 N N1 -1.3891082 0.1495212 0.7816398

5 N N2 -0.5680961 0.0887588 -0.3195267

6 C C4 -1.1959000 0.1623648 -1.6024140

7 O O1 -2.2397536 0.7588736 -1.7357754

8 C C5 -0.5042805 -0.5350105 -2.7565594

9 H H2 1.6388771 -0.2428975 2.0502154

10 H H6 -0.1477495 -1.5320745 -2.4807194

11 H H1 0.3506978 0.0486643 -3.1134891

12 H H10 -1.2281453 -0.6114357 -3.5699406

13 C C6 1.9405593 -0.1448385 -0.8797757

14 H H3 2.8535421 -0.1418511 -0.2775146

15 H H4 1.9830495 0.7255805 -1.5450679

16 H H5 1.9610400 -1.0457160 -1.5028262

17 C C7 -1.1473913 0.0109847 3.2184575

18 H H7 -0.7285733 0.8353614 3.8089736

19 H H8 -0.9079154 -0.9224756 3.7426544

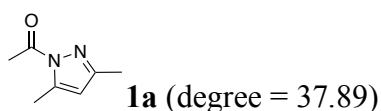
20 H H9 -2.2345027 0.1243424 3.1879650

Point Group = C1 Order = 1 Nsymop = 1

Reason for exit: Successful completion

Properties CPU Time : .41

Properties Wall Time: 1.42



SPARTAN '18 MECHANICS PROGRAM: (x86/Darwin) build 1.3.0

Frequency Calculation

Adjusted 2 (out of 60) low frequency modes

Reason for exit: Successful completion

Mechanics CPU Time : .05

Mechanics Wall Time: .05

SPARTAN '18 Quantum Mechanics Program: (x86/Darwin) build 1.3.0

Job type: Geometry optimization.

Method: RB3LYP

Basis set: 6-31+G\*

Number of basis functions: 210

Number of electrons: 74

Parallel Job: 4 threads

SCF model:

A restricted hybrid HF-DFT SCF calculation will be

performed using Pulay DIIS + Geometric Direct Minimization

Optimization:

Step Energy Max Grad. Max Dist.

1 -457.498662 0.007279 0.096344

2 -457.498826 0.002004 0.019991

3 -457.498840 0.000379 0.003182

Reason for exit: Successful completion

Quantum Calculation CPU Time : 3:46.25

Quantum Calculation Wall Time: 58.96

SPARTAN '18 Properties Program: (x86/Darwin) build 1.3.0

Use of molecular symmetry disabled

Cartesian Coordinates (Angstroms)

Atom X Y Z

-----  
1 C C1 0.7624333 -0.1458861 1.4201725

2 C C2 0.7560632 -0.1019514 0.0456285

3 C C3 -0.5942389 0.0135243 1.8298547

4 N N1 -1.3896612 0.1663454 0.7841831

5 N N2 -0.5659441 0.1117281 -0.3141606

6 C C4 -1.1927095 0.1748111 -1.6018882

7 O O1 -2.1461405 0.8967293 -1.7788741

8 C C5 -0.6072460 -0.6951645 -2.6944758

9 H H2 1.6346602 -0.2638787 2.0502266

10 H H6 -0.3254485 -1.6850104 -2.3210479

11 H H1 0.2825601 -0.2299040 -3.1332551

12 H H10 -1.3607803 -0.7923230 -3.4782043

13 C C6 1.9229137 -0.1612035 -0.8936603

14 H H3 2.8451289 -0.1386886 -0.3062776

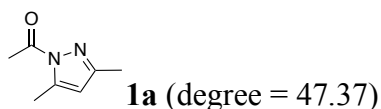
15 H H4 1.9478726 0.6945025 -1.5793233  
16 H H5 1.9392119 -1.0766321 -1.4963514  
17 C C7 -1.1508030 0.0099970 3.2210977  
18 H H7 -0.7310677 0.8307041 3.8161454  
19 H H8 -0.9156762 -0.9265044 3.7416216  
20 H H9 -2.2374851 0.1277152 3.1889095

Point Group = C1 Order = 1 Nsymop = 1

Reason for exit: Successful completion

Properties CPU Time : .40

Properties Wall Time: .41



SPARTAN '18 MECHANICS PROGRAM: (x86/Darwin) build 1.3.0

Frequency Calculation

Adjusted 3 (out of 60) low frequency modes

Reason for exit: Successful completion

Mechanics CPU Time : .05

Mechanics Wall Time: .05

SPARTAN '18 Quantum Mechanics Program: (x86/Darwin) build 1.3.0

Job type: Geometry optimization.

Method: RB3LYP

Basis set: 6-31+G\*

Number of basis functions: 210

Number of electrons: 74

Parallel Job: 4 threads

SCF model:

A restricted hybrid HF-DFT SCF calculation will be

performed using Pulay DIIS + Geometric Direct Minimization

Optimization:

Step Energy Max Grad. Max Dist.

1 -457.497158 0.007718 0.117953

2 -457.497253 0.002715 0.003780

3 -457.497279 0.002254 0.005162

4 -457.497303 0.001975 0.043884

5 -457.497373 0.000250 0.035288

6 -457.497373 0.000295 0.019367

Reason for exit: Successful completion

Quantum Calculation CPU Time : 7:02.92

Quantum Calculation Wall Time: 1:49.07

SPARTAN '18 Properties Program: (x86/Darwin) build 1.3.0

Use of molecular symmetry disabled

Cartesian Coordinates (Angstroms)

Atom X Y Z

-----  
1 C C1 0.7547666 -0.1684020 1.4199290

2 C C2 0.7463875 -0.1026894 0.0445676

3 C C3 -0.5963677 0.0160844 1.8336720

4 N N1 -1.3911039 0.1996650 0.7901834

5 N N2 -0.5679495 0.1457518 -0.3079041

6 C C4 -1.1977924 0.1804860 -1.5994427

7 O O1 -2.0509830 1.0027073 -1.8353369

8 C C5 -0.7221880 -0.8357355 -2.6160796

9 H H2 1.6252351 -0.3089044 2.0477809

10 H H6 -0.5275987 -1.8106323 -2.1592888

11 H H1 0.1995697 -0.4927149 -3.0992203

12 H H10 -1.4919113 -0.9259080 -3.3854596

13 C C6 1.8987731 -0.1748805 -0.9112544

14 H H3 2.8328824 -0.1264265 -0.3442779

15 H H4 1.9004259 0.6604986 -1.6217407

16 H H5 1.9120905 -1.1076240 -1.4872584

17 C C7 -1.1514149 0.0119498 3.2257291

18 H H7 -0.7260942 0.8282582 3.8229809

19 H H8 -0.9225727 -0.9275258 3.7434985

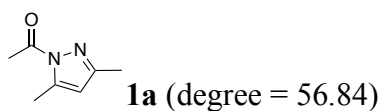
20 H H9 -2.2372451 0.1379577 3.1950836

Point Group = C1 Order = 1 Nsymop = 1

Reason for exit: Successful completion

Properties CPU Time : .40

Properties Wall Time: .41



SPARTAN '18 MECHANICS PROGRAM: (x86/Darwin) build 1.3.0

Frequency Calculation

Adjusted 3 (out of 60) low frequency modes

Reason for exit: Successful completion

Mechanics CPU Time : .05

Mechanics Wall Time: .06

SPARTAN '18 Quantum Mechanics Program: (x86/Darwin) build 1.3.0

Job type: Geometry optimization.

Method: RB3LYP

Basis set: 6-31+G\*

Number of basis functions: 210

Number of electrons: 74

Parallel Job: 4 threads

SCF model:

A restricted hybrid HF-DFT SCF calculation will be performed using Pulay DIIS + Geometric Direct Minimization

Optimization:

Step Energy Max Grad. Max Dist.

1 -457.495507 0.006573 0.030326

2 -457.495638 0.002404 0.009778

3 -457.495649 0.001953 0.012140

4 -457.495659 0.001404 0.055743

5 -457.495645 0.001253 0.030906

6 -457.495671 0.000410 0.011933

7 -457.495673 0.000121 0.005218

Reason for exit: Successful completion

Quantum Calculation CPU Time : 7:59.95

Quantum Calculation Wall Time: 2:03.29

SPARTAN '18 Properties Program: (x86/Darwin) build 1.3.0

Use of molecular symmetry disabled

Cartesian Coordinates (Angstroms)

Atom X Y Z

-----  
1 C C1 0.7517670 -0.1733206 1.4180996  
2 C C2 0.7411730 -0.0950427 0.0416056  
3 C C3 -0.5960993 0.0171903 1.8345198  
4 N N1 -1.3901508 0.2230385 0.7920240  
5 N N2 -0.5663142 0.1762617 -0.3042197



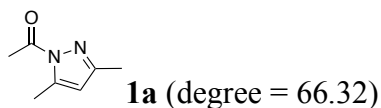
6 C C4 -1.2015283 0.1932634 -1.6002771  
7 O O1 -1.9407544 1.0992979 -1.8993855  
8 C C5 -0.8660045 -0.9563843 -2.5237925  
9 H H2 1.6217960 -0.3269180 2.0434656  
10 H H6 -0.8292368 -1.9065860 -1.9819735  
11 H H1 0.1112610 -0.7962552 -2.9937361  
12 H H10 -1.6196842 -0.9961744 -3.3129994  
13 C C6 1.8811182 -0.1824830 -0.9278823  
14 H H3 2.8246267 -0.1023565 -0.3803604  
15 H H4 1.8570857 0.6272284 -1.6669291  
16 H H5 1.8981492 -1.1354958 -1.4710254  
17 C C7 -1.1515134 0.0053301 3.2266683  
18 H H7 -0.7256177 0.8171950 3.8294854  
19 H H8 -0.9247855 -0.9378279 3.7386610  
20 H H9 -2.2372136 0.1331574 3.1966779

Point Group = C1 Order = 1 Nsymop = 1

Reason for exit: Successful completion

Properties CPU Time : .40

Properties Wall Time: .41



SPARTAN '18 MECHANICS PROGRAM: (x86/Darwin) build 1.3.0

Frequency Calculation

Adjusted 4 (out of 60) low frequency modes

Reason for exit: Successful completion

Mechanics CPU Time : .05

Mechanics Wall Time: .05

SPARTAN '18 Quantum Mechanics Program: (x86/Darwin) build 1.3.0

Job type: Geometry optimization.

Method: RB3LYP

Basis set: 6-31+G\*

Number of basis functions: 210

Number of electrons: 74

Parallel Job: 4 threads

SCF model:

A restricted hybrid HF-DFT SCF calculation will be  
performed using Pulay DIIS + Geometric Direct Minimization

Optimization:

Step Energy Max Grad. Max Dist.

1 -457.494011 0.005544 0.092036

2 -457.494172 0.001818 0.017451

3 -457.494204 0.001167 0.009435

4 -457.494222 0.000917 0.094675

5 -457.494364 0.000589 0.097366

6 -457.494434 0.000870 0.029475

7 -457.494446 0.000634 0.034984

Reason for exit: Successful completion

Quantum Calculation CPU Time : 7:55.13

Quantum Calculation Wall Time: 2:01.96

SPARTAN '18 Properties Program: (x86/Darwin) build 1.3.0

Use of molecular symmetry disabled

Cartesian Coordinates (Angstroms)

Atom X Y Z

-----

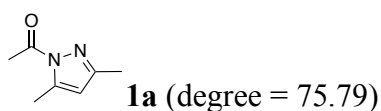
1 C C1 0.7656009 -0.1629979 1.4170733  
2 C C2 0.7507453 -0.0800600 0.0379837  
3 C C3 -0.5831050 -0.0011705 1.8345880  
4 N N1 -1.3841221 0.1904854 0.7900485  
5 N N2 -0.5602552 0.1557975 -0.3017353  
6 C C4 -1.1922725 0.2006335 -1.6079818  
7 O O1 -1.7806282 1.1919386 -1.9597439  
8 C C5 -1.0654329 -1.0584898 -2.4277433  
9 H H2 1.6390560 -0.2993271 2.0416295  
10 H H6 -1.5346232 -1.8885906 -1.8854866  
11 H H1 -0.0151775 -1.3276630 -2.5825725  
12 H H10 -1.5548562 -0.9178929 -3.3932097  
13 C C6 1.8762560 -0.1497938 -0.9495290  
14 H H3 2.8228356 0.0556794 -0.4411205  
15 H H4 1.7641543 0.5877169 -1.7526178  
16 H H5 1.9644765 -1.1417668 -1.4118536  
17 C C7 -1.1380513 -0.0177060 3.2271629  
18 H H7 -0.7226066 0.8002273 3.8289963  
19 H H8 -0.9006507 -0.9571924 3.7411572  
20 H H9 -2.2253174 0.0968126 3.1972325

Point Group = C1 Order = 1 Nsymop = 1

Reason for exit: Successful completion

Properties CPU Time : .40

Properties Wall Time: 1.41



SPARTAN '18 MECHANICS PROGRAM: (x86/Darwin) build 1.3.0

Frequency Calculation

Adjusted 4 (out of 60) low frequency modes

Reason for exit: Successful completion

Mechanics CPU Time : .05

Mechanics Wall Time: .05

SPARTAN '18 Quantum Mechanics Program: (x86/Darwin) build 1.3.0

Job type: Geometry optimization.

Method: RB3LYP

Basis set: 6-31+G\*

Number of basis functions: 210

Number of electrons: 74

Parallel Job: 4 threads

SCF model:

A restricted hybrid HF-DFT SCF calculation will be  
performed using Pulay DIIS + Geometric Direct Minimization

Optimization:

Step Energy Max Grad. Max Dist.

1 -457.493437 0.004890 0.083754

2 -457.493497 0.002072 0.005253

3 -457.493510 0.001870 0.004996

4 -457.493523 0.001702 0.058173

5 -457.493587 0.000229 0.019518

6 -457.493589 0.000219 0.007026

Reason for exit: Successful completion

Quantum Calculation CPU Time : 6:44.85

Quantum Calculation Wall Time: 1:44.13

SPARTAN '18 Properties Program: (x86/Darwin) build 1.3.0

Use of molecular symmetry disabled

Cartesian Coordinates (Angstroms)

Atom X Y Z

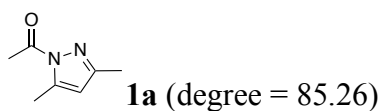
-----  
1 C C1 0.7701302 -0.1437276 1.4239416  
2 C C2 0.7512972 -0.0733362 0.0426577  
3 C C3 -0.5800476 -0.0057750 1.8411381  
4 N N1 -1.3872813 0.1564318 0.7936998  
5 N N2 -0.5629973 0.1242110 -0.2941236  
6 C C4 -1.1790771 0.1914120 -1.6123870  
7 O O1 -1.5999825 1.2393081 -2.0314866  
8 C C5 -1.2574737 -1.1253245 -2.3392953  
9 H H2 1.6464939 -0.2611951 2.0480515  
10 H H6 -1.9108294 -1.7998694 -1.7713172  
11 H H1 -0.2734314 -1.6038146 -2.3923391  
12 H H10 -1.6591716 -0.9769509 -3.3434828  
13 C C6 1.8624055 -0.1391839 -0.9602951  
14 H H3 2.8234840 -0.0165242 -0.4529328  
15 H H4 1.7789954 0.6525704 -1.7142520  
16 H H5 1.8923648 -1.1022308 -1.4874635  
17 C C7 -1.1344404 -0.0170638 3.2342118  
18 H H7 -0.7337329 0.8138415 3.8281179  
19 H H8 -0.8811193 -0.9471932 3.7576417  
20 H H9 -2.2236734 0.0776746 3.2035691

Point Group = C1 Order = 1 Nsymop = 1

Reason for exit: Successful completion

Properties CPU Time : .40

Properties Wall Time: 1.41



SPARTAN '18 MECHANICS PROGRAM: (x86/Darwin) build 1.3.0

Frequency Calculation

Adjusted 5 (out of 60) low frequency modes

Reason for exit: Successful completion

Mechanics CPU Time : .05

Mechanics Wall Time: .05

SPARTAN '18 Quantum Mechanics Program: (x86/Darwin) build 1.3.0

Job type: Geometry optimization.

Method: RB3LYP

Basis set: 6-31+G\*

Number of basis functions: 210

Number of electrons: 74

Parallel Job: 4 threads

SCF model:

A restricted hybrid HF-DFT SCF calculation will be

performed using Pulay DIIS + Geometric Direct Minimization

Optimization:

Step Energy Max Grad. Max Dist.

1 -457.493273 0.002329 0.055086

2 -457.493354 0.001704 0.039290

3 -457.493416 0.000999 0.015835

4 -457.493436 0.000786 0.128531

5 -457.493554 0.000611 0.133620

6 -457.493624 0.001438 0.130615

7 -457.493680 0.001746 0.103621

8 -457.493720 0.001345 0.056593

9 -457.493746 0.000554 0.044844

10 -457.493751 0.000223 0.004842

Reason for exit: Successful completion

Quantum Calculation CPU Time : 11:40.43

Quantum Calculation Wall Time: 2:59.71

SPARTAN '18 Properties Program: (x86/Darwin) build 1.3.0

Use of molecular symmetry disabled

Cartesian Coordinates (Angstroms)

Atom X Y Z

-----

1 C C1 0.7979958 -0.0550612 1.4523341

2 C C2 0.7948146 -0.1012851 0.0709083

3 C C3 -0.5669821 -0.0400245 1.8449354

4 N N1 -1.3686417 -0.0789454 0.7823595

5 N N2 -0.5263409 -0.1554510 -0.2918946

6 C C4 -1.1031927 0.0862797 -1.6123394

7 O O1 -1.2087539 1.2109866 -2.0308030

8 C C5 -1.5887164 -1.1542197 -2.3071749

9 H H2 1.6700707 -0.0370198 2.0928740

10 H H6 -2.3157690 -1.6587353 -1.6588943

11 H H1 -0.7572850 -1.8544569 -2.4559849

12 H H10 -2.0448805 -0.9011101 -3.2659662

13 C C6 1.9134488 -0.0930652 -0.9241925

14 H H3 2.8732967 -0.0838146 -0.4003632

15 H H4 1.8730752 0.7931589 -1.5696348

16 H H5 1.8971445 -0.9793499 -1.5717129

17 C C7 -1.1408778 0.0085726 3.2292900

18 H H7 -0.7711014 0.8811889 3.7814036

19 H H8 -0.8700026 -0.8844076 3.8065723

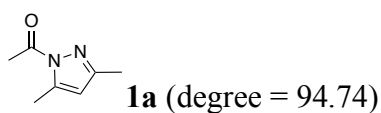
20 H H9 -2.2319753 0.0678409 3.1798834

Point Group = C1 Order = 1 Nsymop = 1

Reason for exit: Successful completion

Properties CPU Time : .41

Properties Wall Time: .42



SPARTAN '18 MECHANICS PROGRAM: (x86/Darwin) build 1.3.0

Frequency Calculation

Adjusted 4 (out of 60) low frequency modes

Reason for exit: Successful completion

Mechanics CPU Time : .05

Mechanics Wall Time: 1.05

SPARTAN '18 Quantum Mechanics Program: (x86/Darwin) build 1.3.0

Job type: Geometry optimization.

Method: RB3LYP

Basis set: 6-31+G\*

Number of basis functions: 210

Number of electrons: 74

Parallel Job: 4 threads

SCF model:

A restricted hybrid HF-DFT SCF calculation will be

performed using Pulay DIIS + Geometric Direct Minimization



Optimization:

Step Energy Max Grad. Max Dist.

1 -457.495729 0.001006 0.012037

2 -457.495749 0.000971 0.005529

3 -457.495761 0.000951 0.007865

4 -457.495780 0.000904 0.149420

5 -457.496020 0.000615 0.068391

6 -457.496042 0.000356 0.022944

7 -457.496049 0.000209 0.007382

Reason for exit: Successful completion

Quantum Calculation CPU Time : 8:10.50

Quantum Calculation Wall Time: 2:06.48

SPARTAN '18 Properties Program: (x86/Darwin) build 1.3.0

Use of molecular symmetry disabled

Cartesian Coordinates (Angstroms)

Atom X Y Z

-----  
1 C C1 0.8058636 -0.0191756 1.4513270

2 C C2 0.8203121 -0.1173998 0.0762794

3 C C3 -0.5652366 -0.0637477 1.8321334

4 N N1 -1.3506140 -0.1975436 0.7694094

5 N N2 -0.4920538 -0.2886490 -0.3012080

6 C C4 -1.0669138 0.0358527 -1.6016359

7 O O1 -0.9638086 1.1503680 -2.0526648

8 C C5 -1.8510510 -1.0874185 -2.2163292

9 H H2 1.6677836 0.0659567 2.1002381

10 H H6 -2.5752343 -1.4592653 -1.4819930

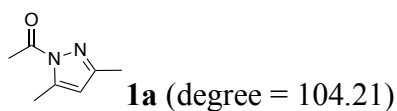
11 H H1 -1.1799680 -1.9223665 -2.4544210  
12 H H10 -2.3598892 -0.7466215 -3.1198180  
13 C C6 1.9499905 -0.0851557 -0.9048847  
14 H H3 2.9028946 -0.0338489 -0.3707669  
15 H H4 1.8812725 0.7875970 -1.5651859  
16 H H5 1.9687536 -0.9819653 -1.5371268  
17 C C7 -1.1517834 0.0165332 3.2094443  
18 H H7 -0.8107535 0.9180409 3.7324854  
19 H H8 -0.8583489 -0.8478333 3.8185933  
20 H H9 -2.2437444 0.0401119 3.1514961

Point Group = C1 Order = 1 Nsymop = 1

Reason for exit: Successful completion

Properties CPU Time : .40

Properties Wall Time: .41



SPARTAN '18 MECHANICS PROGRAM: (x86/Darwin) build 1.3.0

Frequency Calculation

Adjusted 4 (out of 60) low frequency modes

Reason for exit: Successful completion

Mechanics CPU Time : .05

Mechanics Wall Time: .05

SPARTAN '18 Quantum Mechanics Program: (x86/Darwin) build 1.3.0

Job type: Geometry optimization.

Method: RB3LYP

Basis set: 6-31+G\*

Number of basis functions: 210

Number of electrons: 74

Parallel Job: 4 threads

SCF model:

A restricted hybrid HF-DFT SCF calculation will be performed using Pulay DIIS + Geometric Direct Minimization

Optimization:

Step Energy Max Grad. Max Dist.

1 -457.499071 0.001358 0.013128

2 -457.499090 0.001115 0.003636

3 -457.499094 0.001049 0.005663

4 -457.499102 0.000912 0.070598

5 -457.499128 0.000217 0.013704

6 -457.499130 0.000102 0.003040

Reason for exit: Successful completion

Quantum Calculation CPU Time : 6:35.64

Quantum Calculation Wall Time: 1:42.00

SPARTAN '18 Properties Program: (x86/Darwin) build 1.3.0

Use of molecular symmetry disabled

Cartesian Coordinates (Angstroms)

Atom X Y Z

-----  
1 C C1 0.8039679 -0.0170198 1.4485800

2 C C2 0.8199803 -0.1186918 0.0752438

3 C C3 -0.5682156 -0.0646409 1.8296973

4 N N1 -1.3522339 -0.2085936 0.7696186

5 N N2 -0.4929000 -0.2987562 -0.3046745

6 C C4 -1.0653723 0.0305530 -1.5967132

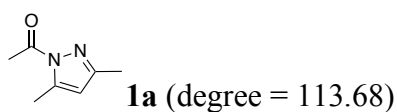
7 O O1 -0.8181342 1.0895564 -2.1240297  
8 C C5 -2.0335108 -0.9961845 -2.1125868  
9 H H2 1.6650822 0.0728638 2.0979421  
10 H H6 -2.7416733 -1.2549034 -1.3179389  
11 H H1 -1.4926647 -1.9143122 -2.3752560  
12 H H10 -2.5582053 -0.6109367 -2.9885878  
13 C C6 1.9538934 -0.0880640 -0.9007537  
14 H H3 2.9047826 -0.0581980 -0.3612663  
15 H H4 1.8967891 0.7936572 -1.5491105  
16 H H5 1.9614069 -0.9756868 -1.5456543  
17 C C7 -1.1535461 0.0243001 3.2068383  
18 H H7 -0.8194743 0.9336648 3.7206520  
19 H H8 -0.8506162 -0.8316196 3.8231766  
20 H H9 -2.2457391 0.0372608 3.1507758

Point Group = C1 Order = 1 Nsymop = 1

Reason for exit: Successful completion

Properties CPU Time : .41

Properties Wall Time: .41



SPARTAN '18 MECHANICS PROGRAM: (x86/Darwin) build 1.3.0

Frequency Calculation

Adjusted 4 (out of 60) low frequency modes

Reason for exit: Successful completion

Mechanics CPU Time : .05

Mechanics Wall Time: 1.05

SPARTAN '18 Quantum Mechanics Program: (x86/Darwin) build 1.3.0

Job type: Geometry optimization.

Method: RB3LYP

Basis set: 6-31+G\*

Number of basis functions: 210

Number of electrons: 74

Parallel Job: 4 threads

SCF model:

A restricted hybrid HF-DFT SCF calculation will be performed using Pulay DIIS + Geometric Direct Minimization

Optimization:

Step Energy Max Grad. Max Dist.

1 -457.502307 0.001554 0.022709

2 -457.502356 0.001033 0.002892

3 -457.502364 0.000924 0.003601

4 -457.502367 0.000857 0.042192

5 -457.502390 0.000422 0.016393

6 -457.502400 0.000125 0.006192

Reason for exit: Successful completion

Quantum Calculation CPU Time : 6:35.72

Quantum Calculation Wall Time: 1:42.10

SPARTAN '18 Properties Program: (x86/Darwin) build 1.3.0

Use of molecular symmetry disabled

Cartesian Coordinates (Angstroms)

Atom X Y Z

-----

1 C C1 0.8003874 -0.0220909 1.4470632

2 C C2 0.8111778 -0.1122078 0.0739347

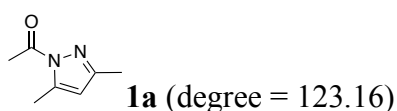
3 C C3 -0.5716096 -0.0586327 1.8340054  
4 N N1 -1.3610037 -0.1888923 0.7778921  
5 N N2 -0.5069117 -0.2746117 -0.3032220  
6 C C4 -1.0742629 0.0409780 -1.5920961  
7 O O1 -0.7038411 1.0176367 -2.2037874  
8 C C5 -2.1830812 -0.8812715 -2.0175876  
9 H H2 1.6647147 0.0547523 2.0938789  
10 H H6 -2.8794168 -1.0281852 -1.1858826  
11 H H1 -1.7654750 -1.8644488 -2.2695822  
12 H H10 -2.6972428 -0.4659246 -2.8859777  
13 C C6 1.9476085 -0.0938714 -0.8992966  
14 H H3 2.8967582 -0.1010789 -0.3557419  
15 H H4 1.9147502 0.7995895 -1.5320770  
16 H H5 1.9312248 -0.9687346 -1.5607976  
17 C C7 -1.1486785 0.0321531 3.2143340  
18 H H7 -0.8194214 0.9472230 3.7211612  
19 H H8 -0.8327839 -0.8176050 3.8325602  
20 H H9 -2.2412769 0.0346626 3.1659574

Point Group = C1 Order = 1 Nsymop = 1

Reason for exit: Successful completion

Properties CPU Time : .40

Properties Wall Time: .41



SPARTAN '18 MECHANICS PROGRAM: (x86/Darwin) build 1.3.0

Frequency Calculation

Adjusted 4 (out of 60) low frequency modes

Reason for exit: Successful completion

Mechanics CPU Time : .05

Mechanics Wall Time: .05

SPARTAN '18 Quantum Mechanics Program: (x86/Darwin) build 1.3.0

Job type: Geometry optimization.

Method: RB3LYP

Basis set: 6-31+G\*

Number of basis functions: 210

Number of electrons: 74

Parallel Job: 4 threads

SCF model:

A restricted hybrid HF-DFT SCF calculation will be

performed using Pulay DIIS + Geometric Direct Minimization

Optimization:

Step Energy Max Grad. Max Dist.

1 -457.505362 0.001810 0.012334

2 -457.505399 0.001626 0.007272

3 -457.505428 0.001420 0.010413

4 -457.505462 0.001160 0.059636

5 -457.505431 0.001310 0.112734

6 -457.505503 0.000954 0.050940

7 -457.505533 0.000244 0.010836

8 -457.505536 0.000071 0.002762

Reason for exit: Successful completion

Quantum Calculation CPU Time : 9:10.12

Quantum Calculation Wall Time: 2:21.41

SPARTAN '18 Properties Program: (x86/Darwin) build 1.3.0

Use of molecular symmetry disabled

Cartesian Coordinates (Angstroms)

Atom X Y Z

-----  
1 C C1 0.7962955 -0.0284565 1.4476176  
2 C C2 0.7986253 -0.1015041 0.0740341  
3 C C3 -0.5742171 -0.0464145 1.8430617  
4 N N1 -1.3720889 -0.1508729 0.7913970  
5 N N2 -0.5266648 -0.2284824 -0.2972218  
6 C C4 -1.0864956 0.0594341 -1.5876053  
7 O O1 -0.6113751 0.9319609 -2.2821534  
8 C C5 -2.3056527 -0.7519157 -1.9339025  
9 H H2 1.6655073 0.0264863 2.0900986  
10 H H6 -2.9931270 -0.7815211 -1.0835822  
11 H H1 -2.0060809 -1.7862176 -2.1463902  
12 H H10 -2.7908235 -0.3238933 -2.8127440  
13 C C6 1.9346250 -0.0986831 -0.8998371  
14 H H3 2.8811689 -0.1789697 -0.3573671  
15 H H4 1.9467453 0.8207659 -1.4943161  
16 H H5 1.8718339 -0.9401125 -1.6000379  
17 C C7 -1.1397498 0.0412356 3.2281610  
18 H H7 -0.8022705 0.9527702 3.7360853  
19 H H8 -0.8218451 -0.8122515 3.8400736  
20 H H9 -2.2326705 0.0489076 3.1890242

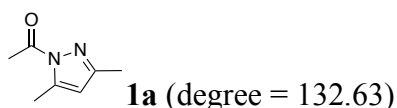
Point Group = C1 Order = 1 Nsymop = 1

Reason for exit: Successful completion

Properties CPU Time : .41



Properties Wall Time: .41



SPARTAN '18 MECHANICS PROGRAM: (x86/Darwin) build 1.3.0

Frequency Calculation

Adjusted 4 (out of 60) low frequency modes

Reason for exit: Successful completion

Mechanics CPU Time : .05

Mechanics Wall Time: 1.05

SPARTAN '18 Quantum Mechanics Program: (x86/Darwin) build 1.3.0

Job type: Geometry optimization.

Method: RB3LYP

Basis set: 6-31+G\*

Number of basis functions: 210

Number of electrons: 74

Parallel Job: 4 threads

SCF model:

A restricted hybrid HF-DFT SCF calculation will be

performed using Pulay DIIS + Geometric Direct Minimization

Optimization:

Step Energy Max Grad. Max Dist.

1 -457.508242 0.002400 0.014060

2 -457.508296 0.002039 0.014496

3 -457.508351 0.001509 0.005596

4 -457.508373 0.001295 0.056818

5 -457.508445 0.000363 0.022164

6 -457.508449 0.000215 0.008091

Reason for exit: Successful completion

Quantum Calculation CPU Time : 6:52.71

Quantum Calculation Wall Time: 1:46.44

SPARTAN '18 Properties Program: (x86/Darwin) build 1.3.0

Use of molecular symmetry disabled

Cartesian Coordinates (Angstroms)

Atom X Y Z

```
-----  
1 C C1 0.7934346 -0.0420362 1.4468872  
2 C C2 0.7884100 -0.0870120 0.0726757  
3 C C3 -0.5755679 -0.0348250 1.8502359  
4 N N1 -1.3810417 -0.1002229 0.8022028  
5 N N2 -0.5440860 -0.1694011 -0.2933568  
6 C C4 -1.0983039 0.0832460 -1.5853328  
7 O O1 -0.5376570 0.8332424 -2.3579422  
8 C C5 -2.4114370 -0.6031718 -1.8557600  
9 H H2 1.6669217 -0.0182996 2.0854901  
10 H H6 -3.0963065 -0.4593850 -1.0161202  
11 H H1 -2.2453784 -1.6830650 -1.9586467  
12 H H10 -2.8373762 -0.2095134 -2.7801665  
13 C C6 1.9248092 -0.0981240 -0.9005176  
14 H H3 2.8646585 -0.2439793 -0.3597559  
15 H H4 1.9798066 0.8413699 -1.4595827  
16 H H5 1.8227218 -0.9050726 -1.6349731  
17 C C7 -1.1304639 0.0430140 3.2399959  
18 H H7 -0.7836146 0.9476174 3.7541152  
19 H H8 -0.8127941 -0.8179825 3.8412784
```

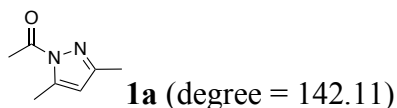
20 H H9 -2.2235609 0.0579026 3.2091343

Point Group = C1 Order = 1 Nsymop = 1

Reason for exit: Successful completion

Properties CPU Time : .41

Properties Wall Time: .41



SPARTAN '18 MECHANICS PROGRAM: (x86/Darwin) build 1.3.0

Frequency Calculation

Adjusted 3 (out of 60) low frequency modes

Reason for exit: Successful completion

Mechanics CPU Time : .05

Mechanics Wall Time: .05

SPARTAN '18 Quantum Mechanics Program: (x86/Darwin) build 1.3.0

Job type: Geometry optimization.

Method: RB3LYP

Basis set: 6-31+G\*

Number of basis functions: 210

Number of electrons: 74

Parallel Job: 4 threads

SCF model:

A restricted hybrid HF-DFT SCF calculation will be

performed using Pulay DIIS + Geometric Direct Minimization

Optimization:

Step Energy Max Grad. Max Dist.

1 -457.510836 0.002559 0.015132

2 -457.510885 0.002230 0.007934

3 -457.510903 0.002082 0.030744

4 -457.510965 0.001566 0.129205

5 -457.511030 0.000905 0.062164

6 -457.511081 0.000546 0.029391

7 -457.511090 0.000138 0.020822

Reason for exit: Successful completion

Quantum Calculation CPU Time : 7:55.05

Quantum Calculation Wall Time: 2:02.21

SPARTAN '18 Properties Program: (x86/Darwin) build 1.3.0

Use of molecular symmetry disabled

Cartesian Coordinates (Angstroms)

Atom X Y Z

-----  
1 C C1 0.7928429 -0.0521553 1.4442291

2 C C2 0.7838409 -0.0731311 0.0698745

3 C C3 -0.5747413 -0.0308306 1.8531824

4 N N1 -1.3845655 -0.0566009 0.8072264

5 N N2 -0.5535918 -0.1122773 -0.2920801

6 C C4 -1.1070643 0.1078364 -1.5838714

7 O O1 -0.4808237 0.7248470 -2.4231562

8 C C5 -2.5014356 -0.4290269 -1.7839624

9 H H2 1.6686854 -0.0545141 2.0799600

10 H H6 -3.1791963 -0.0144770 -1.0325407

11 H H1 -2.5103347 -1.5177172 -1.6558626

12 H H10 -2.8359997 -0.1672864 -2.7891679

13 C C6 1.9212401 -0.0930797 -0.9016652

14 H H3 2.8550692 -0.2706707 -0.3597261

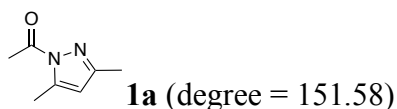
15 H H4 1.9996134 0.8543958 -1.4439989  
16 H H5 1.8019193 -0.8818965 -1.6525518  
17 C C7 -1.1223737 0.0273210 3.2465457  
18 H H7 -0.7667350 0.9207820 3.7741205  
19 H H8 -0.8071352 -0.8455869 3.8316234  
20 H H9 -2.2154604 0.0504049 3.2215029

Point Group = C1 Order = 1 Nsymop = 1

Reason for exit: Successful completion

Properties CPU Time : .41

Properties Wall Time: .41



SPARTAN '18 MECHANICS PROGRAM: (x86/Darwin) build 1.3.0

Frequency Calculation

Adjusted 2 (out of 60) low frequency modes

Reason for exit: Successful completion

Mechanics CPU Time : .05

Mechanics Wall Time: .05

SPARTAN '18 Quantum Mechanics Program: (x86/Darwin) build 1.3.0

Job type: Geometry optimization.

Method: RB3LYP

Basis set: 6-31+G\*

Number of basis functions: 210

Number of electrons: 74

Parallel Job: 4 threads

SCF model:

A restricted hybrid HF-DFT SCF calculation will be

performed using Pulay DIIS + Geometric Direct Minimization

Optimization:

Step Energy Max Grad. Max Dist.

1 -457.513132 0.002329 0.012474

2 -457.513154 0.002212 0.008057

3 -457.513170 0.002092 0.076417

4 -457.513281 0.001113 0.155727

5 -457.513195 0.001475 0.066351

6 -457.513341 0.000337 0.038826

7 -457.513345 0.000170 0.014905

Reason for exit: Successful completion

Quantum Calculation CPU Time : 7:59.10

Quantum Calculation Wall Time: 2:02.98

SPARTAN '18 Properties Program: (x86/Darwin) build 1.3.0

Use of molecular symmetry disabled

Cartesian Coordinates (Angstroms)

Atom X Y Z

-----

1 C C1 0.7928531 -0.0625327 1.4416971

2 C C2 0.7827274 -0.0621428 0.0676186

3 C C3 -0.5740869 -0.0266513 1.8539102

4 N N1 -1.3853644 -0.0185903 0.8094017

5 N N2 -0.5578522 -0.0614724 -0.2920534

6 C C4 -1.1139823 0.1344156 -1.5812241

7 O O1 -0.4398399 0.6069394 -2.4768299

8 C C5 -2.5697312 -0.2361734 -1.7207970

9 H H2 1.6695295 -0.0894483 2.0756865

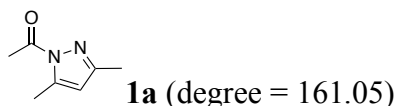
10 H H6 -3.1853733 0.4090123 -1.0866257  
11 H H1 -2.7440167 -1.2651094 -1.3900424  
12 H H10 -2.8549402 -0.1165260 -2.7674220  
13 C C6 1.9218178 -0.0909359 -0.9012835  
14 H H3 2.8528445 -0.2680187 -0.3541434  
15 H H4 2.0052124 0.8523866 -1.4499576  
16 H H5 1.8011633 -0.8825882 -1.6486132  
17 C C7 -1.1178897 0.0121884 3.2492149  
18 H H7 -0.7521052 0.8926510 3.7915738  
19 H H8 -0.8096269 -0.8738150 3.8180670  
20 H H9 -2.2107311 0.0465523 3.2272021

Point Group = C1 Order = 1 Nsymop = 1

Reason for exit: Successful completion

Properties CPU Time : .41

Properties Wall Time: .41



SPARTAN '18 MECHANICS PROGRAM: (x86/Darwin) build 1.3.0

Frequency Calculation

Adjusted 2 (out of 60) low frequency modes

Reason for exit: Successful completion

Mechanics CPU Time : .05

Mechanics Wall Time: .05

SPARTAN '18 Quantum Mechanics Program: (x86/Darwin) build 1.3.0

Job type: Geometry optimization.

Method: RB3LYP

Basis set: 6-31+G\*

Number of basis functions: 210

Number of electrons: 74

Parallel Job: 4 threads

SCF model:

A restricted hybrid HF-DFT SCF calculation will be  
performed using Pulay DIIS + Geometric Direct Minimization

Optimization:

Step Energy Max Grad. Max Dist.

1 -457.514874 0.001662 0.104141

2 -457.514981 0.000826 0.005719

3 -457.514992 0.000685 0.002298

Reason for exit: Successful completion

Quantum Calculation CPU Time : 3:36.01

Quantum Calculation Wall Time: 56.07

SPARTAN '18 Properties Program: (x86/Darwin) build 1.3.0

Use of molecular symmetry disabled

Cartesian Coordinates (Angstroms)

Atom X Y Z

-----  
1 C C1 0.7918906 -0.0780588 1.4406801

2 C C2 0.7815619 -0.0583221 0.0670134

3 C C3 -0.5741588 -0.0223548 1.8550692

4 N N1 -1.3856740 0.0200352 0.8122690

5 N N2 -0.5609843 -0.0249470 -0.2916527

6 C C4 -1.1168525 0.1587810 -1.5787385

7 O O1 -0.4066721 0.4651188 -2.5185001

8 C C5 -2.6117512 -0.0244146 -1.6727732



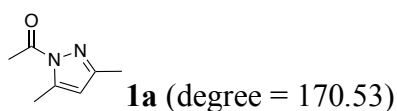
9 H H2 1.6682902 -0.1288394 2.0736938  
10 H H6 -3.1243974 0.7557083 -1.1023071  
11 H H1 -2.9196666 -0.9824606 -1.2424574  
12 H H10 -2.8939853 0.0308634 -2.7255865  
13 C C6 1.9217504 -0.0943640 -0.8998632  
14 H H3 2.8558127 -0.2345834 -0.3467927  
15 H H4 1.9890613 0.8325630 -1.4787954  
16 H H5 1.8125138 -0.9083465 -1.6230521  
17 C C7 -1.1151189 0.0068627 3.2515532  
18 H H7 -0.7524288 0.8872694 3.7962758  
19 H H8 -0.8007685 -0.8793723 3.8165395  
20 H H9 -2.2081326 0.0357445 3.2321447

Point Group = C1 Order = 1 Nsymop = 1

Reason for exit: Successful completion

Properties CPU Time : .40

Properties Wall Time: .41



SPARTAN '18 MECHANICS PROGRAM: (x86/Darwin) build 1.3.0

Frequency Calculation

Adjusted 2 (out of 60) low frequency modes

Reason for exit: Successful completion

Mechanics CPU Time : .05

Mechanics Wall Time: .05

SPARTAN '18 Quantum Mechanics Program: (x86/Darwin) build 1.3.0

Job type: Geometry optimization.

Method: RB3LYP

Basis set: 6-31+G\*

Number of basis functions: 210

Number of electrons: 74

Parallel Job: 4 threads

SCF model:

A restricted hybrid HF-DFT SCF calculation will be  
performed using Pulay DIIS + Geometric Direct Minimization

Optimization:

Step Energy Max Grad. Max Dist.

1 -457.515795 0.001441 0.015557

2 -457.515850 0.001251 0.008074

3 -457.515877 0.001136 0.005736

4 -457.515892 0.001065 0.115563

5 -457.516058 0.000211 0.016934

6 -457.516060 0.000230 0.013336

Reason for exit: Successful completion

Quantum Calculation CPU Time : 6:46.51

Quantum Calculation Wall Time: 1:44.76

SPARTAN '18 Properties Program: (x86/Darwin) build 1.3.0

Use of molecular symmetry disabled

Cartesian Coordinates (Angstroms)

Atom X Y Z

-----

1 C C1 0.7905357 -0.0919719 1.4406573

2 C C2 0.7793065 -0.0443221 0.0682322

3 C C3 -0.5720270 0.0038798 1.8598798

4 N N1 -1.3833801 0.0927764 0.8201472

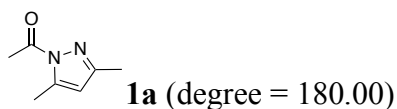
5 N N2 -0.5620909 0.0586351 -0.2856244  
6 C C4 -1.1187514 0.1965358 -1.5760151  
7 O O1 -0.3957707 0.3407807 -2.5457356  
8 C C5 -2.6262334 0.1675700 -1.6465120  
9 H H2 1.6665180 -0.1833385 2.0695536  
10 H H6 -3.0517585 1.0153052 -1.1000155  
11 H H1 -3.0242857 -0.7385436 -1.1805047  
12 H H10 -2.9138582 0.2171370 -2.6981065  
13 C C6 1.9184169 -0.1025123 -0.8983003  
14 H H3 2.8494832 -0.2461499 -0.3412965  
15 H H4 1.9950625 0.8159174 -1.4889107  
16 H H5 1.8021005 -0.9244181 -1.6120913  
17 C C7 -1.1088414 0.0131205 3.2581087  
18 H H7 -0.7125159 0.8630202 3.8274581  
19 H H8 -0.8259706 -0.9004352 3.7954040  
20 H H9 -2.1999890 0.0840989 3.2431877

Point Group = C1 Order = 1 Nsymop = 1

Reason for exit: Successful completion

Properties CPU Time : .40

Properties Wall Time: .41



SPARTAN '18 MECHANICS PROGRAM: (x86/Darwin) build 1.3.0

Frequency Calculation

Adjusted 2 (out of 60) low frequency modes

Reason for exit: Successful completion

Mechanics CPU Time : .05

Mechanics Wall Time: .05

SPARTAN '18 Quantum Mechanics Program: (x86/Darwin) build 1.3.0

Job type: Geometry optimization.

Method: RB3LYP

Basis set: 6-31+G\*

Number of basis functions: 210

Number of electrons: 74

Parallel Job: 4 threads

SCF model:

A restricted hybrid HF-DFT SCF calculation will be  
performed using Pulay DIIS + Geometric Direct Minimization

Optimization:

Step Energy Max Grad. Max Dist.

1 -457.516249 0.000976 0.009473

2 -457.516271 0.000827 0.006154

3 -457.516283 0.000741 0.016257

4 -457.516313 0.000603 0.092628

5 -457.516402 0.000298 0.023437

6 -457.516407 0.000238 0.019025

Reason for exit: Successful completion

Quantum Calculation CPU Time : 6:36.14

Quantum Calculation Wall Time: 1:42.35

SPARTAN '18 Properties Program: (x86/Darwin) build 1.3.0

Use of molecular symmetry disabled

Cartesian Coordinates (Angstroms)

Atom X Y Z

-----

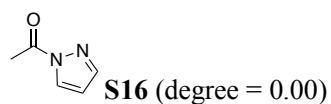
1 C C1 0.7895340 -0.1035935 1.4402491  
2 C C2 0.7796832 -0.0379729 0.0686392  
3 C C3 -0.5699442 0.0228125 1.8612839  
4 N N1 -1.3779208 0.1541526 0.8235097  
5 N N2 -0.5575767 0.1185073 -0.2829196  
6 C C4 -1.1162519 0.2280533 -1.5746099  
7 O O1 -0.3998281 0.1976979 -2.5594515  
8 C C5 -2.6174121 0.3760605 -1.6303947  
9 H H2 1.6630669 -0.2251363 2.0674374  
10 H H6 -2.9404654 1.2672138 -1.0833718  
11 H H1 -3.1096140 -0.4788977 -1.1570993  
12 H H10 -2.9076355 0.4491285 -2.6798160  
13 C C6 1.9174525 -0.1138039 -0.8981023  
14 H H3 2.8519583 -0.2197379 -0.3383465  
15 H H4 1.9787602 0.7821350 -1.5242684  
16 H H5 1.8118815 -0.9639999 -1.5793190  
17 C C7 -1.1069951 0.0183861 3.2594073  
18 H H7 -0.6961782 0.8520684 3.8424100  
19 H H8 -0.8400713 -0.9084228 3.7818504  
20 H H9 -2.1967185 0.1087071 3.2456694

Point Group = C1 Order = 1 Nsymop = 1

Reason for exit: Successful completion

Properties CPU Time : .41

Properties Wall Time: 1.41



MacSPARTAN '16 MECHANICS PROGRAM: (x86/Darwin) build 1.1.2

Frequency Calculation

Adjusted 2 (out of 42) low frequency modes

Reason for exit: Successful completion

Mechanics CPU Time : .04

Mechanics Wall Time: .04

MacSPARTAN '16 Quantum Mechanics Program: (x86/Darwin) build 1.1.2

Job type: Geometry optimization.

Method: RB3LYP

Basis set: 6-31+G\*

Number of basis functions: 164

Number of electrons: 58

Parallel Job: 4 threads

SCF model:

A restricted hybrid HF-DFT SCF calculation will be  
performed using Pulay DIIS + Geometric Direct Minimization

Optimization:

Step Energy Max Grad. Max Dist.

1 -378.862878 0.000114 0.000304

Reason for exit: Successful completion

Quantum Calculation CPU Time : 34.30

Quantum Calculation Wall Time: 10.23

MacSPARTAN '16 Properties Program: (x86/Darwin) build 1.1.2

Reason for exit: Successful completion

Properties CPU Time : .23

Properties Wall Time: .24

SPARTAN '18 Properties Program: (x86/Darwin) build 1.3.0

Use of molecular symmetry enabled

Cartesian Coordinates (Angstroms)

Atom X Y Z

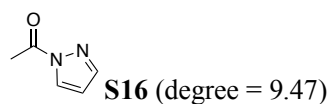
-----  
1 C C1 1.0230383 0.0000000 1.9041227  
2 C C2 0.9228679 0.0000000 0.5371595  
3 C C3 -0.3278087 0.0000000 2.3594030  
4 N N1 -1.1940325 0.0000000 1.3620665  
5 N N2 -0.4246301 0.0000000 0.2330407  
6 C C4 -1.0393026 0.0000000 -1.0540863  
7 O O1 -2.2416572 0.0000000 -1.1713362  
8 C C5 -0.0817834 -0.0000001 -2.2296159  
9 H H2 1.9280371 0.0000000 2.4953933  
10 H H6 0.5612571 -0.8874329 -2.2217851  
11 H H1 0.5612571 0.8874328 -2.2217852  
12 H H10 -0.6780275 0.0000000 -3.1430917  
13 H H11 -0.6926824 0.0000000 3.3789509  
14 H H15 1.6834669 0.0000000 -0.2284363

Point Group = CS Order = 1 Nsymop = 2

Reason for exit: Successful completion

Properties CPU Time : .24

Properties Wall Time: 1.25



MacSPARTAN '16 Quantum Mechanics Program: (x86/Darwin) build 1.1.2

Job type: Geometry optimization.

Method: RB3LYP

Basis set: 6-31+G\*

Number of basis functions: 164

Number of electrons: 58

Parallel Job: 4 threads

SCF model:

A restricted hybrid HF-DFT SCF calculation will be  
performed using Pulay DIIS + Geometric Direct Minimization

Optimization:

Step Energy Max Grad. Max Dist.

1 -378.862557 0.001238 0.011951

2 -378.862575 0.000808 0.022835

3 -378.862598 0.000609 0.023092

4 -378.862614 0.000657 0.073177

5 -378.862620 0.001028 0.018552

6 -378.862629 0.000400 0.011059

7 -378.862632 0.000354 0.007302

8 -378.862633 0.000179 0.009412

9 -378.862634 0.000097 0.003961

Reason for exit: Successful completion

Quantum Calculation CPU Time : 3:50.65

Quantum Calculation Wall Time: 1:01.84

MacSPARTAN '16 Properties Program: (x86/Darwin) build 1.1.2

Reason for exit: Successful completion

Properties CPU Time : .23

Properties Wall Time: .24

SPARTAN '18 Properties Program: (x86/Darwin) build 1.3.0

Use of molecular symmetry disabled

Cartesian Coordinates (Angstroms)



Atom X Y Z

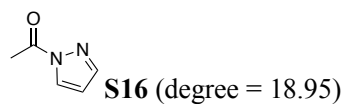
-----  
1 C C1 1.0220680 -0.0185418 1.9032331  
2 C C2 0.9212683 -0.0196842 0.5361434  
3 C C3 -0.3281349 0.0104423 2.3590401  
4 N N1 -1.1945200 0.0311229 1.3618695  
5 N N2 -0.4255022 0.0200357 0.2326745  
6 C C4 -1.0412213 -0.0021047 -1.0540869  
7 O O1 -2.2320510 0.1588981 -1.1781375  
8 C C5 -0.0966273 -0.2171738 -2.2202445  
9 H H2 1.9270988 -0.0359813 2.4941911  
10 H H6 0.4676934 -1.1501145 -2.1134413  
11 H H1 0.6208263 0.6071710 -2.3071613  
12 H H10 -0.6963984 -0.2588635 -3.1304310  
13 H H11 -0.6926539 0.0108949 3.3786994  
14 H H15 1.6809877 -0.0343679 -0.2302729

Point Group = C1 Order = 1 Nsymop = 1

Reason for exit: Successful completion

Properties CPU Time : .30

Properties Wall Time: .31



MacSPARTAN '16 Quantum Mechanics Program: (x86/Darwin) build 1.1.2

Job type: Geometry optimization.

Method: RB3LYP

Basis set: 6-31+G\*

Number of basis functions: 164

Number of electrons: 58

Parallel Job: 4 threads

SCF model:

A restricted hybrid HF-DFT SCF calculation will be performed using Pulay DIIS + Geometric Direct Minimization

Optimization:

Step Energy Max Grad. Max Dist.

1 -378.861759 0.001097 0.026187

2 -378.861784 0.001125 0.010349

3 -378.861801 0.000942 0.017161

4 -378.861812 0.000701 0.037733

5 -378.861824 0.000576 0.010722

6 -378.861826 0.000343 0.007225

7 -378.861828 0.000135 0.001043

Reason for exit: Successful completion

Quantum Calculation CPU Time : 3:00.35

Quantum Calculation Wall Time: 48.67

MacSPARTAN '16 Properties Program: (x86/Darwin) build 1.1.2

Reason for exit: Successful completion

Properties CPU Time : .23

Properties Wall Time: .24

SPARTAN '18 Properties Program: (x86/Darwin) build 1.3.0

Use of molecular symmetry disabled

Cartesian Coordinates (Angstroms)

Atom X Y Z

-----

1 C C1 1.0201132 -0.0356923 1.9024136

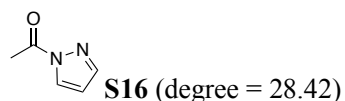
2 C C2 0.9184975 -0.0394719 0.5347858  
3 C C3 -0.3283807 0.0211776 2.3587741  
4 N N1 -1.1947394 0.0598647 1.3613837  
5 N N2 -0.4259218 0.0375733 0.2323463  
6 C C4 -1.0450356 -0.0060679 -1.0540238  
7 O O1 -2.2012642 0.3121802 -1.1987156  
8 C C5 -0.1390133 -0.4292705 -2.1930927  
9 H H2 1.9249925 -0.0690356 2.4928935  
10 H H6 0.3393471 -1.3933842 -1.9907424  
11 H H1 0.6497445 0.3132052 -2.3636658  
12 H H10 -0.7476293 -0.5028380 -3.0954006  
13 H H11 -0.6927973 0.0243843 3.3784290  
14 H H15 1.6767915 -0.0688842 -0.2329673

Point Group = C1 Order = 1 Nsymop = 1

Reason for exit: Successful completion

Properties CPU Time : .28

Properties Wall Time: .28



MacSPARTAN '16 Quantum Mechanics Program: (x86/Darwin) build 1.1.2

Job type: Geometry optimization.

Method: RB3LYP

Basis set: 6-31+G\*

Number of basis functions: 164

Number of electrons: 58

Parallel Job: 4 threads

SCF model:

A restricted hybrid HF-DFT SCF calculation will be  
performed using Pulay DIIS + Geometric Direct Minimization

Optimization:

Step Energy Max Grad. Max Dist.

1 -378.860475 0.001401 0.014081

2 -378.860495 0.001156 0.009568

3 -378.860512 0.000543 0.005668

4 -378.860517 0.000459 0.036579

5 -378.860527 0.000823 0.007156

6 -378.860528 0.000456 0.005813

7 -378.860530 0.000202 0.002931

8 -378.860530 0.000245 0.002137

Reason for exit: Successful completion

Quantum Calculation CPU Time : 3:24.60

Quantum Calculation Wall Time: 54.94

MacSPARTAN '16 Properties Program: (x86/Darwin) build 1.1.2

Reason for exit: Successful completion

Properties CPU Time : .23

Properties Wall Time: .24

SPARTAN '18 Properties Program: (x86/Darwin) build 1.3.0

Use of molecular symmetry disabled

Cartesian Coordinates (Angstroms)

Atom X Y Z

-----  
1 C C1 1.0182023 -0.0480882 1.9023753

2 C C2 0.9170476 -0.0503581 0.5337002

3 C C3 -0.3286446 0.0274937 2.3581308

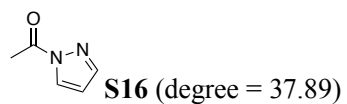
4 N N1 -1.1939235 0.0822415 1.3593913  
5 N N2 -0.4239219 0.0552296 0.2314895  
6 C C4 -1.0481117 -0.0075392 -1.0546515  
7 O O1 -2.1486025 0.4562242 -1.2310254  
8 C C5 -0.2100505 -0.6339478 -2.1496538  
9 H H2 1.9224116 -0.0922836 2.4931897  
10 H H6 0.1564978 -1.6237527 -1.8576015  
11 H H1 0.6586345 -0.0072876 -2.3859995  
12 H H10 -0.8292832 -0.7158177 -3.0441987  
13 H H11 -0.6943918 0.0290855 3.3772682  
14 H H15 1.6747358 -0.0872014 -0.2347717

Point Group = C1 Order = 1 Nsymop = 1

Reason for exit: Successful completion

Properties CPU Time : .30

Properties Wall Time: 1.31



MacSPARTAN '16 Quantum Mechanics Program: (x86/Darwin) build 1.1.2

Job type: Geometry optimization.

Method: RB3LYP

Basis set: 6-31+G\*

Number of basis functions: 164

Number of electrons: 58

Parallel Job: 4 threads

SCF model:

A restricted hybrid HF-DFT SCF calculation will be

performed using Pulay DIIS + Geometric Direct Minimization

Optimization:

Step Energy Max Grad. Max Dist.

1 -378.858705 0.001766 0.047504

2 -378.858728 0.002581 0.024415

3 -378.858744 0.001186 0.005774

4 -378.858752 0.000776 0.009776

5 -378.858760 0.000649 0.005307

6 -378.858762 0.000218 0.004704

7 -378.858763 0.000105 0.007144

8 -378.858764 0.000173 0.000959

Reason for exit: Successful completion

Quantum Calculation CPU Time : 3:29.76

Quantum Calculation Wall Time: 56.42

MacSPARTAN '16 Properties Program: (x86/Darwin) build 1.1.2

Reason for exit: Successful completion

Properties CPU Time : .23

Properties Wall Time: .24

SPARTAN '18 Properties Program: (x86/Darwin) build 1.3.0

Use of molecular symmetry disabled

Cartesian Coordinates (Angstroms)

Atom X Y Z

-----

1 C C1 1.0164229 -0.0600373 1.8998453

2 C C2 0.9136133 -0.0594817 0.5301242

3 C C3 -0.3274133 0.0344210 2.3571381

4 N N1 -1.1929670 0.1051072 1.3582091

5 N N2 -0.4235593 0.0742121 0.2302307

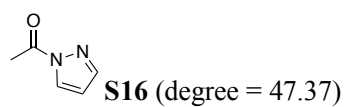
6 C C4 -1.0563380 -0.0119221 -1.0548263  
7 O O1 -2.0838454 0.5812101 -1.2752260  
8 C C5 -0.3061798 -0.8237097 -2.0890680  
9 H H2 1.9208084 -0.1169035 2.4892761  
10 H H6 -0.0645341 -1.8240031 -1.7138040  
11 H H1 0.6356488 -0.3302480 -2.3608212  
12 H H10 -0.9281009 -0.8978323 -2.9825752  
13 H H11 -0.6928352 0.0376275 3.3763256  
14 H H15 1.6697677 -0.1043354 -0.2397946

Point Group = C1 Order = 1 Nsymop = 1

Reason for exit: Successful completion

Properties CPU Time : .30

Properties Wall Time: .31



MacSPARTAN '16 Quantum Mechanics Program: (x86/Darwin) build 1.1.2

Job type: Geometry optimization.

Method: RB3LYP

Basis set: 6-31+G\*

Number of basis functions: 164

Number of electrons: 58

Parallel Job: 4 threads

SCF model:

A restricted hybrid HF-DFT SCF calculation will be  
performed using Pulay DIIS + Geometric Direct Minimization

Optimization:

Step Energy Max Grad. Max Dist.

1 -378.856612 0.002111 0.031584  
2 -378.856639 0.002831 0.018553  
3 -378.856654 0.000824 0.004217  
4 -378.856661 0.000387 0.006656  
5 -378.856662 0.000480 0.001904  
6 -378.856663 0.000295 0.003579  
7 -378.856665 0.000284 0.010827  
8 -378.856667 0.000317 0.009105  
9 -378.856669 0.000385 0.011073  
10 -378.856672 0.000316 0.012450  
11 -378.856674 0.000459 0.025080  
12 -378.856679 0.000529 0.048295  
13 -378.856684 0.000754 0.010503  
14 -378.856688 0.000651 0.006937  
15 -378.856690 0.000183 0.007190  
16 -378.856691 0.000151 0.001557

Reason for exit: Successful completion

Quantum Calculation CPU Time : 6:42.98

Quantum Calculation Wall Time: 1:47.33

MacSPARTAN '16 Properties Program: (x86/Darwin) build 1.1.2

Reason for exit: Successful completion

Properties CPU Time : .23

Properties Wall Time: .24

SPARTAN '18 Properties Program: (x86/Darwin) build 1.3.0

Use of molecular symmetry disabled

Cartesian Coordinates (Angstroms)

Atom X Y Z



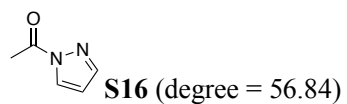
-----  
1 C C1 1.0232710 -0.0476656 1.8936361  
2 C C2 0.9167717 -0.0391011 0.5226295  
3 C C3 -0.3186873 0.0259102 2.3547003  
4 N N1 -1.1879966 0.0946220 1.3566943  
5 N N2 -0.4203720 0.0837533 0.2281943  
6 C C4 -1.0647501 -0.0176005 -1.0563812  
7 O O1 -2.0113179 0.6814387 -1.3212852  
8 C C5 -0.4334400 -1.0012047 -2.0148156  
9 H H2 1.9302712 -0.0942408 2.4799060  
10 H H6 -0.4550243 -2.0123887 -1.5919509  
11 H H1 0.6155229 -0.7503894 -2.2103149  
12 H H10 -0.9856392 -0.9778340 -2.9556223  
13 H H11 -0.6825445 0.0168209 3.3743406  
14 H H15 1.6717138 -0.0641134 -0.2496768

Point Group = C1 Order = 1 Nsymop = 1

Reason for exit: Successful completion

Properties CPU Time : .27

Properties Wall Time: .28



MacSPARTAN '16 Quantum Mechanics Program: (x86/Darwin) build 1.1.2

Job type: Geometry optimization.

Method: RB3LYP

Basis set: 6-31+G\*

Number of basis functions: 164

Number of electrons: 58

Parallel Job: 4 threads

SCF model:

A restricted hybrid HF-DFT SCF calculation will be performed using Pulay DIIS + Geometric Direct Minimization

Optimization:

Step Energy Max Grad. Max Dist.

1 -378.854524 0.002435 0.032986

2 -378.854566 0.001721 0.028453

3 -378.854563 0.001467 0.022817

4 -378.854559 0.002209 0.017359

5 -378.854577 0.000538 0.001754

6 -378.854579 0.000151 0.000979

Reason for exit: Successful completion

Quantum Calculation CPU Time : 2:46.00

Quantum Calculation Wall Time: 44.89

MacSPARTAN '16 Properties Program: (x86/Darwin) build 1.1.2

Reason for exit: Successful completion

Properties CPU Time : .23

Properties Wall Time: 1.24

SPARTAN '18 Properties Program: (x86/Darwin) build 1.3.0

Use of molecular symmetry disabled

Cartesian Coordinates (Angstroms)

Atom X Y Z

-----  
1 C C1 1.0229755 -0.0535517 1.8899995

2 C C2 0.9149542 -0.0363990 0.5173547

3 C C3 -0.3165207 0.0221550 2.3525533

4 N N1 -1.1870318 0.1005399 1.3538466

5 N N2 -0.4194433 0.0950866 0.2269741

6 C C4 -1.0695417 -0.0139693 -1.0611681

7 O O1 -1.9079284 0.7870642 -1.3885280

8 C C5 -0.5775879 -1.1494640 -1.9260450

9 H H2 1.9306421 -0.1049692 2.4747904

10 H H6 -0.7586343 -2.1065651 -1.4226310

11 H H1 0.5020363 -1.0744923 -2.1007861

12 H H10 -1.1009287 -1.1237765 -2.8829350

13 H H11 -0.6803849 0.0098297 3.3720914

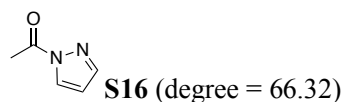
14 H H15 1.6676308 -0.0584789 -0.2580174

Point Group = C1 Order = 1 Nsymop = 1

Reason for exit: Successful completion

Properties CPU Time : .27

Properties Wall Time: .28



MacSPARTAN '16 Quantum Mechanics Program: (x86/Darwin) build 1.1.2

Job type: Geometry optimization.

Method: RB3LYP

Basis set: 6-31+G\*

Number of basis functions: 164

Number of electrons: 58

Parallel Job: 4 threads

SCF model:

A restricted hybrid HF-DFT SCF calculation will be

performed using Pulay DIIS + Geometric Direct Minimization

Optimization:

Step Energy Max Grad. Max Dist.

1 -378.852563 0.002380 0.012757

2 -378.852604 0.000501 0.011420

3 -378.852605 0.000768 0.005135

4 -378.852607 0.000424 0.002877

5 -378.852609 0.000255 0.001649

6 -378.852609 0.000108 0.003742

Reason for exit: Successful completion

Quantum Calculation CPU Time : 2:35.16

Quantum Calculation Wall Time: 42.07

MacSPARTAN '16 Properties Program: (x86/Darwin) build 1.1.2

Reason for exit: Successful completion

Properties CPU Time : .23

Properties Wall Time: .24

SPARTAN '18 Properties Program: (x86/Darwin) build 1.3.0

Use of molecular symmetry disabled

Cartesian Coordinates (Angstroms)

Atom X Y Z

-----

1 C C1 1.0227408 -0.0560022 1.8894536

2 C C2 0.9154095 -0.0322870 0.5148455

3 C C3 -0.3152658 0.0174937 2.3514843

4 N N1 -1.1860133 0.0984346 1.3505069

5 N N2 -0.4168122 0.0983166 0.2269767

6 C C4 -1.0702447 -0.0107662 -1.0666955

7 O O1 -1.7818601 0.8762615 -1.4620992

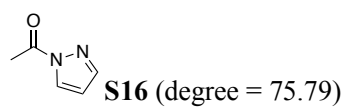
8 C C5 -0.7448738 -1.2694444 -1.8309612  
9 H H2 1.9301933 -0.1092346 2.4743556  
10 H H6 -1.0719707 -2.1438372 -1.2555356  
11 H H1 0.3371306 -1.3688812 -1.9774129  
12 H H10 -1.2459201 -1.2481277 -2.8001885  
13 H H11 -0.6802820 0.0056206 3.3705469  
14 H H15 1.6665610 -0.0524909 -0.2626494

Point Group = C1 Order = 1 Nsymop = 1

Reason for exit: Successful completion

Properties CPU Time : .26

Properties Wall Time: .26



MacSPARTAN '16 Quantum Mechanics Program: (x86/Darwin) build 1.1.2

Job type: Geometry optimization.

Method: RB3LYP

Basis set: 6-31+G\*

Number of basis functions: 164

Number of electrons: 58

Parallel Job: 4 threads

SCF model:

A restricted hybrid HF-DFT SCF calculation will be  
performed using Pulay DIIS + Geometric Direct Minimization

Optimization:

Step Energy Max Grad. Max Dist.

1 -378.851020 0.002167 0.018935

2 -378.851065 0.001693 0.007194

3 -378.851067 0.000959 0.006742

4 -378.851079 0.000472 0.014831

5 -378.851088 0.000653 0.010766

6 -378.851091 0.001092 0.005499

7 -378.851096 0.000637 0.006204

8 -378.851099 0.000389 0.004493

9 -378.851100 0.000321 0.004401

10 -378.851100 0.000128 0.001996

Reason for exit: Successful completion

Quantum Calculation CPU Time : 4:20.22

Quantum Calculation Wall Time: 1:09.71

MacSPARTAN '16 Properties Program: (x86/Darwin) build 1.1.2

Reason for exit: Successful completion

Properties CPU Time : .23

Properties Wall Time: .24

SPARTAN '18 Properties Program: (x86/Darwin) build 1.3.0

Use of molecular symmetry disabled

Cartesian Coordinates (Angstroms)

Atom X Y Z

-----  
1 C C1 1.0267591 -0.0358722 1.8991447

2 C C2 0.9257194 -0.0201458 0.5214425

3 C C3 -0.3127496 0.0065960 2.3542731

4 N N1 -1.1814815 0.0574373 1.3460726

5 N N2 -0.4061833 0.0627370 0.2305318

6 C C4 -1.0541835 -0.0158038 -1.0757355

7 O O1 -1.6050430 0.9502682 -1.5341823

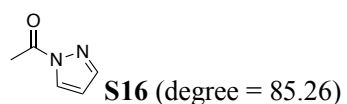
8 C C5 -0.9463811 -1.3611361 -1.7427606  
9 H H2 1.9327894 -0.0630663 2.4879365  
10 H H6 -1.4248044 -2.1173159 -1.1084500  
11 H H1 0.1046091 -1.6545233 -1.8508808  
12 H H10 -1.4271581 -1.3299029 -2.7221603  
13 H H11 -0.6831153 -0.0027794 3.3713201  
14 H H15 1.6788257 -0.0245818 -0.2548241

Point Group = C1 Order = 1 Nsymop = 1

Reason for exit: Successful completion

Properties CPU Time : .24

Properties Wall Time: .25



MacSPARTAN '16 Quantum Mechanics Program: (x86/Darwin) build 1.1.2

Job type: Geometry optimization.

Method: RB3LYP

Basis set: 6-31+G\*

Number of basis functions: 164

Number of electrons: 58

Parallel Job: 4 threads

SCF model:

A restricted hybrid HF-DFT SCF calculation will be  
performed using Pulay DIIS + Geometric Direct Minimization

Optimization:

Step Energy Max Grad. Max Dist.

1 -378.850463 0.001354 0.005998

2 -378.850481 0.001241 0.006289

3 -378.850500 0.001304 0.006614

4 -378.850518 0.001222 0.124889

5 -378.850697 0.001662 0.035748

6 -378.850717 0.000783 0.016707

7 -378.850724 0.000646 0.006117

8 -378.850726 0.000282 0.002123

9 -378.850727 0.000097 0.000947

Reason for exit: Successful completion

Quantum Calculation CPU Time : 3:56.21

Quantum Calculation Wall Time: 1:03.55

MacSPARTAN '16 Properties Program: (x86/Darwin) build 1.1.2

Reason for exit: Successful completion

Properties CPU Time : .23

Properties Wall Time: .24

SPARTAN '18 Properties Program: (x86/Darwin) build 1.3.0

Use of molecular symmetry disabled

Cartesian Coordinates (Angstroms)

Atom X Y Z

-----

1 C C1 1.0375877 0.0383106 1.9255755

2 C C2 0.9565445 0.0057654 0.5453667

3 C C3 -0.3061904 -0.0119771 2.3623201

4 N N1 -1.1614517 -0.0693376 1.3407224

5 N N2 -0.3702131 -0.0647174 0.2389859

6 C C4 -1.0025530 -0.0513914 -1.0828031

7 O O1 -1.3340426 0.9925676 -1.5789859

8 C C5 -1.2017857 -1.4162408 -1.6791751



9 H H2 1.9345767 0.0948721 2.5259156

10 H H6 -1.8291486 -2.0108482 -1.0036840

11 H H1 -0.2390710 -1.9357670 -1.7601420

12 H H10 -1.6720477 -1.3355101 -2.6608358

13 H H11 -0.6907246 -0.0091426 3.3740854

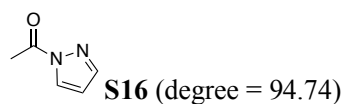
14 H H15 1.7169510 0.0395013 -0.2229608

Point Group = C1 Order = 1 Nsymop = 1

Reason for exit: Successful completion

Properties CPU Time : .26

Properties Wall Time: .26



MacSPARTAN '16 Quantum Mechanics Program: (x86/Darwin) build 1.1.2

Job type: Geometry optimization.

Method: RB3LYP

Basis set: 6-31+G\*

Number of basis functions: 164

Number of electrons: 58

Parallel Job: 4 threads

SCF model:

A restricted hybrid HF-DFT SCF calculation will be

performed using Pulay DIIS + Geometric Direct Minimization

Optimization:

Step Energy Max Grad. Max Dist.

1 -378.851744 0.000928 0.003240

2 -378.851753 0.000995 0.003240

3 -378.851763 0.001014 0.003240

4 -378.851772 0.001015 0.158409

5 -378.852158 0.001008 0.156664

6 -378.852334 0.000894 0.028502

7 -378.852338 0.001084 0.010606

8 -378.852346 0.000278 0.004910

9 -378.852347 0.000203 0.002747

10 -378.852348 0.000256 0.005625

11 -378.852349 0.000320 0.002590

12 -378.852350 0.000353 0.004415

13 -378.852351 0.000338 0.005911

14 -378.852352 0.000288 0.006092

15 -378.852354 0.000327 0.006345

16 -378.852355 0.000314 0.004200

17 -378.852356 0.000182 0.002031

Reason for exit: Successful completion

Quantum Calculation CPU Time : 7:04.10

Quantum Calculation Wall Time: 1:52.70

MacSPARTAN '16 Properties Program: (x86/Darwin) build 1.1.2

Reason for exit: Successful completion

Properties CPU Time : .24

Properties Wall Time: 1.24

SPARTAN '18 Properties Program: (x86/Darwin) build 1.3.0

Use of molecular symmetry disabled

Cartesian Coordinates (Angstroms)

Atom X Y Z

-----

1 C C1 1.0364117 0.1414534 1.9492889

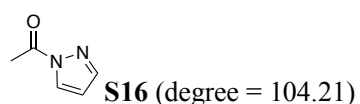
2 C C2 1.0000805 0.0237592 0.5751150  
3 C C3 -0.3092503 -0.0295651 2.3567667  
4 N N1 -1.1195596 -0.2467014 1.3244033  
5 N N2 -0.2951833 -0.2547752 0.2390798  
6 C C4 -0.9174267 -0.1221306 -1.0792963  
7 O O1 -1.0043058 0.9620229 -1.5960464  
8 C C5 -1.4810246 -1.4061953 -1.6147039  
9 H H2 1.9045157 0.3196305 2.5680807  
10 H H6 -2.1595285 -1.8351591 -0.8673460  
11 H H1 -0.6742839 -2.1337912 -1.7675122  
12 H H10 -2.0093954 -1.2267440 -2.5525726  
13 H H11 -0.7226035 -0.0000897 3.3568764  
14 H H15 1.7730480 0.1045028 -0.1766241

Point Group = C1 Order = 1 Nsymop = 1

Reason for exit: Successful completion

Properties CPU Time : .25

Properties Wall Time: 1.25



MacSPARTAN '16 Quantum Mechanics Program: (x86/Darwin) build 1.1.2

Job type: Geometry optimization.

Method: RB3LYP

Basis set: 6-31+G\*

Number of basis functions: 164

Number of electrons: 58

Parallel Job: 4 threads

SCF model:

A restricted hybrid HF-DFT SCF calculation will be  
performed using Pulay DIIS + Geometric Direct Minimization

Optimization:

Step Energy Max Grad. Max Dist.

1 -378.855125 0.001556 0.090000

2 -378.855182 0.002982 0.029786

3 -378.855176 0.003380 0.027148

4 -378.855208 0.002396 0.030248

5 -378.855223 0.001020 0.006902

6 -378.855229 0.000503 0.004782

7 -378.855230 0.000261 0.003833

8 -378.855231 0.000125 0.006550

Reason for exit: Successful completion

Quantum Calculation CPU Time : 3:36.77

Quantum Calculation Wall Time: 58.19

MacSPARTAN '16 Properties Program: (x86/Darwin) build 1.1.2

Reason for exit: Successful completion

Properties CPU Time : .23

Properties Wall Time: .24

SPARTAN '18 Properties Program: (x86/Darwin) build 1.3.0

Use of molecular symmetry disabled

Cartesian Coordinates (Angstroms)

Atom X Y Z

-----  
1 C C1 1.0318776 0.1626977 1.9494579

2 C C2 1.0045363 0.0204153 0.5797524

3 C C3 -0.3141888 -0.0289156 2.3541369

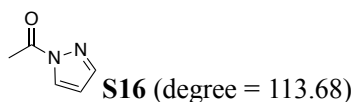
4 N N1 -1.1134448 -0.2848220 1.3249921  
5 N N2 -0.2818422 -0.3025358 0.2396756  
6 C C4 -0.8941368 -0.1441735 -1.0730099  
7 O O1 -0.8045104 0.9076197 -1.6563206  
8 C C5 -1.6874587 -1.3381287 -1.5193664  
9 H H2 1.8923571 0.3695591 2.5702930  
10 H H6 -2.3774560 -1.6294834 -0.7193700  
11 H H1 -1.0151563 -2.1881193 -1.6893848  
12 H H10 -2.2355664 -1.1053832 -2.4338744  
13 H H11 -0.7332035 0.0165197 3.3514214  
14 H H15 1.7770102 0.1101408 -0.1711260

Point Group = C1 Order = 1 Nsymop = 1

Reason for exit: Successful completion

Properties CPU Time : .23

Properties Wall Time: .24



MacSPARTAN '16 Quantum Mechanics Program: (x86/Darwin) build 1.1.2

Job type: Geometry optimization.

Method: RB3LYP

Basis set: 6-31+G\*

Number of basis functions: 164

Number of electrons: 58

Parallel Job: 4 threads

SCF model:

A restricted hybrid HF-DFT SCF calculation will be

performed using Pulay DIIS + Geometric Direct Minimization

Optimization:

Step Energy Max Grad. Max Dist.

1 -378.858510 0.001990 0.027513

2 -378.858537 0.003303 0.055405

3 -378.858440 0.004367 0.046436

4 -378.858564 0.000545 0.014092

5 -378.858563 0.001051 0.009897

6 -378.858569 0.000382 0.003096

7 -378.858569 0.000201 0.002719

Reason for exit: Successful completion

Quantum Calculation CPU Time : 3:10.77

Quantum Calculation Wall Time: 51.39

MacSPARTAN '16 Properties Program: (x86/Darwin) build 1.1.2

Reason for exit: Successful completion

Properties CPU Time : .23

Properties Wall Time: .24

SPARTAN '18 Properties Program: (x86/Darwin) build 1.3.0

Use of molecular symmetry disabled

Cartesian Coordinates (Angstroms)

Atom X Y Z

-----  
1 C C1 1.0325178 0.1616006 1.9466338

2 C C2 0.9980985 0.0181862 0.5788289

3 C C3 -0.3135911 -0.0248710 2.3587535

4 N N1 -1.1184336 -0.2806746 1.3359846

5 N N2 -0.2918703 -0.3024030 0.2440207

6 C C4 -0.8933787 -0.1465050 -1.0652312

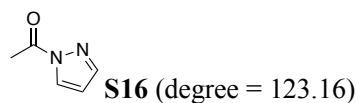
7 O O1 -0.6551800 0.8373320 -1.7244083  
8 C C5 -1.8629284 -1.2359746 -1.4258599  
9 H H2 1.8957656 0.3678408 2.5633089  
10 H H6 -2.5711311 -1.3777266 -0.6025305  
11 H H1 -1.3248503 -2.1829059 -1.5566720  
12 H H10 -2.3880142 -0.9761508 -2.3461722  
13 H H11 -0.7272418 0.0270420 3.3580280  
14 H H15 1.7648267 0.1064889 -0.1775448

Point Group = C1 Order = 1 Nsymop = 1

Reason for exit: Successful completion

Properties CPU Time : .24

Properties Wall Time: .24



MacSPARTAN '16 Quantum Mechanics Program: (x86/Darwin) build 1.1.2

Job type: Geometry optimization.

Method: RB3LYP

Basis set: 6-31+G\*

Number of basis functions: 164

Number of electrons: 58

Parallel Job: 4 threads

SCF model:

A restricted hybrid HF-DFT SCF calculation will be  
performed using Pulay DIIS + Geometric Direct Minimization

Optimization:

Step Energy Max Grad. Max Dist.

1 -378.861797 0.002485 0.043582

2 -378.861869 0.002019 0.018992

3 -378.861895 0.000823 0.004988

4 -378.861902 0.000546 0.014544

5 -378.861910 0.000512 0.005154

6 -378.861912 0.000628 0.007905

7 -378.861914 0.000400 0.012605

8 -378.861917 0.000376 0.011548

9 -378.861918 0.000311 0.013152

10 -378.861919 0.000226 0.007180

Reason for exit: Successful completion

Quantum Calculation CPU Time : 4:18.59

Quantum Calculation Wall Time: 1:09.32

MacSPARTAN '16 Properties Program: (x86/Darwin) build 1.1.2

Reason for exit: Successful completion

Properties CPU Time : .23

Properties Wall Time: .24

SPARTAN '18 Properties Program: (x86/Darwin) build 1.3.0

Use of molecular symmetry disabled

Cartesian Coordinates (Angstroms)

Atom X Y Z

-----  
1 C C1 1.0351484 0.1506598 1.9457248

2 C C2 0.9871903 0.0102800 0.5791818

3 C C3 -0.3126964 -0.0057559 2.3689531

4 N N1 -1.1309352 -0.2431157 1.3538256

5 N N2 -0.3142408 -0.2767407 0.2535962

6 C C4 -0.9036012 -0.1373146 -1.0547715



7 O O1 -0.5286998 0.7463245 -1.7913862

8 C C5 -2.0148861 -1.1081706 -1.3425207

9 H H2 1.9075830 0.3369157 2.5561817

10 H H6 -2.7122741 -1.1387022 -0.4995263

11 H H1 -1.5986635 -2.1171958 -1.4561791

12 H H10 -2.5277731 -0.8157336 -2.2600927

13 H H11 -0.7167540 0.0576919 3.3715265

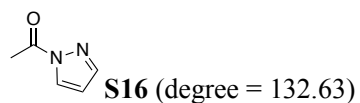
14 H H15 1.7485731 0.0800149 -0.1842486

Point Group = C1 Order = 1 Nsymop = 1

Reason for exit: Successful completion

Properties CPU Time : .24

Properties Wall Time: .24



MacSPARTAN '16 Quantum Mechanics Program: (x86/Darwin) build 1.1.2

Job type: Geometry optimization.

Method: RB3LYP

Basis set: 6-31+G\*

Number of basis functions: 164

Number of electrons: 58

Parallel Job: 4 threads

SCF model:

A restricted hybrid HF-DFT SCF calculation will be  
performed using Pulay DIIS + Geometric Direct Minimization

Optimization:

Step Energy Max Grad. Max Dist.

1 -378.864939 0.002781 0.054097

2 -378.865031 0.002249 0.068802

3 -378.865008 0.003550 0.065868

4 -378.865050 0.001369 0.026369

5 -378.865050 0.001321 0.007838

6 -378.865065 0.000209 0.000936

Reason for exit: Successful completion

Quantum Calculation CPU Time : 2:47.83

Quantum Calculation Wall Time: 45.33

MacSPARTAN '16 Properties Program: (x86/Darwin) build 1.1.2

Reason for exit: Successful completion

Properties CPU Time : .23

Properties Wall Time: .24

SPARTAN '18 Properties Program: (x86/Darwin) build 1.3.0

Use of molecular symmetry disabled

Cartesian Coordinates (Angstroms)

Atom X Y Z

-----

1 C C1 1.0402962 0.1361478 1.9439049

2 C C2 0.9778873 0.0108688 0.5773992

3 C C3 -0.3071216 -0.0000333 2.3788834

4 N N1 -1.1390598 -0.2100244 1.3698759

5 N N2 -0.3339505 -0.2425719 0.2609029

6 C C4 -0.9145829 -0.1234275 -1.0461094

7 O O1 -0.4292628 0.6428662 -1.8492836

8 C C5 -2.1466874 -0.9561027 -1.2692123

9 H H2 1.9210584 0.3030643 2.5481269

10 H H6 -2.8477312 -0.8240285 -0.4399352

11 H H1 -1.8753604 -2.0185462 -1.2957670

12 H H10 -2.6054425 -0.6696608 -2.2166566

13 H H11 -0.6997813 0.0600429 3.3862594

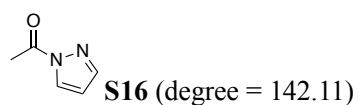
14 H H15 1.7317711 0.0731958 -0.1937213

Point Group = C1 Order = 1 Nsymop = 1

Reason for exit: Successful completion

Properties CPU Time : .24

Properties Wall Time: 1.24



MacSPARTAN '16 Quantum Mechanics Program: (x86/Darwin) build 1.1.2

Job type: Geometry optimization.

Method: RB3LYP

Basis set: 6-31+G\*

Number of basis functions: 164

Number of electrons: 58

Parallel Job: 4 threads

SCF model:

A restricted hybrid HF-DFT SCF calculation will be

performed using Pulay DIIS + Geometric Direct Minimization

Optimization:

Step Energy Max Grad. Max Dist.

1 -378.867705 0.002731 0.055234

2 -378.867806 0.003024 0.069839

3 -378.867793 0.004669 0.053678

4 -378.867841 0.001372 0.017338

5 -378.867858 0.000782 0.007248

6 -378.867864 0.000556 0.002666

7 -378.867866 0.000376 0.007160

8 -378.867868 0.000177 0.001736

9 -378.867869 0.000104 0.000915

Reason for exit: Successful completion

Quantum Calculation CPU Time : 3:54.94

Quantum Calculation Wall Time: 1:03.06

MacSPARTAN '16 Properties Program: (x86/Darwin) build 1.1.2

Reason for exit: Successful completion

Properties CPU Time : .23

Properties Wall Time: 1.24

SPARTAN '18 Properties Program: (x86/Darwin) build 1.3.0

Use of molecular symmetry disabled

Cartesian Coordinates (Angstroms)

Atom X Y Z

-----  
1 C C1 1.0456976 0.1145380 1.9427994

2 C C2 0.9698733 0.0123778 0.5755642

3 C C3 -0.3022432 0.0078316 2.3872959

4 N N1 -1.1475465 -0.1625100 1.3825145

5 N N2 -0.3530906 -0.1918618 0.2665029

6 C C4 -0.9277095 -0.0973541 -1.0391341

7 O O1 -0.3524178 0.5344993 -1.8995123

8 C C5 -2.2551752 -0.7861407 -1.2068241

9 H H2 1.9349538 0.2488578 2.5425117

10 H H6 -2.9432915 -0.4921443 -0.4090227

11 H H1 -2.1202998 -1.8721276 -1.1314882

12 H H10 -2.6630488 -0.5320094 -2.1861704

13 H H11 -0.6842830 0.0613741 3.3991175

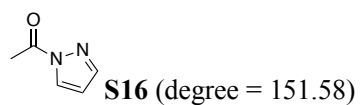
14 H H15 1.7175703 0.0609092 -0.2021860

Point Group = C1 Order = 1 Nsymop = 1

Reason for exit: Successful completion

Properties CPU Time : .26

Properties Wall Time: .27



MacSPARTAN '16 Quantum Mechanics Program: (x86/Darwin) build 1.1.2

Job type: Geometry optimization.

Method: RB3LYP

Basis set: 6-31+G\*

Number of basis functions: 164

Number of electrons: 58

Parallel Job: 4 threads

SCF model:

A restricted hybrid HF-DFT SCF calculation will be

performed using Pulay DIIS + Geometric Direct Minimization

Optimization:

Step Energy Max Grad. Max Dist.

1 -378.870059 0.002392 0.070748

2 -378.870166 0.003040 0.025602

3 -378.870195 0.001240 0.007730

4 -378.870204 0.000418 0.010721

5 -378.870208 0.000279 0.003782

6 -378.870208 0.000520 0.001242

7 -378.870209 0.000389 0.007213

8 -378.870210 0.000237 0.015925

9 -378.870212 0.000257 0.034662

10 -378.870217 0.000417 0.047819

11 -378.870222 0.000412 0.047676

12 -378.870226 0.000261 0.025006

13 -378.870228 0.000224 0.006377

14 -378.870228 0.000118 0.000983

Reason for exit: Successful completion

Quantum Calculation CPU Time : 5:49.66

Quantum Calculation Wall Time: 1:33.10

MacSPARTAN '16 Properties Program: (x86/Darwin) build 1.1.2

Reason for exit: Successful completion

Properties CPU Time : .24

Properties Wall Time: .24

SPARTAN '18 Properties Program: (x86/Darwin) build 1.3.0

Use of molecular symmetry disabled

Cartesian Coordinates (Angstroms)

Atom X Y Z

-----  
1 C C1 1.0520358 0.0925299 1.9400303

2 C C2 0.9674372 0.0263261 0.5715764

3 C C3 -0.2947292 -0.0141873 2.3910639

4 N N1 -1.1477801 -0.1486979 1.3879995

5 N N2 -0.3615337 -0.1482501 0.2668346

6 C C4 -0.9376931 -0.0673856 -1.0337681

7 O O1 -0.3023133 0.4372974 -1.9365342

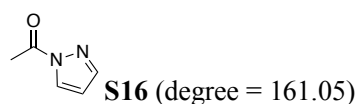
8 C C5 -2.3418753 -0.5972854 -1.1544110  
9 H H2 1.9458341 0.2040157 2.5376011  
10 H H6 -3.0117849 -0.0530303 -0.4815282  
11 H H1 -2.3823206 -1.6511916 -0.8579349  
12 H H10 -2.6668789 -0.4820688 -2.1895636  
13 H H11 -0.6687579 0.0133589 3.4069321  
14 H H15 1.7094058 0.0822135 -0.2109203

Point Group = C1 Order = 1 Nsymop = 1

Reason for exit: Successful completion

Properties CPU Time : .25

Properties Wall Time: .26



MacSPARTAN '16 Quantum Mechanics Program: (x86/Darwin) build 1.1.2

Job type: Geometry optimization.

Method: RB3LYP

Basis set: 6-31+G\*

Number of basis functions: 164

Number of electrons: 58

Parallel Job: 4 threads

SCF model:

A restricted hybrid HF-DFT SCF calculation will be  
performed using Pulay DIIS + Geometric Direct Minimization

Optimization:

Step Energy Max Grad. Max Dist.

1 -378.871887 0.001272 0.003389

2 -378.871898 0.001253 0.005032

3 -378.871907 0.001226 0.003240

4 -378.871917 0.001156 0.090572

5 -378.872017 0.000960 0.016169

6 -378.872023 0.000400 0.005285

7 -378.872025 0.000397 0.002815

8 -378.872026 0.000368 0.012865

9 -378.872027 0.000193 0.012837

10 -378.872028 0.000139 0.013517

Reason for exit: Successful completion

Quantum Calculation CPU Time : 4:05.09

Quantum Calculation Wall Time: 1:05.80

MacSPARTAN '16 Properties Program: (x86/Darwin) build 1.1.2

Reason for exit: Successful completion

Properties CPU Time : .23

Properties Wall Time: .24

SPARTAN '18 Properties Program: (x86/Darwin) build 1.3.0

Use of molecular symmetry disabled

Cartesian Coordinates (Angstroms)

Atom X Y Z

-----  
1 C C1 1.0557844 0.0705399 1.9398236

2 C C2 0.9642283 0.0269352 0.5712836

3 C C3 -0.2922452 -0.0032074 2.3958146

4 N N1 -1.1529564 -0.0947169 1.3948590

5 N N2 -0.3721930 -0.0932524 0.2705500

6 C C4 -0.9449776 -0.0377076 -1.0294230

7 O O1 -0.2561822 0.3063485 -1.9686501



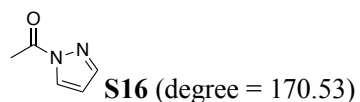
8 C C5 -2.4044248 -0.4004033 -1.1157702  
9 H H2 1.9549410 0.1458754 2.5350146  
10 H H6 -3.0043381 0.2775294 -0.5006297  
11 H H1 -2.5740265 -1.4111797 -0.7298787  
12 H H10 -2.7112693 -0.3371953 -2.1607920  
13 H H11 -0.6602979 0.0152922 3.4140766  
14 H H15 1.7035131 0.0664173 -0.2145267

Point Group = C1 Order = 1 Nsymop = 1

Reason for exit: Successful completion

Properties CPU Time : .24

Properties Wall Time: 1.25



MacSPARTAN '16 Quantum Mechanics Program: (x86/Darwin) build 1.1.2

Job type: Geometry optimization.

Method: RB3LYP

Basis set: 6-31+G\*

Number of basis functions: 164

Number of electrons: 58

Parallel Job: 4 threads

SCF model:

A restricted hybrid HF-DFT SCF calculation will be  
performed using Pulay DIIS + Geometric Direct Minimization

Optimization:

Step Energy Max Grad. Max Dist.

1 -378.872989 0.000979 0.003240

2 -378.872999 0.000938 0.004373

3 -378.873009 0.000904 0.003248

4 -378.873017 0.000853 0.087190

5 -378.873110 0.001241 0.030427

6 -378.873120 0.000399 0.006112

7 -378.873120 0.000147 0.003681

Reason for exit: Successful completion

Quantum Calculation CPU Time : 3:01.46

Quantum Calculation Wall Time: 49.10

MacSPARTAN '16 Properties Program: (x86/Darwin) build 1.1.2

Reason for exit: Successful completion

Properties CPU Time : .23

Properties Wall Time: .24

SPARTAN '18 Properties Program: (x86/Darwin) build 1.3.0

Use of molecular symmetry disabled

Cartesian Coordinates (Angstroms)

Atom X Y Z

-----

1 C C1 1.0584910 0.0497484 1.9397829

2 C C2 0.9628425 0.0286903 0.5712639

3 C C3 -0.2902589 0.0035509 2.3988691

4 N N1 -1.1555346 -0.0471546 1.3993146

5 N N2 -0.3782383 -0.0398642 0.2730107

6 C C4 -0.9488933 -0.0103179 -1.0265786

7 O O1 -0.2279659 0.1695583 -1.9876889

8 C C5 -2.4423643 -0.1952416 -1.0917656

9 H H2 1.9605979 0.0931482 2.5336212

10 H H6 -2.9514231 0.6115667 -0.5548306

11 H H1 -2.7395071 -1.1315911 -0.6097209

12 H H10 -2.7389718 -0.1950046 -2.1417776

13 H H11 -0.6544930 0.0095908 3.4186557

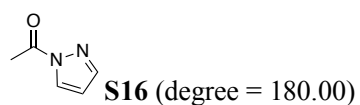
14 H H15 1.7003205 0.0541742 -0.2167370

Point Group = C1 Order = 1 Nsymop = 1

Reason for exit: Successful completion

Properties CPU Time : .24

Properties Wall Time: 1.25



MacSPARTAN '16 Quantum Mechanics Program: (x86/Darwin) build 1.1.2

Job type: Geometry optimization.

Method: RB3LYP

Basis set: 6-31+G\*

Number of basis functions: 164

Number of electrons: 58

Parallel Job: 4 threads

SCF model:

A restricted hybrid HF-DFT SCF calculation will be

performed using Pulay DIIS + Geometric Direct Minimization

Optimization:

Step Energy Max Grad. Max Dist.

1 -378.873347 0.000915 0.003240

2 -378.873356 0.000877 0.003240

3 -378.873365 0.000828 0.003240

4 -378.873373 0.000800 0.082963

5 -378.873473 0.001019 0.022824

6 -378.873480 0.000623 0.003738

7 -378.873481 0.000501 0.002172

8 -378.873483 0.000192 0.006152

9 -378.873484 0.000165 0.012978

10 -378.873486 0.000412 0.015041

11 -378.873487 0.000517 0.020953

12 -378.873488 0.000460 0.013102

13 -378.873489 0.000281 0.004864

Reason for exit: Successful completion

Quantum Calculation CPU Time : 5:17.85

Quantum Calculation Wall Time: 1:24.82

MacSPARTAN '16 Properties Program: (x86/Darwin) build 1.1.2

Reason for exit: Successful completion

Properties CPU Time : .23

Properties Wall Time: .24

SPARTAN '18 Properties Program: (x86/Darwin) build 1.3.0

Use of molecular symmetry disabled

Cartesian Coordinates (Angstroms)

Atom X Y Z

-----  
1 C C1 1.0598612 0.0287455 1.9400661

2 C C2 0.9628395 0.0254751 0.5715710

3 C C3 -0.2895187 0.0262032 2.4000864

4 N N1 -1.1565877 0.0224107 1.4008797

5 N N2 -0.3803018 0.0209251 0.2739778

6 C C4 -0.9491175 0.0158090 -1.0262008

7 O O1 -0.2150363 0.0146886 -1.9943833

8 C C5 -2.4543572 0.0119335 -1.0837248

9 H H2 1.9632603 0.0328234 2.5334819

10 H H6 -2.8619712 0.8935647 -0.5791042

11 H H1 -2.8581581 -0.8623360 -0.5638240

12 H H10 -2.7554484 0.0024699 -2.1323242

13 H H11 -0.6526273 0.0262892 3.4203050

14 H H15 1.7001094 0.0270469 -0.2169715

Point Group = C1 Order = 1 Nsymop = 1

Reason for exit: Successful completion

Properties CPU Time : .24

Properties Wall Time: 1.25

## 2-5-20. Conformational stability of *E/Z* Enol form of **1s**

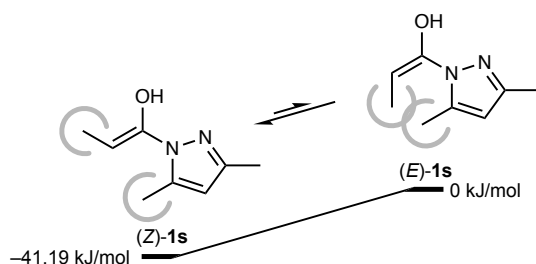
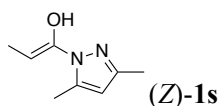


**Figure S8.** *E/Z* geometry of **1s**.

DFT calculation of **1s** was performed using B3LYP/6-31+G\*. **(Z)-1s** is 41.19 kJ/mol more stable than **(E)-1s**.

**Table S4.** Summary of DFT calculation of **(Z)-1s** and **(E)-1s** by using B3LYP/6-31+G\*



SPARTAN '18 MECHANICS PROGRAM: (x86/Darwin) build 1.3.0

Frequency Calculation

Adjusted 5 (out of 69) low frequency modes

Reason for exit: Successful completion

Mechanics CPU Time : .04

Mechanics Wall Time: .05

SPARTAN '18 Quantum Mechanics Program: (x86/Darwin) build 1.3.0

Job type: Geometry optimization.

Method: RB3LYP

Basis set: 6-31+G\*

Number of basis functions: 233

Number of electrons: 82

Parallel Job: 4 threads

SCF model:

A restricted hybrid HF-DFT SCF calculation will be

performed using Pulay DIIS + Geometric Direct Minimization

Optimization:

Step Energy Max Grad. Max Dist.

1 -496.782508 0.034476 0.097289

2 -496.792318 0.008283 0.157900

3 -496.793329 0.004025 0.160980

4 -496.793734 0.001578 0.114757

5 -496.794065 0.004964 0.181296

6 -496.794331 0.002194 0.136081

7 -496.794628 0.003660 0.120082

8 -496.794777 0.002352 0.122715

9 -496.794864 0.000484 0.113914

10 -496.794894 0.000616 0.023186

11 -496.794910 0.000271 0.025190

Reason for exit: Successful completion

Quantum Calculation CPU Time : 18:22.03

Quantum Calculation Wall Time: 4:45.54

SPARTAN '18 Properties Program: (x86/Darwin) build 1.3.0

Reason for exit: Successful completion

Properties CPU Time : .51

Properties Wall Time: .52

SPARTAN '18 Properties Program: (x86/Darwin) build 1.3.0

Use of molecular symmetry disabled

Cartesian Coordinates (Angstroms)

Atom X Y Z

-----  
1 C C1 0.0594579 1.2936402 1.8115895  
2 C C2 0.0572620 1.1772032 0.4320795  
3 C C3 -0.0418367 -0.0210214 2.3239055  
4 N N1 -0.1010207 -0.8976478 1.3254322  
5 N N2 -0.0443444 -0.1693068 0.1684473  
6 C C4 -0.0619797 -0.9348642 -1.0417937  
7 C C7 -0.0835279 -0.4779631 3.7503165  
8 C C8 0.1435090 2.2693079 -0.5851306  
9 H H2 0.1239374 2.2181123 2.3702957  
10 H H3 -0.1364054 -1.5695360 3.7957730  
11 H H5 -0.9563852 -0.0687707 4.2737391  
12 H H7 0.8097621 -0.1525446 4.2971960  
13 H H8 0.1897340 3.2307556 -0.0656174  
14 H H4 1.0402269 2.1807016 -1.2104667  
15 H H9 -0.7289772 2.2868924 -1.2493652  
16 C C5 0.0259912 -0.4427188 -2.2885177

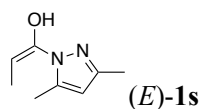
17 H H1 0.1249366 0.6232805 -2.4311112  
18 O O1 -0.1890947 -2.2622024 -0.7994693  
19 H H10 -0.2141089 -2.3707993 0.1774630  
20 C C6 0.0005061 -1.3108178 -3.5158740  
21 H H6 -0.0591922 -2.3708813 -3.2565487  
22 H H11 0.9018367 -1.1596775 -4.1259366  
23 H H12 -0.8602871 -1.0711420 -4.1564060

Point Group = C1 Order = 1 Nsymop = 1

Reason for exit: Successful completion

Properties CPU Time : .59

Properties Wall Time: .60



SPARTAN '18 MECHANICS PROGRAM: (x86/Darwin) build 1.3.0

Frequency Calculation

Adjusted 2 (out of 69) low frequency modes

Reason for exit: Successful completion

Mechanics CPU Time : .04

Mechanics Wall Time: .05

SPARTAN '18 Quantum Mechanics Program: (x86/Darwin) build 1.3.0

Job type: Geometry optimization.

Method: RB3LYP

Basis set: 6-31+G\*

Number of basis functions: 233

Number of electrons: 82

Parallel Job: 4 threads

SCF model:



A restricted hybrid HF-DFT SCF calculation will be  
performed using Pulay DIIS + Geometric Direct Minimization

Optimization:

Step Energy Max Grad. Max Dist.

1 -496.767290 0.053067 0.128544 1

2 -496.776209 0.028317 0.098960 1

3 -496.778250 0.007368 0.089454 1

4 -496.778333 0.004887 0.050848

5 -496.778512 0.002751 0.079130

6 -496.778590 0.001577 0.127689

7 -496.778698 0.002348 0.126292

8 -496.778805 0.003179 0.128190

9 -496.778920 0.003341 0.128617

10 -496.779024 0.004326 0.132022

11 -496.779122 0.004981 0.140478

12 -496.779177 0.004522 0.073890

13 -496.779209 0.002934 0.062737

14 -496.779222 0.000418 0.020946

Reason for exit: Successful completion

Quantum Calculation CPU Time : 22:29.30

Quantum Calculation Wall Time: 5:48.09

SPARTAN '18 Properties Program: (x86/Darwin) build 1.3.0

Reason for exit: Successful completion

Properties CPU Time : .51

Properties Wall Time: 1.52

SPARTAN '18 Properties Program: (x86/Darwin) build 1.3.0

Use of molecular symmetry disabled

Cartesian Coordinates (Angstroms)

Atom X Y Z

-----  
1 C C1 0.9786829 0.0425093 1.7192438  
2 C C2 0.8716660 -0.1382554 0.3533746  
3 C C3 -0.3412174 0.1120759 2.2224404  
4 N N1 -1.2108155 -0.0209939 1.2317205  
5 N N2 -0.4806803 -0.1961947 0.0753516  
6 C C4 -1.2891934 -0.1014352 -1.1157503  
7 C C7 -0.8055573 0.2882652 3.6360046  
8 C C8 2.0045064 -0.4256695 -0.5851608  
9 H H2 1.9030633 0.0773565 2.2809984  
10 H H3 -1.8984812 0.2869932 3.6787942  
11 H H5 -0.4452475 1.2356997 4.0549884  
12 H H7 -0.4339797 -0.5186264 4.2792361  
13 H H8 2.8507257 -0.7953491 0.0021638  
14 H H4 1.7436166 -1.1941558 -1.3164110  
15 H H9 2.3466232 0.4607014 -1.1274484  
16 C C5 -0.9633605 0.0840916 -2.4076341  
17 H H1 -1.8551484 0.0604726 -3.0291660  
18 O O1 -2.6070276 -0.2854484 -0.8168530  
19 H H10 -2.6889102 -0.2158726 0.1597382  
20 C C6 0.3295815 0.2673546 -3.1545906  
21 H H6 1.0241222 0.9527861 -2.6625485  
22 H H11 0.1072874 0.6998601 -4.1360488  
23 H H12 0.8597439 -0.6761647 -3.3424430

Point Group = C1 Order = 1 Nsymop = 1

Reason for exit: Successful completion

Properties CPU Time : .63

Properties Wall Time: .64

## 2-5-21. References

- (1) Hori, M.; Sakakura, A.; Ishihara, K. *J. Am. Chem. Soc.* **2014**, *136*, 13198–13201.
- (2) Ishihara, K.; Fushimu, M. *J. Am. Chem. Soc.* **2008**, *130*, 7532–7533.
- (3) Quach, T. D.; Batey, R. A. *Org. Lett.* **2003**, *5*, 4397–4400.
- (4) Jew, S.-S.; Jeong, B.-S.; Lee, J.-H.; Yoo, M.-S.; Lee, Y.-J.; Park, B.-S.; Kim, M. G.; Park, H.-G. *J. Org. Chem.* **2003**, *68*, 4514–4516.
- (5) Grigg, R.; Husinec, S.; Savić, V. *J. S. Serb. Chem. Soc.* **2010**, *75*, 1–9.
- (6) Jew, S.-S.; Yoo, M.-S.; Jeong, B.-S.; Park II, Y.; Park, H.-G. *Org. Lett.* **2002**, *4*, 4245–4248.
- (7) Cai, X.; Keshavarz, A.; Omaque, J. D.; Stokes, B. J. *Org. Lett.* **2017**, *19*, 2626–2629.
- (8) Jørgensen, M.; Lee, S.; Liu, X.; Wolkowski, J. P.; Hartwig, J. F. *J. Am. Chem. Soc.* **2002**, *124*, 12557–12565.
- (9) Li, B.-F.; Yuan, K.; Zhang, M.-J.; Wu, H.; Dai, L.-X.; Wang, Q. R.; Hou, X.-L. *J. Org. Chem.* **2003**, *68*, 6264–6267.
- (10) Takahashi, E.; Fujisawa, H.; Yanai, T.; Mukaiyama, T. *Chem. Lett.* **2005**, *34*, 604–605.
- (11) Marcé, P.; Lynch, J.; Blacker, A. J.; J. Williams, M. J. *Chem. Commun.* **2016**, *52*, 1436–1438.
- (12) Zhang, H.-J.; Shi, C.-Y.; Zhong, F.; Yin, L. *J. Am. Chem. Soc.* **2017**, *139*, 2196–2199.
- (13) Knör, S.; Khrenov, A. V.; Laufer, B.; Saenko, E. L.; Hauser, C. A. E.; Kessler, H. *J. Med. Chem.* **2007**, *50*, 4329–4339.
- (14) Micuch, P.; Seebach, D. *Helv. Chim. Acta.* **2002**, *85*, 1567–1577.
- (15) Tokumasu, K.; Yazaki, R.; Ohshima, T. *J. Am. Chem. Soc.* **2016**, *138*, 2664–2669.
- (16) Taninokuchim, S.; Yazaki, R.; Ohshima, T. *Org. Lett.* **2017**, *19*, 3187–3190.
- (17) Dauncey, E. M.; Morcillo, S. P.; Douglas, J. J.; Sheikh, N. S.; Leonori, D. *Angew. Chem. Int. Ed.* **2018**, *57*, 744–748.
- (18) Bansode, T. N.; Shilke, J. V.; Dongre, V. G. *Eur. J. Med. Chem.* **2009**, *44*, 5094–5098.
- (19) Huang, Z.; Chen, Q.; Yang, X.; Liu, Y.; Zhang, L.; Lu, T.; Zhou, Q. *Org. Chem. Front.* **2017**, *4*, 967–971.
- (20) Ahmed, B. M.; Mezei, G. *RSC Adv.* **2015**, *5*, 24081–24093.
- (21) Adler, P.; Teskey, C. J.; Kaiser, D.; Holy, M.; Sitte, H. H.; Maulide, N. *Nat. Chem.* **2019**, *11*, 329–334.
- (22) Furuya, T.; Strom, A. E.; Ritter, T. *J. Am. Chem. Soc.* **2009**, *131*, 1662–1663.

- (23) Miyamoto, K.; Tsuchiya, S.; Ohta, H. *J. Fluor. Chem.* **1992**, *59*, 225–232.
- (24) Kim, K.-Y.; Kim, B. C.; Lee, H. B.; Shin, H. *J. Org. Chem.* **2008**, *73*, 8106–8108.
- (25) Gupta, E.; Kand, R.; Mohanan, K. *Org. Lett.* **2017**, *19*, 6016–6019.
- (26) Haro, T. D.; Nevado, C. *Adv. Synth. Catal.* **2010**, *352*, 2767–2772.
- (27) Beeson, T. D.; MacMillan, D. W. C. *J. Am. Chem. Soc.* **2005**, *127*, 8826–8828.
- (28) An analogous UV difference spectrum with a negative/positive band pair around 220/230 nm has been observed for an indolyl model compound of the  $\pi$ -cation interaction. (a) Okada, A.; Miura, T.; Takeuchi, H. *Biochemistry* **2001**, *40*, 6053–6060. (b) Yorita, H.; Otomo, K.; Hiramatsu, H.; Toyama, A.; Miura, T.; Takeuchi, H. *J. Am. Chem. Soc.* **2008**, *130*, 15266–15267.
- (29) Buchanan, S. K.; Dismukes, G. C. *Biochemistry* **1987**, *26*, 5049–5055.
- (30) Liu, S.; Pedersen, L. G. *J. Phys. Chem. A* **2009**, *113*, 3648–3655.
- (31) The geometries of **1a** and Cu(OTf)<sub>2</sub>•2[**1a**] complexes were optimized with gradient-corrected density functional theory (DFT) calculations with B3LYP using 6-31+G\* basis set (gas) which authorizes for Cu(II), after MMFF (molecular mechanics) calculation. For 6-31+G\* basis set for atoms K through Zn, see: Rassolov, V. A.; Pople, J. A.; Ratner, M. A.; Windus, T. L. *J. Chem. Phys.* **1988**, *109*, 1223. For 6-31+G\* basis set for third-row atoms, see: Rassolov, V. A.; Ratner, M. A.; Pople, J. A.; Redfern, P. C.; Curtiss, L. A. *J. Comp. Chem.* **2001**, *22*, 976–984.
- (32) Armstrong, A.; Edmonds, I. D.; Swarbrick, M. E.; Treweeke, N. R. *Tetrahedron* **2005**, *61*, 8423–8442.
- (33) Bordwell, F. G. *Acc. Chem. Res.* **1988**, *21*, 456–463.
- (34) Bordwell, F. G.; Cornforth, F. J. *J. Org. Chem.* **1978**, *43*, 1763–1768.

## Chapter 3

### Thorpe–Ingold Effect and a High-Performance

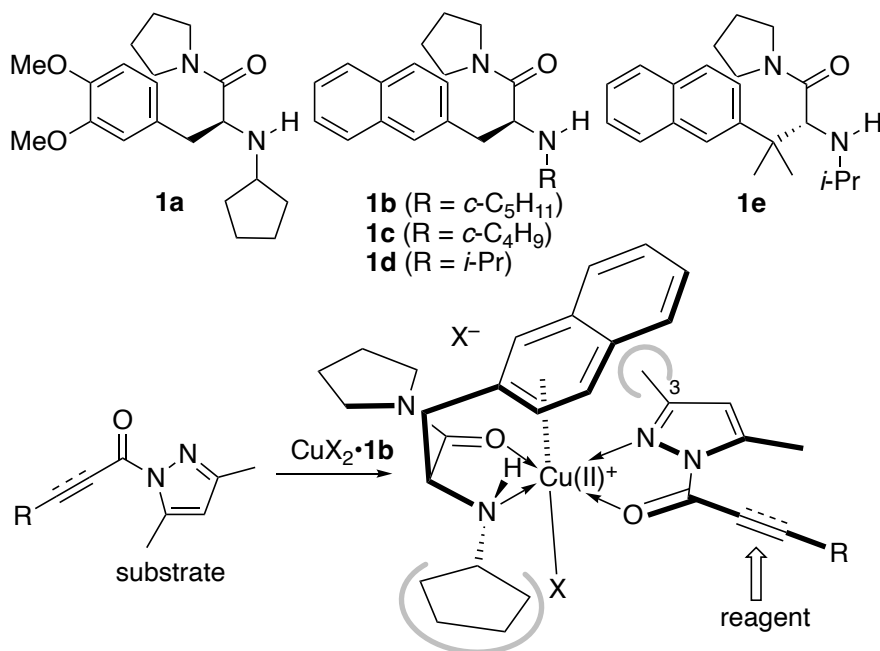
#### Chiral $\pi$ -Cu(II) Catalyst

**Abstract:** The Thorpe–Ingold effect was applied to the design of a chiral ligand of  $\pi$ -copper(II) catalysts for the enantioselective  $\alpha$ -fluorination of *N*-acyl-3,5-dimethylpyrazoles, and also for the enantioselective Mukaiyama–Michael, Diels–Alder, and 1,3-dipolar cycloaddition reactions of *N*-acryloyl-3,5-dimethylpyrazoles. The use of  $\beta,\beta$ -dimethyl- $\beta$ -arylalanine-type ligand gave desired products with higher enantioselectivity compared to with previously reported  $\beta$ -arylalanine-type ligands.

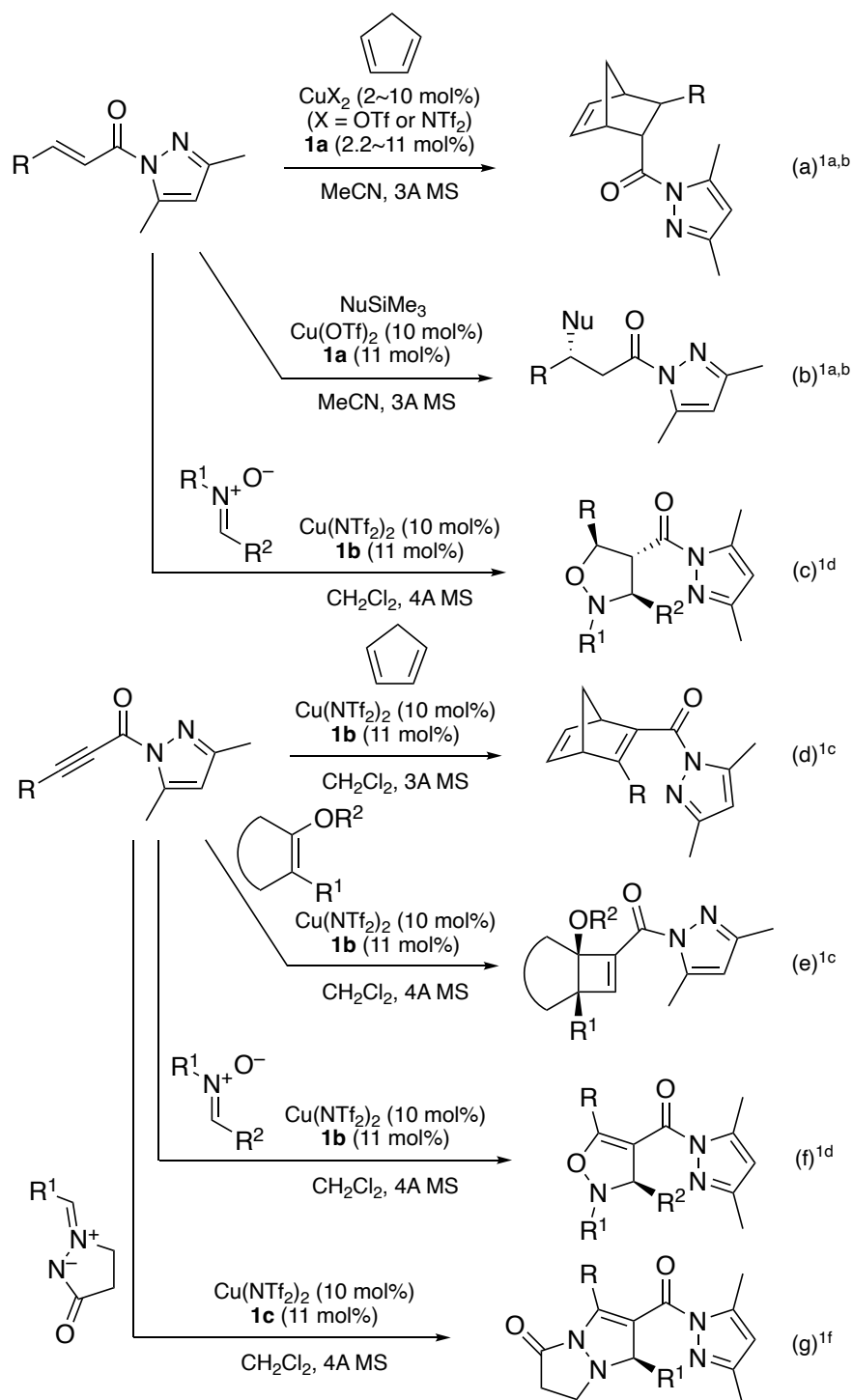
### 3-1. Introduction

L-Amino acids are readily available as natural chiral sources of chiral ligands. Since 2006, we have developed several enantioselective reactions of unsaturated *N*-acyl-3,5-dimethylpyrazoles catalyzed by chiral Lewis acids that are prepared *in situ* from copper(II) salts and chiral amino acid derived  $\alpha$ -aminoamide ligands **1** (Schemes 1 and 2).<sup>1,2</sup> From the perspective of “chiral economy”, chiral amino acid-derived  $\alpha$ -aminoamide ligands **1**, which have a single chiral center, are superior to chiral ligands, which basically include two or more chiral centers, like C<sub>2</sub>- or C<sub>3</sub>-symmetric ligands. Although the side chain of **1** is conformationally flexible by itself, the  $\pi$ -copper(II) interaction between a copper(II) cation and the aromatic ring of the side chain can control the conformation of the side chain to construct an effective asymmetric environment around the copper(II) cation. Furthermore, the Lewis acidity of the copper(II) center is enhanced when X<sup>-</sup> leaves the copper(II) center through  $\pi$ -copper(II) interaction.

**Scheme 1.** Chiral  $\alpha$ -Aminoamide Ligands **1** and  $\pi$ -Copper(II) Complex CuX<sub>2</sub>•**1b**



**Scheme 2.** Chiral  $\pi$ -Copper(II) Complex-Catalyzed Enantioselective Reactions<sup>1</sup>



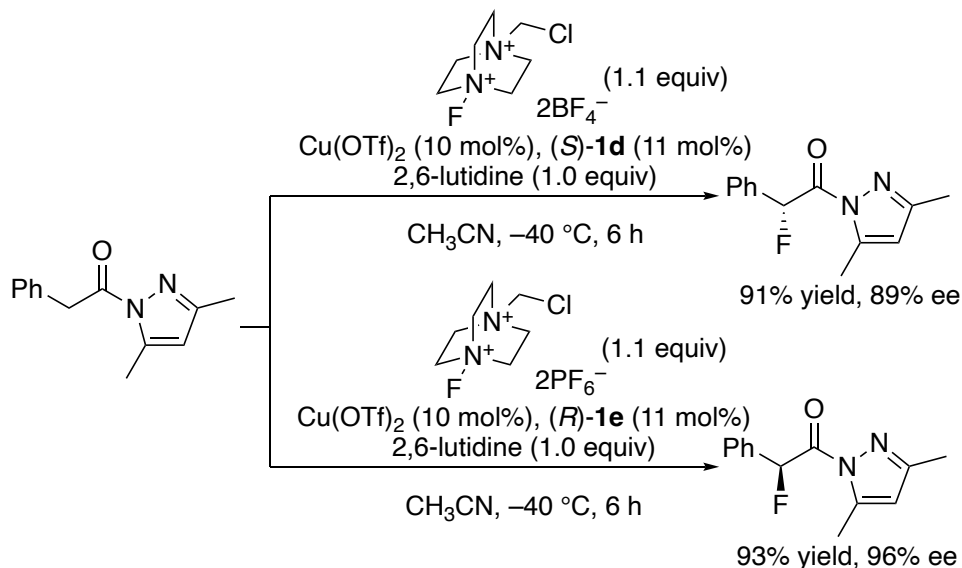
**3-2. Results and Discussion**

In 2020, we developed an enantioselective  $\alpha$ -fluorination of  $\alpha,\beta$ -saturated *N*-acyl-3,5-dimethylpyrazoles with Selectfluor catalyzed by Cu(OTf)<sub>2</sub>•**1d**.<sup>3</sup> For example, the corresponding  $\alpha$ -fluorinated product could be obtained from *N*-phenylacetyl-3,5-dimethylpyrazole in 91% yield with 89% ee. Interestingly, the enantioselectivity was improved to 96% ee with the use of **1e** in place of



**1d** under similar conditions (Scheme 3). In the case of  $\text{Cu}(\text{OTf})_2 \cdot \mathbf{1e}$ , the folded  $\pi$ -copper(II) complex structure might be more stabilized by the Thorpe–Ingold effect.<sup>4</sup>

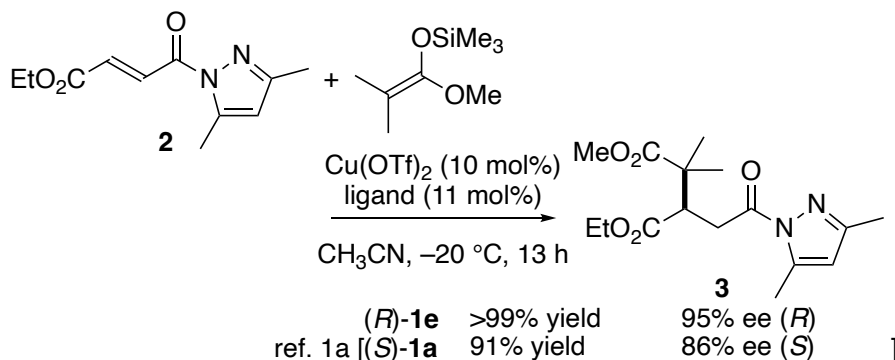
**Scheme 3.** Chiral  $\pi$ -Copper(II) Complex-Catalyzed Enantioselective  $\alpha$ -Fluorination<sup>3</sup>



To ascertain the generality of the effectiveness of **1e** as a chiral ligand of  $\pi$ -copper(II) catalyst, **1e** was examined for use in several different types of reactions of *N*-acryloyl-3,5-dimethylpyrazoles.

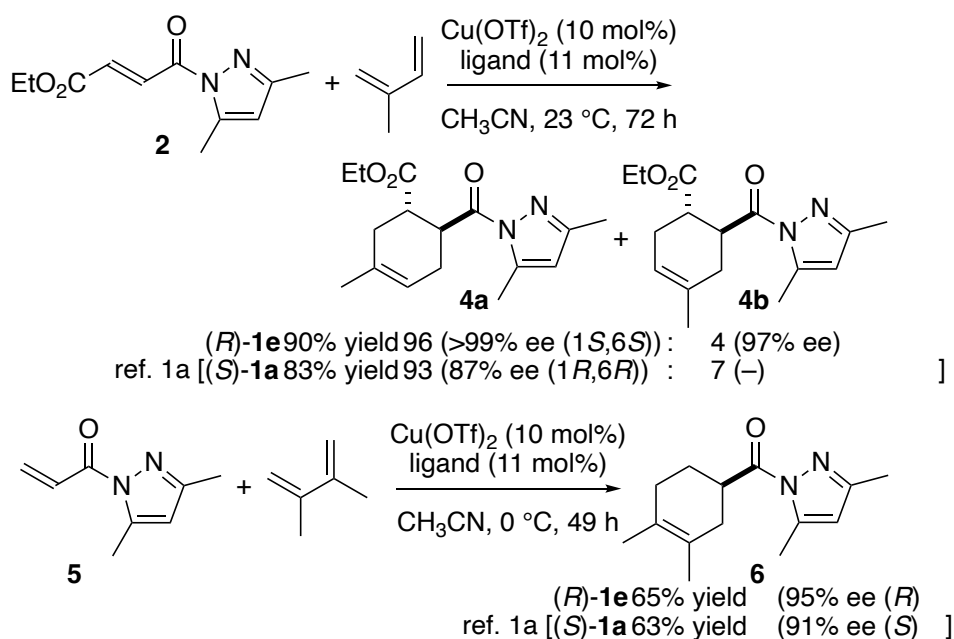
The enantioselective Mukaiyama–Michael reaction of *N*-[ $\beta$ -(ethoxycarbonyl)acryloyl]-3,5-dimethylpyrazole **2** with ketene trimethylsilyl acetal was carried out in the presence of 10 mol% of  $\text{Cu}(\text{OTf})_2 \cdot (\text{R})\text{-1e}$ . As expected, the enantioselectivity of product **3** was improved to 95% ee in comparison with the previous result (86% ee,  $\text{Cu}(\text{OTf})_2 \cdot (\text{S})\text{-1a}$ )<sup>1a</sup> (Scheme 4).

**Scheme 4.** Chiral  $\pi$ -Copper(II) Complex-Catalyzed Enantioselective Mukaiyama–Michael Reaction of **2**



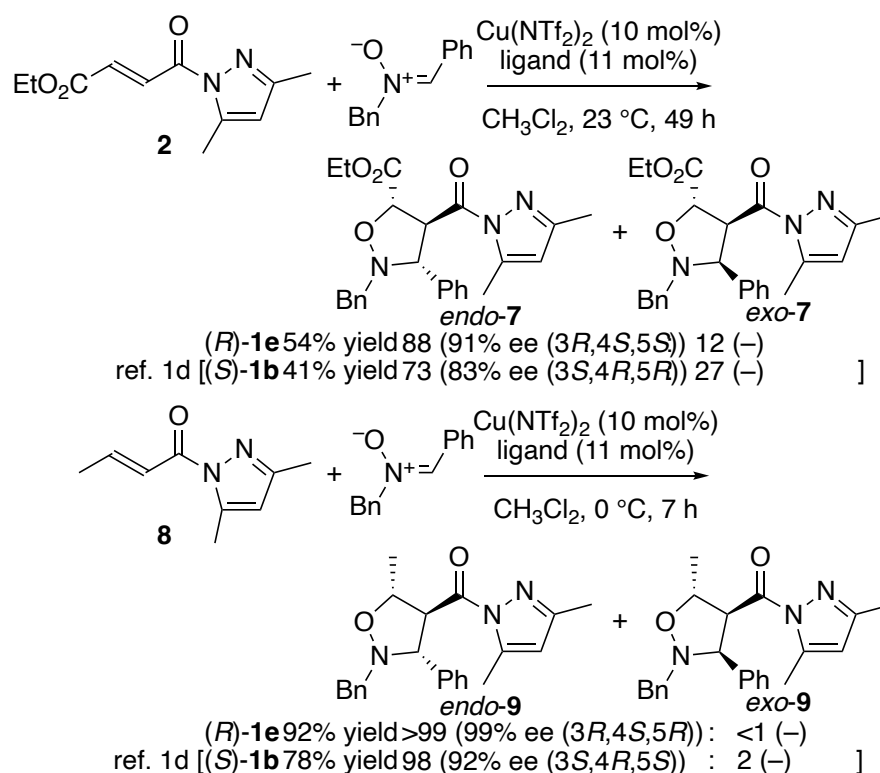
Next, the enantioselective Diels–Alder reaction of **2** with isoprene was carried out in the presence of 10 mol% of  $\text{Cu(OTf)}_2 \cdot (\textit{R})\text{-1e}$ . As expected, the enantioselectivity of product **4a** was improved to >99% ee in comparison with the previous result (87% ee,  $\text{Cu(OTf)}_2 \cdot (\textit{S})\text{-1a}$ )<sup>1a</sup> (Scheme 5). Interestingly, the regioselectivity (**4a** : **4b**) was also improved from 93 : 7 to 96 : 4. The ligand effect of (*R*)-**1e** was also ascertained for the Diels–Alder reaction of *N*-acryloyl-3,5-dimethylpyrazole **5** with 2,3-dimethylbutadiene (Scheme 5).

**Scheme 5.** Chiral  $\pi$ -Copper(II) Complex-Catalyzed Enantioselective Diels–Alder Reactions of **2** and **5**



Next, the enantioselective 1,3-dipolar cycloaddition of **2** with nitron was examined in the presence of 10 mol% of  $\text{Cu}(\text{NTf}_2)_2 \cdot (R)\text{-1e}$ . As expected, the enantioselectivity of *endo*-product **7** was improved to 91% ee in comparison with the previous result (83% ee,  $\text{Cu}(\text{NTf}_2)_2 \cdot (S)\text{-1b}$ )<sup>1d</sup> (Scheme 6). Interestingly, the *endo/exo*-selectivity of **7** was also improved from 88 : 12 to 77 : 23. In a similar way, *endo*-product **9** was obtained in quantitative yield with 99% ee from *N*-crotonoyl-3,5-dimethylpyrazole **8** and nitron (Scheme 6).

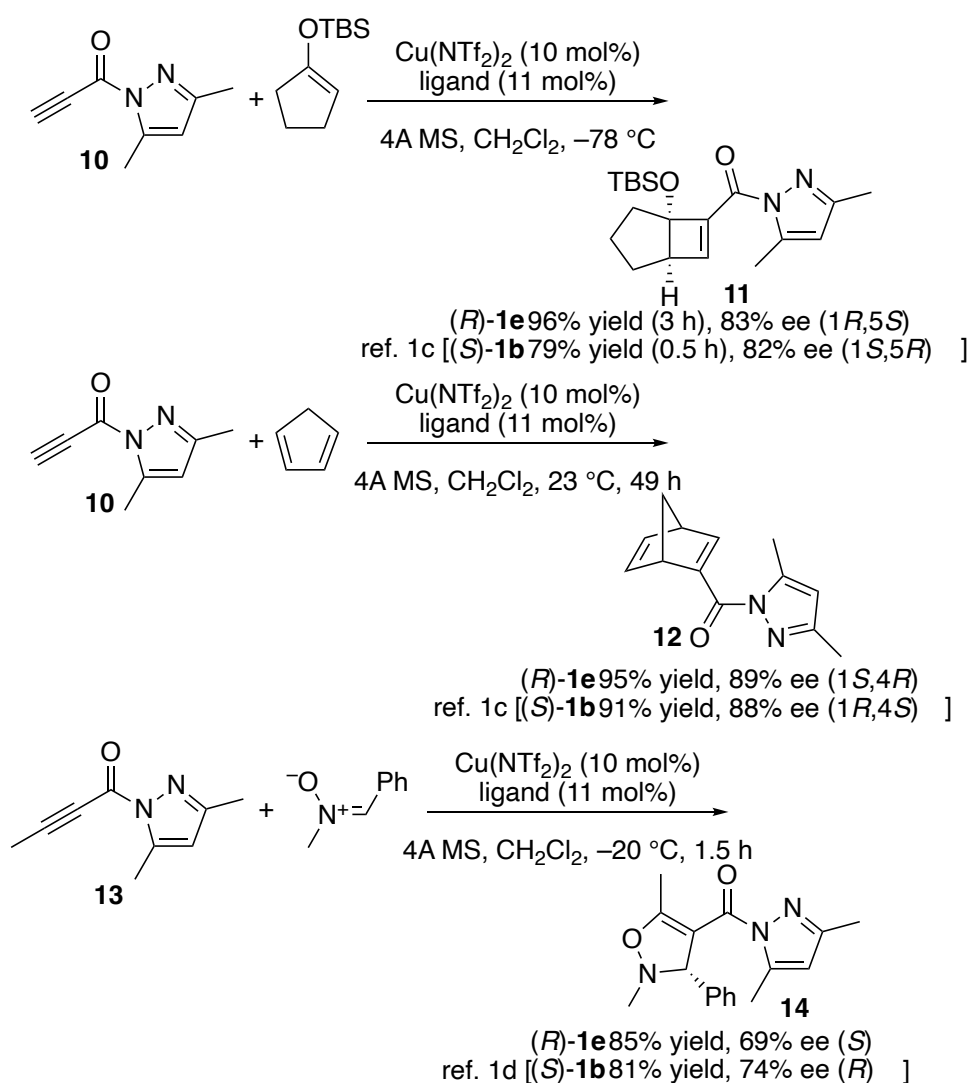
**Scheme 6.** Chiral  $\pi$ -Copper(II) Complex-Catalyzed Enantioselective 1,3-Dipolar Cycloaddition Reactions of **2** and **8** with nitron



Next, we focused on the enantioselective cycloaddition of *N*-propioloyl-3,5-dimethylpyrazoles catalyzed by  $\text{Cu}(\text{OTf})_2 \cdot (R)\text{-1e}$ . However, unexpectedly, the enantioselectivities were not improved in the [2+2] cycloaddition and Diels–Alder reactions of *N*-propioloyl-3,5-dimethylpyrazole **10** (Scheme 7).<sup>1c</sup> The enantioselective 1,3-dipolar cycloaddition of *N*-(but-2-ynoyl)-3,5-dimethylpyrazole **13** with nitron was also examined, but the enantioselectivity was not improved.

(Scheme 7).<sup>1d</sup> In these reactions, if the enantioface discrimination of *N*-propiolyl-3,5-dimethylpyrazoles by Cu(OTf)<sub>2</sub>•(*R*)-**1e** is complete, the enantioselectivity depends on the *endo/exo*-selectivity of nucleophiles. Therefore, the *endo/exo*-selectivity of nucleophiles might be reflected in the enantioselectivity of the cycloadducts. This could be one of the reasons why the Thorpe–Ingold effect of (*R*)-**1e** was not effective for these reactions.

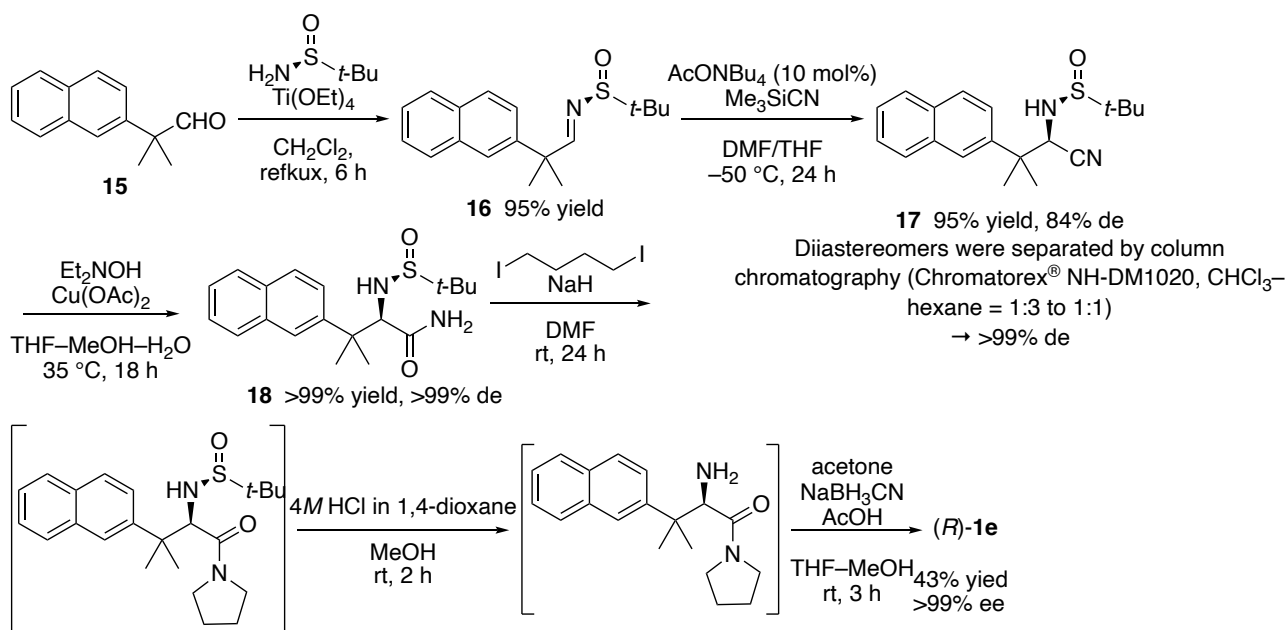
**Scheme 7.** Chiral  $\pi$ -Copper(II) Complex-Catalyzed Enantioselective Cycloaddition Reactions of *N*-Propiolyl-3,5-dimethylpyrazoles **10** and **13**



Chiral ligand **1e** was prepared from 2-methyl-2-(naphthalen-2-yl)propanal (**15**)<sup>5</sup> in 6 steps as shown in Scheme 8.<sup>6</sup> The Strecker reaction of chiral sulfinimine **16** derived from **15** and (*S*)-(-)-*tert*-butylsulfonamide gave  $\alpha$ -amino nitrile **17** with 84% de.<sup>7</sup> Two diastereomers were completely

separated by column chromatography on Chromatorex® NH-DM1020. Hydrolysis of **17** gave primary amide **18** in quantitative yield without epimerization. Thus, **18** was converted to optically pure (*R*)-**1e** in 43% overall yield in three steps.

**Scheme 8.** Preparation of (*R*)-**1e**<sup>3</sup>



### 3-3. Conclusion

In conclusion,  $\beta,\beta$ -dimethyl- $\beta$ -arylalanine-type ligands such as (*R*)-**1e** were more effective than the corresponding  $\beta$ -arylalanine-type ligands such as **1a-d** as chiral ligands for the copper(II) salt-catalyzed enantioselective reactions of *N*-acryloyl-3,5-dimethylpyrazoles due to the conformational stabilization of  $\pi$ -copper(II) complex due to the Thorpe-Ingold effect.

### 3-4. References

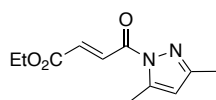
- (1) (1) (a) Ishihara, K.; Fushimi, M. *Org. Lett.* **2006**, *8*, 1921–1924. (b) Ishihara, K.; Fushimi, M. Akakura, M. *Acc. Chem. Res.* **2007**, *40*, 1049–1055. (c) Ishihara, K.; Fushimi, M. *J. Am. Chem. Soc.* **2008**, *130*, 7532–7533. (d) Sakakura, A.; Hori, M.; Fushimi, M.; Ishihara, K. *J. Am. Chem. Soc.* **2010**, *132*, 15550–15552. (e) Sakakura, A.; Ishihara, K. *Chem. Soc. Rev.* **2011**, *40*, 163–172. (f) Hori, M.; Sakakura, A.; Ishihara, K. *J. Am. Chem. Soc.* **2014**, *136*, 13198–13201.
- (2) Yao, L.; Ishihara, K. *Chem. Sci.* **2019**, *10*, 2259–2263.
- (3) Ishihara, K.; Nishimura, K.; Yamakawa, K. *Angew. Chem. Int. Ed.* **2020**, *59*, 17641–17647.
- (4) Beesley, R. M.; Ingold, C. K.; Thorpe, J. F. *J. Chem. Soc. Trans.* **1915**, *107*, 1080–1106.
- (5) (a) Cai, X.; Keshavarz, A.; Omaque, J. D.; Stokes, B. J. *Org. Lett.* **2017**, *19*, 2626–2629. (b) Jørgensen, M.; Lee, S.; Liu, X.; Wolkowski, J. P.; Hartwig, J. F. *J. Am. Chem. Soc.* **2002**, *124*, 12557–12565.
- (6) For the experimental procedures for preparation of (*R*)-**1e**, see ref. 3.
- (7) Li, B.-F.; Yuan, K.; Zhang, M.-J.; Wu, H.; Dai, L.-X.; Wang, Q. R.; Hou, X.-L. *J. Org. Chem.* **2003**, *68*, 6264–6267.

### 3-5. Experimental Section

#### 3-5-1. General methods

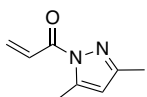
IR spectra were recorded on a JASCO FT/IR-460 plus spectrometer.  $^1\text{H}$  spectra were measured on a JEOL ECS-400 spectrometer (400 MHz) at ambient temperature. Chemical shift in ppm from internal tetramethylsilane (0.00 ppm) in  $\text{CDCl}_3$  on the  $\delta$  scale, multiplicity (s = singlet; d = doublet; t = triplet; m = multiplet), coupling constant (Hz), integration, and assignment.  $^{13}\text{C}$  NMR spectra were measured on a JEOL ECS-400 spectrometer (100 MHz). Chemical shifts were recorded in ppm from the solvent resonance employed as the internal standard ( $\text{CDCl}_3$ : 77.16 ppm). High-performance liquid chromatography (HPLC) analysis was conducted using Shimadzu LC-10 AD coupled diode array-detector SPD-MA-10A-VP and chiral column of Daicel CHIRALCEL AD-H (4.6 mm  $\times$  25 cm), Daicel CHIRALPAK AD-3 (4.6 mm  $\times$  25 cm), Daicel CHIRALPAK ID-3 (4.6 mm  $\times$  25 cm), or Daicel CHIRALPAK OJ-3 (4.6 mm  $\times$  25 cm). For Thin-layer chromatography (TLC) analysis, Merck precoated TLC plates (silica gel 60 F<sub>254</sub> 0.25 mm) was used. Visualization was accomplished by UV light (254 nm). The products were purified by column chromatography on silica gel (E. Merck Art. 9385; Kanto Chemical Co., Inc. 37560). Other materials were obtained from commercial supplies and used without further purification.

### 3-5-2. Characterization of starting materials

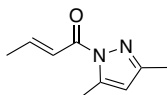


**Ethyl (*E*)-4-(3,5-dimethyl-1*H*-pyrazol-1-yl)-4-oxobut-2-enoate (**2**)**<sup>1</sup>: <sup>1</sup>H NMR (400 MHz,

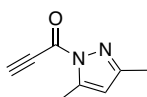
CDCl<sub>3</sub>) δ 8.26 (d, *J* = 15.6 Hz, 1H), 7.01 (d, *J* = 15.6 Hz, 1H), 6.04 (s, 1H), 4.30 (q, *J* = 6.9 Hz, 1H), 2.59 (s, 3H), 2.27 (s, 3H); <sup>13</sup>C NMR (100 MHz, CDCl<sub>3</sub>) δ 165.2, 163.8, 153.0, 144.6, 134.2, 133.7, 112.3, 61.4, 14.5, 14.3, 13.9.



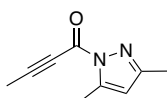
**1-(3,5-Dimethyl-1*H*-pyrazol-1-yl)prop-2-en-1-one (**5**)**<sup>2</sup>: <sup>1</sup>H NMR (400 MHz, CDCl<sub>3</sub>) δ 7.58 (dd, *J* = 17.4, 10.5 Hz, 1H), 6.61 (dd, *J* = 17.4, 0.9 Hz, 1H), 6.00 (s, 1H), 5.99–5.94 (m, 1H), 2.58 (s, 3H), 2.26 (s, 3H); <sup>13</sup>C NMR (100 MHz, CDCl<sub>3</sub>) δ 165.0, 152.3, 144.6, 131.7, 128.4, 111.7, 14.7, 13.9.



**(*E*)-1-(3,5-Dimethyl-1*H*-pyrazol-1-yl)but-2-en-1-one (**8**)**<sup>1</sup>: <sup>1</sup>H NMR (400 MHz, CDCl<sub>3</sub>) δ 7.34–7.16 (m, 2H), 5.98 (s, 1H), 2.57 (s, 3H), 2.26 (s, 3H), 2.01 (dd, *J* = 6.9, 1.4 Hz, 3H); <sup>13</sup>C NMR (100 MHz, CDCl<sub>3</sub>) δ 165.3, 151.9, 146.8, 144.5, 122.7, 111.4, 18.7, 14.8, 13.9.

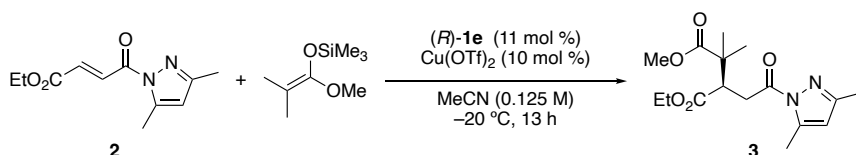


**1-(3,5-Dimethyl-1*H*-pyrazol-1-yl)prop-2-yn-1-one (**10**)**<sup>3</sup>: <sup>1</sup>H NMR (400 MHz, CDCl<sub>3</sub>) δ 6.05 (s, 1H), 3.48 (s, 1H), 2.55 (d, *J* = 0.9 Hz, 3H), 2.30 (s, 3H); <sup>13</sup>C NMR (100 MHz, CDCl<sub>3</sub>) δ 154.8, 151.2, 144.5, 112.6, 82.3, 76.1, 14.1 (2C).



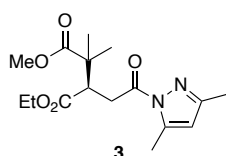
**1-(3,5-Dimethyl-1*H*-pyrazol-1-yl)but-2-yn-1-one (**13**)**<sup>3</sup>: <sup>1</sup>H NMR (400 MHz, CDCl<sub>3</sub>) δ 6.02 (s, 1H), 2.54 (d, *J* = 0.9 Hz, 3H), 2.27 (s, 3H), 2.17 (s, 3H); <sup>13</sup>C NMR (100 MHz, CDCl<sub>3</sub>) δ 153.8, 151.9, 144.0, 111.8, 93.9, 74.2, 14.0, 13.9, 4.7.

### 3-5-3. Procedure for the enantioselective Mukaiyama–Michael Reaction of **2**





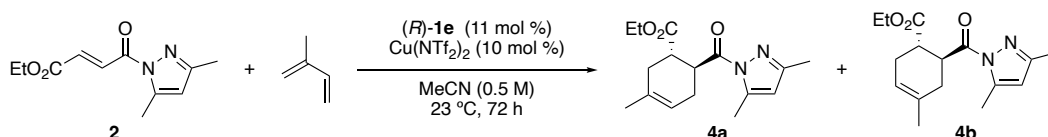
To a mixture of (*R*)-**1e** (11.2 mg, 0.033 mmol) and Cu(OTf)<sub>2</sub> (10.8 mg, 0.030 mmol) in a heat-gun dried 20 mL shlenk flask in MeCN (2.4 mL, dried over activated 4A molecular sieves) were added **2** (66.7 mg, 0.30 mmol) and dimethylketene methyl trimethylsilyl acetal (91 μL, 0.45 mmol) at –20 °C. The reaction mixture was stirred at –20 °C for 13 h. The reaction was quenched with a few drops of triethylamine. The product was washed with saturated aqueous NaHCO<sub>3</sub> solution, extracted with EtOAc, dried over MgSO<sub>4</sub>, filtered and concentrated in vacuo. Purification by chromatography on neutral silica gel (hexane–EtOAc) afforded the desired product **3** (97.1 mg, 100% yield, 95% ee). The ee value was determined by HPLC analysis.



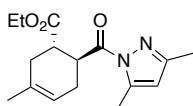
**3**                      4-Ethyl                      1-methyl                      (*R*)-3-(2-(3,5-dimethyl-1*H*-pyrazol-1-yl)-2-oxoethyl)-2,2-

**dimethylsuccinate (3):** <sup>1</sup>H NMR (400 MHz, CDCl<sub>3</sub>) δ 5.94 (s, 1H), 4.23–4.06 (m, 2H), 3.71 (s, 3H), 3.68 (dd, *J* = 18.0, 11.4 Hz, 1H), 3.49 (dd, *J* = 11.4, 2.7 Hz, 1H), 3.12 (dd, *J* = 18.0, 2.7 Hz, 1H), 2.50 (d, *J* = 0.9 Hz, 3H), 2.23 (s, 3H), 1.29 (s, 3H), 1.26 (s, 3H), 1.24 (t, *J* = 7.2 Hz, 3H); <sup>13</sup>C NMR (100 MHz, CDCl<sub>3</sub>) δ 176.8, 172.8, 172.4, 152.2, 144.1, 111.2, 60.9, 52.2, 47.5, 44.0, 33.7, 23.0, 22.9, 14.5, 14.1, 13.9; HPLC analysis; AS-H, *n*-hexane/*i*-PrOH = 9/1, 1.0 mL/min, *t*<sub>R</sub> = 5.0 min (major), *t*<sub>R</sub> = 6.7 min (minor).

### 3-5-4. Procedure for the enantioselective Diels–Alder reaction of **2** and **5**

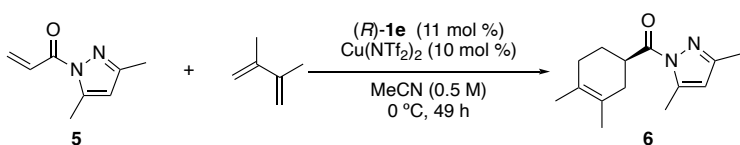


To a mixture of (*R*)-**1e** (11.2 mg, 0.033 mmol) and Cu(NTf<sub>2</sub>)<sub>2</sub> (18.7 mg, 0.030 mmol) in a heat-gun dried 20 mL shlenk flask in MeCN (2.4 mL, dried over activated 4A molecular sieves) were added **2** (66.7 mg, 0.30 mmol) and stirred for 5 min. To the mixture was added isoprene (600 μL, 6.0 mmol) at 23 °C. The reaction mixture was stirred at 23 °C for 72 h. The reaction was quenched with a few drops of triethylamine. The product was washed with saturated aqueous NaHCO<sub>3</sub> solution, extracted with EtOAc, dried over MgSO<sub>4</sub>, filtered and concentrated in vacuo. Purification by chromatography on neutral silica gel (hexane–EtOAc) afforded the desired product **4** (78.5 mg, 90% yield, regioisomeric ratio = 96:4, >99% ee/ 97% ee). Regioisomeric ratio was determined by crude NMR. The ee value was determined by HPLC analysis.

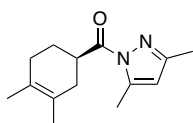


**Ethyl (1*S*,6*S*)-6-(3,5-dimethyl-1*H*-pyrazole-1-carbonyl)-3-methylcyclohex-3-ene-1-**

**carboxylate (4a):**  $^1\text{H}$  NMR (400 MHz,  $\text{CDCl}_3$ )  $\delta$  5.95 (s, 1H), 5.47–5.38 (m, 1H), 4.21–3.99 (m, 3H), 3.07 (dt,  $J$  = 11.4, 5.7 Hz, 2H), 2.68–2.57 (m, 1H), 2.51 (d,  $J$  = 0.9 Hz, 3H), 2.42–2.33 (m, 1H), 2.25–2.03 (m, 2H), 2.23 (s, 3H), 1.71 (s, 3H), 1.18 (t,  $J$  = 7.2 Hz, 3H), 2.23 (s, 3H), 3.08 (quint,  $J$  = 7.8 Hz, 2H);  $^{13}\text{C}$  NMR (100 MHz,  $\text{CDCl}_3$ )  $\delta$  176.6, 175.0, 152.1, 144.1, 132.3, 119.5, 111.3, 60.7, 42.0, 40.9, 32.9, 29.3, 23.1, 14.7, 14.2, 14.0; HPLC analysis; ID-3, *n*-hexane/*i*-PrOH = 99/1, 1.0 mL/min,  $t_{\text{R}}$  = 11.2 min (major, **4b**),  $t_{\text{R}}$  = 13.5 min (major, **4a**),  $t_{\text{R}}$  = 14.8 min (minor, **4a**),  $t_{\text{R}}$  = 20.2 min (minor, **4b**).



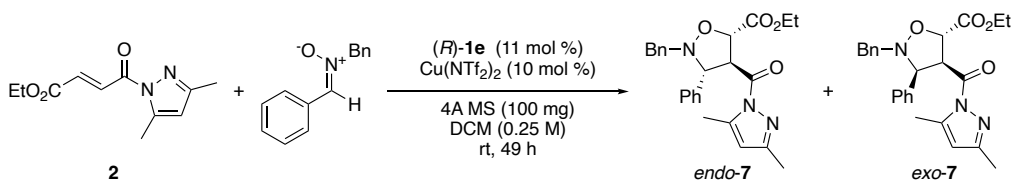
To a mixture of (*R*)-**1e** (11.2 mg, 0.033 mmol) and  $\text{Cu}(\text{NTf}_2)_2$  (18.7 mg, 0.030 mmol) in a heat-gun dried 20 mL shlenk flask in MeCN (1.2 mL, dried over activated 4A molecular sieves) were added **5** (45.1 mg, 0.30 mmol) and stirred for 5 min. To the mixture was added freshly distilled 2,3-dimethylbutadiene (1.2 mL) at 23 °C. The reaction mixture was stirred at 0 °C for 49 h. The reaction was quenched with a few drops of triethylamine. The product was washed with saturated aqueous  $\text{NaHCO}_3$  solution, extracted with EtOAc, dried over  $\text{MgSO}_4$ , filtered and concentrated in vacuo. Purification by chromatography on neutral silica gel (hexane–EtOAc) afforded the desired product **6** (45.0 mg, 65% yield, 95% ee). The ee value was determined by HPLC analysis.



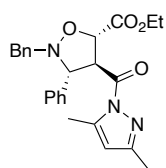
**(*R*)-(3,5-Dimethyl-1*H*-pyrazol-1-yl)(3,4-dimethylcyclohex-3-en-1-yl)methanone (6):**  $^1\text{H}$

NMR (400 MHz,  $\text{CDCl}_3$ )  $\delta$  5.95 (s, 1H), 3.91–3.81 (m, 1H), 2.54 (s, 3H), 2.30–2.11 (m, 2H), 2.23 (s, 3H), 2.05–1.96 (m, 2H), 1.80–1.65 (m, 2H), 1.64 (s, 6H);  $^{13}\text{C}$  NMR (100 MHz,  $\text{CDCl}_3$ )  $\delta$  177.3, 151.8, 144.2, 125.4, 124.1, 111.2, 39.7, 34.3, 31.1, 26.0, 19.1, 19.0, 14.8, 14.0; HPLC analysis; OJ-3, *n*-hexane/*i*-PrOH = 800/1, 1.0 mL/min,  $t_{\text{R}}$  = 7.3 min (minor),  $t_{\text{R}}$  = 8.4 min (major).

**3-5-5. Procedure for the enantioselective 1,3-dipolar cycloaddition of 2 and 8 with nitrene**

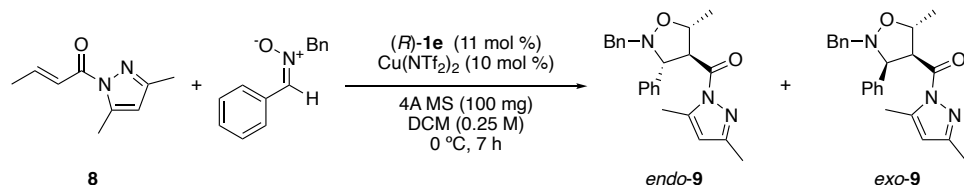


A mixture of (*R*)-**1e** (11.2 mg, 0.033 mmol) and Cu(NTf<sub>2</sub>)<sub>2</sub> (18.7 mg, 0.030 mmol) in a heat-gun dried 20 mL shlenk flask (for in the presence of heat-gun dried powdered 4A molecular sieves (100 mg)) were dissolved in MeCN (0.5 mL, dried over activated 4A molecular sieves) and stirred for 5 min. The solution was concentrated under reduced pressure at room temperature. To the residue were added **2** (66.7 mL, 0.30 mmol), CH<sub>2</sub>CH<sub>2</sub> (1.2 mL), and (*Z*)-*N*-benzyl-1-phenylmethanimine oxide<sup>4</sup> (69.7 mg, 0.33 mmol). The reaction mixture was stirred at rt for 49 h. The reaction mixture was filtered through neutral silica short column (*n*-hexane/EtOAc = 1/1). After evaporation of the organic solvent under reduced pressure, the crude mixture was purified by neutral silica gel column chromatography (*n*-hexane/EtOAc) to give the desired product **7** (70.3 mg, 54% yield, dr = 88:12, 91% ee). Diastereoselective ratio was determined by crude NMR. The ee value was determined by HPLC analysis.



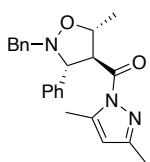
**Ethyl (3*R*,4*S*,5*S*)-2-benzyl-4-(3,5-dimethyl-1*H*-pyrazole-1-carbonyl)-3-phenylisoxazolidine-5-**

**carboxylate (endo-7):** <sup>1</sup>H NMR (400 MHz, CDCl<sub>3</sub>) δ 7.61–7.57 (m, 2H), 7.37–7.29 (m, 4H), 7.29–7.23 (m, 3H), 7.23–7.17 (m, 1H), 5.90 (s, 1H), 5.08 (dd, *J* = 8.2, 4.6 Hz, 1H), 4.78 (d, *J* = 4.1 Hz, 1H), 4.40–4.23 (m, 3H), 4.04 (d, *J* = 15.1 Hz, 1H), 2.52 (s, 3H), 2.04 (s, 3H), 1.32 (t, *J* = 6.9 Hz, 3H); <sup>13</sup>C NMR (100 MHz, CDCl<sub>3</sub>) δ 171.0, 170.5, 152.4, 144.2, 137.7, 137.5, 128.8 (2C), 128.7 (2C), 128.3, 128.2 (2C), 128.2 (2C), 127.0, 111.5, 79.1, 72.5, 61.6, 59.5, 58.8, 14.4, 14.3, 13.8; HPLC analysis; AD-3, *n*-hexane/*i*-PrOH = 9/1, 1.0 mL/min, *t*<sub>R</sub> = 8.6 min (minor), *t*<sub>R</sub> = 14.6 min (major).



A mixture of (*R*)-**1e** (11.2 mg, 0.033 mmol) and Cu(NTf<sub>2</sub>)<sub>2</sub> (18.7 mg, 0.030 mmol) in a heat-gun dried 20 mL shlenk flask (for in the presence of heat-gun dried powdered 4A molecular sieves (100 mg)) were dissolved in MeCN (0.5 mL, dried over 4A molecular sieves) and stirred for 5 min. The solution was concentrated under reduced pressure at room temperature. To the residue were added **8** (49.3 mg, 0.30 mmol), CH<sub>2</sub>CH<sub>2</sub> (1.2 mL), and (*Z*)-*N*-benzyl-1-

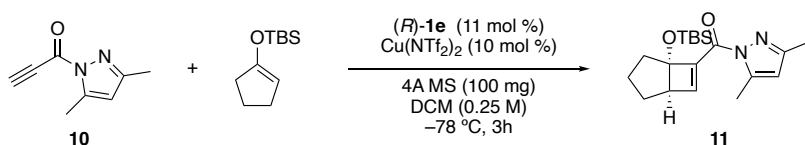
phenylmethanimine oxide<sup>4</sup> (69.7 mg, 0.33 mmol). The reaction mixture was stirred at 0 °C for 7 h. The reaction mixture was filtered through neutral silica short column (*n*-hexane/EtOAc = 1/1). After evaporation of the organic solvent under reduced pressure, the crude mixture was purified by neutral silica gel column chromatography (*n*-hexane/EtOAc) to give the desired product *endo*-**9** (103.6 mg, 92% yield, only *endo* isomer, 99% ee). Diastereoselective ratio was determined by crude NMR.



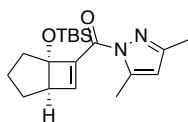
**((3*R*,4*S*,5*R*)-2-Benzyl-5-methyl-3-phenylisoxazolidin-4-yl)(3,5-dimethyl-1*H*-pyrazol-1-**

**yl)methanone (*endo*-**9**):** <sup>1</sup>H NMR (400 MHz, CDCl<sub>3</sub>) δ 7.51 (d, *J* = 7.3 Hz, 2H), 7.39 (d, *J* = 7.3 Hz, 2H), 7.35–7.16 (m, 6H), 5.93 (s, 1H), 4.52 (d, *J* = 7.4 Hz, 1H), 4.46–4.31 (m, 2H), 4.08 (d, *J* = 14.6 Hz, 1H), 3.90 (d, *J* = 14.2 Hz, 1H), 2.55 (s, 3H), 2.14 (s, 3H), 1.69 (d, *J* = 6.0 Hz, 3H); <sup>13</sup>C NMR (100 MHz, CDCl<sub>3</sub>) δ 172.2, 152.3, 144.4, 139.5, 138.3, 128.7 (2C), 128.4 (2C), 128.3 (2C), 128.1 (2C), 127.9, 127.0, 111.6, 78.2, 73.0, 63.7, 59.6, 21.0, 14.6, 13.8; HPLC analysis; AD-3, *n*-hexane/*i*-PrOH = 95/5, 1.0 mL/min, *t*<sub>R</sub> = 6.5 min (minor), *t*<sub>R</sub> = 7.7 min (major).

### 3-5-6. Procedure for the enantioselective cycloaddition reactions of **10** and **13**

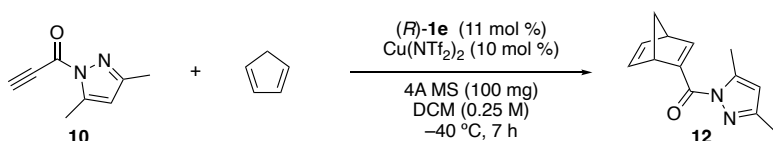


A mixture of (*R*)-**1e** (11.2 mg, 0.033 mmol) and Cu(NTf<sub>2</sub>)<sub>2</sub> (18.7 mg, 0.030 mmol) in a heat-gun dried 20 mL shlenk flask (for in the presence of heat-gun dried powdered 4A molecular sieves (100 mg)) were dissolved in MeCN (0.5 mL, dried over activated 4A molecular sieves) and stirred for 5 min. The solution was concentrated under reduced pressure at room temperature. To the residue were added **10** (44.5 mL, 0.30 mmol), CH<sub>2</sub>CH<sub>2</sub> (1.2 mL), and *tert*-butyl(cyclopent-1-en-1-yloxy)dimethylsilane<sup>5</sup> (238 mg, 1.2 mmol). The reaction mixture was stirred at –78 °C for 3 h. The reaction mixture was filtered through neutral silica short column (*n*-hexane/EtOAc = 1/1). After evaporation of the organic solvent under reduced pressure, the crude mixture was purified by neutral silica gel column chromatography (*n*-hexane/EtOAc) to give the desired product **11** (99.5 mg, 96% yield, 83% ee). The ee value was determined by HPLC analysis.

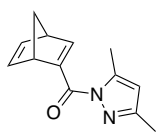


**((1*R*,5*S*)-5-((*tert*-Butyldimethylsilyloxy)bicyclo[3.2.0]hept-6-en-6-yl)(3,5-dimethyl-1*H*-**

**pyrazol-1-yl)methanone (11):** <sup>1</sup>H NMR (400 MHz, CDCl<sub>3</sub>) δ 7.12 (s, 1H), 5.96 (s, 1H), 2.93 (d, *J* = 6.4 Hz, 1H), 2.55 (d, *J* = 0.9 Hz, 3H), 2.33–2.24 (m, 1H), 2.24 (s, 3H), 1.76–1.70 (m, 1H), 1.64–1.36 (m, 4H), 0.86 (s, 9H), 0.06 (s, 3H); <sup>13</sup>C NMR (100 MHz, CDCl<sub>3</sub>) δ 159.9, 152.3, 152.0, 144.7, 140.6, 110.7, 88.6, 54.5, 34.1, 25.9, (3C), 24.9, 23.8, 18.1, 14.6, 14.1, –3.0, –3.1; HPLC analysis; two linear AD-3 columns, *n*-hexane/*i*-PrOH = 800/1, 1.0 mL/min, *t*<sub>R</sub> = 7.6 min (major), *t*<sub>R</sub> = 8.5 min (minor).

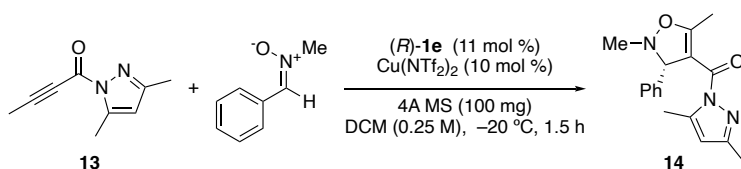


A mixture of (*R*)-**1e** (11.2 mg, 0.033 mmol) and Cu(NTf<sub>2</sub>)<sub>2</sub> (18.7 mg, 0.030 mmol) in a heat-gun dried 20 mL shlenk flask (for in the presence of heat-gun dried powdered 4A molecular sieves (100 mg)) were dissolved in MeCN (0.5 mL, dried over activated 4A molecular sieves) and stirred for 5 min. The solution was concentrated under reduced pressure at room temperature. To the residue were added **10** (44.5 mL, 0.30 mmol), CH<sub>2</sub>CH<sub>2</sub> (1.2 mL), and freshly distilled cyclopentadiene (101 μg, 1.2 mmol). The reaction mixture was stirred at –40 °C for 7 h. The reaction mixture was filtered through neutral silica short column (*n*-hexane/EtOAc = 1/1). After evaporation of the organic solvent under reduced pressure, the crude mixture was purified by neutral silica gel column chromatography (*n*-hexane/EtOAc) to give the desired product **12** (61.3 mg, 95% yield, 89% ee). The ee value was determined by HPLC analysis.

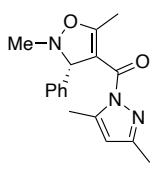


**((1*S*,4*R*)-Bicyclo[2.2.1]hepta-2,5-dien-2-yl)(3,5-dimethyl-1*H*-pyrazol-1-yl)methanone (12):** <sup>1</sup>H

NMR (400 MHz, CDCl<sub>3</sub>) δ 8.17 (d, *J* = 3.7 Hz, 1H), 7.04 (dd, *J* = 4.8, 2.9 Hz, 1H), 6.73 (dd, *J* = 8.2, 4.6 Hz, 1H), 4.10 (d, *J* = 0.9 Hz, 1H), 2.84 (t, *J* = 0.9 Hz, 1H), 2.54 (s, 3H), 2.24 (s, 3H), 2.22 (d, *J* = 6.8 Hz, 1H), 2.10 (d, *J* = 6.4 Hz, 1H); <sup>13</sup>C NMR (100 MHz, CDCl<sub>3</sub>) δ 164.6, 160.8, 151.8, 150.9, 144.8, 144.5, 141.3, 110.7, 72.4, 52.5, 51.9, 14.7, 14.1; HPLC analysis; AD-3, *n*-hexane/*i*-PrOH = 200/1, 1.0 mL/min, *t*<sub>R</sub> = 5.5 min (minor), *t*<sub>R</sub> = 7.3 min (major).



A mixture of (*R*)-**1e** (11.2 mg, 0.033 mmol) and Cu(NTf<sub>2</sub>)<sub>2</sub> (18.7 mg, 0.030 mmol) in 20 mL shlenk flask (for in the presence of heat-gun dried powdered 4A molecular sieves (100 mg)) were dissolved in MeCN (0.5 mL, dried over 4A molecular sieves) and stirred for 5 min. The solution was concentrated under reduced pressure at room temperature. To the residue were added **13** (66.7 mL, 0.30 mmol), CH<sub>2</sub>CH<sub>2</sub> (1.2 mL), and (*Z*)-*N*-methyl-1-phenylmethanimine oxide<sup>4</sup> (48.7 mg, 0.33 mmol). The reaction mixture was stirred at -20 °C for 1.5 h. The reaction mixture was filtered through neutral silica short column (*n*-hexane/EtOAc = 1/1). After evaporation of the organic solvent under reduced pressure, the crude mixture was purified by neutral silica gel column chromatography (*n*-hexane/EtOAc) to give the desired product **14** (75.4 mg, 85% yield, 69% ee). The ee value was determined by HPLC analysis.



**(S)-(3,5-Dimethyl-1H-pyrazol-1-yl)(2,5-dimethyl-3-phenyl-2,3-dihydroisoxazol-4-yl)methanone**

**(14):** <sup>1</sup>H NMR (400 MHz, CDCl<sub>3</sub>) δ 7.26–7.11 (m, 5H), 5.78 (s, 1H), 5.77 (s, 1H), 3.00 (s, 3H), 2.34 (d, *J* = 0.9 Hz), 2.33 (s, 3H), 2.19 (s, 3H); <sup>13</sup>C NMR (100 MHz, CDCl<sub>3</sub>) δ 168.3, 164.8, 150.5, 143.6, 141.4, 128.4 (2C), 127.7, 127.5 (2C), 110.0, 107.2, 47.0, 13.8, 13.7, 13.4; HPLC analysis; AD-3, *n*-hexane/*i*-PrOH = 95/5, 1.0 mL/min, *t*<sub>R</sub> = 5.0 min (major), *t*<sub>R</sub> = 6.5 min (minor).

### 3-5-7. References

1. Kasima, C.; Harada, H.; Kita, I.; Hosomi, A. *Synthesis* **1994**, 61–65.
2. Sibi, M. P.; Miyabe, H. *Org. Lett.* **2002**, *4*, 3435–2438.
3. Brown, R. F. C.; Eastwood, F. W.; Fallon, G. D.; Lee, S. C.; McGearry, R. P. *Aust. J Chem.* **1994**, *47*, 991–1007.
4. Evans, D. A.; Song, H. J.; Fandrick, K. R. *Org. Lett.* **2006**, *8*, 3351–3354.
5. Mander, L. N.; Seti, S. P. *Tetrahedron Lett.* **1984**, *25*, 5953–5956.

## Chapter 4

### A $\pi$ -Cu(II)- $\pi$ Complex as an Extremely Active Catalyst for Enantioselective $\alpha$ -Halogenation of *N*-Acyl-3,5-dimethylpyrazoles

**Abstract:** Novel chiral  $\pi$ -copper(II)- $\pi$  complex-catalyzed enantioselective  $\alpha$ -chlorination and bromination of *N*-acyl-3,5-dimethylpyrazoles are described. The  $\pi$ -copper(II)- $\pi$  complexation of Cu(OTf)<sub>2</sub> with 3-(2-naphthyl)-*L*-alanine-derived amides greatly increases the Lewis acidity, and triggers the *in situ* generation of enolate species without an external base, which has a suppressing effect for  $\alpha$ -chlorination and bromination due to undesired halogen bonding. This strategy provides facile access to  $\alpha$ -halogenated compounds in high yield with excellent enantioselectivity. X-ray crystallographic and ESR analyses of the catalyst complexes suggest that the release of two counter anions (2TfO<sup>-</sup>) from the copper(II) center might be crucial for the efficient activation of *N*-acyl-3,5-dimethylpyrazoles.



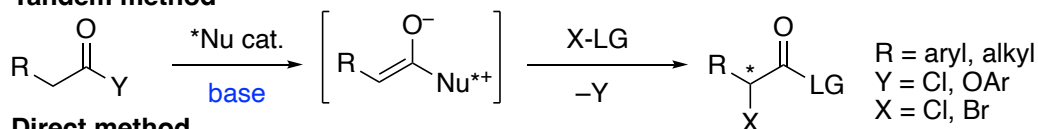
## 4-1. Introduction

Enantioselective carbon–halogen (Cl, Br) bond formations are particularly important due to their potential as synthetic intermediates as well as marine natural products and pharmaceuticals.<sup>1,2</sup> Among the various methods available to build carbon–halogen bonds, the enantioselective electrophilic  $\alpha$ -halogenation of carbonyl compounds is one of the most common. Over the past few decades,  $\alpha$ -halogenation reactions using 1,3-dicarbonyl compounds, aldehydes, and ketones have been well established.<sup>3–5</sup> However, few reports are available on catalytic enantioselective  $\alpha$ -chlorination for carboxylic acid derivatives with  $pK_a$  that are relatively high, and hence it has been considered to be challenging to generate enolate species catalytically.<sup>6</sup> In 2001, Lectka *et al.* reported the cinchona alkaloid-catalyzed enantioselective chlorination<sup>6a,b</sup> and bromination<sup>6a,7</sup>/esterification of acyl chlorides (Tandem method, Scheme 1a). Recently, Waser *et al.* developed a new method using aryl esters in place of acyl chlorides.<sup>6e</sup> In 2009 and 2011, Shibata's group<sup>6c</sup> and Sodeoka's group<sup>6d</sup> independently reported the catalytic enantioselective  $\alpha$ -chlorination of *N*-acylimides (Direct method, Scheme 1a). In 2021, Meggers *et al.* developed the rhodium(III)-catalyzed enantioselective  $\alpha$ -chlorination of *N*-acylpyrazoles with TfCl.<sup>6f</sup> The substrates are limited to *N*-arylacetylimides and corrosive TfCl is needed as a chlorinating reagent in the presence of stoichiometric amounts of base. Despite the notable successes in this area, no highly effective methods have been developed for  $\alpha$ -alkyl-substituted acetyl esters or amides. Most importantly, there have been no successful examples of asymmetric direct  $\alpha$ -bromination reactions for amides or esters.<sup>5</sup>

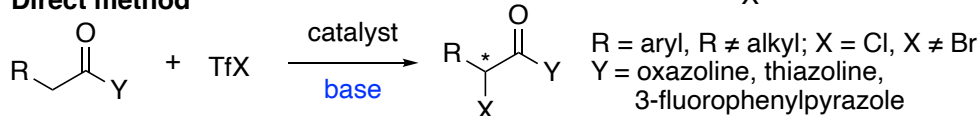
**Scheme 1.** Catalytic Enantioselective  $\alpha$ -Halogenation Reactions of Carboxylic Acid Derivatives

(a) Pioneering works: enantioselective  $\alpha$ -halogenation of carboxylic acid derivatives

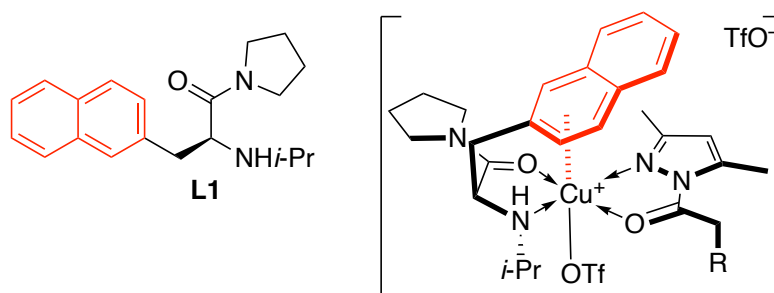
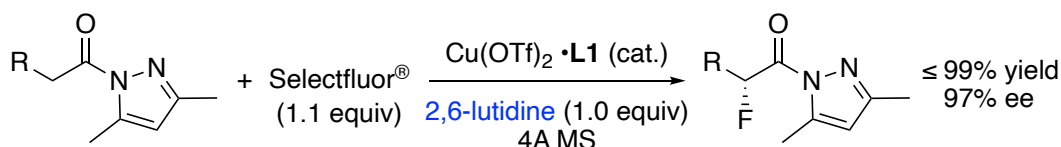
**Tandem method**



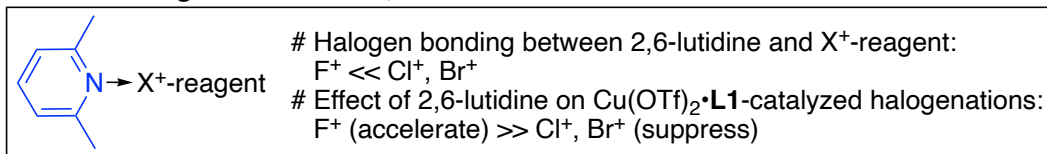
**Direct method**



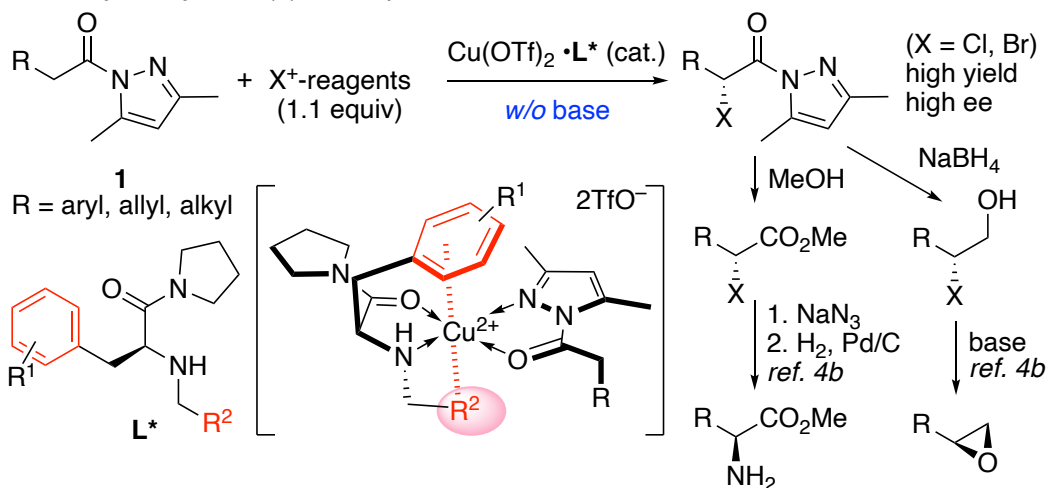
(b) Our previous work: Enantioselective  $\alpha$ -fluorination of *N*-acylpyrazoles catalyzed by  $\pi$ -Cu(II) complexes



**Positive or negative effect of 2,6-lutidine**



(c) **This proposal:** Enantioselective  $\alpha$ -chlorination and bromination of *N*-acylpyrazoles catalyzed by  $\pi$ -Cu(II)- $\pi$  complexes **without base**



Since 2006, we have been interested in  $\pi$ -Cu(II) complexes generated in situ from Cu(OTf)<sub>2</sub> and 3-(2-naphthyl)-L-alanine-derived amides such as **L1** as highly effective chiral Lewis acid catalysts.<sup>8</sup>

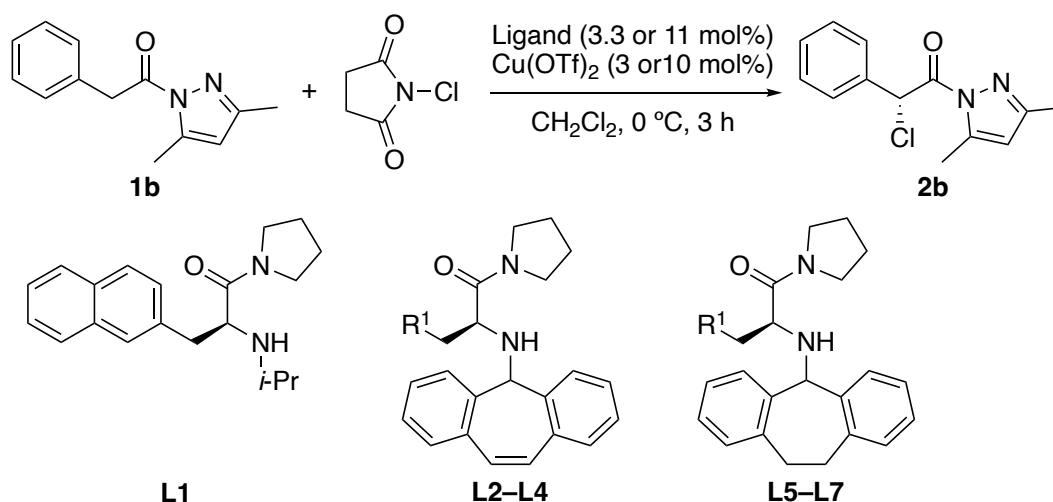
Very recently, we developed the enantioselective  $\alpha$ -fluorination of *N*-acyl-3,5-dimethylpyrazoles **1** catalyzed by chiral  $\pi$ -Cu(II) catalysts in the presence of 2,6-lutidine (Scheme 1b).<sup>9</sup> Mechanistic studies of  $\pi$ -Cu(II) complexes have suggested that the naphthalene moiety of these complexes plays a pivotal role in releasing one counter anion and/or preventing solvents from inactivating the catalysts and thus increasing the Lewis acidity of Cu(II). Inspired by this development, we envisioned that chiral  $\pi$ -Cu(II) catalysts could also promote other halogenation reactions. However, chlorination and bromination were suppressed under the same conditions due to undesired halogen bonding between 2,6-lutidine and X<sup>+</sup>-reagents (X = Cl, Br) (see SI for details).<sup>10</sup> This may be one of the reasons why the development of catalytic enantioselective chlorination and bromination are more difficult than that of enantioselective fluorination. Here we report the enantioselective  $\alpha$ -chlorination and bromination reactions using a novel type of catalytic system (Scheme 1c). We found that the newly designed  $\pi$ -Cu(II)- $\pi$  catalyst was a superior chiral Lewis acid catalyst because two counter anions were released from Cu(II), thus providing the corresponding halogenated carboxamides in high yield with high enantioselectivity without an external base.  $\alpha$ -Halogenated products can be transformed into  $\alpha$ -amino esters and epoxides.<sup>4b</sup>

## 4-2. Results and Discussions

Initial studies on the  $\alpha$ -halogenation reaction were performed with *N*-phenylacetyl-3,5-dimethylpyrazole **1b**, *N*-chlorosuccinimide (NCS), Cu(OTf)<sub>2</sub> (10 mol%), and ligand **L** (11 mol%) in CH<sub>2</sub>Cl<sub>2</sub> at 0 °C for 3 h (Table 1). When we used the previously optimized chiral ligand **L1** in an  $\alpha$ -fluorination reaction in the presence of 2,6-lutidine (1 equiv),<sup>9</sup> the chlorinated product **2b** was formed in low yield with low enantioselectivity (8% yield, 38% ee, entry 1) due to halogen bonding between NCS and 2,6-lutidine. The reaction proceeded more smoothly without 2,6-lutidine (entry 2). Changing the counterion to NTf<sub>2</sub><sup>-</sup> or BF<sub>4</sub><sup>-</sup> also did not effectively promote the reaction (entries 3 and 4).<sup>11</sup> To improve the reactivity and enantioselectivity, we modified the *N*-substituent of the ligand to a sterically demanding 5*H*-dibenzo[*a,d*]cyclo-hepten-5-yl (= trop) group (**L2**). Interestingly, as well as a significant increase in enantioselectivity, a dramatic improvement in reactivity was observed

(90% yield, 96% ee, entry 5). A decrease to 3 mol% catalyst loading resulted in 71% yield. In sharp contrast, the reaction catalyzed by  $\text{Cu}(\text{OTf})_2$  with **L5**, which has an *N*-dibenzosuberyl substituent, gave a moderate yield of **2b** with opposite asymmetric induction (28% yield, -85% ee, entry 9). After screening of the  $\text{R}^1$  group, however, with the decreased reaction rate, 3-indolyl-substituted ligand **L7** gave **2b** with the highest enantioselectivity (78% yield, -97% ee, entry 11). All the ligands with an *N*-dibenzosuberyl group **L5–L7** gave the opposite enantiomer (entries 9–11) whereas ligands bearing an *N*-trop group **L2–L4** always gave **2b** with the same absolute configuration (entries 5–8), indicating that a switch of asymmetric induction was dependent on the difference in the structure of *N*-substituents of the ligand.

**Table 1.** Optimization Studies<sup>a</sup>



entry	Ligand ( $\text{R}^1$ )	<b>2b</b>	
		yield (%) <sup>b</sup>	ee (%) <sup>c</sup>
1 <sup>d</sup>	<b>L1</b> w/ 2,6-lutidine	8	38
2	<b>L1</b> w/o base	54	32
3 <sup>e</sup>	<b>L1</b> w/o base	40	33
4 <sup>f</sup>	<b>L1</b> w/o base	40	34
5	<b>L2</b> (2-naphthyl) w/o base	90 (71) <sup>g</sup>	96 (94) <sup>g</sup>
6 <sup>f</sup>	<b>L2</b> (2-naphthyl) w/o base	85	95

7	<b>L3</b> (phenyl) <i>w/o</i> base	78	65
8	<b>L4</b> (3-indolyl) <i>w/o</i> base	87	68
9	<b>L5</b> (2-naphthyl) <i>w/o</i> base	28	-85
10	<b>L6</b> (phenyl) <i>w/o</i> base	40	-78
11	<b>L7</b> (3-indolyl) <i>w/o</i> base	61 (78) <sup>h</sup>	-93 (-97) <sup>h</sup>

<sup>a</sup> Reactions were performed with **1a** (0.30 mmol), NCS (1.1 equiv), Cu(OTf)<sub>2</sub> (10 mol%), and **L** (11 mol%) in CH<sub>2</sub>Cl<sub>2</sub> (0.2 M) for 3 h at 0 °C. <sup>b</sup> Yields of the isolated **2a**. <sup>c</sup> The ee of **2a** was determined by HPLC analysis. <sup>d</sup> 1.0 equiv of 2,6-lutidine was added. <sup>e</sup> Using Cu(NTf<sub>2</sub>)<sub>2</sub> instead of Cu(OTf)<sub>2</sub>. <sup>f</sup> Using Cu(BF<sub>4</sub>)<sub>2</sub> instead of Cu(OTf)<sub>2</sub>. <sup>g</sup> **1b** (1.5 mmol) was used in the presence of Cu(OTf)<sub>2</sub> (3.0 mol%), **L** (3.3 mol%) and Na<sub>2</sub>SO<sub>4</sub> (100 mg) in CH<sub>2</sub>Cl<sub>2</sub> (1.0 M) for 4 h at 0 °C. <sup>h</sup> In the presence of Na<sub>2</sub>SO<sub>4</sub> (100 mg) and with the reaction time extended to 12 h.

As observed in our previous fluorination reaction catalyzed by the **L1**•Cu(II) complex, the reactivity was greatly influenced by the electron density of the aryl substituent of **L1**. As expected, weak coordination of an aryl group of **L** to Cu(II) was important to release an anionic counterion from Cu(II) and increase the Lewis acidity. Thus, the *in situ*-generated π–Cu(II)–π complex behaved as a fairly active catalyst. To ascertain the π–Cu(II)–π effect, the performance of the ligands was monitored by <sup>1</sup>H NMR analysis, which provided the time-on-stream dependence yield of the chlorinated product **2b** (Fig. 1). Interestingly, **L2** provided the highest catalytic activity over **L1**, **L8**, and **L9**.<sup>12</sup> Importantly, the catalytic activity with **L1** was almost the same as that with **L8**, suggesting that the *N*-trop group of the ligand plays the same role as the aryl group in the complexes. The lowest catalytic activity was observed with **L9**, which has neither an aryl moiety nor an *N*-trop group, thereby highlighting the importance of π–Cu(II) interaction for the activation of Lewis acidity. In addition, the enantioselectivity was low when **L8** and **L9** were used: **L8**, 7 h: **2b** (18% ee); **L9**, 16 h: **2b** (8% ee).

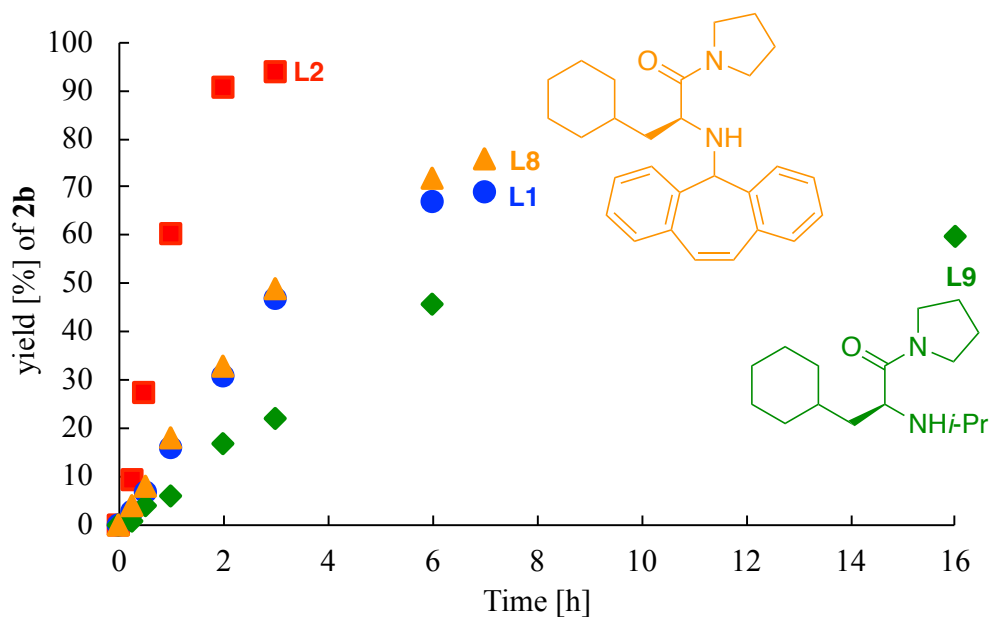
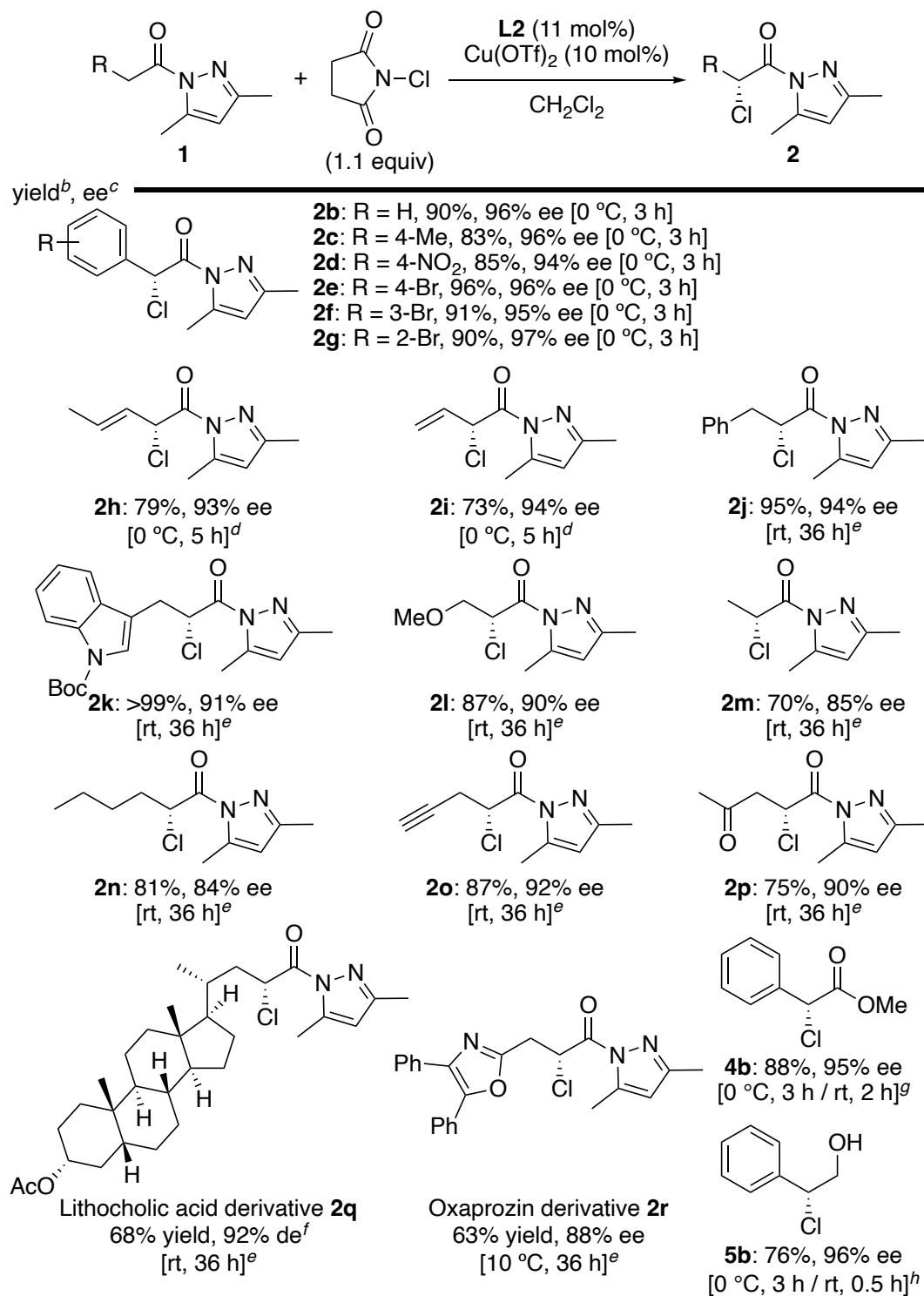


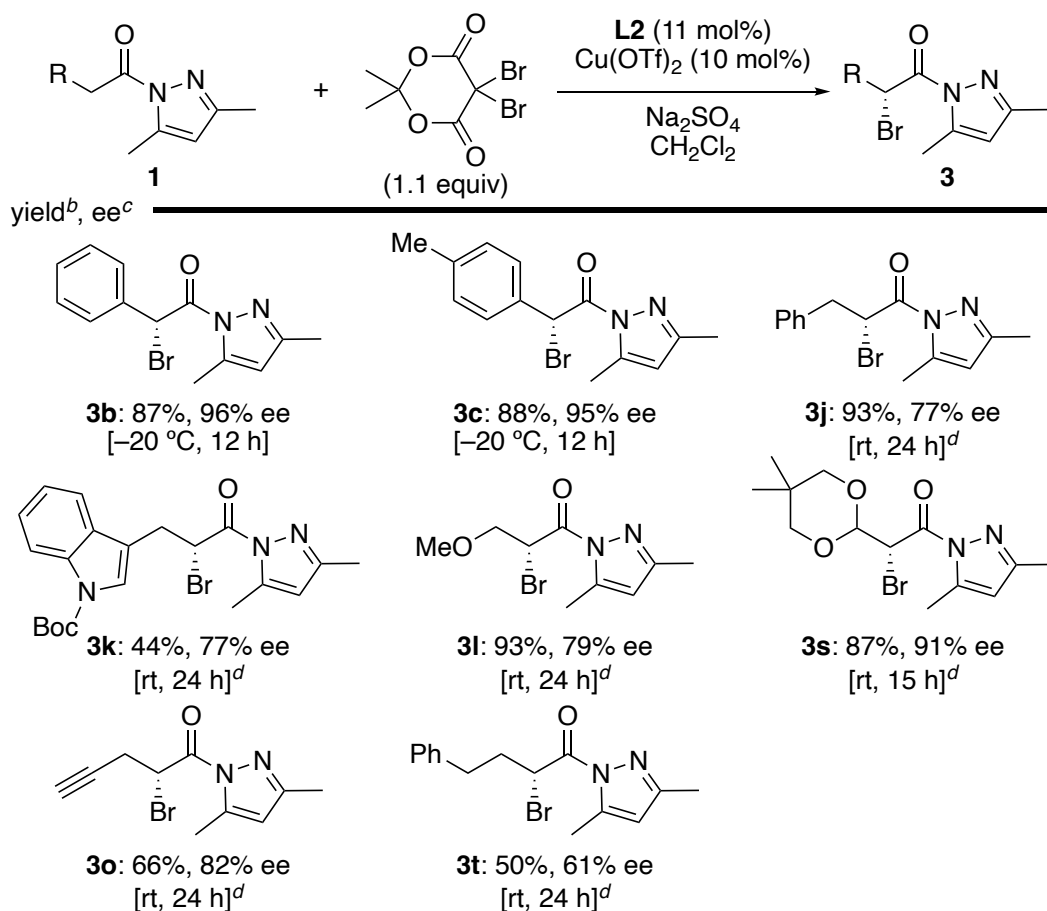
**Figure 1.** Reaction progress analysis of Cu(OTf)<sub>2</sub>•L (10 mol%)-catalyzed  $\alpha$ -chlorination of **1b** with NCS in CH<sub>2</sub>Cl<sub>2</sub> at 0 °C

With the optimal conditions in hand, we demonstrated the generality of the enantioselective  $\alpha$ -chlorination reaction of *N*-acyl-3,5-dimethylpyrazoles **1** (Table 2). Either electron-donating or electron-withdrawing substituents at the phenyl group of **1b–1g** were well tolerated, regardless of their position, and gave **2b–2g** in high yield with high enantioselectivity. Regio- and enantioselective chlorination of **1h** and **1i** (R = alkenyl) occurred at the  $\alpha$ -position to give **2h** and **2i** in good yields with excellent enantioselectivity. Gratifyingly, the chlorination of **1j–1o** (R = CH<sub>2</sub>R', R' = phenyl, indolyl, and methoxy groups) also proceeded well to give **2j–2o** in high yield with high enantioselectivity. To the best of our knowledge, this is the first example of the use of carboxylic acid derivatives for the generation of enolate species without a base. While keeping other carbonyl groups intact, regio- and enantioselective  $\alpha$ -chlorination of **1p** proceeded well. More pharmaceutically relevant Lithocolic acid derivative **1q** and Oxaprozin derivative **1r** were tolerated, albeit the yield was slightly low. The absolute configuration of **2b** was determined to be *R* based on a comparison of the optical rotation with the reported data.<sup>13</sup> It was ascertained that product **2b** could be transformed into the corresponding ester **4b** and alcohol **5b** without racemization.

**Table 2.** Scope of the Enantioselective  $\alpha$ -Chlorination Reaction<sup>a</sup>



<sup>a</sup> Reactions were performed with **1** (0.30 mmol), NCS (1.1 equiv), Cu(OTf)<sub>2</sub> (10 mol%), and **L2** (11 mol%) in CH<sub>2</sub>Cl<sub>2</sub> (0.2 M). <sup>b</sup> Isolated yield. <sup>c</sup> The ee of **2** determined by HPLC analysis. <sup>d</sup> In the presence of Na<sub>2</sub>SO<sub>4</sub> (100 mg). <sup>e</sup> CH<sub>2</sub>Cl<sub>2</sub> (0.5 M) with 4A MS (100 mg). <sup>f</sup> The de of **2q** determined by NMR analysis. <sup>g</sup> One-pot transesterification from **1b** via **2b** was carried out at rt for 1 h by addition of MeOH after  $\alpha$ -chlorination (3 h at 0 °C). <sup>h</sup> Reduction of crude **2b**, which was obtained by  $\alpha$ -chlorination (3 h at 0 °C), with NaBH<sub>4</sub> was carried out at rt for 0.5 h in THF/H<sub>2</sub>O.

**Table 3.** Scope of the Enantioselective  $\alpha$ -Bromination Reaction<sup>a</sup>

<sup>a</sup> Reactions were performed with **1** (0.30 mmol), 5,5-dibromomeldrum's acid (1.1 equiv),  $\text{Cu}(\text{OTf})_2$  (10 mol%), **L2** (11 mol%) and  $\text{Na}_2\text{SO}_4$  (100 mg) in  $\text{CH}_2\text{Cl}_2$  (0.2 M). <sup>b</sup> Isolated yield. <sup>c</sup> The ee of **3** determined by HPLC analysis. <sup>d</sup>  $\text{CH}_2\text{Cl}_2$  (0.5 M).

Subsequently, we investigated the possibility of applying our strategy to the  $\alpha$ -bromination reaction of *N*-acyl-3,5-dimethylpyrazoles **1**. When *N*-bromosuccinimide (NBS) was used in place of NCS, enantioselectivity was unexpectedly low probably due to partial decomposition of **L2**. After the systematic evaluation of electrophilic brominating reagents, we found that 5,5-dibromomeldrum's acid was usable in the presence of anhydrous  $\text{Na}_2\text{SO}_4$  (see SI for details).<sup>14</sup> As with the chlorination reaction, enantioselective  $\alpha$ -bromination proceeded to give the corresponding products **3** in good to excellent yields and enantioselectivities without a base (Table 3).  $\alpha$ -Aryl-substituted products **3b** and **3c** were well tolerated. Hetero-aromatic product **3k** and other electron-withdrawing substituents at the  $\alpha$ -position **3j**, **3l**, **3s**, and **3o** were also obtained. However, moderate



yield and moderate enantioselectivity were observed in the reaction of **1t**. As shown in Figure 1, the naphthalene ring, *N*-5-benzosuberyl-substituted group, and *N*-trop group were shown to be crucial for increasing the reactivity.

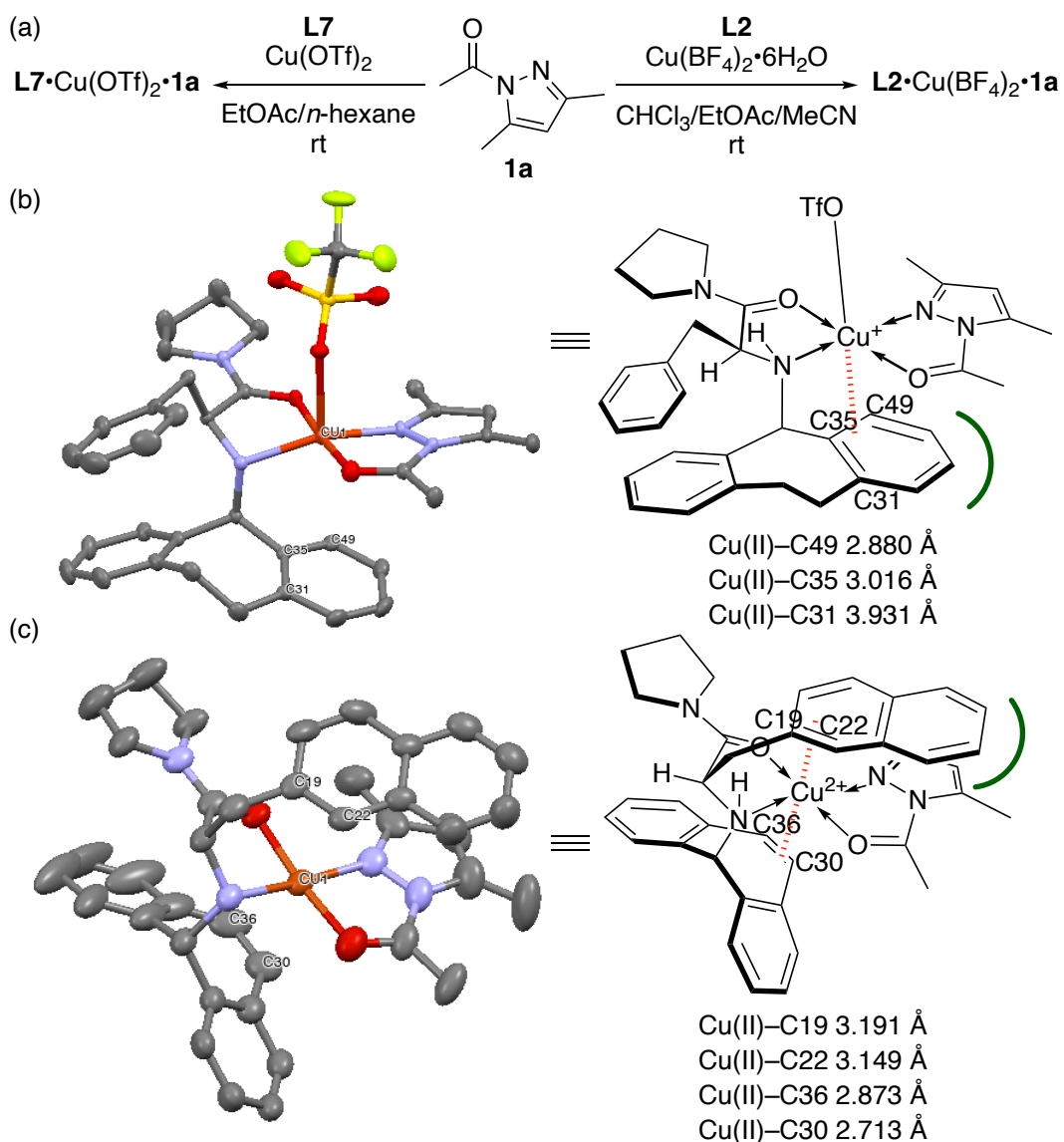


**Figure 2.** (a) The generation of 1:1:1 complexes of **L7**·Cu(OTf)<sub>2</sub>·**1a** and **L2**·Cu(BF<sub>4</sub>)<sub>2</sub>·**1a**. (b) X-ray analysis of **L7**·Cu(OTf)<sub>2</sub>·**1a**. Hydrogen atoms, solvent, and free <sup>-</sup>OTf are omitted for clarity. (c) X-ray analysis of **L2**·Cu(BF<sub>4</sub>)<sub>2</sub>·**1a**. Hydrogen atoms, solvent, and free counterions are omitted for clarity.

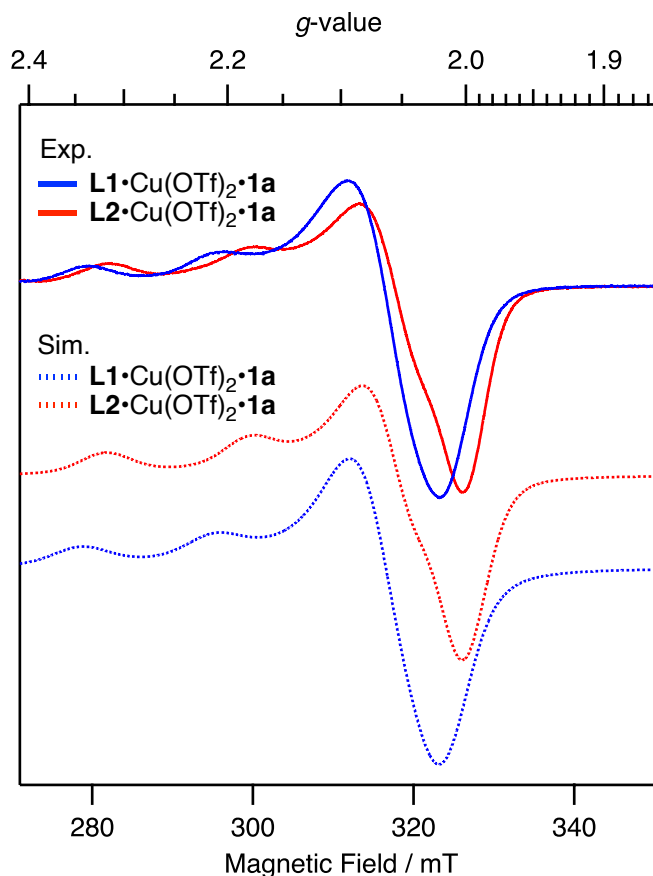


**Figure 2.** ESR spectra (experiments & simulations) of **L7•Cu(OTf)<sub>2</sub>•1a** and **L2•Cu(OTf)<sub>2</sub>•1a** at 30 K.

To get a better understanding of the role of each substituent, we tried to determine the crystal structure of the copper complexes (Fig. 2a). Successfully, we obtained a single crystal of the 1:1:1 complex of **L7•Cu(OTf)<sub>2</sub>•1a** (Fig. 2b). X-ray crystallographic analysis indicated that one side of the aryl moiety of the *N*-5-benzosuberyl-substituted group seems close to the copper center and its distance was around 3 Å, which is considered to be due to  $\pi$ -copper interaction.<sup>15</sup> We believe this interaction is important for both catalytic activity and asymmetric induction. The switch in stereoselectivity in the chlorination reaction using **L5–L7** was consistent with this crystal structure. After an enormous amount of effort, we also succeeded in determining the X-ray crystallographic structure of **L2•Cu(BF<sub>4</sub>)<sub>2</sub>•1a**. Surprisingly, we observed close contact between the copper center and the carbon–carbon double bond of the *N*-trop group, less than 3 Å, as well as  $\pi$ -copper interaction between the naphthyl group and copper.<sup>16</sup> The larger  $\pi$ -face of a naphthyl group than an *N*-trop

group, which is bent against copper, effectively shields the upper face of the  $\alpha$ -carbon of **1b**.

To obtain structural information of copper complexes in a solution state, ESR spectra of **L1**•Cu(OTf)<sub>2</sub>•**1a** and **L2**•Cu(OTf)<sub>2</sub>•**1a** in MeCN at 30 K and simulated spectra are shown in Figure 3. Each experimental spectrum was reproduced with different ESR parameters of axially symmetric *g*-values and hyperfine coupling constants as shown in Table S6. These parameters indicate that the coordination structure of **L2**•Cu(OTf)<sub>2</sub>•**1a** changes from tetrahedrally distorted (6-coordinate) of **L1**•Cu(OTf)<sub>2</sub>•**1a** to axially-coordinate square planar (6-coordinate) depending on two different ligands at the apical position: naphthyl group and <sup>-</sup>OTf.<sup>17</sup>

#### 4-3. Conclusiuon

In summary, we have developed the catalytic enantioselective  $\alpha$ -chlorination and bromination of *N*-acyl-3,5-dimethylpyrazoles. With a newly designed highly active  $\pi$ -Cu(II)- $\pi$  complex, the halogenation reaction of *N*-acyl-3,5-dimethylpyrazoles can be performed using carboxylic acid derivatives with or without an electron-withdrawing group at the  $\alpha$ -position without an external base, which has a suppressing effect due to undesired halogen bonding. X-ray crystallographic analysis of copper complexes and ESR analysis revealed the existence of  $\pi$ -Cu(II)- $\pi$  interaction, which is essential for increasing the reactivity.

#### 4-4. References

- (1) For reviews of chloro-containing drug discovery. Fang, W.-Y.; Ravindar, L.; Rakesh, K. P.; Manukumar, H. M.; Shantharam, C. S.; Alharbi, N. S.; Qin, H.-L. *Eur. J. Med. Chem.* **2019**, *173*, 117–153.
- (2) For selected examples of total synthesis, see: (a) MaGee, D. I.; Mallais, T.; Strunz, G. M. *Can. J. Chem.* **2004**, *82*, 1686–1691. (b) Bardhan, S.; Schmitt, D. C.; Porco, J. A., Jr. *Org. Lett.* **2006**, *8*, 927–930. (c) Britton, R.; Kang, B. *Nat. Prod. Rep.*, **2013**, *30*, 227–236.
- (3) For reviews of catalytic enantioselective  $\alpha$ -chlorination, see: Shibatomi, K.; Narayama, A. *Asian J. Org. Chem.* **2013**, *2*, 812–823.
- (4) For selected examples of  $\alpha$ -chlorination of reactive carbonyl compounds, see: (a) Brochu, M. P.; Brown, S. P.; MacMillan, D. W. C. *J. Am. Chem. Soc.* **2004**, *126*, 4108–4109. (b) Halland, N.; Braunton, A.; Bachmann, S.; Marigo, M.; Jørgensen, K. A. *J. Am. Chem. Soc.* **2004**, *126*, 4790–4791. (c) Marigo, M.; Bachmann, S.; Halland, N.; Braunton, A.; Jørgensen, K. A. *Angew. Chem. Int. Ed.* **2004**, *43*, 5507–5510. (d) Bernardi, L.; Jørgensen, K. A. *Chem. Commun.* **2005**, 1324–1326. (e) Shibata, N.; Kohno, J.; Takai, K.; Ishimaru, T.; Nakamura, S.; Toru, T.; Kanemasa, S. *Angew. Chem. Int. Ed.* **2005**, *44*, 4204–4207. (f) Frings, M.; Bolm, C. *Eur. J. Org. Chem.* **2009**, 4085–4090. (g) Cai, Y.; Wang, W.; Shen, K.; Wang, J.; Hu, X.; Lin, L.; Liu, X.; Feng, X. *Chem. Commun.* **2010**, *46*, 1250–1252. (h) Jiang, J.-J.; Huang, J.; Wang, D.; Yuan, Z.-L.; Zhao, M.-X.; Wang, F.-J.; Shi, M. *Chirality* **2011**, *23*, 272–276. (i) Shibatomi, K.; Soga, Y.; Narayama, A.; Fujisawa, I.; Iwasa, S. *J. Am. Chem. Soc.* **2012**, *134*, 9836–9839. (j) Liu, R. Y.; Wasa, M.; Jacobsen, E. N. *Tetrahedron Lett.* **2015**, *56*, 3428–3430. (k) Shibatomi, K.; Kitahara, K.; Sasaki, N.; Kawasaki, Y.; Fujisawa, I.; Iwasa, S. *Nat. Commun.* **2017**, *8*, 15600. (l) Ponath S.; Menger, M.; Grothues, L.; Webwe, M.; Lentz, D.; Strohmman, C.; Christmann, M. *Angew. Chem. Int. Ed.* **2018**, *57*, 11683–11687. (m) Guan, X.; An, D.; Liu, G.; Zhang, H.; Gao, J.; Zhou, T.; Zhang, G.; Zhang, S. *Tetrahedron Lett.* **2018**, *59*, 2418–2421. (n) Hutchinson, G.; Alamillo-Ferrer, C.; Burés, J. *J. Am. Chem. Soc.* **2021**, *143*, 6805–6809.
- (5) For the enantioselective  $\alpha$ -bromination of aldehydes, see: (a) Bertelsen, S.; Halland, N.;

- Bachmann, S.; Marigo, M.; Braunton, A.; Jørgensen, K. A. *Chem. Commun.* **2005**, 4821–4823.
- (b) Kano, T.; Shirozu, F.; Maruoka, K. *Chem. Commun.* **2010**, 46, 7590–7592. (c) Takeshima, A.; Shimogaki, M.; Kano, T.; Maruoka, K. *ACS Catal.* **2020**, 10, 5959–5963.
- (6) For the enantioselective  $\alpha$ -chlorination of carboxylic acid derivatives, see: (a) Wack, H.; Taggi, A. E.; Hafez, A. M.; Drury, W. J.; Lectka, T. *J. Am. Chem. Soc.* **2001**, 123, 1531–1532. (b) France, S.; Wack, H.; Taggi, A. E.; Hafez, A. M.; Wagerle, T. R.; Shah, M. H.; Dusich, C. L.; Lectka, T. *J. Am. Chem. Soc.* **2004**, 126, 4245–4255. (c) Reddy, D. S.; Shibata, N.; Horikawa, T.; Suzuki, S.; Nakamuwa, S.; Toru, T.; Shiro, M. *Chem. Asian. J.* **2009**, 4, 1411–1415. (d) Hamashima, Y.; Nagi, T.; Shimizu, R.; Tsuchimoto, T.; Sodeoka, M. *Eur. J. Org. Chem.* **2011**, 3675–3578. (e) Stockhammer, L.; Weinzierl, D.; Bögl, T.; Waser, M. *Org. Lett.* **2021**, 23, 6143–6147. (f) Grell, Y.; Xie, X.; Ivlev, S. I.; Meggers, E. *ACS Catal.* **2021**, 11, 11396–11406.
- (7) For the enantioselective  $\alpha$ -bromination of acyl chlorides, see: Dogo-Isonagie, C.; Bekele, T.; France, S.; Wolfer, J.; Weatherwax, A.; Taggi, A. E.; Paull, D. H.; Dudding, T.; Lectka, T. *Eur. J. Org. Chem.* **2007**, 1091–1100.
- (8) (a) Ishihara, K.; Fushimi, M. *Org. Lett.* **2006**, 8, 1921–1924. (b) Ishihara, K.; Fushimi, M.; Akakura, M. *Acc. Chem. Res.* **2007**, 40, 1049–1055. (c) Ishihara, K.; Fushimi, M. *J. Am. Chem. Soc.* **2008**, 130, 7532–7533. (d) Sakakura, A.; Hori, M.; Fushimi, M.; Ishihara, K. *J. Am. Chem. Soc.* **2010**, 132, 15550–15552. (e) Sakakura, A.; Ishihara, K. *Chem. Soc. Rev.* **2011**, 40, 163–172. (f) Hori, M.; Sakakura, A.; Ishihara, K. *J. Am. Chem. Soc.* **2014**, 136, 13198–13201. (g) Yao, L.; Ishihara, K. *Chem. Sci.* **2019**, 10, 2259–2263.
- (9) Ishihara, K.; Nishimura, K.; Yamakawa, K. *Angew. Chem. Int. Ed.* **2020**, 59, 17641–17647.
- (10) See SI (page S20) for experimental results about halogen bonding interactions between 2,6-lutidine and  $X^+$ -reagents. (a) Stilinović, V.; Horvat, G.; Hrenar, T.; Nemeč, V.; Cinčić, D. *Chem. Eur. J.* **2017**, 23, 5244–5257. (b) Anyfanti, G.; Bauzá, A.; Gentiluomo, L.; Rodrigues, J.; Portalone, G.; Frontera, A.; Rissanen, K.; Puttreddy, R. *Front. Chem.* **2021**, 9, 623595.
- (11) For the estimation of weakly coordinating anions, see: (a) Mathieu, B.; Ghosez, L. *Tetrahedron* **2002**, 58, 8219–8226. (b) Krossing, I.; Raabe, I. *Angew. Chem. Int. Ed.* **2004**, 43, 2066–2090.

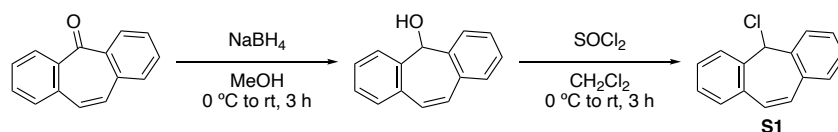
- (c) Krossing, I.; Raabe, I. *Chem. Eur. J.* **2004**, *10*, 5017–5030.
- (12) See SI (page S15) for details of the time-course reaction rate.
- (13) For  $[\alpha]_D = -87.1$  ( $c = 0.74$ ,  $\text{CHCl}_3$ ) of methyl (*R*)-chlorophenylacetate (87% ee), see Ref 6d.
- (14) See SI (page S19) for details of the screening of brominating agents.
- (15) For examples of  $\pi$ -cation interactions between arene and Cu(II), see: (a) van der Helm, D.; Lawson, M. B.; Enwall, E. L. *Acta Crystallogr., Sect. B: Struct. Sci.* **1972**, *28*, 2307–2312. (b) Yorita, H.; Otomo, K.; Hiarmatsu, A.; Toyama, A.; Miura, T.; Takeuchi, H. *J. Am. Chem. Soc.* **2008**, *130*, 15266–15267. (c) Muhonen, H.; Hämäläinen, R. *Chem. Lett.* **1983**, 120–124. (d) Castiñeiras, A.; Sicilia-Zafra, A. G.; González-Pérez, J. M.; Choquesillo-Lazarte, D.; Niclós-Gutiérrez, J. *Inorg. Chem.* **2002**, *41*, 6956–6958.
- (16) For selected examples of the olefin with metal complexes, see: (a) Schönberg, H.; Boulmaâz, S.; Wörle, M.; Liesum, L.; Schweiger, A.; Grützmacher, H. *Angew. Chem. Int. Ed.* **1998**, *37*, 1423–1425. (b) Defieber, C.; Ariger, M. A.; Moriel, P.; Carreira, E. M. *Angew. Chem. Int. Ed.* **2007**, *46*, 3139–3143. (c) Bruin, B. d.; Hetterscheid, D. G. H. *Eur. J. Inorg. Chem.* **2007**, 211–230. (d) Rodríguez-Lugo, R. E., Trincado, M.; Vogt, M.; Twews, F.; Santiso-Quinones, G.; Grützmacher, H. *Nat. Chem.* **2013**, *5*, 342–347. (e) Lichtenberg, C.; Bloch, J.; Gianetti, T. L.; Büttner, T.; Geier, J.; Grützmacher, H. *Dalton Trans.* **2015**, *44*, 20056–20066. (f) Brill, M.; Collado, A.; Cordes, D. B.; Slawin, A. M. Z.; Vogt, M.; Grützmacher, H.; Nolan, S. P. *Organometallics* **2015**, *34*, 263–274. (g) Freitag, B.; Elsen, H.; Pahl, J.; Ballmann, G.; Herrera, A.; Dorta, R.; Harder, S. *Organometallics* **2017**, *36*, 1860–1866. (h) Casas, F.; Trincado, M.; Rodríguez-Lugo, R.; Baneerge, D.; Grützmacher, H. *ChemCatChem* **2019**, *11*, 5241–5251. (i) Martin, J.; Langer, J.; Wiesinger, M.; Elsen, H.; Harder, S. *Eur. J. Inorg. Chem.* **2020**, 2582–2595.
- (17) Sawada, T.; Fukumaru, K.; Sakurai, H. *Chem. Pharm. Bull.* **1996**, *44*, 1009–1016.

#### 4-5-1. General methods

IR spectra were recorded on a JASCO FT/IR-460 plus spectrometer.  $^1\text{H}$  spectra were measured on a JEOL ECS-400 spectrometer (400 MHz) at ambient temperature. Chemical shift in ppm from internal tetramethylsilane (0.00 ppm) in  $\text{CDCl}_3$ , the solvent resonance (2.00 ppm) in acetic acid  $\text{d}_4$ , or the solvent resonance (5.32 ppm) in  $\text{CD}_2\text{Cl}_2$  on the  $\delta$  scale, multiplicity (s = singlet; d = doublet; t = triplet; q = quartet, quin = quintet, m = multiplet), coupling constant (Hz), integration, and assignment.  $^{13}\text{C}$  NMR spectra were measured on a JEOL ECS-400 spectrometer (100 MHz). Chemical shifts were recorded in ppm from the solvent resonance employed as the internal standard ( $\text{CDCl}_3$ : 77.16 ppm), ( $\text{CD}_2\text{Cl}_2$ : 54.00 ppm), ( $\text{CD}_3\text{CN}$ : 1.320 ppm) or acetic acid  $\text{d}_4$ . Optical rotations were measured on Rudolph Autopol IV digital polarimeter. High-performance liquid chromatography (HPLC) analysis was conducted using Shimadzu LC-10 AD coupled diode array-detector SPD-MA-10A-VP and chiral column of Daicel CHIRALCEL OD-3 (4.6 mm  $\times$  25 cm), Daicel CHIRALPAK AS-3 (4.6 mm  $\times$  25 cm), Daicel CHIRALPAK OJ-H (4.6 mm  $\times$  25 cm), Daicel CHIRALPAK ID-3 (4.6 mm  $\times$  25 cm), or Daicel CHIRALPAK IC-3 (4.6 mm  $\times$  25 cm). For Thin-layer chromatography (TLC) analysis, Merck precoated TLC plates (silica gel 60 F<sub>254</sub> 0.25 mm) or silica gel 60 NH<sub>2</sub> F<sub>254</sub>S 0.20 mm) were used. Visualization was accomplished by UV light (254 nm). The products were purified by column chromatography on silica gel (E. Merck Art. 9385; Kanto Chemical Co., Inc. 37560; Fuji Silysia Chemical Ltd. Chromatorex<sup>®</sup> NH-DM1020). High resolution mass spectral analyses (HRMS) were performed at Chemical Instrument Facility, Nagoya University (Bruker Daltonics micrOTOF-QII (ESI), JMS-T100TD (DART)). X-ray diffraction analysis was performed by Rigaku PILATUS-200K. Other materials were obtained from commercial supplies and used without further purification.

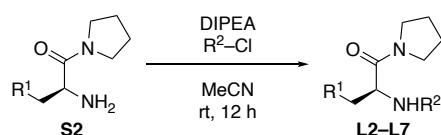
#### 4-5-2. Synthesis of chiral ligands L

Compounds **L1** and **L8** were prepared according to the previous paper.<sup>1,2</sup>

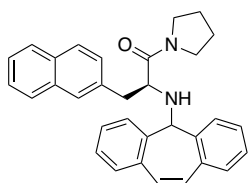


To a solution of dibenzosuberone (2.1 g, 10 mmol) in a mixture of  $\text{MeOH}$  (50 mL) were added  $\text{NaBH}_4$  (760 mg, 20 mmol) at  $0\text{ }^\circ\text{C}$ . The mixture was stirred at ambient temperature for 3 h. After the addition of  $\text{EtOAc}$  (5

mL), the reaction mixture was concentrated in *vacuo*. Purification by short column chromatography (hexane/EtOAc=1/1) afforded a quantitative amount of dibenzosuberanol. To a solution of dibenzosuberanol (2.1g, 10 mmol) in a mixture of CH<sub>2</sub>Cl<sub>2</sub> (30 mL) was added thionyl chloride (SOCl<sub>2</sub>, 2.2 mL, 30 mmol) at 0 °C. The mixture was stirred at ambient temperature for 3 h. The mixture was concentrated in *vacuo*. An excess amount of thionyl chloride was removed by co-evaporation with toluene. The desired product was recrystallized from Et<sub>2</sub>O and hexane to afford 5-Chloro-5*H*-dibenzo[*a,d*]cycloheptane **S1** (2.0 g, 89 % yield) as a pinkish solid.<sup>3</sup> <sup>1</sup>H NMR (400 MHz, CDCl<sub>3</sub>) δ 7.54–7.34 (m, 8H), 7.15 (s, 2H), 6.26 (s, 1H); <sup>13</sup>C NMR (100 MHz, CDCl<sub>3</sub>) δ 136.9 (2C), 134.7 (2C), 131.7 (2C), 130.6 (2C), 128.8 (2C), 128.7 (2C), 128.6 (2C), 67.9.



**S2** except for indole-derived ligands was prepared according to the following procedure.<sup>1,4</sup> To a solution of **S2** (1.0 equiv) in MeCN (0.2 M) were added DIPEA (1.2 equiv) and R<sup>2</sup>-Cl (1.2 equiv) at room temperature. The mixture was stirred for 12 h at ambient temperature. After quenching with 1 M HCl, the resultant mixture was extracted with EtOAc three times. The combined organic layer was washed with saturated aqueous NaHCO<sub>3</sub> and brine. The organic solvent was dried over Na<sub>2</sub>SO<sub>4</sub>, filtered, and concentrated *in vacuo*. Purification by column chromatography on Chromatorex<sup>®</sup> NH-DM1020 (*n*-hexane–EtOAc 10:1 to 3:1) afforded **L2–L7** as a colorless solid.

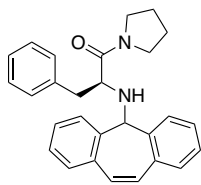


**(S)-2-((5*H*-Dibenzo[*a,d*][7]annulen-5-yl)amino)-3-(naphthalen-2-yl)-1-(pyrrolidin-1-yl)propan-1-one (L2):**

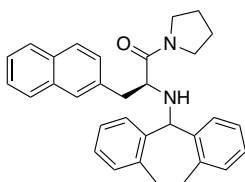
91% yield as a colorless solid.  $[\alpha]^{24}_{\text{D}} 42.4$  (*c* 1.00, CHCl<sub>3</sub>); <sup>1</sup>H NMR (400 MHz, CD<sub>3</sub>COOD) δ 7.82–7.67 (m, 4H), 7.63–7.57 (m, 2H), 7.56–7.35 (m, 8H), 7.28–7.16 (m, 3H), 6.03 (s, 1H), 4.42 (dd, *J* = 11.4, 4.6 Hz, 1H), 3.63 (dd, *J* = 12.4, 4.1 Hz, 1H), 3.02 (t, *J* = 12.4 Hz, 1H), 2.98–2.87 (m, 1H), 2.72–2.61 (m, 1H), 2.61–2.50 (m, 1H), 1.56–1.46 (m, 1H), 1.34–1.12 (m, 2H), 1.12–0.99 (m, 1H), 0.72–0.60 (m, 1H); <sup>13</sup>C NMR (100 MHz, CD<sub>3</sub>COOD) δ 166.0, 136.3, 134.8, 134.2, 133.7, 132.3, 132.0, 131.9, 131.4, 131.2 (2C), 131.1, 130.8, 130.7, 130.6, 130.3, 130.3, 129.9, 129.5, 129.1, 128.5 (2C), 128.4, 127.4, 127.2, 69.6, 60.7, 46.9 (2C), 38.6, 25.7, 24.1; IR (film) 2973, 1632, 1435,



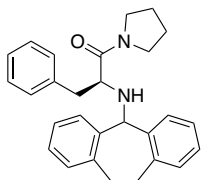
749  $\text{cm}^{-1}$ ; HRMS (ESI+) calcd for  $\text{C}_{32}\text{H}_{31}\text{N}_2\text{O}$   $[\text{M}+\text{H}]^+$  459.2431, found 459.2430.



**(S)-2-((5H-Dibenzo[a,d][7]annulen-5-yl)amino)-3-phenyl-1-(pyrrolidin-1-yl)propan-1-one (L3):** 53% yield as a colorless solid.  $[\alpha]_D^{25}$  29.6 (*c* 1.00,  $\text{CHCl}_3$ );  $^1\text{H}$  NMR (400 MHz,  $\text{CD}_3\text{COOD}$ )  $\delta$  7.82–7.67 (m, 4H), 7.87–7.71 (m, 2H), 7.55–7.37 (m, 6H), 7.28–7.12 (m, 7H), 6.39 (s, 1H), 4.60 (dd, *J* = 11.4, 4.6 Hz, 1H), 3.64 (dd, *J* = 12.4, 4.6 Hz, 1H), 2.96–2.84 (m, 1H), 2.79 (t, *J* = 11.9 Hz, 1H), 2.73–2.61 (m, 2H), 1.72–1.60 (m, 1H), 1.43–1.23 (m, 3H), 1.13–1.10 (m, 1H);  $^{13}\text{C}$  NMR (100 MHz,  $\text{CD}_3\text{COOD}$ )  $\delta$  165.9, 136.4, 134.9, 134.5, 132.5, 132.1, 131.8, 131.7, 131.1, 131.0, 130.8 (4C), 130.6, 130.4, 130.1, 130.1, 129.5 (2C), 128.7, 69.4, 60.9, 47.1, 46.9, 38.6, 25.9, 24.2; IR (film) 1645, 1455, 768  $\text{cm}^{-1}$ ; HRMS (ESI+) calcd for  $\text{C}_{28}\text{H}_{29}\text{N}_2\text{O}$   $[\text{M}+\text{H}]^+$  409.2274, found 409.2274.

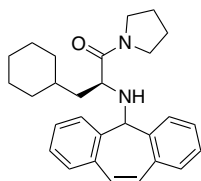


**(S)-2-((10,11-Dihydro-5H-dibenzo[a,d][7]annulen-5-yl)amino)-3-(naphthalen-2-yl)-1-(pyrrolidin-1-yl)propan-1-one (L5):** 82% yield as a colorless solid.  $[\alpha]_D^{25}$  79.6 (*c* 1.00,  $\text{CHCl}_3$ );  $^1\text{H}$  NMR (400 MHz,  $\text{CDCl}_3$ )  $\delta$  7.80–7.73 (m, 1H), 7.73–7.62 (m, 2H), 7.50 (s, 1H), 7.45–7.37 (m, 2H), 7.37–7.29 (m, 1H), 7.23–6.96 (m, 8H), 4.69 (s, 1H), 3.98 (s, 1H), 3.62–3.30 (m, 4H), 3.02–2.72 (m, 3H), 2.70–2.36 (m, 2H), 2.34–2.22 (m, 1H), 1.78–1.64 (m, 1H), 1.64–1.42 (m, 2H), 1.40–1.20 (m, 1H);  $^{13}\text{C}$  NMR (100 MHz,  $\text{CDCl}_3$ )  $\delta$  172.7, 135.8, 133.4, 132.2, 131.1, 130.0, 127.9, 127.9, 127.6, 127.5, 126.0, 126.0, 125.5, 125.4, 59.1, 45.7, 45.6, 40.5, 33.3, 31.4 (2C), 25.8, 24.1; IR (film) 1635, 1436, 770  $\text{cm}^{-1}$ ; HRMS (ESI+) calcd for  $\text{C}_{32}\text{H}_{33}\text{N}_2\text{O}$   $[\text{M}+\text{H}]^+$  461.2587, found 461.2587.

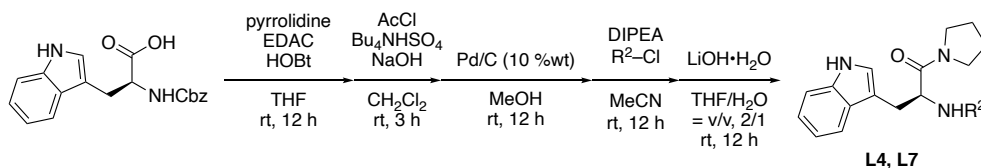


**(S)-2-((10,11-Dihydro-5H-dibenzo[a,d][7]annulen-5-yl)amino)-3-phenyl-1-(pyrrolidin-1-yl)propan-1-one (L6):** 78% yield as a colorless solid.  $[\alpha]_D^{25}$  80.0 (*c* 1.00,  $\text{CHCl}_3$ );  $^1\text{H}$  NMR (400 MHz,  $\text{CDCl}_3$ )  $\delta$  7.35–7.27 (m, 1H), 7.21–6.96 (m, 12H), 4.68 (s, 1H), 4.03 (s, 1H), 3.58–3.35 (m, 3H), 3.34–3.17 (m, 1H), 2.94–2.70 (m, 3H), 2.69–2.47 (m, 2H), 2.40–2.05 (m, 2H), 1.82–1.62 (m, 3H), 1.52–1.36 (m, 1H);  $^{13}\text{C}$  NMR (100 MHz,  $\text{CDCl}_3$ )  $\delta$  172.6,

138.2 (2C), 131.1, 129.9 (2C), 129.4 (3C), 128.1 (3C), 127.9, 127.6, 126.4 (2C), 126.0 (2C), 125.5, 59.2, 45.6, 45.5, 40.5, 33.3, 31.4; IR (film) 1635, 1494, 1220, 1168, 772 $\text{cm}^{-1}$ ; HRMS (ESI<sup>+</sup>) calcd for C<sub>28</sub>H<sub>31</sub>N<sub>2</sub>O [M+H]<sup>+</sup> 411.2431, found 411.2431.

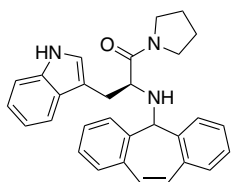


**(S)-2-((5H-Dibenzo[*a,d*][7]annulen-5-yl)amino)-3-cyclohexyl-1-(pyrrolidin-1-yl)propan-1-one (L8):** 54% yield as a colorless solid.  $[\alpha]_D^{23}$   $-36.8$  ( $c$  1.00, CHCl<sub>3</sub>); <sup>1</sup>H NMR (400 MHz, CDCl<sub>3</sub>)  $\delta$  7.79 (d,  $J$  = 6.9 Hz, 1H), 7.62–7.42 (m, 7H), 7.26 (d,  $J$  = 11.9 Hz, 1H), 7.17 (d,  $J$  = 11.9 Hz, 1H), 6.03 (s, 1H), 4.13 (t,  $J$  = 6.9 Hz, 1H), 3.24–3.05 (m, 3H), 2.93–2.79 (m, 1H), 1.94–1.42 (m, 11H), 1.35–1.00 (m, 4H), 0.94–0.72 (m, 2H); <sup>13</sup>C NMR (100 MHz, CD<sub>3</sub>COOD)  $\delta$  167.0, 136.3, 134.8, 132.5, 131.9, 131.3, 131.2, 131.0, 130.9, 130.9, 130.7, 130.5, 130.4, 130.2, 130.0, 69.3, 58.0, 47.3, 39.7, 34.2, 34.1, 34.0, 26.7, 26.6, 26.6, 26.3, 24.4; IR (film) 2921, 2848, 1635, 1422, 1220, 772  $\text{cm}^{-1}$ ; HRMS (ESI<sup>+</sup>) calcd for C<sub>28</sub>H<sub>35</sub>N<sub>2</sub>O [M+H]<sup>+</sup> 415.2744, found 415.2744.



To a solution of *N*-Carbobenzoxy-L-tryptophan (4.8 g, 14.2 mmol) in THF (28 mL) was added 1-hydroxybenzotriazole (HOBt, 2.6 g, 17.0 mmol), pyrrolidine (2.8 mL, 34.0 mmol), and *N*-(3-dimethylaminopropyl)-*N'*-ethylcarbodiimide hydrochloride (EDAC, 3.3 g, 17.0 mmol) at ambient temperature. The mixture was stirred at ambient temperature for 12 h. The reaction was quenched by the addition of 1 M HCl (10 mL). The reaction mixture was extracted with EtOAc (3 × 10 mL), dried over Na<sub>2</sub>SO<sub>4</sub>, filtered, and concentrated *in vacuo*. Purification of the residue by flash column chromatography on silica gel (*n*-hexane/EtOAc = 1/1 to 1/5) afforded the desired product (5.2 g, 94% yield) as a colorless solid. The acetylation of indole was prepared according to the following procedure.<sup>5</sup> To a solution benzyl (S)-3-(1*H*-indol-3-yl)-1-oxo-1-(pyrrolidin-1-yl)propan-2-yl)carbamate (2.0 g, 5.1 mmol) in dry CH<sub>2</sub>Cl<sub>2</sub> (50 mL) were added granular NaOH (1.0 g, 26 mmol) and tetrabutylammonium hydrogen sulfate (173 mg, 0.51 mmol) and the resulting solution was stirred for 15 minutes. AcCl (1.1 mL, 15.3 mmol) was slowly added to the reaction mixture and stirred for 3 h at ambient temperature.

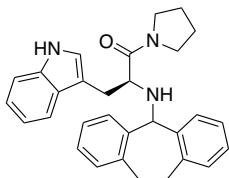
After quenching with 10 mL of water, the resultant mixture was extracted with CHCl<sub>3</sub> three times. The organic solvent was dried over Na<sub>2</sub>SO<sub>4</sub>, filtered, and concentrated *in vacuo*. Purification by column chromatography on Chromatorex<sup>®</sup> NH-DM1020 (*n*-hexane/EtOAc = 1/1 to 1/3) afforded the desired product (1.82 g, 83% yield) as a colorless solid. To a solution of benzyl (*S*)-3-(1-acetyl-1*H*-indol-3-yl)-1-oxo-1-(pyrrolidin-1-yl)propan-2-yl)carbamate (2.0 g, 4.61 mmol) in MeOH (20 mL) was added 10% Pd/C (200 mg), and the mixture was stirred at ambient temperature for 12 h under H<sub>2</sub> atmosphere. The reaction mixture was filtrated through Celite<sup>®</sup> and the filtrate was concentrated under reduced pressure. The reaction mixture was filtered through a silica gel short column on Chromatorex<sup>®</sup> NH-DM1020 (CHCl<sub>3</sub>/MeOH = 20/1 to 5/1) until the product was completely recovered afforded the desired product (>1.38 g, >99% yield) as a colorless oil. To a solution of (*S*)-3-(1-acetyl-1*H*-indol-3-yl)-2-amino-1-(pyrrolidin-1-yl)propan-1-one (1.0 equiv) in MeCN (0.2 *M*) were added DIPEA (1.2 equiv) and R<sup>2</sup>-Cl (1.2 equiv) at room temperature. The mixture was stirred for 12 h at ambient temperature. After quenching with 1 *M* HCl, the resultant mixture was extracted with EtOAc five times (until the desired product was recovered). The combined organic layer was washed with saturated aqueous NaHCO<sub>3</sub> and brine. The organic solvent was dried over Na<sub>2</sub>SO<sub>4</sub>, filtered, and concentrated *in vacuo*. Purification by column chromatography on Chromatorex<sup>®</sup> NH-DM1020 (*n*-hexane/EtOAc = 1/1 to 1/3) afforded the desired product as a colorless solid. A solution of lithium hydroxide (LiOH•H<sub>2</sub>O, 38 mg, 0.92 mmol, 1.5 equiv) in H<sub>2</sub>O (3.0 mL) was added to a solution of amide (301 mg, 1.0 equiv) in THF (3.0 mL). After stirring for 12 h, the mixture containing white precipitate was diluted with 5 mL of Et<sub>2</sub>O, and precipitate was collected. The solid was washed with 1 *M* HCl (5 mL), saturated aqueous NaHCO<sub>3</sub> (5 mL), and water (5 mL), and dried under reduced pressure to give **L4** (212 mg, 77% yield) or **L7** as a colorless solid.



**(*S*)-2-((5*H*-Dibenzo[*a,d*][7]annulen-5-yl)amino)-3-(1*H*-indol-3-yl)-1-(pyrrolidin-1-yl)propan-1-one (L4):**

[ $\alpha$ ]<sub>D</sub><sup>26</sup> 12.0 (*c* 0.10, CHCl<sub>3</sub>); <sup>1</sup>H NMR (400 MHz, CD<sub>3</sub>COOD)  $\delta$  7.73–7.66 (m, 1H), 7.63–7.56 (m, 1H), 7.54–7.34 (m, 7H), 7.31 (d, *J* = 8.3 Hz, 1H), 7.23–7.15 (m, 2H), 7.11 (t, *J* = 7.3 Hz, 1H), 7.05–6.96 (m, 2H), 5.99 (s, 1H), 4.20 (dd, *J* = 10.5, 5.0 Hz, 1H), 3.51 (dd, *J* = 13.8, 5.0 Hz, 1H), 3.14 (dd, *J* = 13.8, 11.0 Hz, 1H), 2.87–2.75 (m, 1H),

2.74–2.62 (m, 1H), 2.61–2.49 (m, 1H), 1.81–1.71 (m, 1H), 1.35–1.21 (m, 2H), 1.05–0.91 (m, 1H), 0.89–0.74 (m, 1H); <sup>13</sup>C NMR (100 MHz, CD<sub>3</sub>COOD) δ 166.6, 137.2, 136.1, 134.8, 132.3, 131.7, 131.4, 131.2, 131.0, 130.8, 130.7, 130.4, 130.0, 127.8, 125.8, 122.9, 120.3, 118.9, 112.5, 107.4, 69.4, 60.6, 47.3, 47.0, 28.2, 25.7, 24.1; IR (film) 3194, 1650, 1220, 1095, 772 cm<sup>-1</sup>; HRMS (ESI+) calcd for C<sub>30</sub>H<sub>30</sub>N<sub>3</sub>O [M+H]<sup>+</sup> 448.2383, found 448.2387.

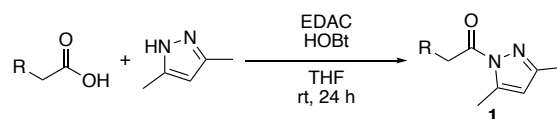


**(S)-2-((10,11-Dihydro-5H-dibenzo[*a,d*][7]annulen-5-yl)amino)-3-(1H-indol-3-yl)-1-(pyrrolidin-1-yl)propan-**

**1-one (L7):** 55% yield as a colorless solid.  $[\alpha]_D^{23}$  63.2 (*c* 1.00, CHCl<sub>3</sub>); <sup>1</sup>H NMR (400 MHz, CD<sub>2</sub>Cl<sub>2</sub>) δ 9.11 (s, 1H), 7.46 (d, *J* = 7.8 Hz, 2H), 7.26–7.00 (m, 9H), 6.91 (s, 1H), 4.78 (s, 1H), 4.14 (s, 1H), 3.70–3.40 (m, 3H), 3.40–3.25 (m, 1H), 3.16–2.19 (m, 7H), 1.75–1.12 (m, 4H); <sup>13</sup>C NMR (100 MHz, CD<sub>2</sub>Cl<sub>2</sub>) δ 173.7, 136.7, 131.5, 130.4, 128.3, 128.1, 128.0, 126.4, 126.1, 123.6, 122.0, 119.3, 119.1, 112.0, 111.7, 58.9, 46.2, 46.0, 33.6, 32.0 (2C), 30.5, 26.1, 24.4; IR (film) 3420, 1616, 1456, 1220, 772 cm<sup>-1</sup>; HRMS (ESI+) calcd for C<sub>30</sub>H<sub>32</sub>N<sub>3</sub>O [M+H]<sup>+</sup> 450.2540, found 450.2532.

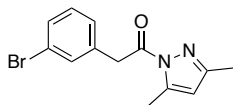
#### 4-5-3. Preparation of acylpyrazoles **1**

Compounds **1b**, **1c**, **1d**, **1e**, **1g**, **1h**, **1i**, **1j**, **1k**, **1m**, **1n**, **1o**, **1p**, and **1q** were prepared according to the previous paper.<sup>2</sup>

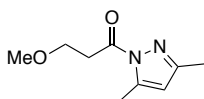


The round bottom flask equipped with a magnetic stirring bar and 3-way glass stopcock was evacuated and filled with argon (three cycles). To the solution of carboxylic acid (1.0 equiv) in THF (0.5 M) were added EDC•HCl (1.2 equiv), HOBT (1.2 equiv), 3,5-dimethylpyrazole (2.2 equiv) at room temperature. After stirring for 24 h at room temperature, the reaction was quenched by 1 M HCl. The resultant mixture was extracted with EtOAc, and the combined organic layer was washed with sat. NaHCO<sub>3</sub> solution and brine successively. The resulting organic layers were dried over Na<sub>2</sub>SO<sub>4</sub>. After removal of the solvent under reduced pressure, the crude mixture was purified by silica gel column chromatography (*n*-hexane/EtOAc = 30/1 to 20/1) to afford desired *N*-

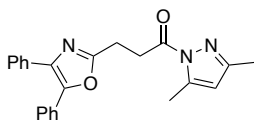
acylpyrazole **1**.



**1-(3-Bromophenyl)-2-(3,5-dimethyl-1H-pyrazol-1-yl)ethan-1-one (1f):** 5 mmol scale, 88% yield as a colorless solid.  $^1\text{H}$  NMR (400 MHz,  $\text{CDCl}_3$ )  $\delta$  7.52 (s, 1H), 7.41 (d,  $J = 7.3$  Hz, 1H), 7.29 (d,  $J = 7.3$  Hz, 1H), 7.21 (t,  $J = 7.3$  Hz, 1H), 5.99 (s, 1H), 4.40 (s, 2H), 2.52 (s, 3H), 2.27 (s, 3H);  $^{13}\text{C}$  NMR (100 MHz,  $\text{CDCl}_3$ )  $\delta$  171.3, 152.5, 144.5, 136.4, 133.1, 130.4, 130.1, 128.8, 122.6, 111.7, 41.4, 14.6, 14.0; IR (KBr) 3111, 1732, 1582, 1358, 1245, 963, 744  $\text{cm}^{-1}$ ; HRMS (ESI+) calcd for  $\text{C}_{13}\text{H}_{13}\text{BrN}_2\text{NaO}$   $[\text{M}+\text{Na}]^+$  315.0103, found 315.0100.

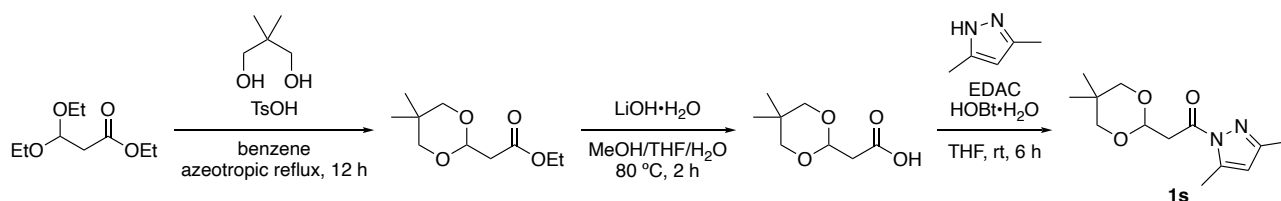


**1-(3,5-Dimethyl-1H-pyrazol-1-yl)-3-methoxypropan-1-one (1l):** 10 mmol scale, 60% yield as a colorless solid.  $^1\text{H}$  NMR (400 MHz,  $\text{CDCl}_3$ )  $\delta$  5.95 (s, 1H), 3.81 (t,  $J = 7.8$  Hz, 2H), 3.39 (s, 3H), 3.38 (t,  $J = 6.4$  Hz, 2H), 2.55 (s, 3H), 2.23 (s, 3H);  $^{13}\text{C}$  NMR (100 MHz,  $\text{CDCl}_3$ )  $\delta$  171.9, 152.1, 144.1, 111.2, 67.6, 58.9, 35.7, 14.6, 13.9; IR (KBr) 3105, 2897, 1718, 1583, 1356, 1121, 963, 741  $\text{cm}^{-1}$ ; HRMS (ESI+) calcd for  $\text{C}_9\text{H}_{14}\text{N}_2\text{NaO}_2$   $[\text{M}+\text{Na}]^+$  205.0947, found 205.0941.

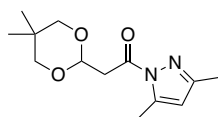


**1-(3,5-Dimethyl-1H-pyrazol-1-yl)-3-(4,5-diphenyloxazol-2-yl)propan-1-one (1r):** 3.36 mmol scale, 79% yield as a colorless solid.  $^1\text{H}$  NMR (400 MHz,  $\text{CDCl}_3$ )  $\delta$  7.66–7.61 (m, 2H), 7.60–7.54 (m, 2H), 7.39–7.28 (m, 6H), 5.97 (s, 1H), 3.71 (t,  $J = 7.8$  Hz, 2H), 3.29 (t,  $J = 7.4$  Hz, 2H), 2.55 (d,  $J = 0.9$  Hz, 3H), 2.23 (s, 3H);  $^{13}\text{C}$  NMR (100 MHz,  $\text{CDCl}_3$ )  $\delta$  172.3, 162.1, 152.3, 145.5, 144.2, 135.3, 132.7, 129.2, 128.7 (2C), 128.6 (2C), 128.5, 128.1, 128.0 (2C), 126.6 (2C), 111.3, 32.7, 23.1, 14.6, 13.9; IR (film) 1732, 1386, 962, 771, 694  $\text{cm}^{-1}$ ; HRMS (ESI+) calcd for  $\text{C}_{23}\text{H}_{22}\text{N}_3\text{O}_2$   $[\text{M}+\text{H}]^+$  372.1707, found 372.1704.

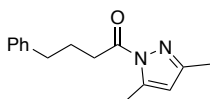
**Preparation of 2-(5,5-dimethyl-1,3-dioxan-2-yl)-1-(3,5-dimethyl-1H-pyrazol-1-yl)ethan-1-one (1s)**



Based on a literature procedure,<sup>6</sup> a mixture of ethyl 3,3-diethoxypropanoate (981  $\mu\text{L}$ , 5.0 mmol), 2,2-dimethylpropane-1,3-diol (521 mg, 5.0 mmol), 4-toluenesulfonic acid hydrate (9.5 mg, 0.05 mmol), and benzene (10 mL) was heated under the azeotropic condition to remove EtOH. After 12 h, the mixture was cooled to room temperature and neutralized with sat.  $\text{NaHCO}_3$  aq., extracted 2 times with  $\text{Et}_2\text{O}$ . The resulting organic layers were dried over  $\text{Na}_2\text{SO}_4$ . After removal of the solvent under reduced pressure, the crude mixture was purified by short silica gel column chromatography ( $n$ -hexane/ $\text{EtOAc}$  = 10/1) to give ester. A solution of lithium hydroxide ( $\text{LiOH}\cdot\text{H}_2\text{O}$ , 1.0 g, 24.6 mmol, 3.0 equiv) in  $\text{H}_2\text{O}$  (5 mL) was added to a solution of ester in THF (5 mL) and MeOH (5 mL). After stirring for 2 h at 80  $^\circ\text{C}$ , the mixture was cooled to room temperature and concentrated *in vacuo* and acidified with 1  $M$  HCl. The aqueous layer was extracted with  $\text{CHCl}_3$  ( $2 \times 10$  mL) and  $\text{EtOAc}$  ( $3 \times 10$  mL) and the combined organic layers were washed with brine (20 mL) and dried over  $\text{Na}_2\text{SO}_4$ . The solvent was removed under reduced pressure to give the corresponding carboxylic acid as a colorless solid (869 mg, 100%).



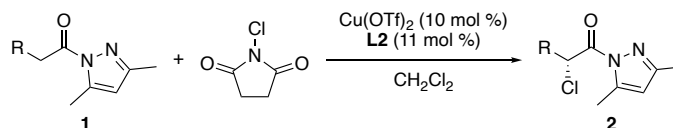
**2-(5,5-Dimethyl-1,3-dioxan-2-yl)-1-(3,5-dimethyl-1H-pyrazol-1-yl)ethan-1-one (1s):** 5.0 mmol scale, >99% yield as a colorless solid.  $^1\text{H}$  NMR (400 MHz,  $\text{CDCl}_3$ )  $\delta$  5.94 (d,  $J$  = 0.9 Hz, 1H), 5.07 (t,  $J$  = 5.5 Hz, 1H), 3.65–3.59 (m, 2H), 3.52–3.46 (m, 4H), 2.53 (d,  $J$  = 0.9 Hz, 3H), 2.22 (s, 3H), 1.21 (s, 3H), 0.73 (s, 3H);  $^{13}\text{C}$  NMR (100 MHz,  $\text{CDCl}_3$ )  $\delta$  170.0, 152.3, 144.2, 111.4, 98.9, 41.5, 30.2, 23.1 (2C), 22.0 (2C), 14.6, 14.0; IR (film) 1955, 1733, 1352, 1134, 961, 772  $\text{cm}^{-1}$ ; HRMS (DART+) calcd for  $\text{C}_{13}\text{H}_{21}\text{N}_2\text{O}_3$   $[\text{M}+\text{H}]^+$  253.1552, found 253.15497.



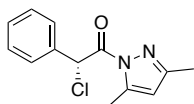
**1-(3,5-Dimethyl-1H-pyrazol-1-yl)-4-phenylbutan-1-one (1t):** 5.0 mmol scale, 77% yield as a colorless solid.  $^1\text{H}$  NMR (400 MHz,  $\text{CDCl}_3$ )  $\delta$  7.31–7.26 (m, 2H), 7.25–7.15 (m, 3H), 5.94 (s, 1H), 3.14 (t,  $J$  = 7.4 Hz, 2H), 2.73 (t,  $J$  = 7.3 Hz, 2H), 2.53 (d,  $J$  = 0.9 Hz, 3H), 2.23 (s, 3H), 3.08 (quint,  $J$  = 7.8 Hz, 2H);  $^{13}\text{C}$  NMR (100 MHz,

CDCl<sub>3</sub>)  $\delta$  174.0, 151.9, 144.1, 141.8, 128.6 (2C), 128.5 (2C), 126.0, 111.1, 35.3, 34.8, 26.1, 14.7, 13.9; IR (film) 1541, 1507, 1220, 772 cm<sup>-1</sup>; HRMS (ESI+) calcd for C<sub>15</sub>H<sub>18</sub>N<sub>2</sub>NaO [M+Na]<sup>+</sup> 265.1311, found 265.1323.

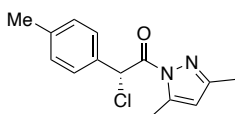
#### 4-5-4. General procedure for the enantioselective $\alpha$ -chlorination reaction of **1b** (Table 2)



A mixture of **L2** (15.1 mg, 0.033 mmol) and copper(II) triflate (10.9 mg, 0.030 mmol) in a 20 mL shlenk flask (for in the presence of heat-gun dried pellet 4A MS (100 mg)) were dissolved in acetonitrile (0.5 mL, dried over 4A molecular sieves). After stirring for 10 minutes, the solution was concentrated under reduced pressure at room temperature. To the residue were added **1**, CH<sub>2</sub>Cl<sub>2</sub> (1.5 mL) and, *N*-chlorosuccinimide (NCS, 44.1 mg, 0.33 mmol), and the mixture was stirred at 0 °C or temperature for 3–36 h. The reaction mixture was filtered through a neutral silica short column (*n*-hexane/EtOAc = 1/1). After evaporation of the organic solvent under reduced pressure, the crude mixture was purified by neutral silica gel column chromatography (*n*-hexane/EtOAc = 30/1 to 9/1) to give the desired product **2**. The enantiomeric excess (ee) was determined through chiral HPLC analysis.

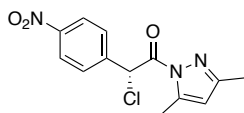


**(R)-2-Chloro-1-(3,5-dimethyl-1H-pyrazol-1-yl)-2-phenylethan-1-one (2b):**  $[\alpha]_D^{24} = 33.7$  (*c* 1.00, CHCl<sub>3</sub>, 96% ee); <sup>1</sup>H NMR (400 MHz, CDCl<sub>3</sub>)  $\delta$  7.64–7.62 (m, 2H), 7.38–7.29 (m, 3H), 6.94 (s, 1H), 5.98 (s, 1H), 2.52 (d, *J* = 0.9 Hz, 3H), 2.23 (s, 3H); <sup>13</sup>C NMR (100 MHz, CDCl<sub>3</sub>)  $\delta$  167.6, 153.1, 145.0, 135.9, 129.1, 128.8 (4C), 112.4, 57.7, 14.4, 14.0; IR (KBr) 1736, 1377, 1355, 961, 772, 727 cm<sup>-1</sup>; HRMS (ESI+) calcd for C<sub>13</sub>H<sub>13</sub>ClNaN<sub>2</sub>O [M+Na]<sup>+</sup> 271.0609, found 271.0608; HPLC analysis; OD-3, *n*-hexane/*i*-PrOH = 99/1, 0.5 mL/min, *t*<sub>R</sub> = 10.7 min (minor), *t*<sub>R</sub> = 11.7 min (major).

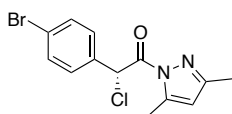


**(R)-2-Chloro-1-(3,5-dimethyl-1H-pyrazol-1-yl)-2-(*p*-tolyl)ethan-1-one (2c):**  $[\alpha]_D^{25} = 47.7$  (*c* 1.00, CHCl<sub>3</sub>, 96% ee); <sup>1</sup>H NMR (400 MHz, CDCl<sub>3</sub>)  $\delta$  7.52 (d, *J* = 7.8 Hz, 2H), 7.16 (d, *J* = 7.8 Hz, 2H), 6.91 (s, 1H), 5.96 (s, 1H),

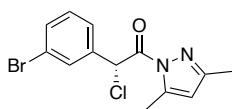
2.52 (d,  $J = 0.9$  Hz, 3H), 2.33 (s, 3H), 2.22 (s, 3H);  $^{13}\text{C}$  NMR (100 MHz,  $\text{CDCl}_3$ )  $\delta$  167.7, 153.0, 145.0, 139.2, 133.0, 129.5 (2C), 128.7 (2C), 112.3, 57.7, 21.3, 14.4, 14.0; IR (KBr) 2927, 1589, 1737, 1377, 1351, 961, 747  $\text{cm}^{-1}$ ; HRMS (ESI+) calcd for  $\text{C}_{14}\text{H}_{15}\text{ClN}_2\text{NaO}$   $[\text{M}+\text{Na}]^+$  285.0765, found 285.0767; HPLC analysis: AS-3, *n*-hexane/*i*-PrOH = 99/1, 0.5 mL/min,  $t_{\text{R}} = 10.8$  min (minor),  $t_{\text{R}} = 15.2$  min (major).



**(R)-2-Chloro-1-(3,5-dimethyl-1H-pyrazol-1-yl)-2-(4-nitrophenyl)ethan-1-one (2d):**  $[\alpha]_{\text{D}}^{25} = 51.3$  ( $c$  1.00,  $\text{CHCl}_3$ , 94% ee);  $^1\text{H}$  NMR (400 MHz,  $\text{CDCl}_3$ )  $\delta$  8.24–8.20 (m, 2H), 7.84–7.79 (m, 2H), 6.99 (s, 1H), 6.02 (s, 1H), 2.53 (s, 3H), 2.23 (s, 3H);  $^{13}\text{C}$  NMR (100 MHz,  $\text{CDCl}_3$ )  $\delta$  166.5, 153.7, 148.2, 145.3, 129.9 (2C), 124.0 (2C), 112.8, 56.7, 14.4, 14.0; IR (KBr) 1736, 1525, 1378, 1348, 961, 733  $\text{cm}^{-1}$ ; HRMS (DART+) calcd for  $\text{C}_{13}\text{H}_{13}\text{ClN}_3\text{O}_3$   $[\text{M}+\text{H}]^+$  294.0645, found 294.06489; HPLC analysis: AS-3, *n*-hexane/*i*-PrOH = 99/1, 0.5 mL/min,  $t_{\text{R}} = 40.8$  min (minor),  $t_{\text{R}} = 46.7$  min (major).



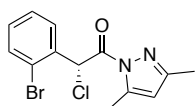
**(R)-2-(4-Bromophenyl)-2-chloro-1-(3,5-dimethyl-1H-pyrazol-1-yl)ethan-1-one (2e):**  $[\alpha]_{\text{D}}^{25} = 55.2$  ( $c$  1.00,  $\text{CHCl}_3$ , 96% ee);  $^1\text{H}$  NMR (400 MHz,  $\text{CDCl}_3$ )  $\delta$  7.52–7.42 (m, 4H), 6.88 (s, 1H), 5.99 (s, 1H), 2.52 (s, 3H), 2.23 (s, 3H);  $^{13}\text{C}$  NMR (100 MHz,  $\text{CDCl}_3$ )  $\delta$  167.2, 153.3, 145.1, 135.0, 132.0, 130.5, 123.5, 112.5, 57.1, 14.4, 14.0; IR (KBr) 1731, 1590, 1488, 1377, 1352, 759  $\text{cm}^{-1}$ ; HRMS (ESI+) calcd for  $\text{C}_{13}\text{H}_{12}\text{BrClN}_2\text{NaO}$   $[\text{M}+\text{Na}]^+$  348.9714, found 348.9713; HPLC analysis: AS-3, *n*-hexane/*i*-PrOH = 99/1, 0.5 mL/min,  $t_{\text{R}} = 11.6$  min (minor),  $t_{\text{R}} = 16.3$  min (major).



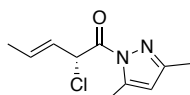
**(R)-2-(3-Bromophenyl)-2-chloro-1-(3,5-dimethyl-1H-pyrazol-1-yl)ethan-1-one (2f):**  $[\alpha]_{\text{D}}^{24} = 30.1$  ( $c$  1.00,  $\text{CHCl}_3$ , 95% ee);  $^1\text{H}$  NMR (400 MHz,  $\text{CDCl}_3$ )  $\delta$  7.79 (s, 1H), 7.57 (d,  $J = 7.8$  Hz, 1H), 7.46 (d,  $J = 7.8$  Hz, 1H), 7.22 (d,  $J = 7.8$  Hz, 1H), 6.88 (s, 1H), 6.00 (s, 1H), 2.53 (s, 3H), 2.23 (s, 3H);  $^{13}\text{C}$  NMR (100 MHz,  $\text{CDCl}_3$ )  $\delta$  167.1, 153.4, 145.1, 138.0, 132.3, 131.9, 130.3, 127.5, 122.7, 112.6, 56.9, 14.4, 14.0; IR (KBr) 1735, 1590, 1377, 1352, 961, 758  $\text{cm}^{-1}$ ; HRMS (ESI+) calcd for  $\text{C}_{13}\text{H}_{12}\text{BrClN}_2\text{NaO}$   $[\text{M}+\text{Na}]^+$  348.9714, found 348.9718; HPLC analysis:



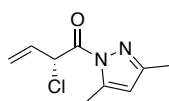
AS-3, *n*-hexane/*i*-PrOH = 99/1, 1.0 mL/min,  $t_R$  = 5.6 min (minor),  $t_R$  = 8.6 min (major).



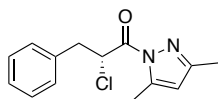
**(R)-2-(2-Bromophenyl)-2-chloro-1-(3,5-dimethyl-1H-pyrazol-1-yl)ethan-1-one (2g):**  $[\alpha]_D^{25} = 62.9$  ( $c$  1.00, CHCl<sub>3</sub>, 97% ee); <sup>1</sup>H NMR (400 MHz, CDCl<sub>3</sub>)  $\delta$  7.69 (d,  $J$  = 7.8, 1.4 Hz, 1H), 7.57 (dd,  $J$  = 8.0, 1.4 Hz, 1H), 7.34 (ddd,  $J$  = 8.0, 7.8, 1.4 Hz, 1H), 7.23 (s, 1H), 7.19 (ddd,  $J$  = 7.8, 7.8, 1.4 Hz, 1H), 5.98 (s, 1H), 2.55 (s, 3H), 2.21 (s, 3H); <sup>13</sup>C NMR (100 MHz, CDCl<sub>3</sub>)  $\delta$  167.1, 153.3, 144.8, 135.8, 133.1, 130.5, 130.0, 128.1, 123.9, 112.3, 57.8, 14.3, 14.0; IR (KBr) 1735, 1589, 1377, 1354, 961, 744 cm<sup>-1</sup>; HRMS (ESI+) calcd for C<sub>13</sub>H<sub>12</sub>BrClN<sub>2</sub>NaO [M+Na]<sup>+</sup> 348.9714, found 348.9712; HPLC analysis: OD-3, *n*-hexane/*i*-PrOH = 99/1, 0.5 mL/min,  $t_R$  = 13.3 min (minor),  $t_R$  = 16.9 min (major).



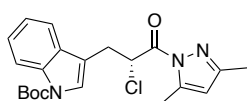
**(R,E)-2-Chloro-1-(3,5-dimethyl-1H-pyrazol-1-yl)pent-3-en-1-one (2h):**  $[\alpha]_D^{25} = 65.6$  ( $c$  1.00, CHCl<sub>3</sub>, 93% ee); <sup>1</sup>H NMR (400 MHz, CDCl<sub>3</sub>)  $\delta$  6.27 (d,  $J$  = 8.7 Hz, 1H), 6.02 (s, 1H), 6.08–5.97 (m, 1H), 5.91–5.82 (m, 1H), 2.55 (d,  $J$  = 0.9 Hz, 3H), 2.25 (s, 3H), 1.77 (dd,  $J$  = 6.4, 1.4 Hz, 3H); <sup>13</sup>C NMR (100 MHz, CDCl<sub>3</sub>)  $\delta$  168.0, 153.1, 145.1, 133.5, 125.7, 112.4, 56.3, 18.1, 14.5, 14.0; IR (neat) 2929, 1734, 1588, 1383, 1360, 962, 807 cm<sup>-1</sup>; HRMS (ESI+) calcd for C<sub>10</sub>H<sub>13</sub>ClN<sub>2</sub>NaO [M+Na]<sup>+</sup> 235.0609, found 235.0603; HPLC analysis: AS-3, *n*-hexane/*i*-PrOH = 99/1, 1.0 mL/min,  $t_R$  = 4.9 min (minor),  $t_R$  = 5.4 min (major).



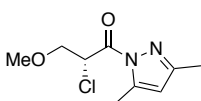
**(R)-2-Chloro-1-(3,5-dimethyl-1H-pyrazol-1-yl)but-3-en-1-one (2i):**  $[\alpha]_D^{24} = 54.8$  ( $c$  1.00, CHCl<sub>3</sub>, 94% ee); <sup>1</sup>H NMR (400 MHz, CDCl<sub>3</sub>)  $\delta$  6.29 (d,  $J$  = 8.2 Hz, 1H), 6.20 (ddd,  $J$  = 17.0, 10.1, 8.2 Hz, 1H), 6.03 (s, 1H), 5.58 (d,  $J$  = 16.5 Hz, 1H), 5.40 (d,  $J$  = 10.1 Hz, 1H), 2.55 (d,  $J$  = 0.9 Hz, 3H), 2.25 (s, 3H); <sup>13</sup>C NMR (100 MHz, CDCl<sub>3</sub>)  $\delta$  167.5, 153.3, 145.1, 132.4, 120.9, 112.4, 56.6, 14.4, 14.0; IR (film) 1731, 1375, 958, 925 cm<sup>-1</sup>; HRMS (ESI+) calcd for C<sub>9</sub>H<sub>12</sub>ClN<sub>2</sub>O [M+H]<sup>+</sup> 199.0633, found 199.0634; HPLC analysis: AS-3, *n*-hexane/*i*-PrOH = 99/1, 1.0 mL/min,  $t_R$  = 4.9 min (minor),  $t_R$  = 5.3 min (major).



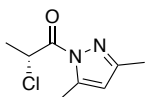
**(R)-2-Chloro-1-(3,5-dimethyl-1H-pyrazol-1-yl)-3-phenylpropan-1-one (2j):**  $[\alpha]_D^{27} = -34.5$  (*c* 1.00, CHCl<sub>3</sub>, 94% ee); <sup>1</sup>H NMR (400 MHz, CDCl<sub>3</sub>) δ 5.94 (dd, *J* = 8.2, 6.4 Hz, 1H), 7.32–7.23 (m, 5H), 5.99 (s, 1H), 3.53 (dd, *J* = 14.2, 6.4 Hz, 1H), 3.23 (dd, *J* = 14.2, 8.2 Hz, 1H), 2.54 (d, *J* = 0.9 Hz, 3H), 2.24 (s, 3H); <sup>13</sup>C NMR (100 MHz, CDCl<sub>3</sub>) δ 168.7, 153.1, 144.9, 136.4, 129.7 (2C), 128.6 (2C), 127.3, 112.3, 56.5, 40.6, 14.5, 14.0; IR (neat) 1732, 1588, 1383, 962, 743, 699 cm<sup>-1</sup>; HRMS (ESI+) calcd for C<sub>14</sub>H<sub>15</sub>ClN<sub>2</sub>NaO [M+Na]<sup>+</sup> 285.0765, found 285.0767; HPLC analysis: AS-3, *n*-hexane/*i*-PrOH = 99/1, 0.5 mL/min, *t*<sub>R</sub> = 10.2 min (minor), *t*<sub>R</sub> = 12.0 min (major).



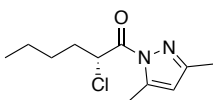
**tert-Butyl (R)-3-(2-chloro-3-(3,5-dimethyl-1H-pyrazol-1-yl)-3-oxopropyl)-1H-indole-1-carboxylate (2k):**  $[\alpha]_D^{25} = 10.8$  (*c* 1.00, CHCl<sub>3</sub>, 91% ee); <sup>1</sup>H NMR (400 MHz, CDCl<sub>3</sub>) δ 8.12 (d, *J* = 7.8 Hz, 1H), 7.67 (d, *J* = 7.8 Hz, 1H), 7.51 (s, 1H), 7.36–7.20 (m, 2H), 6.05–6.02 (m, 1H), 6.00 (s, 1H), 3.63 (ddd, *J* = 14.7, 56.0, 0.9 Hz, 1H), 3.37–3.30 (m, 1H), 2.53 (d, *J* = 0.9 Hz, 3H), 2.24 (s, 3H), 1.66 (s, 9H); <sup>13</sup>C NMR (100 MHz, CDCl<sub>3</sub>) δ 14.0, 14.4, 28.3 (3C), 30.9, 55.5, 83.8, 112.2, 115.4 (2C), 119.1, 122.6, 124.6, 124.9, 130.2, 135.5, 145.0, 149.7, 153.2, 168.8; IR (film) 2979, 1734, 1380, 1256, 1158, 1086, 749 cm<sup>-1</sup>; HRMS (ESI+) calcd for C<sub>21</sub>H<sub>24</sub>ClN<sub>3</sub>NaO<sub>3</sub> [M+Na]<sup>+</sup> 424.1398, found 424.1393; HPLC analysis: AS-3, *n*-hexane/*i*-PrOH = 99/1, 1.0 mL/min, *t*<sub>R</sub> = 5.5 min (minor), *t*<sub>R</sub> = 6.7 min (major).



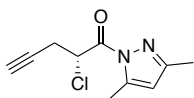
**(R)-2-Chloro-1-(3,5-dimethyl-1H-pyrazol-1-yl)-3-methoxypropan-1-one (2l):**  $[\alpha]_D^{26} = -9.3$  (*c* 1.00, CHCl<sub>3</sub>, 90% ee); <sup>1</sup>H NMR (400 MHz, CDCl<sub>3</sub>) δ 6.02 (s, 1H), 5.89 (dd, *J* = 7.3, 6.0 Hz, 1H), 4.01 (dd, *J* = 10.1, 7.3 Hz, 1H), 3.85 (dd, *J* = 10.3, 6.0 Hz, 1H), 3.42 (s, 3H), 2.56 (d, *J* = 0.9 Hz, 3H), 2.25 (s, 3H); <sup>13</sup>C NMR (100 MHz, CDCl<sub>3</sub>) δ 167.6, 153.3, 144.9, 112.4, 73.4, 59.5, 52.8, 14.5, 14.0; IR (neat) 1734, 1589, 1387, 1360, 1124, 957 cm<sup>-1</sup>; HRMS (ESI+) calcd for C<sub>9</sub>H<sub>13</sub>ClN<sub>2</sub>NaO<sub>2</sub> [M+Na]<sup>+</sup> 239.0558, found 239.0554; HPLC analysis: OD-3, *n*-hexane/*i*-PrOH = 99/1, 0.5 mL/min, *t*<sub>R</sub> = 10.9 min (minor), *t*<sub>R</sub> = 12.0 min (major).



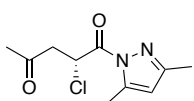
**(R)-2-Chloro-1-(3,5-dimethyl-1H-pyrazol-1-yl)propan-1-one (2m):**  $[\alpha]_D^{25} = -22.0$  (*c* 1.00, CHCl<sub>3</sub>, 85% ee); <sup>1</sup>H NMR (400 MHz, CDCl<sub>3</sub>) δ 6.02 (s, 1H), 5.82 (q, *J* = 6.9 Hz, 1H), 2.56 (s, 3H), 2.25 (s, 3H), 1.78 (d, *J* = 6.9 Hz, 3H); <sup>13</sup>C NMR (100 MHz, CDCl<sub>3</sub>) δ 169.8, 153.1, 145.0, 112.2, 51.7, 21.3, 14.5, 14.0; IR (neat) 1734, 1541, 1507, 1379, 772 cm<sup>-1</sup>; HRMS (DART+) calcd for C<sub>8</sub>H<sub>12</sub>ClN<sub>2</sub>O [M+H]<sup>+</sup> 187.0638, found 187.06372; HPLC analysis: AS-3, *n*-hexane/*i*-PrOH = 99/1, 0.5 mL/min, *t*<sub>R</sub> = 9.9 min (minor), *t*<sub>R</sub> = 10.7 min (major).



**(R)-2-Chloro-1-(3,5-dimethyl-1H-pyrazol-1-yl)hexan-1-one (2n):**  $[\alpha]_D^{25} = -3.2$  (*c* 1.00, CHCl<sub>3</sub>, 84% ee); <sup>1</sup>H NMR (400 MHz, CDCl<sub>3</sub>) δ 6.02 (s, 1H), 5.73 (dd, *J* = 8.2, 6.0 Hz, 1H), 2.56 (s, 3H), 2.24 (s, 3H), 2.22–2.05 (m, 1H), 2.05–1.95 (m, 1H), 1.57–1.30 (m, 4H), 0.95 (t, *J* = 7.3 Hz, 3H); <sup>13</sup>C NMR (100 MHz, CDCl<sub>3</sub>) δ 169.6, 153.0, 144.9, 112.2, 56.2, 34.3, 28.2, 22.2, 14.5, 13.9; IR (neat) 1735, 1382, 1357, 961 cm<sup>-1</sup>; HRMS (DART+) calcd for C<sub>11</sub>H<sub>18</sub>ClN<sub>2</sub>O [M+H]<sup>+</sup> 229.1108, found 229.11035; HPLC analysis: AS-3, *n*-hexane/*i*-PrOH = 99/1, 1.0 mL/min, *t*<sub>R</sub> = 4.1 min (minor), *t*<sub>R</sub> = 4.4 min (major).

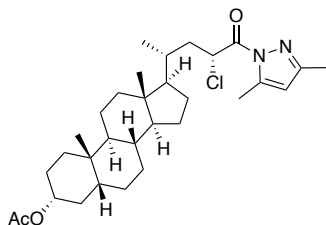


**(R)-2-Chloro-1-(3,5-dimethyl-1H-pyrazol-1-yl)pent-4-yn-1-one (2o):**  $[\alpha]_D^{25} = -11.6$  (*c* 1.00, CHCl<sub>3</sub>, 92% ee); <sup>1</sup>H NMR (400 MHz, CDCl<sub>3</sub>) δ 6.03 (s, 1H), 5.83 (t, *J* = 7.4 Hz, 1H), 3.08 (ddd, *J* = 16.9, 7.3, 2.7 Hz, 1H), 2.97 (ddd, *J* = 16.9, 6.8, 2.7 Hz, 1H), 2.56 (s, 3H), 2.26 (s, 3H), 2.10 (t, *J* = 2.3 Hz, 1H); <sup>13</sup>C NMR (100 MHz, CDCl<sub>3</sub>) δ 167.5, 153.5, 145.0, 112.5, 78.7, 71.7, 53.0, 24.9, 14.4, 14.0; IR (neat) 3295, 2928, 1732, 1387, 1332 cm<sup>-1</sup>; HRMS (ESI+) calcd for C<sub>10</sub>H<sub>11</sub>ClN<sub>2</sub>NaO [M+Na]<sup>+</sup> 233.0452, found 233.0456; HPLC analysis: AS-3, *n*-hexane/*i*-PrOH = 99/1, 1.0 mL/min, *t*<sub>R</sub> = 6.3 min (minor), *t*<sub>R</sub> = 7.2 min (major).

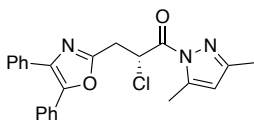


**(R)-2-Chloro-1-(3,5-dimethyl-1H-pyrazol-1-yl)pentane-1,4-dione (2p):**  $[\alpha]_D^{25} = -15.6$  (*c* 1.00, CHCl<sub>3</sub>); <sup>1</sup>H NMR (400 MHz, CDCl<sub>3</sub>) δ 6.02 (s, 1H), 5.99 (dd, *J* = 9.2, 5.5 Hz, 1H), 3.50 (dd, *J* = 18.3, 9.2 Hz, 1H), 3.15 (dd, *J* = 17.8,

5.0 Hz, 1H), 2.53 (s, 3H), 2.26 (s, 3H), 2.22 (s, 3H);  $^{13}\text{C}$  NMR (100 MHz,  $\text{CDCl}_3$ )  $\delta$  204.8, 168.5, 153.3, 144.9, 112.4, 49.5, 47.9, 30.0, 14.4, 14.1; IR (film) 1716, 1387, 1220, 772  $\text{cm}^{-1}$ ; HRMS (ESI+) calcd for  $\text{C}_{10}\text{H}_{13}\text{ClN}_2\text{NaO}_2$   $[\text{M}+\text{Na}]^+$  251.0558, found 251.0567; HPLC analysis: AS-3, *n*-hexane/*i*-PrOH = 50/1, 1.0 mL/min,  $t_{\text{R}}$  = 13.0 min (minor),  $t_{\text{R}}$  = 14.2 min (major).

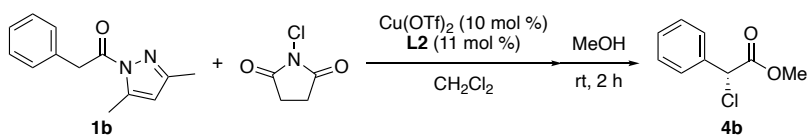


**(3R,5R,8R,9S,10S,13R,14S,17R)-17-((2R,4R)-4-Chloro-5-(3,5-dimethyl-1H-pyrazol-1-yl)-5-oxopentan-2-yl)-10,13-dimethylhexadecahydro-1H-cyclopenta[*a*]phenanthren-3-yl acetate (2q):**  $^1\text{H}$  NMR (400 MHz,  $\text{CDCl}_3$ )  $\delta$  6.01 (s, 1H), 5.83 (dd,  $J$  = 11.2, 2.7 Hz, 1H), 4.78–4.67 (m, 1H), 2.55 (s, 3H), 2.24 (s, 3H), 2.16–2.07 (m, 1H), 2.03 (s, 3H), 1.95–1.76 (m, 6H), 1.75–0.97 (m, 22H), 0.93 (s, 3H), 0.70 (s, 3H);  $^{13}\text{C}$  NMR (100 MHz,  $\text{CDCl}_3$ )  $\delta$  170.8, 170.0, 152.9, 144.9, 112.1, 74.5, 56.6, 56.5, 55.6, 43.1, 42.0, 40.7, 40.5, 40.3, 35.9, 35.1, 34.7, 33.5, 32.3, 28.4, 27.1, 26.7, 26.4, 24.3, 23.5, 21.6, 20.9, 18.1, 14.5, 14.0, 12.2; IR (film) 2931, 2867, 1734, 1588, 1380, 1244, 1027  $\text{cm}^{-1}$ ; HRMS (ESI+) calcd for  $\text{C}_{31}\text{H}_{47}\text{ClN}_2\text{NaO}_3$   $[\text{M}+\text{Na}]^+$  553.3167, found 553.3156.

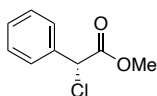


**(R)-2-Chloro-1-(3,5-dimethyl-1H-pyrazol-1-yl)-3-(4,5-diphenyloxazol-2-yl)propan-1-one (2r):**  $[\alpha]_{\text{D}}^{25}$  = 10.0 (*c* 1.00,  $\text{CHCl}_3$ , 88% ee);  $^1\text{H}$  NMR (400 MHz,  $\text{CDCl}_3$ )  $\delta$  7.61–7.51 (m, 4H), 7.39–7.28 (m, 6H), 6.26 (t,  $J$  = 7.3 Hz, 1H), 6.02 (s, 1H), 3.74 (dd,  $J$  = 16.0, 7.3 Hz, 1H), 3.61 (dd,  $J$  = 16.0, 7.4 Hz, 1H), 2.57 (d,  $J$  = 0.9 Hz, 3H), 2.23 (s, 3H);  $^{13}\text{C}$  NMR (100 MHz,  $\text{CDCl}_3$ )  $\delta$  168.0, 158.5, 153.4, 146.0, 145.0, 135.4, 132.3, 128.9, 128.8 (3C), 128.6 (2C), 128.2, 128.0 (2C), 126.7 (2C), 112.4, 52.1, 33.7, 14.4, 14.0; IR (film) 1733, 1387, 962, 772  $\text{cm}^{-1}$ ; HRMS (ESI+) calcd for  $\text{C}_{23}\text{H}_{20}\text{ClN}_3\text{NaO}_2$   $[\text{M}+\text{Na}]^+$  428.1136, found 428.1132; HPLC analysis: AS-3, *n*-hexane/*i*-PrOH = 99/1, 1.0 mL/min,  $t_{\text{R}}$  = 10.0 min (minor),  $t_{\text{R}}$  = 17.5 min (major).

## 5. Procedure for the one-pot transformation of 1b to 4b (Table 2)

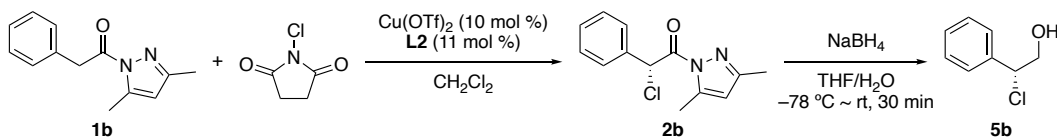


A mixture of **L2** (15.1 mg, 0.033 mmol) and copper(II) triflate (10.9 mg, 0.030 mmol) in a 20 mL shlenk flask were dissolved in acetonitrile (0.5 mL, dried over 4A molecular sieves). After stirring for 10 minutes, the solution was concentrated under reduced pressure at room temperature. To the residue were added **1b**, CH<sub>2</sub>Cl<sub>2</sub> (1.5 mL) and, *N*-chlorosuccinimide (NCS, 44.1 mg, 0.33 mmol), and the mixture was stirred at 0 °C to temperature for 3 h. The reaction mixture was filtered through neutral silica short column (*n*-hexane/EtOAc = 1/1). To a reaction mixture was added dry methanol (1.5 mL) and the reaction mixture was stirred at room temperature for 2 h. The reaction mixture was filtered through a neutral silica short column (*n*-hexane/EtOAc = 10/1). After evaporation of the organic solvent under reduced pressure, the crude mixture was purified by neutral silica gel column chromatography (*n*-hexane/EtOAc = 20/1) to give the desired product **4b** (48.9 mg, 88% yield).<sup>[6]</sup> The enantiomeric excess (ee) was determined through chiral HPLC analysis.



**Methyl (*R*)-2-chloro-2-phenylacetate (4b):** [ $\alpha$ ]<sub>D</sub><sup>24</sup> = -113.0 (*c* 0.74, CHCl<sub>3</sub>, 95% ee) [lit.<sup>7</sup> [ $\alpha$ ]<sub>D</sub> = -87.1 (*c* 0.74, CHCl<sub>3</sub>, 87% ee for *R* enantiomer)]; <sup>1</sup>H NMR (400 MHz, CDCl<sub>3</sub>)  $\delta$  7.51–7.48 (m, 2H), 7.41–7.35 (m, 3H), 5.37 (s, 1H), 3.78 (s, 3H); <sup>13</sup>C NMR (100 MHz, CDCl<sub>3</sub>)  $\delta$  169.0, 135.8, 129.5, 129.0 (2C), 128.1 (2C), 59.1, 53.5; HPLC analysis: OD-H, *n*-hexane/*i*-PrOH = 99/1, 1.0 mL/min, *t*<sub>R</sub> = 8.4 min (major), *t*<sub>R</sub> = 9.4 min (minor).

#### 4-5-6. Procedure for the transformation of **1b** to **5b**

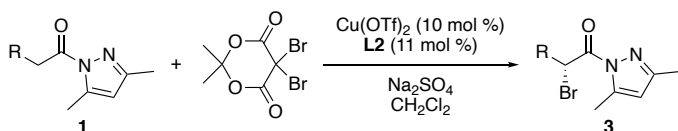


A mixture of **L2** (15.1 mg, 0.033 mmol) and copper(II) triflate (10.9 mg, 0.030 mmol) in a heat-gun dried 20 mL shlenk flask were dissolved in acetonitrile (0.5 mL, dried over 4A molecular sieves). After stirring for 10 minutes, the solution was concentrated under reduced pressure at room temperature. To the residue were added **1b**, CH<sub>2</sub>Cl<sub>2</sub> (1.5 mL) and, *N*-chlorosuccinimide (NCS, 44.1 mg, 0.33 mmol), and the mixture was stirred at 0 °C or temperature for 3 h. The reaction mixture was filtered through a neutral silica short column (*n*-hexane/EtOAc = 10/1). After evaporation of the organic solvent under reduced pressure, the crude mixture was moved to 20 mL round bottom flask, then THF (2.4 mL) and H<sub>2</sub>O (0.6 mL) were added to the shlenk flask and the reaction mixture

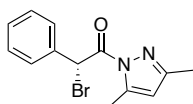
was cooled to  $-78\text{ }^{\circ}\text{C}$ . To the solution was added  $\text{NaBH}_4$  (45.4 mg, 1.20 mmol, 4.00 equiv) and the reaction flask was removed from acetone bath and stirred for 30 min at room temperature. After quenching with 1 M HCl, the resultant mixture was extracted with  $\text{CHCl}_3$ . The combined organic layer was washed with brine, and dried over  $\text{Na}_2\text{SO}_4$ . After evaporation of the organic solvent under reduced pressure, the crude mixture was purified by neutral silica gel column chromatography ( $n$ -hexane/EtOAc = 7/1 to 3/1) to give the product **5b** (35.8 mg, 76% yield over 2 steps, 96% ee) as a light yellow oil.

**(R)-2-chloro-2-phenylethan-1-ol (5b):**<sup>8</sup>  $[\alpha]_{\text{D}}^{24} = -145.2$  ( $c$  1.00,  $\text{CHCl}_3$ , 96% ee);  $^1\text{H NMR}$  (400 MHz,  $\text{CDCl}_3$ )  $\delta$  7.43–7.33 (m, 5H), 5.00 (dd,  $J = 7.4, 5.5$  Hz), 3.95–3.93 (m, 2H), 2.12 (brs, 1H);  $^{13}\text{C NMR}$  (100 MHz,  $\text{CDCl}_3$ )  $\delta$  137.9, 129.1, 129.0 (2C), 127.6 (2C), 68.1, 65.0; HPLC analysis: ID-3,  $n$ -hexane/ $i$ -PrOH = 9/1, 1.0 mL/min,  $t_R = 9.3$  min (minor),  $t_R = 12.2$  min (major).

#### 4-5-7. General procedure for the enantioselective $\alpha$ -bromination reaction of **1**

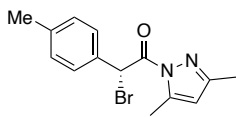


A mixture of **L2** (15.1 mg, 0.033 mmol) and copper(II) triflate (10.9 mg, 0.030 mmol) in a 20 mL schlenk flask in the presence of heat-gun dried  $\text{Na}_2\text{SO}_4$  (100 mg) was dissolved in acetonitrile (0.5 mL, dried over 4A molecular sieves). After stirring for 10 minutes, the solution was concentrated under reduced pressure at room temperature. To the residue were added **1**,  $\text{CH}_2\text{Cl}_2$  (1.0 mL) and, 5,5-dibromomeldrum's acid (99.6 mg in 0.5 mL of  $\text{CH}_2\text{Cl}_2$ , 0.33 mmol), and the mixture was stirred at  $-20\text{ }^{\circ}\text{C}$  to room temperature for 12-24 h. (For the reaction of **1b** and **1c**, started from  $-78\text{ }^{\circ}\text{C}$  for 5 minutes and then raise to  $-20\text{ }^{\circ}\text{C}$ ). The reaction mixture was filtered through a neutral silica short column ( $n$ -hexane/EtOAc = 1/1). After evaporation of the organic solvent under reduced pressure, the crude mixture was purified by neutral silica gel column chromatography ( $n$ -hexane/EtOAc = 30/1 to 9/1) to give the desired product **3**. The enantiomeric excess (ee) was determined through chiral HPLC analysis.

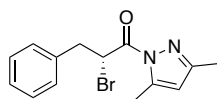


**(R)-2-Bromo-1-(3,5-dimethyl-1H-pyrazol-1-yl)-2-phenylethan-1-one (3b):**  $[\alpha]_{\text{D}}^{28} = -18.6$  ( $c$  1.00,  $\text{CHCl}_3$ , 96% ee);  $^1\text{H NMR}$  (400 MHz,  $\text{CDCl}_3$ )  $\delta$  7.69–7.67 (m, 2H), 7.39–7.32 (m, 3H), 6.98 (d,  $J = 0.9$  Hz, 1H), 5.99 (s, 1H), 2.53 (d,  $J = 0.9$  Hz, 3H), 2.24 (s, 3H);  $^{13}\text{C NMR}$  (100 MHz,  $\text{CDCl}_3$ )  $\delta$  167.7, 153.0, 145.1, 135.8, 129.5 (2C), 129.3, 128.8 (2C), 112.5, 45.8, 14.6, 14.0; IR (neat) 3031, 2928, 1731, 1588, 1377, 1356, 961, 693  $\text{cm}^{-1}$ ;  $\text{C}_{13}\text{H}_{13}\text{BrN}_2\text{NaO}$

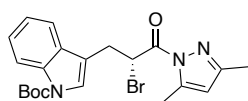
[M+Na]<sup>+</sup> 315.0103, found 315.0100; HPLC analysis: AS-3, *n*-hexane/*i*-PrOH = 99/1, 1.0 mL/min, *t*<sub>R</sub> = 6.1 min (minor), *t*<sub>R</sub> = 7.3 min (major).



**(R)-2-Bromo-1-(3,5-dimethyl-1H-pyrazol-1-yl)-2-(*p*-tolyl)ethan-1-one (3c):** [ $\alpha$ ]<sup>27</sup><sub>D</sub> = -10.8 (*c* 1.00, CHCl<sub>3</sub>, 95% ee); <sup>1</sup>H NMR (400 MHz, CDCl<sub>3</sub>)  $\delta$  7.57 (d, *J* = 7.7 Hz, 2H), 7.17 (d, *J* = 8.2 Hz, 2H), 6.96 (s, 1H), 5.99 (s, 1H), 2.53 (s, 3H), 2.33 (s, 3H), 2.23 (s, 3H); <sup>13</sup>C NMR (100 MHz, CDCl<sub>3</sub>)  $\delta$  167.7, 152.9, 145.1, 139.4, 132.8, 129.6 (2C), 129.4 (2C), 112.4, 45.9, 21.4, 14.6, 14.4, 14.0; IR (neat) 3650, 3032, 1734, 1385, 1362, 961, 751 cm<sup>-1</sup>; HRMS (ESI<sup>+</sup>) calcd for C<sub>14</sub>H<sub>15</sub>BrN<sub>2</sub>NaO [M+Na]<sup>+</sup> 329.0260, found 329.0253; HPLC analysis: AS-3, *n*-hexane/*i*-PrOH = 99/1, 1.0 mL/min, *t*<sub>R</sub> = 6.1 min (minor), *t*<sub>R</sub> = 6.7 min (major).

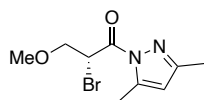


**(R)-2-Bromo-1-(3,5-dimethyl-1H-pyrazol-1-yl)-3-phenylpropan-1-one (3j):** [ $\alpha$ ]<sup>25</sup><sub>D</sub> = -48.0 (*c* 1.00, CHCl<sub>3</sub>, 77% ee); <sup>1</sup>H NMR (400 MHz, CDCl<sub>3</sub>)  $\delta$  7.31–7.22 (m, 5H), 5.97 (s, 1H), 5.94 (d, *J* = 7.8 Hz, 1H), 3.61 (dd, *J* = 14.2, 7.8 Hz, 1H), 3.35 (dd, *J* = 14.2, 7.4 Hz, 1H), 2.52 (d, *J* = 0.9 Hz, 3H), 2.21 (s, 3H); <sup>13</sup>C NMR (100 MHz, CDCl<sub>3</sub>)  $\delta$  168.9, 152.9, 144.8, 137.2, 129.6 (2C), 128.7 (2C), 127.2, 112.3, 44.6, 40.3, 14.5, 14.0; IR (neat) 1726, 1588, 1382, 962, 742, 700 cm<sup>-1</sup>; HRMS (ESI<sup>+</sup>) calcd for C<sub>14</sub>H<sub>15</sub>BrN<sub>2</sub>NaO [M+Na]<sup>+</sup> 329.0260, found 329.0256; HPLC analysis: OD-3, *n*-hexane/*i*-PrOH = 99/1, 0.5 mL/min, *t*<sub>R</sub> = 12.4 min (major), *t*<sub>R</sub> = 16.0 min (minor).

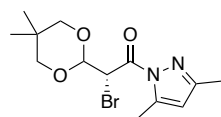


**tert-Butyl (R)-3-(2-bromo-3-(3,5-dimethyl-1H-pyrazol-1-yl)-3-oxopropyl)-1H-indole-1-carboxylate (3k):** [ $\alpha$ ]<sup>25</sup><sub>D</sub> = -27.2 (*c* 1.00, CHCl<sub>3</sub>, 77% ee); <sup>1</sup>H NMR (400 MHz, CDCl<sub>3</sub>)  $\delta$  8.11 (d, *J* = 6.9 Hz, 1H), 7.65 (d, *J* = 7.3 Hz, 1H), 7.50 (s, 1H), 7.36–7.22 (m, 2H), 6.03 (t, *J* = 6.9 Hz, 1H), 5.98 (s, 1H), 3.72 (dd, *J* = 15.1, 8.2 Hz, 1H), 3.44 (dd, *J* = 15.1, 6.4 Hz, 1H), 2.52 (d, *J* = 0.9 Hz, 3H), 2.21 (s, 3H), 1.65 (s, 9H); <sup>13</sup>C NMR (100 MHz, CDCl<sub>3</sub>)  $\delta$  169.0, 153.0, 149.7, 144.8, 135.4, 130.1, 124.7, 124.6, 124.6, 122.7, 119.1, 116.3, 115.4, 112.4, 43.4, 30.3, 28.3 (3C), 14.5, 14.0; IR (film) 3734, 3649, 1733, 1541, 1507, 1357, 772 cm<sup>-1</sup>; HRMS (ESI<sup>+</sup>) calcd for C<sub>21</sub>H<sub>24</sub>BrN<sub>3</sub>NaO<sub>3</sub> [M+Na]<sup>+</sup> 468.0893, found 468.0873; HPLC analysis: OD-3, *n*-hexane/*i*-PrOH = 99/1, 1.0 mL/min, *t*<sub>R</sub> = 6.9 min

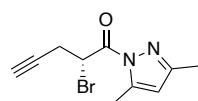
(major),  $t_R = 8.0$  min (minor).



**(R)-2-Bromo-1-(3,5-dimethyl-1H-pyrazol-1-yl)-3-methoxypropan-1-one (31):**  $[\alpha]_D^{25} = -54.0$  ( $c$  1.00,  $\text{CHCl}_3$ , 79% ee);  $^1\text{H}$  NMR (400 MHz,  $\text{CDCl}_3$ )  $\delta$  6.02 (d,  $J = 0.9$  Hz, 1H), 5.86 (dd,  $J = 8.7, 5.5$  Hz, 1H), 4.09 (dd,  $J = 10.1, 8.7$  Hz, 1H), 3.82 (dd,  $J = 10.1, 5.5$  Hz, 1H), 3.42 (s, 3H), 2.56 (d,  $J = 0.9$  Hz, 3H), 2.25 (s, 3H);  $^{13}\text{C}$  NMR (100 MHz,  $\text{CDCl}_3$ )  $\delta$  168.1, 153.1, 144.9, 112.5, 72.9, 59.5, 40.1, 15.0, 14.0; IR (film) 2928, 1729, 1382, 1307, 1114, 956  $\text{cm}^{-1}$ ; HRMS (ESI+) calcd for  $\text{C}_9\text{H}_{13}\text{BrN}_2\text{NaO}_2$   $[\text{M}+\text{Na}]^+$  283.0053, found 283.0036; HPLC analysis: OD-3,  $n$ -hexane/ $i$ -PrOH = 99/1, 1.0 mL/min,  $t_R = 5.7$  min (major),  $t_R = 7.6$  min (minor).

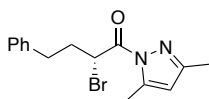


**(R)-2-Bromo-2-(5,5-dimethyl-1,3-dioxan-2-yl)-1-(3,5-dimethyl-1H-pyrazol-1-yl)ethan-1-one (3s):**  $[\alpha]_D^{24} = -1.2$  ( $c$  1.00,  $\text{CHCl}_3$ , 91% ee);  $^1\text{H}$  NMR (400 MHz,  $\text{CDCl}_3$ )  $\delta$  6.01 (s, 1H), 5.01 (d,  $J = 6.9$  Hz, 1H), 5.82 (d,  $J = 6.9$  Hz, 1H), 3.74 (dd,  $J = 11.0, 2.7$  Hz, 1H), 3.64 (dd,  $J = 11.0, 2.8$  Hz, 1H), 3.53 (dd,  $J = 11.0, 5.5$  Hz, 2H), 2.54 (s, 3H), 2.24 (s, 3H), 1.21 (s, 3H), 0.75 (s, 3H);  $^{13}\text{C}$  NMR (100 MHz,  $\text{CD}_3\text{CN}$ )  $\delta$  168.1, 153.1, 144.9, 112.5, 72.9, 59.5, 40.1, 15.0, 14.0; IR (film) 1733, 1541, 1507, 1457, 1356  $\text{cm}^{-1}$ ; HRMS (ESI+) calcd for  $\text{C}_{13}\text{H}_{19}\text{BrN}_2\text{NaO}_3$   $[\text{M}+\text{Na}]^+$  353.0471, found 353.0471; HPLC analysis: OD-3,  $n$ -hexane/ $i$ -PrOH = 99/1, 1.0 mL/min,  $t_R = 6.8$  min (major),  $t_R = 10.1$  min (minor).



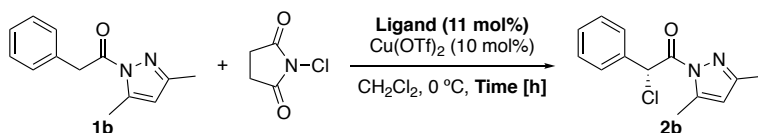
**(R)-2-Bromo-1-(3,5-dimethyl-1H-pyrazol-1-yl)pent-4-yn-1-one (3o):**  $[\alpha]_D^{25} = -61.2$  ( $c$  1.00,  $\text{CHCl}_3$ , 82% ee);  $^1\text{H}$  NMR (400 MHz,  $\text{CDCl}_3$ )  $\delta$  6.03 (s, 1H), 5.82 (dd,  $J = 7.8, 6.9$  Hz, 1H), 3.16 (ddd,  $J = 17.0, 7.8, 2.7$  Hz, 1H), 3.00 (ddd,  $J = 17.4, 7.3, 2.8$  Hz, 1H), 2.56 (d,  $J = 0.9$  Hz, 3H), 2.26 (s, 3H), 2.11 (t,  $J = 2.8$  Hz, 1H);  $^{13}\text{C}$  NMR (100 MHz,  $\text{CDCl}_3$ )  $\delta$  168.0, 153.2, 144.9, 112.6, 79.7, 71.4, 40.7, 24.6, 14.4, 14.1; IR (neat) 3293, 1726, 1385, 1330  $\text{cm}^{-1}$ ; HRMS (ESI+) calcd for  $\text{C}_{10}\text{H}_{11}\text{BrN}_2\text{NaO}$   $[\text{M}+\text{Na}]^+$  276.9947, found 276.9950s; HPLC analysis: OD-3,  $n$ -hexane/ $i$ -PrOH = 99/1, 1.0 mL/min,  $t_R = 7.4$  min (major),  $t_R = 10.1$  min (minor).





**(R)-2-Bromo-1-(3,5-dimethyl-1H-pyrazol-1-yl)-4-phenylbutan-1-one (3t):**  $[\alpha]_D^{24} = -7.6$  ( $c$  1.00,  $\text{CHCl}_3$ , 61% ee);  $^1\text{H NMR}$  (400 MHz,  $\text{CDCl}_3$ )  $\delta$  7.31–7.18 (m, 5H), 6.00 (s, 1H), 5.73 (dd,  $J = 7.8, 6.4$  Hz, 1H), 2.93–2.82 (m, 1H), 2.81–2.70 (m, 1H), 2.58–2.35 (m, 2H), 2.53 (d,  $J = 0.9$  Hz, 3H), 2.23 (s, 3H);  $^{13}\text{C NMR}$  (100 MHz,  $\text{CDCl}_3$ )  $\delta$  169.2, 152.8, 144.9, 140.3, 128.6 (2C), 128.6 (2C), 126.4, 112.4, 44.6, 36.0, 33.6, 14.5, 14.0; IR (neat) 1730, 1381, 772  $\text{cm}^{-1}$ ; HRMS (DART+) calcd for  $\text{C}_{15}\text{H}_{18}\text{BrN}_2\text{O}$   $[\text{M}+\text{H}]^+$  321.0603, found 321.06031; HPLC analysis: IC-3,  $n$ -hexane/EtOAc = 24/1, 0.5 mL/min,  $t_R = 11.5$  min (minor),  $t_R = 13.2$  min (major).

#### 4-5-8. The details of reaction progress analysis of chlorination of **1b** with L1, L2, L8, or L9 (Fig. 1)



**Procedure for the time-course reaction progresses:** A mixture of **L** (0.033 mmol) and copper(II) triflate (10.9 mg, 0.030 mmol) in a 20 mL shlenk flask was dissolved in acetonitrile (0.5 mL, dried over 4A molecular sieves). After stirring for 10 minutes, the solution was concentrated under reduced pressure at room temperature. To the residue were added phenanthrene (25.7 mg, 0.15 mmol) as internal standard and **1b** (44.3 mg, 0.30 mmol),  $\text{CH}_2\text{Cl}_2$  (1.5 mL) and,  $N$ -chlorosuccinimide (NCS, 44.1 mg, 0.33 mmol). The mixture was stirred at 0 °C to temperature. The sampling of the reaction mixture at the corresponding time was filtered through a neutral silica short column ( $n$ -hexane/EtOAc = 1/1). After evaporation of the organic solvent under reduced pressure, the NMR yield of **2b** was calculated based on an internal standard.

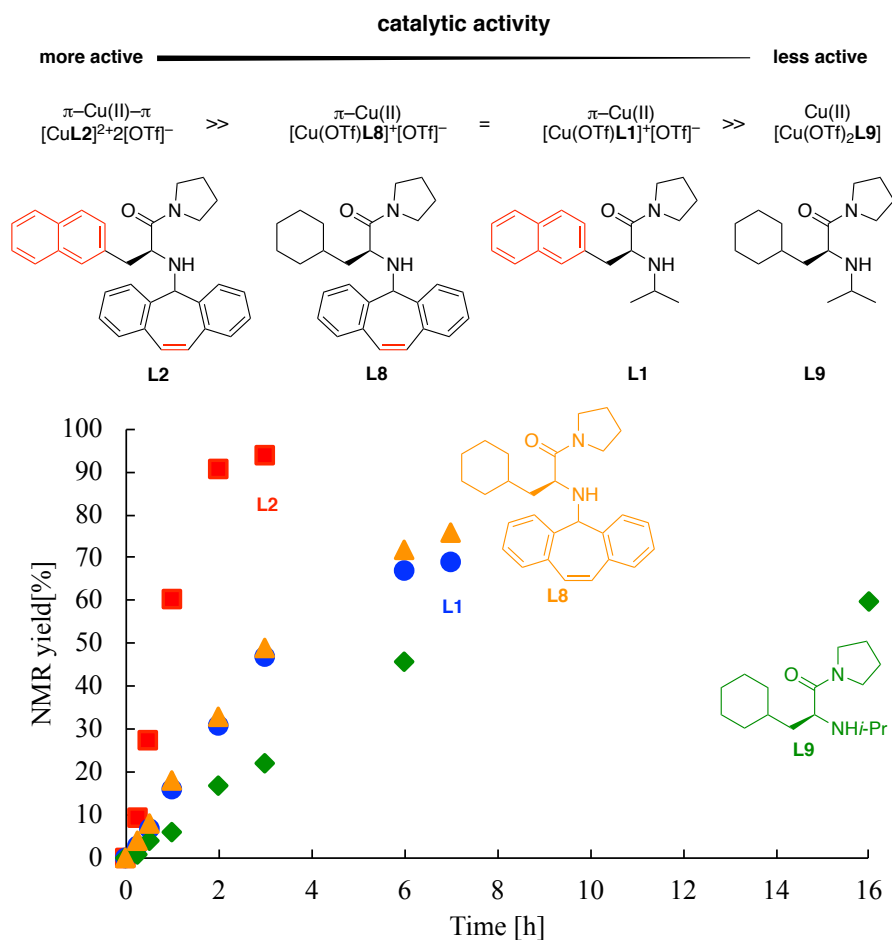


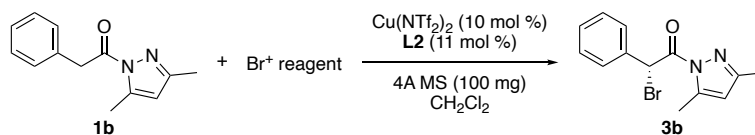
**Figure. 1** Reaction progress analysis of chlorination of **1b** with different ligands

**Table S1. The details of the chlorination of 1b**

Entry	0	1	2	3	4	5	6	7	7
Time [h]	0	0.25	0.5	1	2	3	6	7	16
<b>L2</b>	0	9	27	60	91	94	–	–	–
<b>L1</b>	0	3	7	16	31	47	67	69	–
<b>L8</b>	0	4	8	18	33	49	72	76	–
<b>L9</b>	0	1	4	6	17	22	46	–	60

#### 4-5-9. Optimization of the $\alpha$ -bromination reaction of **1b**

**Table S2. Screening of the brominating reagents<sup>a</sup>**



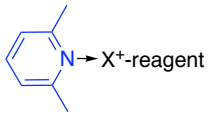
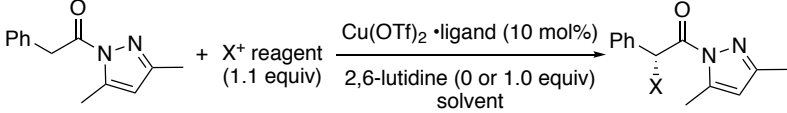
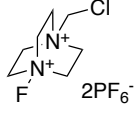
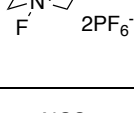
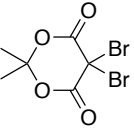
Entry	Temperature, Time	Br <sup>+</sup> reagent	<b>3b</b>	
			Conversion (%) <sup>b</sup>	Ee (%) <sup>c</sup>
1	0 °C, 12 h		>99 (79) <sup>d</sup>	0
2	0 °C, 12 h		>99 (60) <sup>d</sup>	0
3	0 °C, 12 h		>99 (0) <sup>d</sup>	–
4	0 °C, 12 h		95 (95) <sup>d</sup>	25
5	–20 °C, 12 h		95 (95) <sup>d</sup>	25
6	–20 °C, 12 h		>99 (0) <sup>d</sup>	–
7	–20 °C, 12 h, then 0 °C, 12 h, then rt, 36 h		30 (30) <sup>d</sup>	–
8	–20 °C, 12 h		83–86 <sup>e</sup>	70–86
9 <sup>f</sup>	–20 °C, 12 h		82 <sup>e</sup>	79
10 <sup>g</sup>	–20 °C, 12 h		27	24
11 <sup>h</sup>	–78 °C, 5 min, then –20 °C, 12 h		87 <sup>e</sup>	96

<sup>a</sup> Unless otherwise noted, **1b** (0.3 mmol), Br<sup>+</sup> reagent (1.1 equiv),  $\text{Cu}(\text{NTf}_2)_2$  (10 mol%), **L2** (11 mol%), and 4A MS

(100 mg) were added in CH<sub>2</sub>Cl<sub>2</sub> (1.5 mL). <sup>b</sup> Based on NMR analysis. <sup>c</sup> The ee of **3b** determined by HPLC analysis. <sup>d</sup> The ratio of **3b** based on NMR analysis. <sup>e</sup> Isolated yield. <sup>f</sup> 0.55 equivalent of Br<sup>+</sup> reagent was added. <sup>g</sup> **1b** (0.3 mmol), Br<sup>+</sup> reagent (1.1 equiv), Cu(OTf)<sub>2</sub> (10 mol%), **L2** (11 mol%), and Na<sub>2</sub>SO<sub>4</sub> (100 mg) were added in CH<sub>2</sub>Cl<sub>2</sub> (1.5 mL). <sup>h</sup> **1b** (0.3 mmol), Br<sup>+</sup> reagent (1.1 equiv) dissolved in CH<sub>2</sub>Cl<sub>2</sub> (0.5 mL), Cu(OTf)<sub>2</sub> (10 mol%), **L2** (11 mol%), and Na<sub>2</sub>SO<sub>4</sub> (100 mg) were added in CH<sub>2</sub>Cl<sub>2</sub> (1.0 mL).

#### 4-5-10. The investigation of halogen bonding

**Table S3. Effect of 2,6-lutidine for the enantioselective  $\alpha$ -halogenation**

		# Halogen bonding between 2,6-lutidine and X <sup>+</sup> -reagent: F <sup>+</sup> << Cl <sup>+</sup> , Br <sup>+</sup>		# Effect of 2,6-lutidine on Cu(OTf) <sub>2</sub> · <b>L1</b> -catalyzed halogenations: F <sup>+</sup> (accelerate) >> Cl <sup>+</sup> , Br <sup>+</sup> (suppress)	
					
X <sup>+</sup> reagent	conditions	Ligand	2,6-lutidine	yield (%)	ee (%)
	MeCN, 4A MS	<b>L1</b>	0	7	–
	–40 °C, 1 h	<b>L1</b>	1.0	98	91
	MeCN, 4A MS	<b>L2</b>	0	26	–
	–40 °C, 1 h	<b>L2</b>	1.0	92	80
NCS	CH <sub>2</sub> Cl <sub>2</sub>	<b>L1</b>	0	54	32
	0 °C, 3 h	<b>L1</b>	1.0	8	38
	CH <sub>2</sub> Cl <sub>2</sub> , Na <sub>2</sub> SO <sub>4</sub>	<b>L1</b>	0	32	21
	–20 °C, 12 h	<b>L1</b>	1.0	3	–

**NMR experiment for the investigation of halogen bonding:** A mixture of X<sup>+</sup> reagent (0.1 mmol) and 2,6-lutidine (13  $\mu$ L, 0.1 mmol) (or individuals) in NMR tube was dissolved in CD<sub>2</sub>Cl<sub>2</sub> or CD<sub>3</sub>CN (1.0 mL). The measurement was conducted at –40°C, –20 °C, 0 °C, 20 °C, respectively.

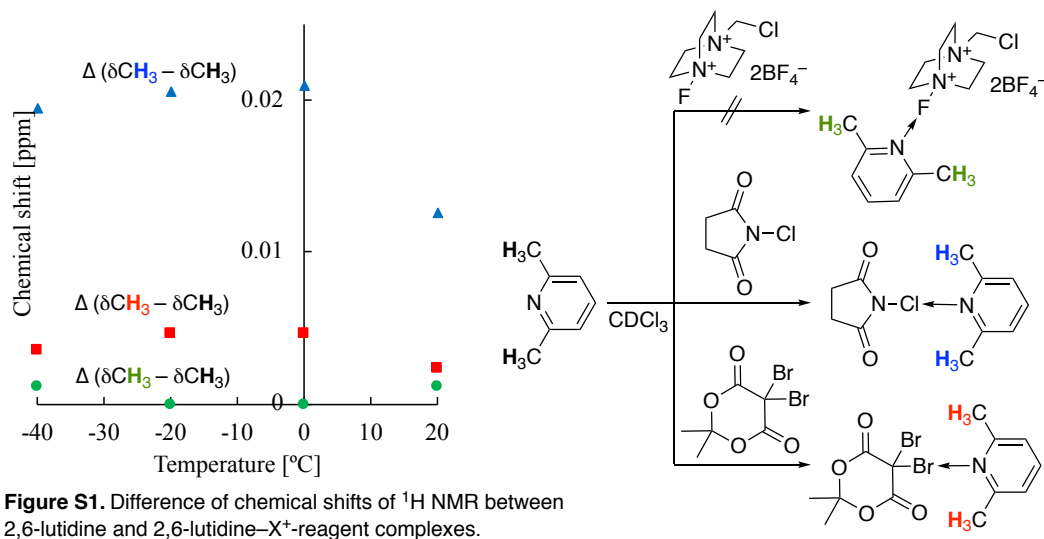
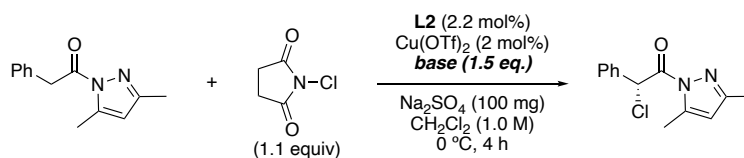


**Table S4.** The details of halogen bonding

Temperature [°C]	20	0	-20	-40
NCS + lutidine	2.4723	2.4715	2.4631	2.4517
Lutidine	2.4597	2.4505	2.4425	2.4322
Delta	0.0126	0.021	0.0206	0.0195
Br + lutidine	2.4620	2.4551	2.4471	2.4357
lutidine	2.4597	2.4505	2.4425	2.4322
delta	0.0023	0.0046	0.0046	0.0035
Selectfluor + lutidine	2.4280	2.4223	2.4142	2.4074
lutidine	2.4268	2.4223	2.4142	2.4062
delta	0.0012	0	0	0.0012

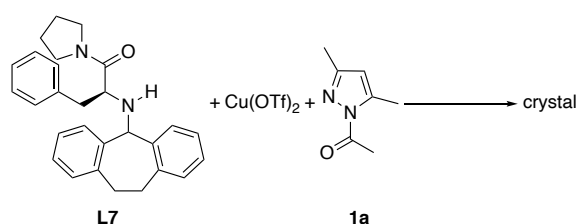
#### 4-5-11. Screening of bases

**Table S5.** Screening of bases on the enantioselective α-chlorination



Entry	Base	Yield (%)	<i>ee</i> (%)
1	none	39	92
2	K <sub>2</sub> CO <sub>3</sub>	NR	–
3	NEt <sub>3</sub>	11	–
4	Na <sub>2</sub> HPO <sub>4</sub>	18	88
5	NMM	24	0

#### 4-5-12. X-ray diffraction analysis of L7•Cu(OTf)<sub>2</sub>•1a complex



**Preparation of a crystal sample:** L7 (82.1 mg, 0.20 mmol), Cu(OTf)<sub>2</sub> (72.3 mg, 0.20 mmol), and 1a (27.3 mg, 0.20 mmol) were placed in a Schlenk test tube under argon atmosphere and dissolved in dry acetonitrile (1 mL). Then the solution was stirred for 1 h at room temperature. The volatile was removed *in vacuo*, and then ethyl acetate (1 mL) was added to give a clear solution, and *n*-hexane was added until the white precipitate appeared at room temperature. The mixture was then heated with a drier to give a clear solution. The solution was passed through a membrane filter (0.50 μm pore size). The solution was settled at room temperature, and a single crystal was obtained within a week.

**Crystal data of L7•Cu(OTf)<sub>2</sub>•1a complex (Figure 2a):** Formula C<sub>41</sub>H<sub>48</sub>CuF<sub>6</sub>N<sub>4</sub>O<sub>10</sub>S<sub>2</sub>, blue, orthorhombic, space group *P21 21 21*, *a* = 14.6616(11) Å, *b* = 15.7092(13) Å, *c* = 19.6198(16) Å, α = 90.0000°, β = 90.0000°, γ = 90.0000°, *V* = 4518.9(6) Å<sup>3</sup>, *Z* = 4, ρ<sub>calc</sub> = 1.468 g/cm<sup>3</sup>, λ(MoKα) = 0.71075 Å, *T* = 123 K. 10264 reflections collected, and 605 parameters were used for the solution of the structure. *R*<sub>1</sub> = 0.0411 and *wR*<sub>2</sub> = 0.1084. GOF = 1.033. Flack *x* parameter = 0.003(7).—Crystallographic data (excluding structure factors) for the structure reported in this paper have been deposited with the Cambridge Crystallographic Data Centre as supplementary publication no. CCDC-2106621. Copies of the data can be obtained free of charge on application to CCDC, 12 Union Road, Cambridge CB2 1EZ, UK [Fax: int. code + 44(1223)336-033; E-mail: deposit@ccdc.cam.ac.uk; Web

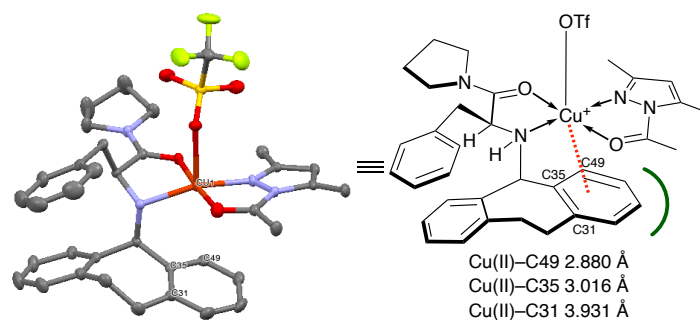
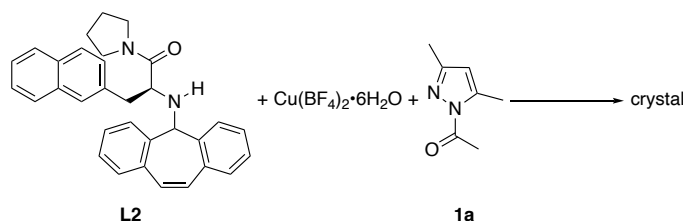


**Figure 2b.** X-ray diffraction analysis of a 1:1:1 complex of **L7**•Cu(OTf)<sub>2</sub>•**1a** (ORTEP Drawing)

#### 4-5-13. X-ray diffraction analysis of **L2**•Cu(BF<sub>4</sub>)<sub>2</sub>•**1a** complex



**Preparation of a crystal sample:** **L2** (45.9 mg, 0.10 mmol), Cu(BF<sub>4</sub>)<sub>2</sub>•6H<sub>2</sub>O (34.5 mg, 0.10 mmol), and **1a** (13.8 mg, 0.10 mmol) were placed in a Schlenk test tube under argon atmosphere and dissolved in dry acetonitrile (1 mL). Then the solution was stirred for 1 h at room temperature. The volatile was removed *in vacuo*, and then CHCl<sub>3</sub>/ethyl acetate/CH<sub>3</sub>CN = v/v, 10/8/5 was added to give a clear solution at room temperature. The solution was passed through a membrane filter (0.50 μm pore size). The solution was settled at room temperature, and a single crystal was obtained within a week.

**Crystal data of **L7**•Cu(OTf)<sub>2</sub>•**1a** complex (Figure 2c):** Formula C<sub>40</sub>H<sub>41</sub>B<sub>2</sub>Cl<sub>3</sub>CuF<sub>8</sub>N<sub>4</sub>O<sub>2</sub>, blue, orthorhombic, space group *P21 21 21*, *a* = 13.070(2) Å, *b* = 14.339(3) Å, *c* = 21.988(4) Å, α = 90.0000°, β = 90.0000°, γ = 90.0000°, *V* = 4120.8(13) Å<sup>3</sup>, *Z* = 4, ρ<sub>calc</sub> = 1.535 g/cm<sup>3</sup>, λ(MoKα) = 0.71075 Å, *T* = 123 K. 9455 reflections collected, and 543 parameters were used for the solution of the structure. *R*<sub>1</sub> = 0.0659 and *wR*<sub>2</sub> = 0.1912. GOF = 1.009. Flack *x* parameter = 0.012(7).—Crystallographic data (excluding structure factors) for the structure reported in this paper have been deposited with the Cambridge Crystallographic Data Centre as supplementary publication no. CCDC-2106620. Copies of the data can be obtained free of charge on application to CCDC, 12 Union Road, Cambridge CB2 1EZ, UK [Fax: int. code + 44(1223)336-033; E-mail: [deposit@ccdc.cam.ac.uk](mailto:deposit@ccdc.cam.ac.uk); Web page: <http://www.ccdc.cam.ac.uk/pages/Home.aspx>]. Due to close contacts between protons of highly disordered

terminal methyl groups with high thermal parameters (Alert level A).

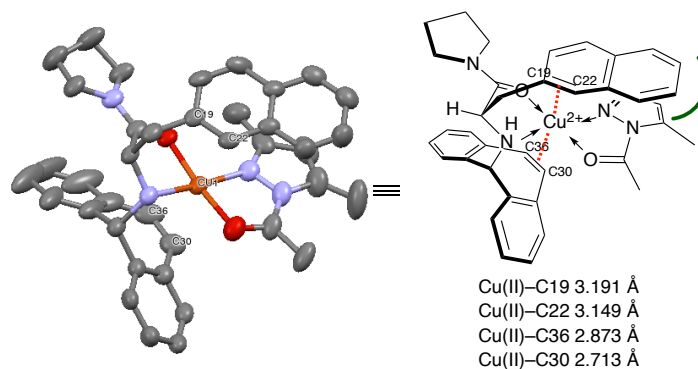


**Figure 2c.** X-ray diffraction analysis of a 1:1:1 complex of **L2**•Cu(BF<sub>4</sub>)<sub>2</sub>•**1a** (ORTEP Drawing)

#### 4-5-14. ESR spectral analyses of **L2**•Cu(OTf)<sub>2</sub>•**1a** and **L5**•Cu(OTf)<sub>2</sub>•**1a** complexes

##### 1. Sample preparation

In the presence of heat-gun-dried pellet 4A molecular sieves (100 mg), **L1** (0.1 mmol, 31.0 mg) or **L2** (0.1 mmol, 45.9 mg), Cu(OTf)<sub>2</sub> (0.1mmol, 36.1 mg) and **1a** (0.1 mmol, 13.8 mg) were dissolved in 3.0 mL of acetonitrile (dried over activated 4A molecular sieves). The solution was stirred for 10 min under N<sub>2</sub> and carefully into quartz ESR tubes of i. d. 1 mm x o. d. 3 mm filled enough to the height of ESR cavity and were degassed and filled with N<sub>2</sub> gas before sealing the tubes.

##### 2. ESR measurement

The ESR spectra were measured at 30 K with JEOL JES-RE1X spectrometer equipped with liquid helium cryostat (ES-CT470). The sample tubes were set to the ESR cavity, and their temperatures were controlled by the cryostat. Microwave power of 0.1 mW at 30 K was adequate to avoid spectral saturation. The sweep width of a magnetic field was set to 310±40 mT. Microwave frequency (ca. 9.14 GHz) and magnetic field of the spectrometer were monitored using a microwave frequency counter (Hewlett-Packard, 53150A) and an NMR field meter (Echo Electronics Co. Ltd., EFM-2000AX), respectively.

##### 3. ESR simulation

The observed ESR spectra were simulated with “pepper” function for solid state cw ESR in Easyspin software v5.2.30.<sup>9</sup> ESR parameters of axial symmetric *g*-values (*g*<sub>||</sub>, *g*<sub>⊥</sub>), axial symmetric hyperfine coupling constants



( $A_{\parallel}$ ,  $A_{\perp}$ ), a line width of Lorentzian and Gaussian line shapes and the ratio of both lines were optimized with “esfit” program for least square fitting in the Easyspin. The results of simulations are summarized in Figure 3 and Table S6.

**Table S6. Best-fit ESR parameters of L1•Cu(OTf)<sub>2</sub>•1a and L2•Cu(OTf)<sub>2</sub>•1a**

Compounds	g-value			A-value $\times 10^{-4}$ / $\text{cm}^{-1}$		
	$g_{\text{iso}}$	$g_{\parallel}$	$g_{\perp}$	$A_{\text{iso}}$	$A_{\parallel}$	$A_{\perp}$
<b>L1•Cu(OTf)<sub>2</sub>•1a</b>	2.1351	2.2765	2.0588	62.9	171.8	8.5
<b>L2•Cu(OTf)<sub>2</sub>•1a</b>	2.1179	2.2475	2.0531	69.9	182.9	13.5

The simulated spectra in Fig. 3 shown in dotted lines were coincide with the experimental ones (solid line) very well. The order of  $g_{\parallel} > g_{\perp} > g_e$  ( $g$  value of free electron as 2.002319) for both compounds indicates that the ground state of  $d$ -orbital of the Cu atom in their compounds is  $d_{x^2-y^2}$ , which is related to the coordinate structures of elongated octahedral, square pyramidal or square planner.<sup>10</sup> Sakurai *et al.* categorized the coordinate structures of Cu(II) complexes from the relationship between  $g_{\text{iso}}$  and  $A_{\text{iso}}$ .<sup>11</sup> According to their categorization,  $g_{\text{iso}}$  and  $A_{\text{iso}}$  values of 2.1179 and  $69.9 \times 10^{-4} \text{ cm}^{-1}$  for **L2•Cu(OTf)<sub>2</sub>•1a** correspond to the structure of axially-coordinate square planar, and those of 2.1351 and  $62.9 \times 10^{-4} \text{ cm}^{-1}$  for **L1•Cu(OTf)<sub>2</sub>•1a**. to the structures between square planar and tetrahedral. These ESR parameters indicate that the coordination structure of **L1•Cu(OTf)<sub>2</sub>•1a** changes from axially-coordinate square planar (6-coordinate) of **L2•Cu(OTf)<sub>2</sub>•1a** to axially-coordinate tetrahedrally distorted (6-coordinate) depending on two different ligands at the apical position, naphthyl group and <sup>-</sup>OTf.

#### 4-5-15. References

- (1) Hori, M.; Sakakura, A.; Ishihara, K. *J. Am. Chem. Soc.* **2014**, *136*, 13198–13201.
- (2) Ishihara, K.; Nishimura, K.; Yamakawa, K. *Angew. Chem. Int. Ed.* **2020**, *59*, 17641–17647.
- (3) Zhang, Y.; Lu, Z.; Desai, A.; Wulff, W. D. *Org. Lett.* **2008**, *10*, 5429–5432.
- (4) Ishihara, K.; Fushimi, M. *J. Am. Chem. Soc.* **2008**, *130*, 7532–7533.
- (5) Coste, A.; Toumi, M.; Wright, K.; Razafimahaléo, V.; Couty, F.; Marrot, J.; Evano, G. *Org. Lett.* **2008**, *10*, 3841–3844.
- (6) Tietze, L.-F.; Meier, H.; Voß, E. *Synthesis* **1988**, *4*, 274–277.
- (7) Hamashima, Y.; Nagi, T.; Shimizu, R.; Tsuchimoto, T.; Sodeoka, M.; *Eur. J. Org. Chem.* **2011**, 3675–3678.
- (8) Yang, L.; Li, X.; Wang, Y.; Li, C.; Wu, X.; Zhang, Z.; Xie, X. *Tetrahedron* **2020**, *76*, 131114.
- (9) Stoll, S.; Schweiger, A. *J. Mag. Reson.* **2006**, *178*, 42–55.
- (10) Garribba, E.; Micera, G. *J. Chem. Edu.* **2006**, *83*, 1229–1232.
- (11) Sawada, T.; Fukumaru, K.; Sakurai, H. *Chem. Pharm. Bull.* **1996**, *44*, 1009–1016.

## Research Achievement

### • Publications

- (1) “Enantio- and Site-selective  $\alpha$ -Fluorination of *N*-Acyl-3,5-dimethylpyrazoles Catalyzed by Chiral  $\pi$ -Cu(II) Complexes”  
Ishihara, K.; Nishimura, K.; Yamakawa, K. *Angew. Chem. Int. Ed.* **2020**, *59*, 17641–17647.  
紹介記事: 名古屋大学プレスリリース(2020年7月14日)  
[日本の研究.com\(2020年7月15日\)](#)  
[化学工業日報\(2020年7月15日、第3面\)](#)、  
[毎日新聞\(2020年8月31日、第21面\)](#)
- (2) “A  $\pi$ -Cu(II)- $\pi$  Complex as an Extremely Active Catalyst for Enantioselective  $\alpha$ -Halogenation of *N*-Acyl-3,5-dimethylpyrazoles”  
Nishimura, K.; Wang, Y.; Ogura, Y.; Ishihara, K. *ACS. Catal.* **2022**, *12*, 1012–1017.
- (3) “Thorpe–Ingold Effect on High-Performance Chiral  $\pi$ -Copper(II) Catalyst”  
Nishimura, K.; Ishihara, K. *manuscript under review*.

### • Award

- (1) 日本化学会東海支部長賞 (2017年3月27日)
- (2) 第7回CSJ化学フェスタ 優秀ポスター発表賞 (2017年11月13日)
- (3) 第113回有機合成シンポジウム 優秀ポスター賞(2018年9月14日)
- (4) 鏡友会賞(2019年3月25日)
- (5) 独立行政法人日本学生支援機構 第一種奨学金 業績優秀者半額返還免除 (博士前期課程) (2019年5月31日)
- (6) 2019年度ホシザキ奨学金奨学生 (2019年7月～)
- (7) CSJ Student Presentation Award 2021 (March 31, 2021)
- (8) 名大鏡友会「博士学術賞」(2021年10月12日)
- (9) 第52回中部化学関係学協会支部連合秋季大会 (静岡)「VIP賞」(2021年11月30日)

## Conference Presentation

### • Oral Presentation

- (1) 「キラル $\pi$ -銅(II)触媒を用いるアシルピラゾールのエナンチオ選択的 $\alpha$ -ハロゲン化反応」  
○ 西村和揮、王彦兆、小倉義浩、山川勝也、石原一彰  
日本化学会第 97 春季年会、慶應義塾大学、2017 年 3 月 16 日[A 講演]
- (2) 「キラル $\pi$ -銅(II)触媒を用いるアシルピラゾールのエナンチオ選択的 $\alpha$ -フッ素化反応」  
○ 西村和揮、王彦兆、小倉義浩、山川勝也、石原一彰  
日本化学会第 98 春季年会、日本大学、2019 年 3 月 20 日[A 講演]
- (3) 「キラル $\pi$ -銅(II)触媒を用いる活性アミドのエナンチオ選択 $\alpha$ -フッ素化反応」  
○ 西村和揮、山川勝也、石原一彰  
日本化学会第 99 春季年会、甲南大学、2019 年 3 月 19 日[A 講演]
- (4) 「Enantio- and Site-selective  $\alpha$ -Fluorination of *N*-Acyl-3,5-dimethylpyrazoles Catalyzed by Chiral  $\pi$ -Cu(II) Complexes」  
○ Kazuki Nishimura, Katsuya Yamakawa, Kazuaki Ishihara  
日本化学会第 100 春季年会、東京理科大学、2020 年 3 月 23 日 [英語 B 講演]
- (5) 「Enantioselective  $\alpha$ -Halogenation of *N*-Acyl-3,5-Dimethylpyrazoles Catalyzed by Chiral  $\pi$ -Cu(II)- $\pi$  Complexes」  
○ Kazuki Nishimura, Yanzhao Wang, Yoshihiro Ogura, Kazuaki Ishihara  
日本化学会第 101 春季年会、A20-2am-08、オンライン方式、2021 年 3 月 20 日 [英語 B 講演]
- (6) 「キラル  $\pi$ -銅(II)- $\pi$  触媒によるアシルピラゾール類のエナンチオ選択的 $\alpha$ -ハロゲン化反応」  
○ 西村和揮、WANG Yanzhao、小倉義浩、石原一彰  
中部化学関係学協会支部連合秋季大会 (静岡)、B5-11、オンライン形式、2021 年 10 月 31 日

• Poster Presentation

- (1) 「キラル $\pi$ -銅(II)触媒を用いるアシルピラゾールのエナンチオ選択的 $\alpha$ -ハロゲン化反応」  
○ 西村和揮、王彦兆、小倉義浩、山川勝也、石原一彰  
第 52 会有機反応若手の会、鷹洞温泉 涼風荘、2017 年 7 月 12 日
  
- (2) 「Chiral  $\pi$ -Cu(II) Catalysts for Enantioselective  $\alpha$ -Halogenation of Acylpyrazoles」  
○ Kazuki Nishimura, Kazuaki Ishihara  
The 8th International Meeting on Halogen Chemistry (HALCHEM VIII), Inuyama International Sightseeing Center, 13th September, 2017 [国際会議]
  
- (3) 「キラル $\pi$ -銅(II)触媒を用いるアシルピラゾールのエナンチオ選択的 $\alpha$ -ハロゲン化反応」  
○ 西村和揮、石原 一彰  
日本化学会秋季事業第 7 回 CSJ 化学フェスタ、タワーホール船堀、2017 年 10 月 17 日
  
- (4) 「キラル $\pi$ -銅(II)触媒によるアシルピラゾールのエナンチオ選択的 $\alpha$ -ハロゲン化反応」  
○ 西村和揮、王彦兆、小倉義浩、山川勝也、石原一彰  
ITbM/IGER Chemistry Workshop 2017、名古屋大学、2017 年 11 月 6 日
  
- (5) 「Rational Design of Copper(II)-L-Amino Acid Derivative Catalysts for the Enantioselective  $\alpha$ -Halogenation Reaction」  
○ 西村和揮、王彦兆、小倉義浩、山川勝也、石原一彰  
名古屋大学 L 大学院・IGER 平成 29 年度年次報告会、名古屋大学・豊田講堂、2018 年 1 月 10 日
  
- (6) 「L-アミノ酸誘導体-銅(II)触媒によるキラル $\alpha$ -ハロアミドのエナンチオ選択的分岐合成」  
○ 西村和揮、王彦兆、小倉義浩、山川勝也、石原一彰  
第 113 回有機合成シンポジウム、名古屋大学、2018 年 6 月 6 日
  
- (7) 「キラル $\pi$ -銅(II)触媒を用いる $\alpha$ -ハロアミドのエナンチオ選択的分岐型合成」  
○ 西村和揮、王彦兆、小倉義浩、山川勝也、石原一彰  
第 51 会有機金属若手の会、京都レイクフォレストリゾート、2018 年 7 月 2 日
  
- (8) 「キラル $\pi$ -銅(II)触媒を用いるエナンチオ選択的 $\alpha$ -フッ素化反応」

○ 西村和揮、山川勝也、石原一彰

ITbM/IGER Chemistry Workshop 2018、名古屋大学、2018年12月10日

(9) 「キラル $\pi$ -銅(II)触媒を用いるエナンチオ選択的 $\alpha$ -フッ素化反応」

○ 西村和揮、山川勝也、石原一彰

GTR キックオフミーティング、名古屋大学、2019年1月8日

(10) 「キラル $\pi$ -銅(II)触媒を用いるエナンチオ選択的 $\alpha$ -フッ素化反応」

○ 西村和揮、山川勝也、石原一彰

第52回有機金属若手の会 夏の学校、倉敷せとうち児島ホテル、2019年6月24日

(11) 「キラル $\pi$ -銅(II)触媒によるアシルピラゾールのエナンチオ選択的 $\alpha$ -フッ素化反応の開発」

○ 西村和揮、山川勝也、石原一彰

長良川国際会議場&ぎふ長良川温泉ホテルパーク、2019年9月17-19日

(12) 「Enantioselective  $\alpha$ -halogenation of N-acyl-3,5-dimethylpyrazoles catalyzed by chiral  $\pi$ -Cu(II)- $\pi$  complexes」

○ Kazuki Nishimura, Yanzhao Wang, Yoshihiro Ogura, Akira Sakakura, Kazuaki Ishihara

GTR Annual Meeting 2020、P-102、名古屋大学、2021年1月9日

## Acknowledgements

I would like to express my grateful acknowledgment to my supervisors, Professor Kazuaki Ishihara whose encouragement and helpful suggestions have been indispensable to the completion of the present thesis.

I am indebted to Professor Manabu Hatano (Kobe Pharmaceutical University), Associate Professor Muhammet Uyanik, Dr. Takahiro Horibe, and Assistant Professor Shuhei Ohmura for their practical and fruitful discussions. I especially thank Dr. Katsuya Yamakawa for collaborative research. I am also very grateful to Associate Professor Jun Kumagai, Dr. Yanzhao Wang, and Dr. Yoshihiro Ogura. It is pleasant to express my appreciation to the former and present colleagues, especially Dr. Kenji Yamashita, Dr. Yuta Goto, Dr. Tasuya Mutsuga, Dr. Haruka Okamoto, Dr. Lu Yao, Dr. Lu Yanhui, Dr. Tatsuhiro Sakamoto, Dr. Kohey Nishioka, Dr. Naoto Sahara, Dr. Takuya Mochizuki, Dr. Yasutaka Tsuji, and Mr. Hiroki Tanaka, Mr. Keita Nakagawa, Mr. Masato Sakakibara, Mr. Kosuke Nishio, Mr. Ohta Katade, Mr. Takehiro Kato, Mr. Rin Hiramatsu, Mr. Ryutaro Kondo, Mr. Kohei Toh, Mr. Takashi Hazeyama, Mr. Ng Ji Qi, Mr. Weiwei Guo, Mr. Kei Katagiri, Mr. Hiroyuki Hayashi, Mr. Shinichi Ishizaki, Mr. Toshihiro Yasui, Mr. Tatsuya Ishikawa, Mr. Hiro Arima, Mr. Jianhao Huang, Ms. Xue Zhao, Mr. Kai Matsui, Mr. Kazuki Takeda, Ms. Sachiko Kumagai, Ms. Haruna Kato, Mr. Yasuo Tsukimori, Mr. Shogo, Yamamoto, Mr. Kosuke Nomura, and all of my colleagues in Ishihara group. I also would like to express my gratitude to Michiko Yoshimura for her dedicated support in administrative work.

I am very grateful to the Fellowships from the Program for Leading Graduate Schools “Integrative Graduate Education and Research in Green Natural Sciences”, MEXT, Japan, “Graduate Program of Transformative Chem-Bio Research” in Nagoya University, supported by MEXT (WISE program), JST SPRING and HOSHIZAKI Scholarship.

I would like to express special thanks to Professors Takashi Ooi, Toshio Nishikawa, Yoshihiko Yamamoto, and Associate Professor Jun Kumagai for serving on my discussion committee.

I wish to thank my family and friends, who made this work possible through for their support and sacrifice.

January 2022  
Kazuki Nishimura